

M₁ AND M₄ MUSCARINIC ACETYLCHOLINE RECEPTOR REGULATION OF
NEUROTRANSMISSION AND CELL EXCITABILITY IN RODENT
HIPPOCAMPUS AND PREFRONTAL CORTEX

By

Jana Kristin Shirey-Rice

Dissertation

Submitted to the Faculty of the
Graduate School of Vanderbilt University
in partial fulfillment of the requirements
for the degree of

DOCTOR OF PHILOSOPHY

in

Pharmacology

May, 2010

Nashville, Tennessee

Approved:

Professor P. Jeffrey Conn

Professor Ariel Y. Deutch

Professor Danny G. Winder

Professor C. David Weaver

ABSTRACT

Muscarinic acetylcholine receptors (mAChRs), specifically M₁ and M₄ subtypes, provide viable targets for the treatment of multiple central nervous system disorders. However, highly selective activators of either M₁ or M₄ have not been available, making it difficult to determine the *in vivo* effects of selective activation of these receptors. We have used cheminformatics and medicinal chemistry to develop new, highly selective M₁ and M₄ positive allosteric modulators (PAMs). VU10010 potentiated the functional M₄ response to acetylcholine while having no activity at other mAChR subtypes. Whole-cell patch clamp recordings revealed that VU10010 increased carbachol-induced depression of transmission at excitatory but not inhibitory synapses at the Schaffer collateral-CA1 (SC-CA1) synapse in the hippocampus. Chemical optimization of VU10010 afforded two centrally penetrant analogs, VU0152099 and VU0152100, which are also potent, selective M₄ PAMs. Interestingly, these compounds reversed amphetamine-induced hyperlocomotion in rats, a model that is predictive of clinical antipsychotic efficacy in humans.

A growing body of literature also supports M₁ receptors as a viable target for treatment of disorders involving impaired cognitive function. Data in this thesis reports the molecular characterization of a novel compound, BQCA, which is a potent, highly selective PAM of the rat M₁ receptor. BQCA induced a robust inward current and increased spontaneous EPSCs in mPFC layer V pyramidal cells, effects which were absent in acute slices from M₁ receptor knockout mice. Furthermore, multiple single-unit recordings were obtained from the mPFC of rats which showed that BQCA increased

firing of pyramidal cells *in vivo*. BQCA also restored discrimination reversal learning in a transgenic mouse model of AD and regulated non-amyloidogenic APP processing *in vitro*.

Together, these studies provide compelling evidence while M₄ inhibits excitatory transmission at the SC-CA1 synapse, M₁ receptor activation induces a dramatic excitation of PFC neurons. Newly developed highly selective ligands that activate or potentiate M₁ and M₄ provide exciting tools that will be useful in further delineating the individual roles of these receptors in the efficacy of drugs like acetyl cholinesterase inhibitors and xanomeline.

ACKNOWLEDGEMENTS

First and foremost, I want to extend my gratitude to my advisor, Dr. P. Jeffrey Conn for allowing me to join his laboratory and perform my graduate work there. Dr. Conn has provided unwavering support and guidance throughout the time I've spent as a graduate student in his lab. He has served as a role model for me not only as a scientist but as a person; he has such a passion for science coupled with an exceptionally kind heart and a genuine desire to contribute to our understanding of human disease with the ultimate goal being the development of better treatments for devastating CNS disorders. I have been continually inspired not just by his relentless pursuit of scientific progress but by the dignity and diplomacy with which he does so. His ability to bring together a bright, like-minded group of researchers has also greatly contributed to my happiness and success in lab over the years. I thank all the members of the Conn lab, past and present, who have infinitely blessed and enriched my life both in and outside the lab. None of the research in this thesis would have been possible without my funding sources (NIH T32 Training Grant and NIMH Ruth L. Kirschstein Individual Predoctoral National Research Service Award). I would like to acknowledge my thesis committee members; Drs. Ariel Deutch, C. David Weaver, and Danny Winder have taught me so much. They were always available to answer questions and not only offer direction for my thesis project but also to give great advice on how to successfully maneuver my way through graduate school life. They gave me confidence through the many times when I doubted my abilities or my work and helped me believe in myself because they did. I'm especially

grateful for invaluable advice from Dr. Winder on how to find and obtain a post-doctoral position during the final stages of my thesis research.

My family and friends have also provided endless support. I'm so blessed to have parents who always believe I can do anything I set out to do; thank you, mom and dad, for constantly reminding me how proud you are of me and for your encouragement throughout every stage of my life. I am so grateful for the friendships I've developed with my lab mates over the years. The numerous members of the Conn lab have committed tremendous time and effort to my training and have been great mentors and friends to me. My heartfelt gratitude goes to Drs. Ashley Brady, Alice Rodriguez, Doug Sheffler, Zixiu Xiang, Paulianda Jones, Jennifer Ayala, and Meredith Noetzel not only for their help with experiments and publications but also for their amazing friendship and boundless support. I would also like to thank Dr. Elaine Sanders-Bush for giving me a job as a research assistant before I entered graduate school; it was in her lab that I first discovered my interests in pharmacology and neuroscience. She was such a shining example of a strong, bright, determined female scientist who really inspired me.

I would finally like to acknowledge my husband, Jarrett, who has been a consistently positive force in my life; he kept me grounded as I faced the difficult and stressful times that are part of getting a graduate degree. He so often saw me at my worst and showed me nothing but open arms. I couldn't imagine a more perfect person with whom to share this exciting time in my life. I contribute much of my success to his selfless support, and I am deeply grateful to have found my perfect match.

TABLE OF CONTENTS

	Page
ABSTRACT	ii
ACKNOWLEDGEMENTS	iv
LIST OF TABLES	x
LIST OF FIGURES	xi
LIST OF ABBREVIATIONS	xiv
 Chapter	
I. INTRODUCTION	1
Cholinergic biosynthesis and neuroanatomy	1
Acetylcholine receptors	4
Muscarinic acetylcholine receptor subtypes, signaling, and function	4
Muscarinic regulation of hippocampal physiology	10
Electrophysiological effects of mAChR activation in the hippocampus	12
Muscarinic modulation of GABAergic transmission in the hippocampus	15
NMDA receptor modulation by mAChRs	17
Presynaptic M ₂ and M ₄ may regulate excitatory and inhibitory synaptic transmission	18
Role of muscarinic cholinergic signaling in hippocampal LTP	19
Muscarinic modulation and induction of LTD in the hippocampus	24
mAChR modulation of hippocampal physiology: conclusions	26
Prefrontal cortical physiology and function	27
Role of mAChRs in the mPFC	28
Postsynaptic effects of mAChRs in cortical neurons	29
Cholinergic modulation of cortical neurotransmission	32
mAChRs modulation of long-term changes in cortical synaptic strength	35
mAChR modulation of cortical physiology: conclusions	42
Pharmacology of muscarinic receptors	43
Models of receptor activation	43
Allosteric ligands of mAChRs	45
Development of early allosteric ligands of mAChRs	48
New ligands are highly selective for the M ₄ mAChR subtype	50
Advances in the development of novel selective activators of M ₁	52
mAChR pharmacology and novel allosteric ligands: conclusions	61

Muscarinic receptors as therapeutic targets	62
Xanomeline	65
mAChR subtypes involved in the therapeutic efficacy of xanomeline.....	66
The dopamine hypothesis of schizophrenia.....	67
Therapeutic promise of mAChR ligands: conclusions	69
II: MATERIALS AND METHODS.....	70
Compounds and materials.....	70
Chemistry methods	70
Chemical database mining for LY2033298 analogs.....	70
General syntheses of compounds VU10001-VU10010.....	71
General medicinal chemistry methods, M ₄ PAM libraries	74
General medicinal chemistry methods, M ₁ PAM libraries	77
JetMilling.....	82
Stable recombinant cell line establishment and cell culture	82
Calcium mobilization assays.....	83
GIRK-mediated thallium flux assay	85
Ancillary pharmacology assays	86
Equilibrium radioligand binding assays.....	86
[³⁵ S]GTPγS binding assays.....	88
Electrophysiology	88
Hippocampal whole cell patch clamp recordings	89
mPFC layer V whole cell patch clamp recordings.....	91
<i>In vivo</i> mPFC unit activity recordings	93
Pharmacokinetic profiling.....	94
M ₄ PAMS VU0152099 and VU0152100	94
M ₁ PAM BQCA.....	96
Mouse and rat behavior.....	98
Amphetamine-induced hyperlocomotion.....	98
Reversal learning	99
Amyloid precursor protein processing.....	105
IIIa: M₄ POSITIVE ALLOSTERIC MODULATORS REDUCE EXCITATORY POSTSYNAPTIC CURRENTS AT THE SC-CA1 SYNAPSE.....	107
Introduction.....	107
Results.....	112
Database mining of the ChemBridge chemical library yields a focused library of 232 compounds	112
Primary screening hits are robust, subtype selective allosteric potentiators of rat M ₄	116
Chemical optimization of primary M ₄ allosteric potentiator hits	117
Characterization of novel compounds in the VU10000 series.....	119
VU10010 binds allosterically and increases M ₄ receptor affinity for ACh.....	125
VU10010 enhances M ₄ coupling to downstream effector proteins	128

VU10010 enhances muscarinic depression of excitatory post-synaptic currents in hippocampal CA1 pyramidal cells.....	131
Muscarinic depression of inhibitory post synaptic currents is not affected by M ₄ potentiation.....	134
VU10010 potentiates CCh-induced reduction of EPSCs in wild-type but not M ₄ knockout mice.....	136
Discussion.....	137
IIIb: CENTRALLY ACTIVE ALLOSTERIC POTENTIATORS OF THE M ₄ MUSCARINIC ACETYLCHOLINE RECEPTOR REVERSE AMPHETAMINE-INDUCED HYPERLOCOMOTOR ACTIVITY IN RATS.....	141
Introduction.....	141
Results.....	144
Chemical lead optimization	144
Screening paradigm for analog libraries.....	147
VU0152099 and VU0152100 are potent positive allosteric modulators of M ₄ in two independent <i>in vitro</i> assays.....	150
VU0152099 and VU0152100 are selective for the M ₄ mAChR subtype.....	154
VU0152099 and VU0152100 bind to an allosteric site on the M ₄ receptor and increase ACh affinity.....	159
VU0152099 and VU0152100 exhibit improved physiochemical and pharmacokinetic properties compared to VU10010.....	161
VU0152099 and VU0152100 exhibit <i>in vivo</i> activity in rat.....	163
Discussion.....	165
IV: A SELECTIVE ALLOSTERIC POTENTIATOR OF THE M ₁ mAChR INCREASES ACTIVITY OF MEDIAL PREFRONTAL CORITICAL NEURONS AND RESTORES IMPAIRMENTS IN REVERSAL LEARNING.....	169
Introduction.....	169
Results.....	171
A panel of 21 compounds related to BQCA has a range of activities as allosteric potentiators at the rat M ₁ mAChR.....	171
BQCA is a potent and selective positive allosteric modulator of the rat M ₁ receptor <i>in vitro</i>	175
BQCA is functionally selective for the M ₁ mAChR subtype.....	177
BQCA does not compete for orthosteric antagonist binding but increases ACh affinity at the rM ₁ receptor.....	181
Activation of the M ₁ receptor induces an inward current in rat mPFC layer V pyramidal cells and this effect is potentiated by BQCA.....	183
BQCA does not potentiate CCh-mediated inward currents in M ₁ knockout mice.....	186
CCh increases mPFC spontaneous EPSC amplitude and frequency.....	188
The effect of CCh on sEPSC amplitude and frequency is inhibited by M ₁ antagonist VU0255035.....	190

BQCA increases sEPSCs and potentiates the effect of a sub-threshold concentration of CCh on sEPSC frequency	192
CCh and BQCA have no effect on miniature EPSCs	194
BQCA has no effect on sEPSCs in slices from M ₁ receptor knockout mice	196
BQCA has excellent brain penetration and increases the firing rate of mPFC neurons <i>in vivo</i> in rats	200
Acute administration of BQCA restores impairment in reversal learning in Tg2576 mice	204
BQCA regulates non-amyloidogenic APP processing	207
Discussion	210
V: SUMMARY AND FUTURE DIRECTIONS	213
REFERENCES	231

LIST OF TABLES

Table		Page
1	Media and Odor Pairings for reversal learning.....	104
2	Example of Experimental Design for reversal learning.....	104
3	Identification numbers of compounds and hits from the ChemBridge library	114
4	Radioligand binding parameters for mAChR-expressing cell lines	126
5	Structures, activities and ACh CRC fold-shifts of M ₄ PAM library five analogs	149
6	Selectivity of VU0152099 and VU0152100 determination in radioligand binding assays in the LeadProfilingScreen® by MDS Pharma	156
7	Pharmacokinetic analysis of VU0152099 and VU0152100	162
8	Pharmacokinetic analysis of BQCA	201
9	BQCA reverses impairments in discrimination learning in Tg2576 mice.....	205

LIST OF FIGURES

Figure		Page
1	Schematic model of cholinergic biosynthesis and neurotransmission in the central nervous system.....	3
2	Database mining yields a series of compounds from the ChemBridge library with allosteric potentiator activity at the rat M ₄ receptor	111
3	Lead compounds robustly potentiate M ₄ -mediated calcium mobilization and are selective for M ₄ relative to other mAChR subtypes	115
4	Synthesis of compounds in the VU10000 series.....	118
5	Chemical optimization generates compounds that potentiate M ₄ -mediated calcium mobilization with greater efficacy than lead compound 791236.....	121
6	VU10010 is selective for the rM ₄ receptor relative to the other mAChRs	123
7	VU10010 showed no agonist, antagonist, or potentiator activity at two GPCRs unrelated to rM ₄ mAChR	124
8	Compound VU10010 binds to an allosteric site on M ₄ mAChR and causes an increase in affinity for ACh and M ₄ -mediated [³⁵ S]GTPγS binding	127
9	VU10010 does not compete for binding at rM ₁ , hM ₂ , hM ₃ , or hM ₅	130
10	VU10010 potentiates CCh-induced reduction of EPSCs but not IPSCs at rat hippocampal Shaffer collateral-CA1 synapses	133
11	VU10010 potentiates CCh-induced reduction of EPSCs in wild-type but not in M ₄ knockout mice.....	135
12	Chemical structures of xanomeline and VU10010	143
13	Chemical optimization of VU10010 using a diversity-oriented approach to achieve soluble, centrally penetrant M ₄ positive allosteric modulators.....	146
14	Screening paradigm for analog libraries 7-15 allowing for the rapid triage of inactive analogs.....	148
15	VU0152099 and VU0152100 are potent positive allosteric modulators of rM ₄ <i>in vitro</i>	151

16	VU0152099 and VU0152100 potentiate GIRK-mediated thallium flux in response to ACh in HEK cells expressing human M ₄	153
17	VU0152099 and VU0152100 are functionally selective for the M ₄ mAChR subtype	155
18	Millipore GPCR Profiler™ Functional Screen for VU0152099 selectivity	158
19	VU0152099 and VU0152100 bind allosterically and increase ACh affinity at rM ₄	160
20	Pharmacokinetic profiling of VU0152099 and VU0152100 in rats	162
21	VU0152099 and VU0152100 inhibit amphetamine-induced hyperlocomotor activity in rats without causing sedation	164
22	Twenty-one putative M ₁ receptor PAMs were synthesized and evaluated at the rM ₁ mAChR for their ability to potentiate an EC ₂₀ concentration of ACh.....	173
23	Four of the compounds initially identified as robust M ₁ potentiators of the calcium response were further characterized <i>in vitro</i> at the rM ₁ mAChR	174
24	BQCA (VU0238386) is a potent positive allosteric modulator of the rM ₁ receptor <i>in vitro</i>	176
25	The presence of BQCA has no effect on the ACh concentration response curve at any other mAChR subtype	179
26	Millipore GPCR Profiler BQCA selectivity data.....	180
27	BQCA does not compete for orthosteric antagonist binding and induces a robust leftward shift in ACh affinity at the rM ₁ receptor.....	182
28	CCh-induced inward current in mPFC layer V pyramidal cells is reduced by M ₁ receptor antagonist VU0255035 and potentiated by BQCA.....	185
29	BQCA does not potentiate CCh-mediated inward currents in M ₁ knockout mice	187
30	Muscarinic receptor activation increases mPFC spontaneous EPSC amplitude and frequency	189
31	The effect of CCh on sEPSC amplitude and frequency is inhibited by VU0255035.....	191
32	BQCA increases sEPSCs and potentiates a sub-threshold concentration of CCh to increase sEPSC frequency.....	193

33	CCh and BQCA have no effect on miniature EPSC amplitude and frequency in rat mPFC layer V pyramidal cells.....	195
34	BQCA has no effect and does not potentiate the CCh effect on sEPSCs in M ₁ receptor knockout mice.....	198
35	Pharmacokinetic profiling of BQCA in rats	201
36	BQCA increases the firing rate of mPFC neurons <i>in vivo</i> in rats	203
37	Effects of acute administration of BQCA on discrimination learning in Tg2576 mice.....	206
38	BQCA regulates non-amyloidogenic APP processing	209

LIST OF ABBREVIATIONS

77-LH-28-1	Centrally penetrant M ₁ agonist
A β	Amyloid precursor protein cleavage product produced by β -secretase and subsequent γ -secretase cleavage
AC42	M ₁ allosteric agonist
ACh	Acetylcholine
AChE	Acetyl cholinesterase
ACSF	Artificial cerebrospinal fluid
AD	Alzheimer's disease
AF267	Muscarinic receptor agonist reported to be M ₁ -selective
ANOVA	Analysis of variance
AP-5	(2 <i>R</i>)-amino-5-phosphonovaleric acid, competitive NMDAR antagonist
APP	Amyloid precursor protein
ATP	Adenosine triphosphate
Brucine	First reported M ₁ positive allosteric modulator
BQCA	Benzylquinolone carboxylic acid, M ₁ PAM
CAR	Conditioned avoidance responding
CCh	Carbachol, non-selective muscarinic agonist
CD	Compound discrimination
CDR	Compound discrimination reversal
c-fos	Transcription factor belonging to the immediate early gene family
CID	Collision-induced dissociation

CNS	Central nervous system
CNQX	6-cyano-7-nitroquinoxaline-2,3-dione, AMPA/kainate receptor antagonist
CRC	Concentration response curve
D ₂	D ₂ dopamine receptor
DA	Dopamine
DAR	Dopamine receptor
DCC	Dicyclohexylcarbodiimide
DIEA	Diisopropylethyl amine
DMEM	Dulbecco's Modified Eagle Medium
DMSO	Dimethyl sulfoxide
EDTA	Ethylenediaminetetraacetic acid
EGTA	Ethylene glycol tetraacetic acid
ELISA	Enzyme-linked immunosorbent assay
EPSC	Excitatory postsynaptic current
EPSP	Excitatory postsynaptic potential
ERK	Extracellular signal-regulated kinase
GABA	γ -aminobutyric acid
GDP	Guanosine 5'-diphosphate
GFP	Green fluorescent protein
GIRK	G protein-coupled inwardly rectifying potassium
Glu	Glutamic acid
GPCR	G protein-coupled receptor

Gq _{i5}	Chimeric Gq _α protein containing the five c-terminal amino acid residues corresponding to those of Gi _α
GTPγS	Guanosine 5'-[γ-thio]triphosphate
HOBt	Hydroxybenzotriazole
<i>i.p.</i>	Intraperitoneally
IPSC	Inhibitory postsynaptic current
IPSP	Inhibitory postsynaptic potential
[³ H]-NMS	<i>l</i> -[N-methyl- ³ H]scopolamine
LC-MS-MS	Liquid chromatography followed by tandem mass spectrometry
LTD	Long-term depression
LTP	Long-term potentiation
LY2033298	M ₄ positive allosteric modulator
M ₁ – M ₅	Muscarinic acetylcholine receptor subtypes 1 - 5
mAChR	Muscarinic acetylcholine receptor
MAPK	Mitogen-activated protein kinase
mGluR	Metabotropic glutamate receptor
mPFC	Medial prefrontal cortex
NAM	Negative allosteric modulator
NIH	National Institutes of Health
NMDA	<i>N</i> -Methyl-D-aspartate
Oxotremorine	Non-selective muscarinic receptor agonist
PAM	Positive allosteric modulator
P-gp	P-glycoprotein
PLCβ	Phospholipase C β

PPI	Prepulse inhibition (of the acoustic startle reflex)
PPR	Paired pulse ratio
rpm	Revolutions per minute
SAR	Structure-Activity-Relationship
<i>s.c.</i>	Subcutaneously
SC-CA1	Shaffer collateral-CA1
SD	Simple discrimination
SDR	Simple discrimination reversal
SDS-PAGE	Sodium dodecyl sulfate polyacrylamide gel electrophoresis
S.E.M.	Standard error of the mean
TBPB	M ₁ allosteric agonist
Tg2576 mice	Mice over-expressing a 695 amino acid splice form (Swedish mutations K670N and M671L) of the human amyloid precursor protein (APP ₆₉₅)
VU0029767	M ₁ positive allosteric modulator
VU0090157	M ₁ positive allosteric modulator
VU0152099	Centrally penetrant M ₄ positive allosteric modulator
VU0152100	Centrally penetrant M ₄ positive allosteric modulator
VU0177548	M ₁ allosteric agonist
VU0184670	M ₁ allosteric agonist
VU0207811	M ₁ allosteric agonist
VU0255035	Centrally penetrant orthosteric M ₁ -selective antagonist
VU0357017	M ₁ allosteric agonist
VU10010	M ₄ positive allosteric modulator

CHAPTER I

INTRODUCTION

Cholinergic biosynthesis and neuroanatomy

A detailed understanding of cholinergic synthesis and neurotransmission is now available as a result of diverse research techniques, including biochemical analysis, molecular genetics, and microscopy (**Fig. 1**) (Krnjevic, 1969; Csillik, 1975). In the presynaptic terminal, acetylcholine (ACh) is synthesized from its precursors acetyl coenzyme A (acetyl CoA) and choline by the enzyme choline acetyltransferase (ChAT). ACh is packaged into synaptic vesicles by the vesicular acetylcholine transporter (VAChT) and subsequently released into the synaptic cleft. Synaptic vesicles containing the neurotransmitter can bind and activate pre- and post-synaptic acetylcholine receptors only for a brief time until it is degraded by acetylcholinesterase (AChE). Following degradation, the precursor choline is taken up into the presynaptic axon terminal by a high affinity choline transporter (CHT). This reuptake process is the rate limiting step in acetylcholine biosynthesis.

Cholinergic nuclei in the basal forebrain, a group of structures in the medial and ventral telencephalon, contain large numbers of neurons that project to the hippocampus, amygdala, and cerebral cortex and provide the majority of cholinergic innervation to these areas (Mufson et al., 2000). The basal forebrain is divided into several distinct regions that send bundles of axons to their respective targets. Projection cholinergic neurons in the medial septum and the diagonal band of Broca project to the hippocampus,

while neurons in the nucleus basalis of Meynert project broadly to the neocortex as well as to the amygdala. These cholinergic projections provide one of the most crucial neuromodulatory inputs to the forebrain in humans and other mammals. Cholinergic interneurons in the striatum also release ACh within local circuits where muscarinic receptors modulate the activity of medium spiny neurons. Cholinergic neurons are distinguished among other features by the presence of ChAT, the enzyme that is responsible for ACh biosynthesis these neurons.

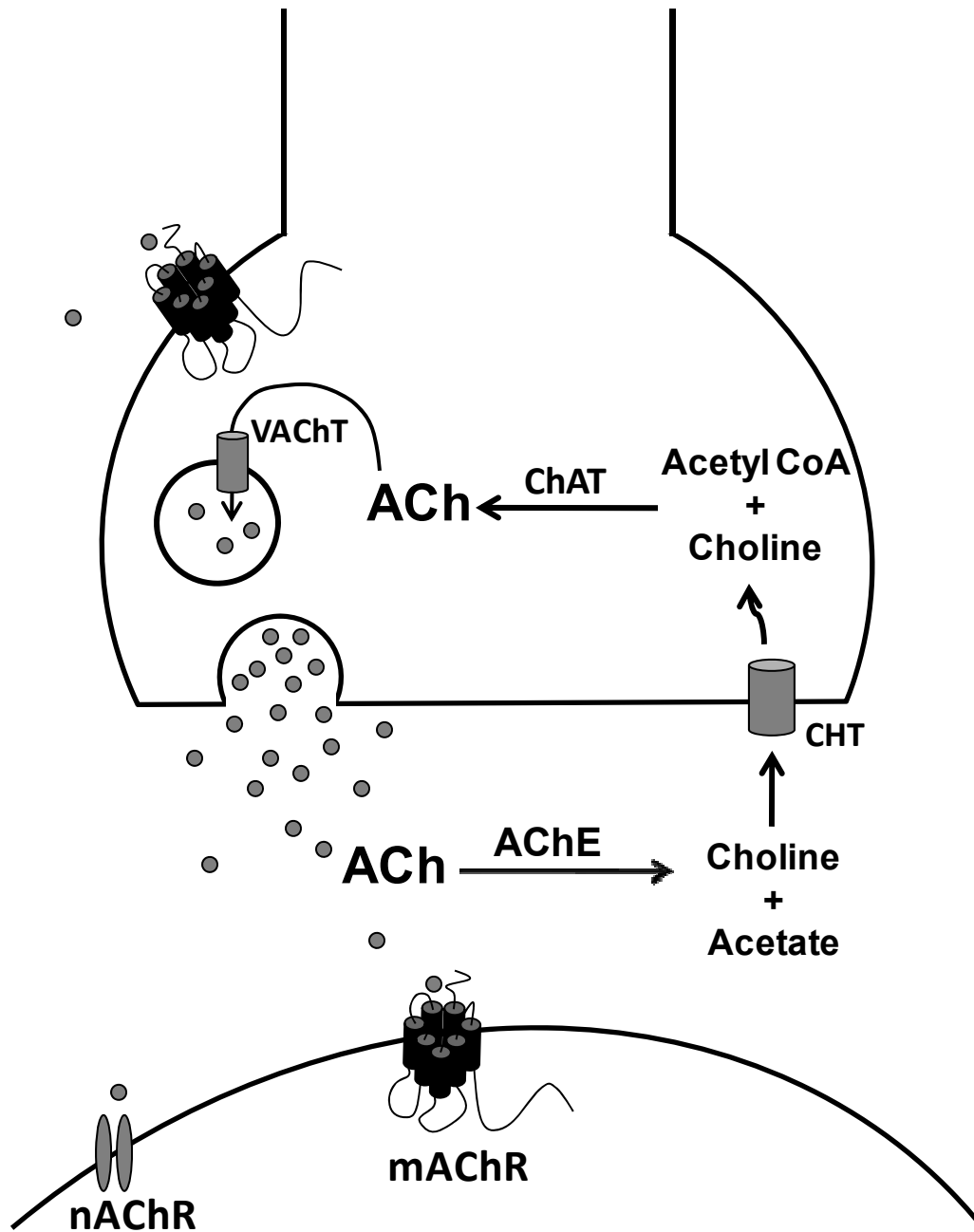


Figure 1. Schematic model of cholinergic biosynthesis and neurotransmission in the central nervous system. Acetylcholine (ACh) is synthesized in presynaptic nerve terminals by the enzyme choline acetyltransferase (ChAT), packaged into synaptic vesicles by the vesicular acetylcholine transporter (VAcHT), and released into the synaptic cleft. Intact ACh can bind and activate nicotinic and muscarinic acetylcholine receptors on both pre- and post-synaptic membranes until it is degraded by the enzyme acetylcholinesterase (AChE). The biosynthetic precursor choline is then taken up into the presynaptic terminal by the high affinity choline transporter (CHT) with choline reuptake being the rate-limiting step in ACh synthesis.

Acetylcholine Receptors

ACh, the first neurotransmitter to be identified, activates two families of receptors that mediate its action in target tissues: nicotinic receptors, which function as ligand-gated cation channels that participate in rapid postsynaptic neurotransmission, and muscarinic receptors (mAChR), which are members of family A G-protein coupled receptors (GPCRs) and play a role in modulating the activity of many circuits within the CNS. These two classes of receptor families were originally named for their specific activation by nicotine and muscarine, respectively, but have been extensively characterized since that time on a molecular basis. This thesis will focus on muscarinic acetylcholine receptor subtypes. The diversity and complexity of muscarinic cholinergic signaling is facilitated in part by five distinct receptor subtypes, M₁-M₅, the genes for which were cloned in the mid to late 1980s (Bonner et al., 1987; Peralta et al., 1987; Bonner et al., 1988). These intronless genes encode muscarinic receptor proteins that have the typical structural features of the seven transmembrane helix GPCR superfamily, the largest family of cell-surface receptors and key regulators of a wide variety of physiological processes (Lefkowitz, 2007). In general, when the receptor is activated GDP is converted to GTP on the G protein resulting in its dissociation from the receptor. Subsequently, the G protein dissociated into α and $\beta\gamma$ subunits, which both activate downstream signaling cascades.

Muscarinic acetylcholine receptor subtypes, signaling, and function

The five receptor subtypes are highly homologous in the ACh binding domain; their signaling properties are quite different, however. M₁, M₃, and M₅ preferentially

couple to $G\alpha_q$ proteins to activate phospholipase C (PLC) and cause a subsequent release of calcium from intracellular stores as well as an increase in phosphatidylinositol turnover and activation of protein kinase C (PKC) (Wess, 1996). The major mechanism of calcium release from endoplasmic reticulum stores in CA1 pyramidal neurons is via production of inositol 1,4,5-triphosphate (IP_3) induced by mAChR activation. In addition M_1 , M_3 and M_5 receptors have also been shown to activate phospholipase A_2 (PLA_2), phospholipase D (PLD) and tyrosine kinases (Wess, 1996). M_2 and M_4 receptors couple predominantly to $G\alpha_{i/o}$ proteins to inhibit adenylate cyclase and cause a decrease in cyclic AMP levels. Activation of $Gi_{\beta\gamma}$ subunits by M_2 and M_4 subtypes also modulate a variety of ionic channels including voltage-gated calcium channels as well as inwardly rectifying potassium channels. All subtypes of muscarinic receptors have been shown to activate extracellular signal related kinase (ERK), a signaling protein involved in cell growth, differentiation and survival (Hulme (a) et al., 2003).

In situ hybridization experiments following the cloning of mAChR subtype genes revealed that individual subtypes were expressed in partially overlapping tissues, with some regions, including the hippocampus, expressing all five mAChR subtypes (Buckley et al., 1988; Weiner et al., 1990). A series of studies using subtype-selective antibodies has illustrated the distinct neuroanatomical localization of the mAChR subtypes in brain and have provided important clues as to their function in neural circuits (Levey et al., 1991; Mrzljak et al., 1993; Levey et al., 1994; Hersch and Levey, 1995; Levey et al., 1995b; Rouse and Levey, 1996; Rouse et al., 1998; Rouse et al., 2000b).

The M_1 receptor is expressed at very high levels in multiple brain regions including cortex, hippocampus, and striatum (Wess, 2003). In the cortex, M_1 is localized

to pyramidal cells and is prominent in the neuropil of layers II/III and VI (Levey et al., 1991). M₁ is expressed broadly throughout the hippocampus, including in pyramidal neuron cell bodies and dendritic processes in the stratum radiatum and stratum oriens, and in the molecular layer and granule cells of the dentate gyrus (Levey et al., 1995b). In the striatum, M₁ is found in the majority of dopamine-2 receptor (D₂)-expressing medium spiny neurons as well as in the neuropil. At the electron microscopy level, M₁ can be visualized at the postsynaptic density of asymmetrical synapses, suggesting a role in modulating excitatory neurotransmission (Hersch et al., 1994). Studies using knockout mice have suggested a role for M₁ in learning and memory, and it has been demonstrated that M₁ potentiates NMDA receptor currents (Marino et al., 1998) and is the sole mAChR responsible for muscarinic activation of extracellular signal-regulated kinase (ERK 1/2) in the hippocampus, a protein involved in synaptic plasticity (Berkeley et al., 2001; Hamilton and Nathanson, 2001). M₁ knockout mice are less susceptible to pilocarpine-induced seizures and have a phenotype that is similar to that seen in animal models of psychosis, including hyperactivity, increased dopamine release, and a heightened response to amphetamine (Gerber et al., 2001; Miyakawa et al., 2001). Interestingly, M₁ knockout mice perform as well as their wild-type littermates in the Morris water maze, a paradigm commonly used to assess hippocampal-dependent spatial memory; however, performance was impaired under certain experimental conditions in the eight-arm radial maze and in fear conditioning studies (Miyakawa et al., 2001). These animals only exhibited a mild reduction in hippocampal long-term potentiation (LTP), an electrophysiological phenomenon associated with learning and memory (Anagnostaras et al., 2003). The profound hyperactivity phenotype of these animals (Gerber et al., 2001;

Miyakawa et al., 2001) makes it unclear whether some of the behavioral impairments are actually due to cognitive impairments. This caveat aside, $M_1^{-/-}$ mice display significant impairments in non-matching-to-sample working memory and consolidation (Anagnostaras et al., 2003), implicating these receptors in cortical memory function and tasks requiring prefrontal cortical signaling (Hamilton and Nathanson, 2001). Based on these studies using genetically altered mice as well as a growing body of clinical and pre-clinical data, the M_1 receptor subtype is viewed as one of the most exciting therapeutic targets for the treatment of neurological disorders such as Alzheimer's disease (AD) and schizophrenia (Fisher, 2008b; Conn et al., 2009b).

M_2 is the most widespread mAChR subtype in brain; it is expressed predominantly on presynaptic terminals and has been shown to function as an autoreceptor controlling ACh release in the hippocampus and cerebral cortex but not in striatum (Zhang et al., 2002a). M_2 has a distinct laminar distribution in the cortical neuropil of layer IV and the junction between layers V/VI, and is also present on interneuron cell bodies (Levey et al., 1991). Close inspection revealed that M_2 is expressed both pre-and post-synaptically (Mrzljak et al., 1993). In the hippocampus, M_2 localizes to discrete bands of cell bodies and processes along the oriens/alveus border, and is also found in processes along the pyramidal cell layer, most prominently in the CA3 region (Levey et al., 1995b). There is a high expression level of M_2 in the basal forebrain, in both cholinergic and noncholinergic cells, as well as in the neuropil (Levey et al., 1995a). M_2 also mediates parasympathetic decreases in the force of contraction and in the rate of cardiac contraction by inhibiting voltage-gated calcium channels and activating inwardly rectifying potassium channels (Caulfield and Birdsall, 1998). Studies

in M₂ knockout mice have demonstrated a physiological role for this protein in locomotion, regulation of body temperature, and response to pain (Gomez et al., 2001). These mice have deficits in behavioral flexibility and working memory as well as in passive avoidance (Seeger et al., 2004; Tzavara et al., 2004).

The M₃ receptor is expressed at relatively low levels in brain, accounting for only 5-10% of total mAChRs in various brain regions (Levey et al., 1994). By immunohistochemistry, M₃ can be seen to localize to multiple brain regions, including cortex, hippocampus, olfactory bulb, amygdala, striatum, thalamus, and pons. Subcellularly, M₃ appears in cell bodies and proximal dendrites, suggesting a postsynaptic localization, and also as a diffuse, punctate reaction product in the neuropil that may reflect presynaptic terminals or dendritic processes. In the CNS, M₃ helps regulate the release of several neurotransmitters, including dopamine in the striatum, GABA and glycine in the dorsal horns of the spinal cord, and endocannabinoids (Zhang et al., 2002a; Ohno-Shosaku et al., 2003; Zhang et al., 2006; Zhang et al., 2007). Studies in M₃ knockout mice have also implicated this subtype in multiple peripheral and autonomic functions, including arterial vasodilation, insulin release, glandular secretion (including salivation), weight gain, and smooth muscle contraction in the stomach, trachea, and urinary bladder (Matsui et al., 2000; Yamada et al., 2001b; Duttaroy et al., 2004; Khurana et al., 2004). It is believed that activation of peripheral M₃ receptors leads to severe side effects such as excess salivation and GI distress induced by cholinergic agonists and AChE inhibitors used to treat AD.

The M₄ receptor is expressed at somewhat lower levels than other mAChR subtypes in cortical laminae, and is localized to discrete layers in the hippocampus,

including the stratum radiatum and stratum oriens in CA1 and the inner molecular layer of the dentate gyrus. In the striatum where M₄ is most highly expressed, dense patches of receptor expression are observed that correspond to postsynaptic sites on medium spiny neurons. Analogous to the autoinhibitory role that M₂ plays in the hippocampus and cortex, M₄ is the major autoreceptor in the striatum responsible for feedback regulation of ACh release from the presynaptic terminal (Zhang et al., 2002b). M₄ has been shown to participate in regulating dopaminergic signaling and release, and M₄ knockout mice show increased basal and dopamine-regulated locomotor responses (Gomez et al., 1999; Zhang et al., 2002a). These animals are hypersensitive to agents that disrupt prepulse inhibition of the acoustic startle response, a measure of sensorimotor gating which is also disrupted in schizophrenic patients (Felder et al., 2001). *In vivo* microdialysis studies revealed that M₄ knockout mice also have elevated basal dopamine levels in the nucleus accumbens and that these mice show heightened dopamine efflux in response to psychostimulants like D-amphetamine and phencyclidine (Tzavara et al., 2004).

Levels of the M₅ receptor approach the lower limits of specific detection in brain as determined by quantitative immunoprecipitation and immunohistochemistry, although M₅ mRNA is detectable in multiple brain tissues. M₅ knockout mice have revealed roles for M₅ in dilation of cerebral blood vessels and in reward and reinforcement behaviors, specifically in response to drugs of abuse such as morphine and cocaine (Yamada et al., 2001a; Basile et al., 2002; Thomsen et al., 2005). Further support for the role of M₅ in drug addiction came with the finding that these animals exhibit less severe withdrawal symptoms after chronic morphine exposure as well as decreased cocaine conditioned

place preference and reduced acute cocaine self-administration (Fink-Jensen et al., 2003; Thomsen et al., 2005).

Muscarinic regulation of hippocampal physiology and function

The hippocampus is a key cortical structure that plays an important role in a number of normal physiological processes, including processing of complex spatial and temporal patterns and formation of short- and long-term memory. In addition, the hippocampus is a primary site of pathology in certain neurological disorders, such as AD and temporal lobe epilepsy. Because of this, much effort has been directed at developing a detailed understanding of the synaptic organization of the hippocampus as well as the cellular mechanisms involved in regulation of synaptic transmission in this structure (see (Brown and Zador, 1990) for review). Glutamate is the primary neurotransmitter at each of the three major excitatory synapses in the hippocampal formation. In addition, neuromodulators from extrinsic afferents (ie. acetylcholine, serotonin, norepinephrine) regulate transmission through the hippocampus by activating GTP-binding protein-linked receptors. Regulation of hippocampal function by these neuromodulators dramatically influences net transmission through the hippocampus and participates in a variety of different physiological and pathological conditions.

The hippocampus is commonly viewed as a relatively simple circuit consisting of three major excitatory synapses. The primary input to the hippocampus is from the entorhinal cortex which sends excitatory afferents to the dentate gyrus (DG) via the perforant path; the entorhinal cortex collects polymodal information from other cortical areas and relays this information to dentate granule cells. Mossy fibers from the dentate

granule cells project to area CA3 of the hippocampus which in turn sends afferents via the Schaffer collateral to hippocampal area CA1. Afferents from CA1 pyramidal cells then provide the major output of the hippocampus. Each subregion of the hippocampus also has intrinsic circuits and connections within (associational) and between (commissural) hippocampi. Glutamate is the excitatory neurotransmitter at each of the three major excitatory synapses in the hippocampal formation. In addition, neuromodulators from extrinsic afferents (ie. acetylcholine, serotonin, norepinephrine) regulate transmission through the hippocampus by activating GTP-binding protein-linked receptors. Regulation of hippocampal function by these neuromodulators dramatically influences net transmission through the hippocampus and participates in a variety of different physiological and pathological conditions.

One of the major neuromodulatory inputs to the hippocampus is a large bundle of cholinergic projections from the medial septum and the diagonal band of Broca (Brown and Zador, 1990), and these cholinergic projections make synaptic contact with widespread but highly specific targets in the hippocampus. A large number of animal and human studies suggest that cholinergic projections to the hippocampus play a critical role in memory and attention mechanisms. For instance, blockade of muscarinic receptors or lesions of the septo-hippocampal projections produce memory and attentional deficits (Drachman and Leavitt, 1974; Bartus et al., 1982; Dekker et al., 1991; Fibiger et al., 1991; Nilsson et al., 1992; Callahan et al., 1993). Also, the theta rhythm, an electroencephalographic measure of the arousal response in the hippocampus which may be involved in attention and filtering of sensory information, is regulated by cholinergic septal input and can be induced by muscarinic agonists and abolished by

muscarinic antagonists (Colom et al., 1991; Vinogradova et al., 1993). Furthermore, abundant evidence suggests that the clinical syndrome associated with AD results, at least in part, from failed neurotransmission at cholinergic synapses in the hippocampus and neocortex. The basal forebrain neurons that provide the majority of cholinergic innervation of the neocortex and hippocampus degenerate with AD (Whitehouse et al., 1982; Arendt et al., 1983) and this is accompanied by a depletion of presynaptic cholinergic markers in these brain regions (Bowen et al., 1976; Davies and Maloney, 1976; Perry et al., 1978; Whitehouse et al., 1982). Furthermore, lesions of basal forebrain neurons or pharmacological blockade of muscarinic receptors, experimentally in animals (Dunnett, 1985; Dekker et al., 1991; Fibiger, 1991; Voytko et al., 1994) or naturally in humans (Drachman and Leavitt, 1974; Drachman, 1977; Bartus et al., 1982; Damasio et al., 1985), impairs learning, memory, and attention. Evidence suggests that cholinergic transmission in the hippocampus is mediated primarily by mAChRs and that these receptors are likely to mediate the cholinergic involvement in learning and memory (Coyle et al., 1983; Brown and Zador, 1990; Fibiger, 1991).

Electrophysiological effects of mAChR activation in the hippocampus

Multiple mAChR subtypes are expressed in the hippocampus (Hulme et al., 1990; Caulfield, 1993; Levey et al., 1995b) where they are involved in regulating various aspects of hippocampal physiology. Early studies showed that mAChR activation induces a number of direct excitatory effects on hippocampal pyramidal cells and reduces both excitatory (Hounsgaard, 1978; Segal, 1982; Dutar and Nicoll, 1988; Sheridan and Sutor, 1990; Williams and Johnston, 1990; Burgard et al., 1993) and inhibitory (Krnjevic

et al., 1981; Bilkey and Goddard, 1985) synaptic transmission in the hippocampus. Another well characterized electrophysiological effect of muscarinic receptor activation in hippocampal pyramidal cells using the intracellular recording technique is a slow post-synaptic potential (Cole and Nicoll, 1984a); repetitive electrical stimulation of cholinergic fibers terminating in stratum oriens evokes a series of membrane potential changes. First is a series of fast excitatory postsynaptic potentials (EPSPs) followed by an inhibitory postsynaptic potential (IPSP); these are followed by a slow EPSP that lasts on the order of 20-30 seconds. The slow EPSP could be induced by ionophoretic application of ACh and was blocked by atropine and was dependent on action potential firing and calcium (Cole and Nicoll, 1984a).

Muscarinic receptors modulate a large number of ionic conductances in pyramidal neurons through both direct and indirect biochemical interactions; the conductances known to be modulated by mAChRs in hippocampal pyramidal cells include several potassium currents (I_M , the muscarine sensitive K^+ current; I_{AHP} , the Ca^{2+} -activated K^+ current underlying spike frequency adaptation; I_{leak} , the background leak current) (Halliwell, 1990). Exogenously applied muscarinic agonists induce a pronounced membrane potential depolarization and increased membrane resistance (Cole and Nicoll, 1984b), and direct electrical stimulation of cholinergic afferents in the hippocampus causes a similar mAChR-dependent membrane potential depolarization (Segal, 1982; Cole and Nicoll, 1984b; Madison et al., 1987; Pitler and Alger, 1990; Morton and Davies, 1997). This response often results in a sustained action potential discharge, in part arising from a pronounced reduction in spike frequency adaptation (Cole and Nicoll, 1984b). Activation of mAChRs increases cell firing and depresses the I_{AHP} that is due to

a calcium-activated potassium conductance, as mentioned above. It is thought that this conductance, at least in part, is responsible for a dampening of action potential discharge during depolarizing current injections. These excitatory effects of ACh are mediated by mAChRs because they are completely blocked by atropine, a non-selective muscarinic antagonist, but not by nicotinic antagonists. mAChR activation also potentiates two mixed cation currents (I_h , the hyperpolarization-activated cation current; I_{cat} , the Ca^{2+} -dependent non-specific cation current) (Halliwell, 1990; Colino and Halliwell, 1993) and modulates the activity of both voltage-dependent Ca^{2+} currents and several ligand-gated receptors including *N*-methyl-D-aspartate (NMDA) receptors (Markram and Segal, 1990b, a, 1992; Harvey et al., 1993; Marino et al., 1998; Sur et al., 2003). In addition, mAChR agonists increase pyramidal cell excitability indirectly by reducing GABA-mediated synaptic inhibition (Krnjevic et al., 1981; Bilkey and Goddard, 1985). Presynaptically, activation of mAChRs inhibits excitatory afferents, reducing the release of glutamate through inhibition of voltage-gated calcium channels (Qian and Saggau, 1997; Fernandez de Sevilla et al., 2002; Fernandez de Sevilla and Buno, 2003). More recently, muscarinic agonists have also been shown to inhibit L-type calcium currents in superior cervical ganglion (SCG) neurons (Liu et al., 2006) and enhance R-type, but not T-type, Ca^{2+} currents in hippocampal CA1 pyramidal neurons, an effect that required PKC activation (Tai et al., 2006).

Subsequent studies examining specific mAChR subtypes involved in some of these electrophysiological effects have shown that depolarization of hippocampal pyramidal neurons is likely mediated, at least in part, by the M_1 receptor subtype as inward currents recorded in voltage clamp mode from CA3 pyramidal cells were

markedly reduced in M₁ knockout mice as compared to wild-types (Fisahn et al., 2002). The muscarinic potentiation of I_{CAT} contributes to the depolarization of pyramidal neurons. Muscarine caused an increase in magnitude of I_h in wild-type but not M₁ knockout mice, indicated that the M₁ subtype is responsible for this effect in CA3 cells; conversely, there was no effect of muscarinic agonists on I_M in the M₁ knockout supporting data by Rouse et al. (Rouse et al., 2000a) indicating a lack of M₁ modulation of this current in CA1 pyramidal cells.

Muscarinic modulation of GABAergic transmission in the hippocampus

Extrahippocampal γ -aminobutyric acid (GABA)ergic afferents originating from the medial septum and diagonal band of Broca innervate the hippocampus and target solely hippocampal interneurons and cholinergic afferents which in turn target both pyramidal cells and interneurons (Frotscher and Leranth, 1985). Acetylcholine is a powerful presynaptic modulator of synaptic transmission at both excitatory glutamatergic and inhibitory GABAergic synapses with modulation being both cell type and pathway specific. Furthermore, GABAergic interneurons can inhibit cholinergic release presynaptically through GABA_B receptors (Morton et al., 2001). The role of mAChRs in modulating activity of GABAergic inhibitory neurons is complex; studies have shown that mAChR activation of individual interneurons in the hippocampus yields differential effects on resting membrane potential (McQuiston and Madison, 1999a, b). Among several subpopulations of GABAergic interneurons, muscarinic receptor activation produces a pure hyperpolarizing response, a biphasic response in which an initial hyperpolarization is followed by a secondary depolarizing phase, a slow membrane

potential oscillatory response, or no response. Immunocytochemical findings suggested cell type-specific localization of mAChRs in different subtypes of interneurons (Levey et al., 1995b) which likely explains the variable muscarinic effects observed in these cells. This diversity of interneuron responses also likely reflects a highly heterogeneous population of GABAergic interneurons with respect to their connectivity and neurochemistry. A more recent study investigated mAChR function in a morphologically identifiable class of stratum oriens interneurons, the stratum oriens-lacunosum moleculare (O-LM) interneurons; they exhibit a muscarinic-induced afterdepolarization that is associated with the inhibition of several potassium conductances and the activation of I_{CAT} (Lawrence et al., 2006). In these interneurons, muscarine abolished the afterhyperpolarization (AHP) current and induced a switch in firing frequency from accommodating to accelerating during the depolarizing current injection. The AHP was replaced by a prominent afterdepolarization in the presence of muscarine. In another set of cells that exhibited strong spike frequency accommodation and broad rebound spikes, mAChR activation was accompanied by a reduction in input resistance and shunting of firing. Finally, muscarinic receptor activation increases the frequency and amplitude of spontaneous IPSCs but depresses monosynaptically evoked IPSCs and the frequency of miniature IPSCs (Behrends and ten Bruggencate, 1993).

NMDAR modulation by mAChRs

As previously stated, one of the most prominent effects of mAChR activation in the hippocampus and other forebrain regions is potentiation of currents through the NMDA subtype of ionotropic glutamate receptor (Markram and Segal, 1990b; Harvey et al., 1993; Calabresi et al., 1998; Marino et al., 1998; Lu et al., 1999; Marino and Conn, 2002). The M₁ receptor likely enhances currents through NMDARs through a PKC-dependent activation of the non-receptor tyrosine kinase (Src) signaling cascade (Calabresi et al., 1998; Lu et al., 1999). The NMDA receptor plays a critical role in regulating hippocampal and cortical function and is thought to be important for the cognition-enhancing and attention-promoting effects of mAChR activation. In addition, the NMDA receptor may play an important role in regulation of circuits that are disrupted in schizophrenia and other psychotic disorders (Coyle et al., 2002; Marino and Conn, 2002; Tsai and Coyle, 2002). Competitive and non-competitive antagonists of the NMDA receptor can induce a psychotic state that closely resembles that seen in schizophrenic patients. Furthermore, co-agonists at the NMDA receptor, such as glycine and D-cycloserine produce improvements in the symptoms of schizophrenic patients. Thus, a large number of clinical and animal studies have led to the hypothesis that potentiation of NMDA receptor currents in these regions could have an antipsychotic action. Based on this, it is possible that mAChR-induced potentiation of NMDA receptor function plays important roles in the therapeutic efficacy of mAChR activation in psychotic disorders.

Presynaptic M₂ and M₄ receptors may regulate excitatory and inhibitory synaptic transmission

Many studies have indicated that mAChR-induced reduction of transmission at excitatory synapses in the hippocampus is mediated presynaptically. Based on early immunocytochemical studies, the most likely mAChRs involved in the presynaptic actions of mAChR agonists are M₂ and M₄ since both of these receptors are predominantly localized presynaptically in each major subsector of the hippocampus. Consistent with this, a large body of research suggests that presynaptic receptors involved in regulating neurotransmitter release are often coupled to inhibition of adenylyl cyclase, and M₂ and M₄ both couple to this effector system. While both M₂ and M₄ are localized presynaptically, M₂ immunoreactivity is not present in granule cells and pyramidal cells, but is highly localized in inhibitory interneurons (Levey et al., 1995b). Since dentate granule cells and CA3 pyramidal cells provide the majority of excitatory input to areas CA3 and CA1 respectively, this makes M₄ a more likely candidate for the mAChR involved in regulating glutamate release. In contrast, if M₂ is localized on presynaptic terminals of inhibitory interneurons, M₂ would be in an ideal position for regulating GABA release and thereby reducing GABA-mediated synaptic inhibition.

One mechanism of presynaptic inhibition of neurotransmitter release involves the modulation of presynaptic calcium channels that are involved in vesicle fusion and release. Early indirect (Valentino and Dingledine, 1981) and more recent studies have shown that muscarinic inhibition of synaptic transmission in the hippocampus is presynaptic and relies at least in part on muscarinic blockade of N-type and P/Q-type voltage dependent calcium channels at the SC-CA1 synapse (Qian and Saggau, 1997) and in the associational-commissural fiber system of CA3 (Vogt and Regehr, 2001).

Activation of mAChRs with carbachol (CCh), a muscarinic agonist, increases the paired-pulse facilitation index of evoked EPSCs at CA1 synapses and also decreased the coefficient of variation ratio, indicating that CCh inhibits synaptic transmission via activation of presynaptic mAChRs which causes a reduction in the reliability of glutamate release (Fernandez de Sevilla et al., 2002). Electrical stimulation of cholinergic terminals in stratum oriens/alveus also causes a decrease in evoked CA1 EPSCs by presynaptically inhibiting glutamate release via activation of mAChRs as indicated by parallel changes in PPF index and EPSC variance (Fernandez de Sevilla and Buno, 2003). Although ACh has been shown to suppress excitatory transmission at mossy fiber synapses in CA3 through modulation of GABA_B receptor activity (K. E. Vogt and W. G. Regehr, 2001), presynaptic inhibition at CA1 seems to be independent of GABAergic transmission (Kremin et al., 2006). Although experiments to confirm a presynaptic mechanism of action were not carried out, we have found that selective potentiation of M₄ receptors with the PAM VU10010 enhances muscarinic depression of evoked excitatory but not inhibitory postsynaptic currents in CA1 neurons (**Chapter IIIa**).

Role of muscarinic cholinergic signaling in hippocampal LTP

Of particular relevance to issues of synaptic plasticity, mAChR activation enhances agonist-evoked currents through the NMDA subtype of glutamate receptor (Markram and Segal, 1990b; Harvey et al., 1993; Marino et al., 1998). The NMDA receptor is known to play a critical role in several forms of hippocampal long-lasting synaptic plasticity which are thought to underlie learning and memory. Consistent with

this, mAChR activation can also induce or enhance long term potentiation (LTP) of excitatory synaptic responses in the hippocampus (Blitzer et al., 1990; Burgard and Sarvey, 1990; Markram and Segal, 1990b; Abe et al., 1994; Auerbach and Segal, 1996; Shinoe et al., 2005). Because long-term alterations in efficacy of glutamate transmission contribute to memory mechanisms (Bliss and Collingridge, 1993; Malenka and Bear, 2004), induction of long-term synaptic changes by cholinergic receptors may underlies the cholinergic dependence of normal memory processing. Furthermore, because of the postulated role of NMDA receptors and LTP in learning and memory, it has been suggested that the mAChR subtype that mediates these responses may be an excellent target for therapeutic agents useful in the treatment of AD.

Early studies using sharp microelectrodes revealed that ionophoretic application of ACh caused an initial reduction in EPSP amplitude followed by a gradual and long-lasting facilitation of EPSP amplitude in CA1 pyramidal cells that was not associated with a change in input resistance (Markram and Segal, 1990b). Atropine blocked both the suppressing and facilitating effects of ACh. These studies also indicated that ACh enhanced the slow NMDA-mediated component of the EPSP and that responses to NMDA application in current clamp mode were also potently facilitated by both ACh and oxotremorine-M, a muscarinic agonist. Muscarinic facilitation of both EPSP amplitude and NMDA responses were independent of changes in voltage or K^+ conductances as the facilitation was not affected by clamping cells at resting membrane potentials or by the inclusion of cesium in recording electrodes.

Burgard and Sarvey (1990) showed a concentration-dependent ability of muscarine in the dentate gyrus to facilitate LTP induction by subthreshold titanic

stimulation (Burgard and Sarvey, 1990); Blitzer et al. (1990) demonstrated a significant depression of the CA1 field EPSP with high doses of CCh which, when controlled for, enhanced tetanus-induced LTP (Blitzer et al., 1990). Subsequent reports indicated that bath application of 750 nM carbachol also induced a long-lasting (>45 min post drug washout) facilitation of intracellularly recorded EPSPs; muscarinic potentiation of field EPSPs was also seen and was dependent on CCh concentration and time of drug application (Auerbach and Segal, 1994). Only with 20-minute CCh application was sustained LTP produced. This phenomenon was termed LTP_m and was completely blocked by atropine; when antagonist was added to the bath after the establishment of LTP, no effect was seen indicating that induction but not maintenance of LTP_m was mediated by mAChRs. These studies also indicated that LTP_m requires involvement of intracellular calcium stores and protein kinases but is activity independent. Interestingly, CCh still induced LTP_m in the presence of the 10 μ M NMDAR antagonist (2*R*)-amino-5-phosphonopentanoate (APV), a concentration that did block tetanus-induced LTP, suggesting that the two mechanisms were somewhat divergent. It was also demonstrated that 0.1 μ M CCh (a concentration that did not induce LTP alone) facilitated LTP caused by a subthreshold tetanic stimulus and that LTP_m and tetanus-induced LTP were mutually occlusive phenomena. Therefore, the mechanisms of LTP_m and tetanus-induced LTP seemed to converge at a point downstream of NMDA receptor activation (Auerbach and Segal, 1994). LTP_m was later shown to not be accompanied by a change in the size of the afferent fiber volley or by a change in paired-pulse potentiation, consistent with a postsynaptic locus of CCh action (Auerbach and Segal, 1996). Intracellular recordings from CA1 pyramidal cells in voltage clamp mode revealed that 0.5 μ M CCh transiently

potentiated NMDA responses but that responses to AMPA increased gradually and remained potentiated after drug washout.

The M_1 receptor is a likely candidate for the mAChR subtype involved in the facilitation of LTP induction. For instance, evidence suggests that mAChR-induced facilitation of LTP is mediated by a postsynaptic mechanism, and depends on the release of calcium from intracellular stores (Auerbach and Segal, 1994). The M_1 receptor is the most abundant postsynaptically localized mAChR subtype in CA1 pyramidal cells. Furthermore, M_1 is coupled to phosphoinositide hydrolysis and activation of this receptor leads to release of intracellular calcium. Thus, it seemed plausible that the mAChR-induced facilitation of LTP induction is mediated by the M_1 receptor. Recent studies have indicated that M_1 is indeed the subtype most likely mediating cholinergic modulation of synaptic plasticity in the mouse hippocampus. Experiments focusing on enhancement of electrically induced LTP by low concentrations of CCh or by repetitive stimulation in the stratum oriens, which presumably trigger release of endogenous ACh from cholinergic terminals, revealed that the enhancing effect was abolished in M_1 knockout but not in M_3 knockout mice (Shinoe et al., 2005). While concentrations of 500 nM to 5 μ M CCh induced a transient depression of field excitatory postsynaptic potentials (fEPSPs) at the SC-CA1 synapse, 50 nM had no effect alone on fEPSPs. This is in contrast to what had been reported in rat where low doses of CCh induced LTP. This could be a result of differences in mAChR expression and receptor density between species; as shown in Chapters IIIa and IV, we have also seen a difference in potency of CCh on various electrophysiological responses between rat and mouse. Regardless, Shinoe et al. reported that 50 nM CCh significantly increased LTP elicited by high

frequency stimulation (HFS, 100 Hz for 1 sec) of SC afferent fibers. Stimulation of stratum oriens thirty seconds prior to the HFS to cause endogenous ACh release also potentiated the degree of LTP. While HFS-LTP remained intact in both M₁ and M₃ knockout animals, CCh-induced enhancement of LTP was absent in only the M₁ knockout supporting a role for M₁ in mediating this effect. The same was shown to be true after stratum oriens stimulation (Shinoe et al., 2005).

One recent set of studies by Fernández de Sevilla et al. (2008) revealed that a brief puff of ACh applied at the apical dendritic shaft of a CA1 pyramidal cell induces a postsynaptic calcium elevation and LTP of excitatory postsynaptic currents (EPSCs) evoked by stimulation of SC-CA1 afferents. Because changes in postsynaptic responses can be mediated by a change in α -amino-3-hydroxyl-5-methyl-4-isoxazole-propionate receptor (AMPA) density at the postsynaptic membrane, the content of recombinant tagged GluR1 and GluR2, subunits of AMPARs, was analyzed before and after ACh treatment using two-photon microscopy. Indeed, ACh induced an increase in GluR1 and GluR2 containing AMPARs at the spine surface without a change in spine volume. Results also suggested that LTP induced by ACh was mediated through a postsynaptic mechanism as shown by a lack of effect of ACh on the paired-pulse ratio or the fiber volley of fEPSPs evoked by Schafer Collateral (SC) stimulation, and LTP in this case was NMDA independent. Because levels of ACh released from the medial septum rise during tasks that require attention, it could be postulated that this form of plasticity could be induced *in vivo*. Tetanic stimulation of the medial septum using chronically implanted stimulating electrodes did in fact induce a long-lasting synaptic enhancement of fEPSPs at CA1 synapses *in vivo* (Fernandez de Sevilla et al., 2008). A key difference between

the ACh-induced LTP reported by Fernández de Sevilla et al. and the synaptic enhancement induced by CCh in earlier studies (Auerbach and Segal, 1994, 1996) is a dependence on NMDAR activity.

Muscarinic modulation and induction of LTD in the hippocampus

Interestingly, M_1 activation also seems to induce a novel form of long-term depression (LTD) often termed mLTD (Scheiderer et al., 2006). At hippocampal CA3-CA1 synapses, bath application of a high concentration of CCh (50 μ M) elicits a robust transient depression of the dendritic fEPSP which is followed by LTD after agonist washout. This mLTD was prevented by atropine, by the M_1 toxin MTx-7 (Potter, 2001), and by pirenzepine but not by the nAChR antagonist methyllycaconitine. The expression of mLTD was independent of GABA_A receptor activity and appeared to be via a postsynaptic mechanism. It was also postulated that the acute presynaptic depression and mLTD involve separate mechanisms and that the presynaptic depression is not required for mLTD induction. Lastly, similar to LTP_m described by Auerbach and Segal (1994), mLTD was blocked in the presence of the NMDAR antagonist D,L-APV (Auerbach and Segal, 1994). In contrast to LTP_m however, mLTD is activity dependent; mLTD requires presynaptic activity because cessation of stimulation of presynaptic afferents during CCh application prevented induction of plasticity when CA3 cell bodies were removed from the slice. Thus mLTD is both activity- and NMDAR-dependent. Interestingly, this Hebbian form of LTD is lost after medial septal lesioning but is rescued by sympathetic sprouting of noradrenergic fibers from the superior cervical ganglia into hippocampus. This sprouting of sympathetic fibers appears to stimulate cholinergic reinnervation as

indicated by new VAChT-positive fibers in the hippocampus, and the appearance of these new fibers correlates with the rescue of mLTD.

In a subsequent publication, McCutchen et al. (2006) found that mLTD did not affect subsequent electrical induction of LTP; mLTD was also able to depotentiate LTP. That is, application of CCh could cause a population of CA1 pyramidal cells exhibiting LTP after high frequency stimulation to undergo an acute depression and then return to the baseline fEPSP slope level (McCutchen et al., 2006).

Electrical induction of LTD using low frequency stimulation (LFS-LTD) is both activity- and NMDA receptor dependent; since both LFS-LTD and mLTD share those characteristics, occlusion studies were performed to confirm a shared mechanism between the two types of LTD. Not surprisingly, prior saturation of LFS-LTD occluded induction of mLTD by CCh application. Unexpectedly, however, when the converse experiment was performed, saturating levels of mLTD did *not* occlude further depression induced by subsequent LFS. In other words, even after multiple CCh applications to insure saturated mLTD, application of LFS induced roughly 25% more depression of the fEPSP. Further studies revealed that CCh treatment prior to LFS caused LFS-LTD to become independent of NMDARs at hippocampal CA1 synapses but not in layer IV-layer II/III synapses in visual cortex where LFS-LTD is also normally NMDA-dependent. The fact that the switch in LFS-LTD does not occur in visual cortex suggests that this may be a cholinergic mechanisms specific to hippocampal synapses and that there is perhaps more flexibility in the induction mechanisms available to mediate hippocampal LTD (McCoy and McMahon, 2007). Finally, induction of mLTD seems to require ERK activation; application of U0126, a MEK inhibitor, before and during CCh treatment

completely blocks mLTD. Induction of this form of synaptic plasticity also required activity of Src kinase but not PLC (Scheiderer et al., 2008).

Muscarinic modulation of hippocampal physiology: conclusions

It is likely that these cellular actions of mAChR activation are directly related to the behavioral effects of activation of hippocampal mAChRs. For instance, the combined reduction of excitatory synaptic transmission with an increase in excitability of pyramidal cells could increase the signal to noise ratio of signaling through the hippocampus. Such modulation of signal to noise ratio occurs with some other neurotransmitters and has been proposed to play an important role in regulation of attentiveness to sensory stimuli (Madison and Nicoll, 1986). In addition, selective potentiation of NMDA receptor responses could critically modulate synaptic plasticity that is involved in learning and memory. Consistent with this, mAChR activation modulates LTP and LTD of excitatory synaptic responses in the hippocampus. A complete understanding of the roles of mAChRs in both normal and pathological hippocampal function will require a detailed understanding of the cellular mechanisms involved in these responses as well as the specific mAChR subtypes that mediate each of these responses. While preliminary studies using mice lacking each of the individual mAChR subtypes have provided important clues about the function of these subtypes in mediating many of the electrophysiological effects described above, we now have selective activators of M₁ and M₄ that will be described further in subsequent chapters. It will be important to confirm initial findings in knockout mice as well as to further delineate the roles of these two receptor subtypes in modulating hippocampal physiology. Studies using the M₄ positive

allosteric modulator VU10010 (see **Chapter IIIa**) revealed that this mAChR subtype is involved in modulation of excitatory but not inhibitory transmission at the SC-CA1 synapse in rats and mice.

Prefrontal cortical physiology and function

An important projection from the hippocampus is to the prefrontal cortex (PFC), a cortical region that integrates information from multiple other brain regions; PFC function is the target of many neuromodulators including acetylcholine. The PFC receives glutamatergic inputs from the thalamus and primary sensory cortices, from the brainstem, and from the hippocampus (Groenewegen and Uylings, 2000; Dalley et al., 2004; Vertes, 2006), and this merging of information in the PFC is implicated in higher executive functioning. Cholinergic input to the PFC regulates attention (Muir et al., 1992; Hasselmo, 1995), memory (DeSousa et al., 1994), and anxiety induction processes (Berntson et al., 1998). Dysfunction of mAChRs and muscarinic-mediated signaling pathways has been linked to Fragile X mental retardation (Volk et al., 2007), AD (Fisher, 2008b), and aging (Joseph et al., 1993). Lesions of the medial PFC (mPFC) result in cognitive deficits that resemble symptoms of schizophrenia and Alzheimer's disease (Kolb, 1984, 1990; Heckers et al., 1998).

Among a number of glutamatergic afferents projecting to the PFC, the afferents originating in the hippocampus are especially crucial in supporting memory and cognitive function. Previous work has shown that the CA1 and subiculum of ventral hippocampus send ipsilateral, unidirectional projections that terminate on neurons in the mPFC (Jay and Witter, 1991; Jay et al., 1992). This hippocampal-mPFC pathway has been described

as projecting anteriorly through the fornix, and it ultimately ascends dorsally to terminate on neurons within the nucleus accumbens and a region of the mPFC that includes the infralimbic and prelimbic cortices. The functional integrity of the hippocampal-mPFC network and the flow of information between these two brain regions are critical to the proper functioning of the mPFC in memory formation (O'Donnell and Grace, 1995; O'Donnell et al., 2002; Goto and O'Donnell, 2003).

Role of mAChRs in the mPFC

Cholinergic afferents to the prelimbic and infralimbic cortices, the major components of the medial prefrontal cortex (mPFC), originate primarily in the basal forebrain nucleus basalis magnocellularis, the diagonal band of Broca, and the mesopontine laterodorsal nucleus (Lehmann et al., 1980; Satoh and Fibiger, 1986; Gaykema et al., 1990). Cholinergic input to the cortex plays a vital role in supporting processes requiring arousal, attention, memory, and learning (Phillis, 2005); in addition to being released from inputs from the basal forebrain nuclei, ACh is also released from local circuit neurons in the mPFC, and ACh release increases during performance of attentional tasks (Passetti et al., 2000). In contrast, lesions of cholinergic nuclei that project to the mPFC impair cue detection and attentional performance whereas augmentation of cholinergic transmission enhances behavioral arousal and locomotor activity (Day et al., 1991; McGaughy et al., 2002; Parikh et al., 2007). Of the five mAChR subtypes, M₁ and M₂ are the predominant subtypes expressed in the mPFC with M₁ mainly localizing postsynaptically at asymmetrical (glutamatergic) synapses and M₂ localizing both pre- and postsynaptically (Volpicelli and Levey, 2004). Activation of

mAChRs results in an array of effects on the excitability and firing properties of cortical neurons, and these effects involve different cellular mechanisms. In addition, mAChRs play a role in modulating long-term strengthening and weakening of synaptic transmission in this brain region which appears to be input-specific. Modulation of electrophysiological behavior and plasticity of cortical circuits, particularly in the PFC, by ACh is thought to play a critical role in attention and memory (Gill et al., 2000; Passetti et al., 2000; Anagnostaras et al., 2003; Sarter et al., 2005).

Postsynaptic effects of mAChRs in cortical neurons

Similar to the effects seen in hippocampal pyramidal cells, ACh causes a marked depolarization and increase in membrane excitability and repetitive spiking in cortical pyramidal cells (Benardo and Prince, 1982; Andrade, 1991; Krnjevic, 2004; Carr and Surmeier, 2007). Many ionic currents have been implicated in mediating this depolarization; one of these is a voltage-dependent nonselective cation current (Haj-Dahmane and Andrade, 1996; Klink and Alonso, 1997; Fisahn et al., 2002). Studies in hippocampal and sensorimotor cortices have indicated this increase in excitability can be attributed to the inhibition of three main potassium currents: the calcium-activated potassium current underlying the afterhyperpolarization (I_{AHP}), a voltage-dependent leak potassium current (I_{leak}), and the voltage-dependent M-current (I_M). The involvement of a potassium current-mediated mechanism was supported by the increase in input resistance and a dependence on membrane potential; barium and tetraethylammonium (TEA), potassium channel blockers, also reduced CCh-induced inward currents (Haj-Dahmane and Andrade, 1996). However, the CCh-induced current did not reverse at the

reveral potential of potassium (E_K) but persisted as an inward current at membrane potentials 10-20 mV negative to the predicted E_K for potassium. Intracellular cesium, which blocks a wide range of potassium channels, also did not inhibit the CCh-induced inward current. These results indicated that another ion conductance was likely involved in this muscarinic effect. Subsequent studies implicated the involvement of a non-selective cation current in muscarinic depolarization of mPFC layer V neurons (Haj-Dahmane and Andrade, 1996). Similar findings in entorhinal cortex did not support a role for potassium conductances in this effect but rather a calcium-dependent cationic conductance largely permeable to sodium (Klink and Alonso, 1997). Conflicting data support the involvement of an inwardly rectifying potassium current through a channel containing Kir2 subunits; these channels are open at the resting membrane potential and help set the resting membrane potential in PFC pyramidal neurons and also play a role in integration of excitatory synaptic inputs (Day et al., 2005). Carr and Surmeier (2007) found the CCh-induced inward current to be sensitive to barium and cesium that block Kir2 channels, and showed that mAChR activation reduces Kir2 channel currents by depleting membrane phosphatidylinositol 4,5-bisphosphate (PIP₂) as this modulation was blocked by PLC but not PKC inhibitors (Carr and Surmeier, 2007).

The calcium-dependent non-selective cation current mentioned above has also been shown to contribute to the fast afterdepolarization (fADP) that follows an action potential triggered by depolarizing current injection (Haj-Dahmane and Andrade, 1997). This fADP is prominently displayed by pyramidal neurons of layer V in rat PFC. Interestingly, these cells also exhibit a muscarinic-induced slow afterdepolarization (sADP) (Haj-Dahmane and Andrade, 1998). Buffering of intracellular calcium prevented

the mAChR-induced sADP, and ion substitution experiments implicated the flow of sodium ions into the cell but not the flux of potassium or chloride. The muscarinic sADP therefore is likely mediated by a calcium- and voltage-sensitive nonselective cation current and could represent a mechanism by which mAChRs modulate neuronal excitability in the PFC. Due to the calcium-dependence of the sADP, the involvement of calcium channel modulation by mAChRs has been investigated. A recent study has implicated TRPC (transient receptor potential) ion channels in the muscarinic sADP (Yan et al., 2009); these channels allow calcium flux into cells in response to a variety of stimuli usually linked to phosphatidylinositol signal transduction pathways. Data indicates that the current underlying the sADP induced by mAChR activation is carried through TRPC channels containing TRPC5 or TRPC6 subunits and occurs through a mechanism involving $G\alpha_q$ and PLC β 1 signaling.

Pyramidal cells normally respond to a sustained current injection with a high initial firing rate followed by a slowing of this rate. The voltage-sensitive potassium current (I_M) and voltage-dependent calcium influx which activates a calcium-sensitive potassium current (I_{AHP}) are both thought to underlie this accommodation or adaptation in cell firing rate by pyramidal cells in response to sustained depolarization. Activation of mAChRs decreases both of these potassium currents which, in turn, allows neurons to fire in a more sustained manner in response to sustained afferent input. Cholinergic agonists also cause a strong increase in the firing rate of cortical neurons, and this increase in firing rate was demonstrated to result from a slow depolarization of cortical pyramidal cells due at least in part to blockade of potassium currents (Krnjevic et al., 1971; Hasselmo and McGaughy, 2004). The muscarinic inhibition of the calcium-

dependent potassium currents underlying afterhyperpolarization also supports a role of mAChRs in modulating voltage-dependent calcium channels. Indeed, mAChR modulation of L-, N-, P/Q- and R-type calcium channels pre- and postsynaptically in both hippocampal and cortical neurons occurs through G-protein dependent mechanisms (Perez-Burgos et al., 2008).

In accordance with the excitatory effects of selective M₁ receptor activation in rat and mouse layer V mPFC pyramidal cells described in this thesis, a recent study using M₁ knockout mice shows that activation of this receptor subtype mediates cholinergic modulation of excitability in these neurons (Gulledge et al., 2009). Interestingly, short focal application of ACh near the soma of the recorded neuron produced a hyperpolarization and pronounced inhibition of spiking followed by spike acceleration when ACh was delivered during periods of action potential generation by depolarizing current injection in layer V but not as robustly in layer II/III neurons. This effect was abolished in slices from M₁ knockout but not M₃ or M₅ knockout mice. Tonic cholinergic excitation using bath-applied CCh depolarized layer V neurons and also suppressed the afterhyperpolarization in addition to generating a slow afterdepolarization, effects that were also absent in M₁ knockout slices (Gulledge et al., 2009).

Cholinergic modulation of cortical neurotransmission

Despite a consistent reporting of increases in cortical neuronal excitability in response to cholinergic agonists, many discrepancies exist in studies examining the effects of cholinomimetic drugs on glutamatergic transmission; data suggests that the effect of ACh on synaptic transmission is region- and input specific (Hasselmo and

Bower, 1992; Gil et al., 1997; Gullledge et al., 2007; Eggermann and Feldmeyer, 2009; Gullledge et al., 2009). In addition, varying concentrations of ACh induce either depression or facilitation of glutamatergic transmission; this principle holds true when examining the effects of CCh on long-term changes in synaptic transmission as discussed below. By employing stimulation of either layer Ia or Ib in rat piriform cortex slices, Hasselmo and Bower found that CCh, muscarine, and ACh strongly reduced responses stimulated from intrinsic fibers in layer Ib but not from afferent fibers from layer Ia; this suggested that mAChR activation decreases excitatory transmission within intracortical circuits but not from afferent inputs (Hasselmo and Bower, 1992). In slices containing somatosensory cortex and ventrobasal thalamus, muscarine depressed EPSPs at both thalamocortical (TC) and intracortical (IC) synapses onto layer III pyramidal cells whereas nicotine selectively enhanced responses from TC synapses and had no effect on IC synapses. Muscarine increased the paired-pulse ratio at both TC and IC synapses, suggesting a presynaptic mechanism of action (Gil et al., 1997). In addition, GABA released by an intracortical stimulus selectively suppresses transmitter release from IC synapses but not TC synapses by activating presynaptic GABA_B receptors. Taken together, these results indicate that cholinergic receptors selectively modulate of intrinsic versus afferent synapses.

Acetylcholine also modulates activity and GABA release from cortical GABAergic interneurons differentially depending on cell subtype (Kawaguchi, 1997). Despite the relatively low abundance of inhibitory neocortical interneurons, these cells have profuse axonal arborizations such that a single GABAergic interneuron can control hundreds of excitatory pyramidal cells (Kruglikov and Rudy, 2008). Recordings from

these interneurons revealed that ACh induces inhibitory postsynaptic potentials in neocortical cells indirectly through cortical GABAergic cells; CCh also induces an increase in spontaneous IPSC in frontal cortical pyramidal cells, an effect that was dependent on action potential firing as it was suppressed by the fast sodium channel blocker tetrodotoxin (TTX). While fast-spiking and late-spiking GABAergic cells were not depolarized by CCh, this muscarinic agonist did appear to depolarize somatostatin-immunoreactive and vasoactive intestinal peptide (VIP)-positive GABAergic cells (Kawaguchi, 1997) indicating that muscarinic modulation of inhibitory interneurons is cell-type specific. Paradoxically, muscarine and oxotremorine decrease the amplitude of electrically evoked inhibitory postsynaptic currents in layer II/II neurons in rat auditory cortex (Salgado et al., 2007) and in the mouse layer V somatosensory cortex (Kruglikov and Rudy, 2008) via a presynaptic mechanism. Furthermore, mAChR activation potentiates GABA_A currents in acutely dissociated PFC neurons, an effect that required pretreatment with insulin. This effect was blocked by inhibitors of PKC, broad-spectrum protein tyrosine kinase, and Src inhibitors (Ma et al., 2003). This array of muscarinic effects on GABAergic release and transmission likely results from the cortical expression of multiple mAChR subtypes both pre- and postsynaptically where they have both excitatory and inhibitory effects on different populations of inhibitory neurons.

Of particular relevance to muscarinic modulation of prefrontal cortical signaling in AD, a relationship between beta amyloid (A β), ACh, and GABAergic signaling has been established. Exposure of cortical slices to fibril A β peptides activated PKC and CamKII in addition to inducing action potential firing and enhancing spontaneous EPSCs in mPFC layer V neurons; these effects were blocked by oxotremorine. In addition,

mAChR activation caused a PKC-dependent increase in spontaneous IPSC amplitude and frequency (Gu et al., 2003). Interestingly, this muscarinic modulation of sIPSCs was impaired in an APP mutant mouse model of AD (Zhong et al., 2003). These authors also showed that persistent spiking of layer V neurons induced by CCh was independent of PKC activation and was intact in APP transgenic mice, suggesting that muscarinic modulation of inhibitory transmission is selectively impaired in these animals.

mAChRs modulation of long-term changes in cortical synaptic strength

Cholinergic receptors have been shown to play a role in cortical synaptic plasticity in a number of cortical regions. Similar to the cholinergic activity-dependent long-term depression of EPSPs observed in hippocampus (Scheiderer et al., 2006), carbachol induces LTD of synaptic responses when paired-pulse stimulation is delivered to layer IV and field EPSPs were recorded from layer III of rat visual cortex (Kirkwood et al., 1999). A key difference is that in hippocampus, agonist treatment alone without any low-frequency stimulation induced LTD; a paired pulse stimulation protocol was required to reveal muscarinic LTD in visual cortex. Therefore CCh, in conjunction with paired-pulse stimulation, induces an activity-dependent and homosynaptic form of LTD. CCh also facilitated LTD induction using a low-frequency stimulation protocol in visual cortex. Muscarinic-induced LTD required NMDAR activity as it was blocked in the presence of AP5.

Subsequent studies have shown that mLTD in visual cortex has a postsynaptic locus of expression as indicated by the fact that there was no change in the paired pulse ratio during expression of the long-lasting depression induced by CCh (McCoy and

McMahon, 2007). A change in PPR is usually indicative of a presynaptic locus of expression, whereas no change indicates a postsynaptic locus. In contrast to results reported by Kirkwood et al. (1999), these authors found no effect of the NMDA antagonist APV in mLTD induction or maintenance. They did however show that the L-type Ca^{2+} blocker nifedipine inhibited mLTD whereas picrotoxin had no effect which indicates that mLTD induction is not due to an increase in inhibitory transmission but requires activity of L-type Ca^{2+} channels. McCoy and McMahon also found that mLTD in visual cortex was independent of PKC but was partially dependent on PLC activation. A prominent signaling cascade downstream of M_1 receptor activation is the Src tyrosine kinase which leads to the phosphorylation and activation of MEK which subsequently phosphorylates and activates ERK1/2 (Chan et al., 2005). The Src inhibitor PP2 completely blocked mLTD as did the ERK1/2 inhibitor U0126, indicating that activation of the MEK/ERK1/2 cascade is required for this form of plasticity to occur. In the hippocampus, Src activation has also been implicated in muscarinic modulation of NMDA currents (Lu et al., 1999); since mLTD in visual cortex may or may not require NMDAR activity, it is unclear whether there is a link between these two phenomena. Lastly, the maintenance of mLTD in visual cortex which can last on the order of 2.5 hours can be blocked by protein synthesis inhibitors (McCoy and McMahon, 2007). Translation of new proteins is not required for the induction of mLTD but for maintenance of the depression long-term. Inhibiting transcription of mRNAs had no effect on either the induction, expression, or the long-term maintenance of mLTD.

Reduction of cortical cholinergic innervations produces a shift from LTP to LTD that can be prevented by exogenous application of ACh (Kuczewski et al., 2005); this

suggests a regulatory action of ACh on the direction of synaptic plasticity (LTP vs. LTD). In a recent study by Origlia et al. (2006), an approach using mAChR knockout mice indicated that M₂/M₄ receptors were necessary for TBS-induced LTP whereas M₁/M₃ receptors were necessary for LFS-LTP in visual cortex. Interestingly, this group showed that in the absence of any muscarinic agonist, atropine was able to fully block TBS-induced LTP and LFS-LTD in layer II/III of visual cortex after stimulation of layer IV. This data indicates that mAChR activity, unlike in hippocampus, is required for induction of LTP and LTD using standard electrical stimulus protocols. Furthermore, theta-burst stimulation failed to induce LTP in M₂/M₄ double knock-outs, and LFS failed to induce LTD in but instead induced LTP in M₁/M₃ double knock-outs. In single knockout studies, M₂ and M₄ knockouts exhibited normal LTP after TBS whereas the M₃ knockout showed no LTD after LFS and the M₁ knockout actually exhibited LTP after a low frequency stimulation protocol that induces LTD in wild-type animals. Application of the PLC inhibitor U73122 had a similar effect on the response to LFS as when M₁ receptors were absent; in other words, blocking PLC caused LTP to be induced by the LFS protocol. Similarly, treatment of slices with pertussis toxin blocked the ability of TBS to induce LTP supporting the idea that activation of M₂/M₄ receptors and the downstream activation of Gi/o proteins underlie LTP induction. These studies indicate that the direction of synaptic plasticity in visual cortex depends on the combined activity of different mAChR subtypes (Origlia et al., 2006). It could be postulated that if there was a loss or decrease in particular mAChR subtype expression or function, this would tip the balance of muscarinic modulation of LTP and LTD and induce a bias in one direction or another.

More directly relevant to the studies described in this thesis is the finding that mAChR activation also induces very robust LTD in layer V pyramidal cells of the mPFC (Huang and Hsu, 2009). Whole cell patch clamp studies in voltage clamp mode revealed that CCh induces a dose-dependent acute depression of EPSCs evoked by stimulation of layer V apical dendrites, and that the acute depression is followed by a long-lasting depression of excitatory transmission. Very high concentrations of CCh were used (10, 50, and 100 μ M), but the short- and long-term effects of 50 μ M CCh were completely blocked by 1 μ M atropine and 100 nM pirenzepine, indicating that the depression is indeed mediated by mAChRs. CCh also transiently depressed monosynaptic IPSCs in the presence of 6-cyano-7-nitroquinoxaline-2,3-dione (CNQX) and APV, but IPSCs returned to baseline levels upon agonist washout indicating that mLTD is selective for excitatory synaptic transmission. This depression of excitatory synaptic transmission still occurred in the presence of NMDA antagonist D-APV indicating that mLTD is NMDAR independent, a finding similar to what was observed in the visual cortex by McCoy and McMahon (2007). In contrast to mLTD at CA1 and visual cortical synapses, however, this form of plasticity in layer V mPFC is activity independent; if electrical stimulation ceased during CCh addition, mLTD was still induced when stimulation resumed. Activation of ionotropic and metabotropic glutamate receptors was also not required for induction of mLTD. GDP β S which disrupts G protein-coupled signaling blocked the long-term but not the acute depression induced by CCh, suggesting that the acute depression is likely presynaptic whereas the LTD requires postsynaptic G protein activation. mLTD also required activation of PLC, PKC, and IP₃ receptors. Intriguingly, as opposed to mLTD in visual cortex (McCoy and McMahon, 2007) and hippocampus

(Scheiderer et al., 2008), long-term depression induced by CCh in layer V mPFC pyramidal cells was not blocked by Src kinase and MEK inhibitors PP2 and U0126, respectively (Huang and Hsu, 2009). Another discrepancy was seen with the use of the L-type Ca^{2+} blocker nimodipine which inhibited mLTD in visual cortex but not in mPFC. mLTD in the mPFC appeared to have a presynaptic locus of expression that did not require postsynaptic clathrin-mediated endocytosis of AMPARs. Data indicated that activation of postsynaptic mAChR signaling suppresses glutamatergic synaptic transmission through a presynaptic effect on neurotransmitter release; it was therefore hypothesized that a retrograde messenger was involved in the expression of mLTD. The nitric oxide synthase (NOS) inhibitor L-NAME blocked mLTD induction; inhibitor studies also showed that mLTD was dependent on activation of presynaptic sGC/PKG signaling pathway initiated by postsynaptic nitric oxide (NO) production. Finally, to ascertain whether endogenous ACh release, as opposed to exogenously applied CCh, can modulate LTD, a paired-pulse LFS (PP-LFS) protocol was used to induce a stable form of LTD measured using field EPSPs. The magnitude of PP-LFS-LTD was significantly reduced by atropine and pirenzepine and enhanced by the cholinesterase inhibitor eserine. These results indicate that endogenous ACh does in fact play a critical role in LTD in these neurons. Occlusion experiments also showed that PP-LFS-LTD and mLTD share a common mechanism (Huang and Hsu, 2009).

Also of particular interest in relation to our findings in mPFC layer V neurons is the finding that mAChRs modulate excitatory afferents from the hippocampus which project to the mPFC (Wang and Yuan, 2009). Parent et al. (2009) identified a bundle of afferent fibers that project to the mPFC from the ventral hippocampus in acute slice

preparations; *in vivo* track tracing and optic studies revealed that the afferent bundle did not include contributions from the mediodorsal nucleus of the thalamus, amygdala, or lateral hypothalamus/medial forebrain bundle (Parent et al., 2009). Although there have been numerous studies examining the result of hippocampal monosynaptic projections to the mPFC *in vivo* (Laroche et al., 1990; Degenetais et al., 2003; Romcy-Pereira and Pavlides, 2004), the majority of electrophysiological studies examining neurotransmission *in vitro* in acute slices of the mPFC have employed placement of a stimulating electrode in different layers of the mPFC. This is possible due to the fact that pyramidal neurons in this brain region have elaborate dendrites that extend into both deep and superficial layers of the cortex. The mPFC, like other cortical regions, not only contains local circuits but receives innervations of afferents that are not spatially resolved. Therefore synaptic responses resulting from general laminar stimulation are a product of stimulating mixed populations of axonal fibers, and this type of stimulation often results in polysynaptic responses. Studies by Parent et al. (2009) indicate that hippocampal afferent fibers can be identified and stimulated in modified coronal mouse brain slices containing the mPFC, and that stimulation of these fibers produces monosynaptic responses that undergo bidirectional plasticity in response to patterned stimulation. This finding provides an exciting opportunity to further explore neurotransmission and informational flow from the hippocampus to the mPFC and the ways in which mAChRs may contribute to and modulate this flow.

Employing this modified coronal slice preparation, Wang and Yuan (2009) recorded monosynaptic EPSPs in current clamp mode from mPFC layer II/III and layer V pyramidal cells during stimulation of afferents from the ventral hippocampus. They

found that bath application of 20 μ M CCh for 10 min depressed EPSP slope and that this depression lasted >45 min after agonist washout; this muscarinic effect was evident in recordings from both layer II/II and layer V. In other words, muscarinic LTD occurs not only in hippocampus and visual cortex but also in mPFC neurons, and this mLTD can be induced by CCh application after stimulation of deep or superficial cortical layers or after stimulation of newly proposed hippocampal afferents to the mPFC. It was also shown that mLTD at hippocampal-mPFC glutamatergic synapses was not affected by GABA_A and GABA_B antagonists (Wang and Yuan, 2009). It is important to note that when layer I was stimulated and whole cell EPSPs recorded in layer II/III, CCh induced an acute depression but not a long-lasting one; Huang and Hsu (as described above, 2009) saw confounding results when stimulating and recording from layer V or when stimulating layer II/III and recording in layer V. In both scenarios, mLTD could be induced. One critical difference is that Wang and Yuan used slices from mice whereas studies from Huang and Hsu employed rat slices. This may go to show, however, that the stimulation and recording location within the mPFC have quite an impact on plasticity phenomena and that a more consistent, direct examination of the hippocampal-mPFC pathway may yield more reliable data.

Paired pulse facilitation studies indicated that mLTD upon stimulation of hippocampal afferents was induced via a presynaptic mechanism, and interruption of electrical stimulation during CCh application prevented mLTD which indicated activity dependence (Wang and Yuan, 2009). Acute and long-term depression of EPSPs by CCh were both intact in the presence of NMDAR antagonist APV but not with the addition of the L-type Ca²⁺ blocker nifedipine indicating that mLTD at hippocampal-mPFC synapses

is NMDA independent but relies on Ca^{2+} influx through voltage gated L-type calcium channels. Upon the observations that mAChR antagonists AF-DX 116 and pirenzepine induced differential modulation of mLTD and that the mechanism of depression seemed presynaptic, the authors concluded that presynaptic M_2 receptors mediated mLTD. These antagonists are not selective, however, and evidence presented by Huang and Hsu (2009) supporting a role for the retrograde signaling molecule nitric oxide seems much more conclusive (Huang and Hsu, 2009). This scenario would explain the involvement of a post-synaptic G_q -coupled mAChR as well as presynaptic inhibition of glutamate release seen by both sets of researchers.

mAChR modulation of cortical physiology: conclusions

Acetylcholine release in cortical areas of the brain results in a multi-faceted array of electrophysiological responses in both pyramidal neurons and GABAergic interneurons by activating both mAChRs and nAChRs. ACh is a powerful modulator of numerous ion channels that contribute to the excitability and firing patterns of cortical neurons both at rest and in response to intracortical and afferent inputs from multiple brain regions including the thalamus and hippocampus. The diversity of cholinergic receptor subtypes and layer-specific expression contributes to the complex cell type- and input-dependent consequences of mAChR activation. In this thesis, we show that the selective activation of the M_1 receptor induces an inward current and an increase in spontaneous EPSCs in layer V pyramidal neurons in rat and mouse mPFC, a cortical region implicated in attentional processes and cognition. These effects are decreased in M_1 knockout mice. Potentiation of M_1 also increases the firing rate of rat mPFC neurons

in vivo. Finally, the selective M₁ PAM BQCA reverses impairments in a form of learning that requires normal functioning of the PFC in a mouse model of AD. These studies lend further support for a critical role of M₁ in supporting normal function of the PFC.

Pharmacology of muscarinic receptors

Our lack of understanding of the physiological roles of specific mAChRs is largely due to the historical lack of pharmacological agents that are highly selective for individual subtypes. Previous efforts have failed to develop highly selective traditional (orthosteric) agonists of the individual muscarinic receptors. This is likely due to the high conservation of the orthosteric (primary) ACh binding region across muscarinic receptor subtypes (Eglen, 2005), making it difficult to develop subtype selective ligands that bind to this site (Felder et al., 2000). However, in recent years, we and others have been highly successful in developing allosteric modulators and agonists of GPCRs. These compounds provide unprecedented selectivity for the intended receptor and can have behavioral effects *in vivo* that are very similar to those of direct acting agonists.

Models of receptor activation

The binding of an agonist to the receptor can be theoretically modeled. One type of model, the two-state model also referred to as the ternary model of binding posits that the receptor exists in two conformations; an inactive conformation and an active conformation (Gether, 2000). In this model, the agonists are able to bind to receptors in the active conformation and thus shift the equilibrium toward that of activated receptors.

Antagonists bind to both the inactive and active conformations, resulting in no change in equilibrium. In contrast, inverse agonists bind to the inactive form of the receptor resulting in a shift in equilibrium towards inactive receptors (Gether, 2000). This is quantified by the cooperativity factor α , which is based on the affinity of the ligand for the active state of the receptor compared to the affinity for the inactive state (Christopoulos and Kenakin, 2002; Hulme (a) et al., 2003). This model is expanded further in the extended ternary complex model to incorporate binding of G proteins to the receptor (Hulme (a) et al., 2003). In this case, the receptor again exists in inactive and active conformations. However, the receptor in the active state (either bound or unbound by ligand) now binds to the G protein (Hulme (a) et al., 2003). It should be noted that the G protein could also bind to the inactive form of the receptor (Christopoulos and Kenakin, 2002). In this model it is also possible that multiple G proteins have the ability to bind to the active receptor conformation, which would allow for potential specificity in receptor signaling (Kenakin, 2003).

Molecules bind to the receptor in a specific manner to activate (agonists), block (antagonists) or decrease (inverse agonists) receptor activation. Agonists have both affinity and intrinsic efficacy for the receptor, whereas antagonists possess only affinity; an inverse agonist has negative efficacy (Christopoulos and El-Fakahany, 1999). The action of an agonist is dependent on the system that it is being studied, thus it can only be defined as a partial or full agonist for the system in which the response is measured. When a system has spare receptors this means that only a fraction of the receptors need to be activated to get a maximal response. Additionally, it is important to note that a receptor saturating concentration of a drug in one system may not be saturating in a different system.

There are different classes of allosteric modulators; positive allosteric modulators or potentiators are thought to result in a conformation change at the orthosteric site that results in higher affinity for the orthosteric ligand. Allosteric agonists result in increased G protein coupling irrespective of the action on the orthosteric site; and allosteric antagonists result in a decrease in receptor affinity and/or make the G protein less likely to couple to the receptor (Christopoulos and Kenakin, 2002; Wess, 2005).

Furthermore, ligands that bind in an allosteric manner can induce conformational changes in the receptor which can result in the modulation of receptor activity (Christopoulos, 2002). In allosteric interactions the binding of one ligand affects the ability of another ligand to bind. This occurs in a reciprocal manner between the two ligands (Birdsall et al., 1996). Changes in receptor conformation can result in change in receptor affinity. While positive cooperativity results in an increase in affinity, negative cooperativity results in a decrease in affinity and neutral cooperativity results in no change in affinity (Christopoulos, 2002). The action of a particular allosteric modulator may also be ligand specific. Thus, it may be possible to get some degree of subtype selectivity based in cooperativity rather than affinity (Lanzafame et al., 2006).

Allosteric ligands of mAChRs

Despite tremendous efforts by multiple industry and academic scientists, previous efforts have failed to produce highly selective traditional (orthosteric) agonists of the M₁ muscarinic receptor. This is likely due to the fact that the ACh binding site is highly conserved, making it difficult to develop agonists at M₁ that are devoid of activity at the other mAChR subtypes. In addition to the difficulty in developing M₁ agonists that are

highly selective, there are a number of problems associated with the use of direct acting agonists as drugs. These include adverse effects associated with excessive activation of the receptor, greater receptor desensitization than may occur with more indirect approaches, and loss of activity dependence of receptor activation. Another approach to achieving receptor activation that has been highly successful for ligand-gated ion channels is development of allosteric modulators of receptor function. Allosteric ligands do not bind to the orthosteric neurotransmitter binding site and do not directly activate the receptor but bind to another site on the receptor and potentiate the effects of a orthosteric agonist. A classical example of this approach is the use of benzodiazepines to potentiate GABA_A receptor function (Mohler et al., 2002). Because allosteric potentiators require the endogenous agonist for activity, they maintain activity-dependence of receptor activation. This is thought to reduce adverse effects that can be associated with direct-acting agonists and may also reduce the level of desensitization. In recent years, we (Marino et al., 2003; O'Brien et al., 2003; Lindsley et al., 2004; O'Brien et al., 2004; Galici et al., 2005; Kinney et al., 2005; Brady et al., 2008; Shirey et al., 2008; Bridges et al., 2009; Marlo et al., 2009) and others (Christopoulos, 2002; Gasparini et al., 2002; Rees et al., 2002; Soudijn et al., 2002; Waelbroeck, 2003) have been highly successful in developing allosteric potentiators of GPCRs. In many cases, these compounds provide unprecedented selectivity for the intended receptor and can have behavioral effects *in vivo* that are very similar to those of direct acting agonists. In the case of mAChRs, a major goal has been to develop allosteric ligands that selectively increase the activity of M₁ or M₄ receptors. Allosteric activators can also include allosteric agonists, which act at a site removed from the orthosteric site to directly activate the receptor in the absence of ACh, in contrast to positive allosteric

modulators (PAMs), which do not activate the receptor directly but potentiate activation of the receptor by the orthosteric agonists. Lastly, it is possible for a single molecule to have both allosteric potentiator and allosteric agonist activity (May et al., 2007; Conn et al., 2009a).

As stated earlier, previous attempts to develop orthosteric agonists that are highly selective for individual mAChR subtypes have failed because of the high degree of conservation of the orthosteric ACh-binding site. Although there have been reports of subtype-selective M₁ agonists in the patent and primary literature, subsequent studies across multiple systems have revealed that previous orthosteric agonists are not highly selective when evaluated across multiple systems. A reason for this is that the claims of selectivity of these agents were based on functional efficacy rather than selective binding to individual mAChR subtypes. Because of this, a weak partial agonist at multiple mAChR subtypes might seem to be selective in cell lines in which there is little or no receptor reserve but might have robust agonist activity at these same mAChR subtypes in native systems that have high receptor reserve. Because high receptor reserve is common for mAChRs in native tissues, these agents often activate multiple mAChR subtypes in animal models and humans (Felder et al., 2000; Wess et al., 2007; Langmead et al., 2008b). A recent example, AF267, was suggested to have selective agonist activity at M₁ but displays a similar selectivity profile to previous orthosteric agonists and activates multiple mAChR subtypes (i.e. M₁, M₃ and M₅) (Jones et al., 2008). As discussed further elsewhere in this introduction, the muscarinic agonist developed by Eli Lilly, xanomeline, suffers from this same lack of selectivity across multiple mAChR subtypes (Langmead et al., 2008b). These studies do not rule out the possibility that highly selective agonists of individual mAChR

subtypes will eventually be developed but do raise a need for also considering other strategies for identifying agents that selectively activate individual subtypes of this receptor family.

Development of early allosteric ligands of mAChRs

Work by several laboratories (Jakubik et al., 1997; Lazareno et al., 1998; Fawzi et al., 2001; Lazareno, 2004) identified a diverse array of chemotypes that possess PAM activity at the M₁ and M₄ mAChR subtypes. The first mAChR PAM reported was brucine (Jakubik et al., 1997; Lazareno et al., 1998), which acts as an allosteric potentiator at M₁. Brucine is a weak M₁ PAM requiring high micromolar concentrations for activity and induces only a two-fold increase in ACh affinity at the M₁ receptor. However, brucine is relatively selective for M₁ and this provided an important proof of concept that it would be possible to develop selective PAMs for this important mAChR subtype. Equilibrium and non-equilibrium radioligand-binding studies with brucine, the mAChR antagonist radioligand [³H]-*N*-methyl-scopolamine ([³H]NMS) and unlabeled ACh were consistent with a ternary allosteric model in which both the orthosteric and allosteric ligands bind to the receptor simultaneously and modify the affinities of each other.

Discovery of brucine was followed by the discovery of thiochrome as an M₄ PAM (Lazareno et al., 2004) and SCH-202676 as a PAM of multiple GPCR subtypes including M₁ (Fawzi et al., 2001; Lanzafame and Christopoulos, 2004). Thiochrome was especially interesting in that it provided M₄ subtype selectivity. This compound increases the affinity of ACh three- to fivefold at M₄ and increased ACh potency in activating M₄ in functional assays but has no effect on ACh affinity at M₁, M₂ or M₅ (Lazareno et al., 2004).

Interestingly, thiochrome has no effect on the equilibrium binding of [³H]-NMS to the five human mAChRs (M₁–M₅) but inhibits the [³H]NMS dissociation from M₁–M₄. This indicates that the selectivity of thiochrome for M₄ is due to selective cooperativity rather than selective interactions with this single mAChR subtype.

Another major breakthrough in mAChR pharmacology came when Spalding et al. (2002) identified AC42 as the first in a novel class of compounds that bind to a secondary ectopic site on the M₁ receptor (Spalding et al., 2002). AC42 acts at a site that is clearly distinct from the orthosteric ACh site and involves transmembrane domains one and seven (but not three, five, and six, which contribute to the orthosteric site). AC42 is an allosteric agonist rather than an allosteric potentiator in that it activates the receptor directly rather than potentiating the response to ACh. This compound fully activates the M₁ receptor and is highly selective for M₁ relative to other mAChR subtypes. As with allosteric potentiators, this selectivity is likely to be achieved by targeting a site distinct from the orthosteric ACh binding site. Mutations that render the receptor insensitive to ACh agonists do not alter activity of AC42. Also, activity of AC42 can be eliminated by mutations that do not alter activation of the receptor by ACh (Spalding et al., 2002).

Unfortunately, brucine, AC-42 and other early mAChR allosteric agonists and PAMs lacked the pharmacological profiles and physicochemical properties required to be useful tools to probe the effect of allosteric activation of mAChRs in more complex native systems. For instance, these compounds have off-target activities at other receptors and have relatively low potencies at M₁ or M₄. This, combined with poor solubility in physiological buffer systems, prevented their use for studies in tissue or animal model systems. However, discovery of these early compounds provided an important advance in

establishing the potential of developing more selective activators of M₁ and other mAChR subtypes by targeting allosteric sites.

New ligands are highly selective for the M₄ mAChR subtype

Another major breakthrough came with the discovery of a novel highly selective allosteric potentiator of M₄, LY2033298, by Felder and coworkers at Eli Lilly (Chan et al., 2008). This compound does not activate M₄ directly but induces a robust potentiation of the M₄-mediated response to ACh. This compound is highly selective at M₄ and has no discernable activity at the other mAChR subtypes. Site-directed mutagenesis studies revealed that residue D432 in the third extracellular loop (o3) of the receptor is involved in the potentiating effects of LY2033298. When co-administered with a low dose (0.1 – 0.3 mg/kg) of oxotremorine, LY2033298 attenuated conditioned avoidance responding (CAR) and reversed apomorphine-induced disruption of the prepulse inhibition (PPI) of the acoustic startle response. Potentiation of M₄ also augmented oxotremorine-stimulated dopamine (DA) release in dialysate from prefrontal cortex but not nucleus accumbens supporting a role for M₄ in modulating mesocortical but not mesolimbic DA levels. Authors reported a diminished potency of this compound at the rat M₄ (rM₄) receptor compared to the human receptor (hM₄), and this statement was based on the ability of LY2033298 to enhance binding of [³H]-oxotremorine-M to CHO hM₄ cell membranes and rat striatal membranes in a dose-dependent manner. The lack of effect of the PAM when administered alone on CAR, PPI, and DA release was therefore postulated to be due to this species difference (Chan et al., 2008). Functional data using recombinant cell lines expressing rM₄ or hM₄ wild-type and mutant receptors indicated that the response to ACh

was similar between species, but no data examining potentiation by LY2033298 in this assay was shown.

Employing a cheminformatics approach based on LY2033298, coupled with medicinal chemistry, we identified a new series of ligands that interact with an allosteric site on the M₄ receptor (no displacement of [³H]-NMS in binding assays) which not only potentiate the receptor, but also confer complete subtype selectivity versus M₁, M₂, M₃ and M₅ (Shirey et al., 2008). The lead compound in this series, VU100010, possesses an EC₅₀ for potentiation of ~400 nM and shifts the functional ACh response curve 47-fold to the left. As described further in this thesis in Chapter IIIa, binding studies indicate that VU100010 exerts its allosteric potentiation of M₄ by increasing the affinity of the receptor for ACh and downstream coupling to G proteins. Electrophysiological studies indicate that VU100010 modulates hippocampal synaptic transmission at excitatory but inhibitory CA1 synapses in acute slices (Shirey et al., 2008).

Despite this notable advance in mAChR pharmacology, VU10010 suffered from poor physiochemical properties (logP~4.5) and *in vivo* studies proved infeasible because we were unable to formulate VU10010 into a homogeneous solution in any acceptable vehicle, regardless of salt form or particle size. Several nonhomogenous suspensions were prepared and dosed *i.p.*, but VU10010 was not found to be centrally active. In order to evaluate the role of selective M₄ activation *in vivo*, VU10010 required further chemical optimization. The subsequent development and characterization of two novel analogs of VU10010 that are CNS penetrant following systemic administration are described in Chapter IIIb of this thesis (Brady et al., 2008). VU0152099 and VU0152100 were identified as M₄ PAMS with EC₅₀ values for potentiation of the response to ACh of

approximately 400 nM. These novel modulators maintained the high degree of mAChR subtype selectivity shown by VU10010 and also showed functional selectivity in a screen of 15 other GPCRs that are highly expressed in the CNS. Similar to the binding profile of VU10010, VU0152099 and VU0152100 did not compete for orthosteric [³H]NMS binding but increased M₄ receptor affinity for ACh. The most exciting finding in this series of studies was that VU0152099 and VU0152100 exhibited improved physiochemical and pharmacokinetic properties as compared to VU10010; in contrast, to the high logP of VU10010 (4.5), both VU0152099 and VU0152100 possessed logPs of 3.65 and 3.6, respectively, a full order of magnitude less lipophilic than VU10010. As a consequence, both VU0152099 and VU0152100 displayed improved physiochemical properties and afforded homogeneous dosing solutions in multiple vehicles acceptable for *in vivo* studies. Furthermore, both compounds exhibited substantial systemic absorption and brain penetration after systemic dosing with the PK profile of VU0152100 being superior as shown by a higher AUC (0-∞) value, a measurement of bioavailability. Subsequent studies in an animal model used to predict antipsychotic efficacy showed that both novel M₄ PAMS substantially reduced amphetamine-induced hyperlocomotion (Brady et al., 2008). It will be of critical importance to further evaluate these compounds and their efficacy in other animal models of psychosis and cognition to yield a deeper understanding of the role of this receptor subtype in human diseases like schizophrenia and AD.

Advances in the development of novel selective activators of M₁

Over the past few years, several novel selective M₁ agonists and allosteric potentiators have been identified. These compounds are providing important new tools to

evaluate the potential utility of selective activators of M₁ for treatment of AD and other CNS disorders. For instance, TBPB (Jones et al., 2008) and 77-LH-28-1 (Langmead et al., 2008b; Thomas et al., 2008) have been reported as agonists of M₁. Since the discovery of AC42, Acadia has developed a number of related compounds that have unprecedented selectivity for M₁ relative to other mAChR subtypes, are orally bioavailable, and readily cross the blood brain barrier. These compounds provide an exciting new approach for developing therapeutic agents to selectively activate M₁. In addition, they provide new tools that can be used to determine the physiological roles of M₁ in the central nervous system and test the hypothesis that activation of M₁ has effects that would predict antipsychotic efficacy in humans. Both of these compounds are systemically active and are proving to be useful for *in vivo* studies of M₁ activation.

TBPB selectively activates M₁ in cell lines and has no agonist activity at any other mAChR subtypes. Mutations that reduce the activity of orthosteric agonists have no effect on the response to TBPB, and Schild analysis of the blockade of TBPB effects with the orthosteric antagonist atropine reveals that TBPB does not interact with the orthosteric site in a competitive manner. These data are consistent with the predictions of an allosteric ternary complex model for the actions of two molecules that interact with distinct sites (May et al., 2007; Conn et al., 2009a) and are consistent with the hypothesis that TBPB acts as an allosteric M₁ agonist. However, recent studies have shown that TBPB acts as an antagonist at M₂-M₅ receptors (Lebois et al., 2009) and also has off-target activity at D₂ receptors (Jones et al., 2008). Despite the fact that TBPB does not significantly occupy D₂ sites at doses that produced efficacy *in vivo*, these findings do complicate data interpretation from studies using this compound.

Interestingly, TBPB induces M_1 -dependent potentiation of NMDA currents in hippocampal pyramidal cells, an action that is thought to be important for the cognition-enhancing effects of mAChR activation. By contrast, TBPB does not reduce inhibitory or excitatory synaptic transmission in these neurons, effects thought to be mediated by M_2 and M_4 mAChRs, respectively (Jones et al., 2008). Of particular relevance to AD pathology, early studies in cell lines indicate that TBPB induces an increase in processing of the amyloid precursor protein (APP) towards the non-amyloidogenic pathway and decreased $A\beta$ production *in vitro* (Jones et al., 2008). This is consistent with previous extensive studies indicating that mAChR activation has favorable effects on amyloid precursor protein processing in animal models and in humans (Nitsch et al., 2000; Fisher, 2008a; Caccamo et al., 2009) and provides further support to the hypothesis that selective activation of M_1 might have disease-modifying effects in the treatment of AD in addition to its potential efficacy in acutely enhancing cognition in patients suffering from this disorder. TBPB is systemically active and crosses the blood–brain barrier, making this a useful tool for studies of cognition-enhancing effects of M_1 -selective agonists. These encouraging results provide strong support for the utility of M_1 allosteric agonists in activating this crucial mAChR subtype in the CNS without inducing the adverse effects associated with less selective mAChR agonists.

A second systemically active M_1 agonist, 77-LH-28-1 was discovered as a structural analog of AC-42 (Langmead et al., 2008b; Thomas et al., 2008). 77-LH-28-1 is somewhat selective for M_1 relative to other mAChR subtypes but does have weak agonist activity at M_3 at higher concentrations. Interestingly, in contrast to the effects of atropine on the response to TBPB, the orthosteric antagonist scopolamine induces parallel rightward

shifts in the 77-LH-28-1 concentration–response relationship (Langmead et al., 2008b). Consistent with this, recent radioligand-binding studies reveal that 77-LH-28-1 binds to the orthosteric site in a competitive manner (Thomas et al., 2008). However, extensive mutagenesis studies combined with functional studies and analysis of the effects of 77-LH-28-1 on binding of an orthosteric antagonist are consistent with an allosteric mode of agonist action of this compound. These studies raise the possibility that 77-LH-28-1 might be what has been referred to as a ‘bi-topic’ ligand that binds to a site that overlaps with the orthosteric site but also includes an allosteric site that modulates orthosteric-site affinity (Lebon et al., 2009). Electrophysiological studies indicated that 77-LH-28-1 increased activity of hippocampal CA1 pyramidal cells *in vitro* and *in vivo* and also induced synchronous network activity in the gamma and/or theta frequency bands in the hippocampus (Langmead et al., 2008b). Interestingly, 77-LH-28-1 selectively activates the coupling of M₁ to Gα_q and Gα_s signaling without activating the coupling of M₁ to Gα_i in Chinese hamster ovary cells (Thomas et al., 2008); this indicates that this compound might preferentially activate different responses to M₁ activation. Such differential effects of allosteric agonists on various responses to M₁ activation could prove to be crucially important in determining the *in vivo* and ultimately therapeutic potential of allosteric M₁ agonists.

None of the novel M₁ allosteric agonists described above are entirely selective for the M₁ subtype and have properties that limit their use in determining the roles of M₁ in native systems; an exciting development in the field of muscarinic pharmacology has been the recent discovery of M₁ allosteric agonists VU0184670 and VU0357017 (Lebois et al., 2009). These compounds are chemically optimized analogs of M₁ allosteric agonists

identified in a primary high-throughput screen in the Vanderbilt Screening Center for GPCRs, Ion Channels and Transporters, initiated and supported by the NIH Molecular Libraries Roadmap. A diversity-oriented synthesis/iterative screening approach was used to rapidly explore structure-activity relationships (SAR) of novel compounds with the goal being to improve potency while maintaining subtype selectivity. Neither initial hits from the primary screen (VU0207811, VU0177548) nor the two chemically optimized analogs (VU0184670, VU0357017) displayed any agonist or antagonist activity at M₂-M₅, and the optimized leads also possessed an exceptionally clean ancillary pharmacology profile when assessed in a Panlab lead profiling screen of sixty-eight GPCRs, ion channels, and transporter targets (Lebois et al., 2009). Thus, these newer generation M₁ allosteric agonists represent a major breakthrough and are much more highly selective and have improved physiochemical properties compared to previous allosteric or orthosteric M₁ agonists. Mutagenesis studies revealed that residues located in the extracellular loop three (o3) and the first helical turn of transmembrane seven (TM7) of the M₁ receptor were critical for activity of VU0184670. This same region of M₄ was also implicated in the actions of M₄ PAM LY2033298 (Chan et al., 2008). Both M₁ allosteric agonist lead compounds were found to possess a high degree of solubility in aqueous solutions and were centrally penetrant after systemic administration with VU0184670 possessing a superior pharmacokinetic profile. Similar to what was found with TBPB, VU0184670 also potentiates NMDAR currents evoked by NMDA application in hippocampal CA1 pyramidal cells. An exciting finding was that acute *i.p.* administration of VU0357017 reversed cognitive deficits induced by the orthosteric mAChR antagonist scopolamine in a

contextual fear conditioning paradigm, a measure of hippocampal dependent learning (Lebois et al., 2009).

In addition to the discovery of novel M₁-selective allosteric agonists, exciting progress has been made in the discovery of novel M₁ PAMs that serve as allosteric potentiators of this receptor. For instance, multiple M₁ allosteric potentiators have recently been identified in a high-throughput functional-screening campaign (Marlo et al., 2009). These molecules belong to several structurally distinct chemical scaffolds and include compounds that are selective for M₁ relative to other mAChR subtypes. None of the compounds identified had agonist activity but each behaved as a pure PAM and induced parallel leftward shifts in the ACh concentration–response relationships. None of the novel M₁ PAMs competes for binding at the orthosteric ACh-binding site. The two most selective compounds, VU0090157 and VU0029767, were studied in detail and induced progressive shifts in ACh affinity at M₁ that are consistent with their effects in a functional assay; this indicates that they mechanistically enhance M₁ activity by increasing ACh affinity. However, these compounds were strikingly different in their ability to potentiate responses at a mutant M₁ receptor that exhibits decreased affinity for ACh and in their ability to affect responses of the allosteric M₁ agonist TBPB. Furthermore, VU0090157 induced similar potentiation in M₁ activation of PLC and PLD activity, whereas VU0029767 potentiated activation of PLC but not PLD signaling. This provides another example of an ability of novel M₁ PAMs to differentially regulate coupling of the receptor to different signaling pathways. Based on this, it is possible that different M₁ PAMs will have different actions on different responses to M₁ activation in native systems.

In a recent publication, researchers reported an encouraging advance in the discovery of benzyl quinolone carboxylic acid (BQCA) as a highly selective and efficacious allosteric potentiator for M₁ (Ma et al., 2009). As with VU0090157 and VU0029767, BQCA has no direct agonist activity but induces a robust leftward shift of the concentration–response relationship of ACh at activating M₁. BQCA has no activity at M₂, M₃, M₄, or M₅. This compound markedly increased two markers of neuronal activation, *c-fos* and *arc*, in multiple brain regions including cortex in wild-type but not M₁ knockout mice as detected by *in situ* hybridization. Similar to data from studies in our lab, BQCA did not compete for orthosteric [³H]NMS binding but increased affinity of M₁ for ACh (see **Chapter IV**). Residues Y179 and W400 which lie in the second (o2) and third (o3) extracellular loop of the receptor were shown to be required for the potentiation of M₁ by BQCA as mutations of these residues completely illuminated potentiation. Interestingly, BQCA is systemically active and fully reversed the cognitive impairment induced by scopolamine in a contextual fear-conditioning model of episodic-like memory (Ma et al., 2009). In addition, BQCA induces changes in electroencephalography oscillations in a manner that is consistent with a potential cognition-enhancing effect. These findings provide exciting new data in support of the hypothesis that it will be possible to develop highly selective M₁ PAMs that have potential for cognition-enhancing effects in animal models.

In agreement with findings by Ma et al. (2009), our lab has also characterized the M₁ PAM, BQCA; our results are discussed in detail in **Chapter IV** of this thesis. We also found BQCA to be highly selective for M₁ relative to other mAChRs as well as to a panel of other GPCRs (Shirey et al., 2009). Because studies in M₁ knockout mice supported a

role for this receptor in supporting cognitive behaviors requiring normal functioning of the prefrontal cortex (PFC) (Anagnostaras et al, 2003), we sought to examine the effect of selective M₁ activation in mPFC pyramidal cells. Nonselective mAChR activation with CCh induced a robust inward current, and BQCA increased the inward current induced by a low concentration of CCh. We also found that CCh dose-dependently increased excitatory drive to these cells as seen by an increase in spontaneous EPSCs, and that BQCA potentiates this effect as well. Furthermore, systemic administration of BQCA drastically increases the firing rate of mPFC pyramidal cells *in vivo* in multichannel single unit recordings and is able to reverse impairments in PFC-dependent learning in a mouse model of AD (Shirey et al., 2009). Together, studies by our group (Lebois et al., 2009; Shirey et al., 2009) and Ma et al. (2009) support a pivotal role for the M₁ receptor in modulating both hippocampal- and PFC-dependent learning and suggest that this mAChR subtype represents an exciting potential therapeutic target for the treatment of CNS disorders characterized by memory and cognitive impairment.

Lastly, it is important to note that, at present, the mechanisms underlying the selectivities of muscarinic allosteric agonists and PAMs are not fully established. The initial rationale driving this approach is that allosteric ligands bind to evolutionarily less-conserved allosteric sites on the M₁ or M₄ receptor, as opposed to the highly conserved orthosteric (ACh) binding site and might, therefore, bind selectively to allosteric sites on individual mAChR subtypes. This hypothesis has been clearly established for metabotropic glutamate receptors where selective binding of allosteric ligands to individual subtypes has been established as the basis for the selectivity of some ligands (Conn et al., 2009a). However, this does not rule out the possibility that these compounds bind to

allosteric sites on multiple mAChR subtypes with similar affinities but that selectivity is conferred by selective cooperativity with orthosteric-site agonists (May et al., 2007; Conn et al., 2009a), as has been suggested for the functionally selective PAM activity of thiochrome on M₄ (Lazareno et al., 2004). If this is the case, it is possible that selectivity of these compounds will vary depending on the system in which their effects are measured. Thus, it will be crucial to develop a clear understanding of the molecular basis for the observed selectivity in future studies. Optimally, this should be addressed with radioligands that act at the allosteric but not the orthosteric sites. However, studies involving detailed analysis of effects of allosteric compounds on binding of orthosteric-site ligands in addition to mutagenesis studies will also shed light on this important issue. Finally, it will be critical to understand whether selectivity of PAMs holds constant in the presence of multiple different classes of orthosteric agonists; examples of probe dependence of allosteric modulators are now surfacing (Kenakin, 2008). Preliminary findings by our group and others with the M₄ PAM LY2033298 and related analogs suggest that selectivity of these compounds across mAChR subtypes exists in the presence of ACh but not another orthosteric agonist, oxotremorine. Considering that co-administration of low doses of systemically active muscarinic agonists may be required to see efficacy of PAMs in different behavioral models, it will be critical to explore selectivity profiles of allosteric modulators not only in careful radioligand binding experiments but also in multiple functional assays *in vitro* with different classes of orthosteric agonists.

mAChR pharmacology and novel allosteric ligands: conclusions

Exciting new data from animal and clinical studies indicate that ligands at mAChR subtypes might provide a novel approach to the treatment of multiple CNS disorders. This includes compelling evidence that selective increases in the activity of M₁ and M₄ could provide a novel approach to the treatment of AD and schizophrenia and perhaps have efficacy in treating psychosis and cognitive impairment in other neurodegenerative diseases. Major advances have been made in establishing selective allosteric agonists and PAMs of both M₁ and M₄ as an alternative approach to orthosteric agonists for the development of selective receptor activators. These molecules have now been optimized for use in animal models, and early studies indicate that they have effects in animal models that predict efficacy in the treatment of these disorders. In addition to potential clinical utility of selective mAChR activators, abundant clinical and animal studies indicate that highly selective antagonists of specific mAChR subtypes might have utility in the treatment of other CNS disorders including dystonia, Parkinson's disease, epilepsy and others (Bymaster et al., 2002; Bymaster et al., 2003c; Bymaster et al., 2003b; Katzenschlager et al., 2003; Wess et al., 2007; Fisher, 2008b; Langmead et al., 2008a; Conn et al., 2009b). In each case, subtype selectivity will be a key to achieving clinical efficacy in the absence of adverse effects. For other GPCRs, it has been possible to discover allosteric modulators that serve as allosteric activators or inhibitors (i.e. NAMs) of receptor function (Gasparini et al., 1999; Mannaioni et al., 2001; Campbell et al., 2004). Thus, it might be possible to discover selective allosteric antagonists of mAChR subtypes. Indeed, a recent high-throughput screening campaign that focused on M₁ PAMs was also successful in identifying NAMs of mAChR subtypes that are still under development (Marlo et al.,

2009). These exciting advances are providing a fundamental advance in our approaches to regulating mAChRs as drug targets and may provide a novel approach to treatment of AD and schizophrenia in addition to other CNS-related disorders.

Muscarinic receptors as therapeutic targets

A prominent characteristic of AD is a degeneration of a group of cholinergic projection neurons in the basal forebrain that project from the medial septum and nucleus basalis of Meynert to the hippocampus and other forebrain areas involved in cognition, learning and memory (Francis et al., 1999). There is a subsequent decrease in the synaptic levels of ACh that seem to correlate with cognitive impairment, and in AD, there is can be up to a ninety percent loss of cholinergic neurons in the basal forebrain. A large number of animal and human studies suggest that these cholinergic projections play a critical role in memory and attention mechanisms and that the clinical syndrome associated with AD results, at least in part, from failed neurotransmission at cholinergic synapses (Bartus et al., 1982; Whitehouse et al., 1982; Arendt et al., 1983; Damasio et al., 1985; Reinikainen et al., 1990; Fibiger, 1991; Voytko et al., 1994; Auld et al., 2002). Evidence suggests that cholinergic transmission in the forebrain is mediated primarily by mAChRs and these receptors are likely to mediate the cholinergic involvement in learning and memory (Coyle et al., 1983; Brown and Zador, 1990; Fibiger et al., 1991). Despite a loss in presynaptic cholinergic markers such as the vesicular ACh transporter and the choline transporter as well as presynaptic M₂ receptor expression, it appears that postsynaptic M₁ and M₃ receptors remain intact whereas presynaptic M₄ levels have been shown to increase in AD (Flynn et al., 1995b; Flynn et al., 1995a).

These studies suggest that agents that enhance cholinergic transmission could be clinically useful for ameliorating the loss of cognitive function in patients with AD and other memory disorders. Some of the earliest therapies developed for the treatment of AD employed the strategy of inhibiting the enzyme responsible for degrading ACh, acetylcholinesterase (AChE). The cholinergic hypothesis of AD has been partially substantiated by clinical trials with AChE inhibitors such as tacrine, rivastigmine, donepezil, and galantamine, establishing dose-related improvements in measures of cognitive performance and quality of life (Davis et al., 1992; Farlow et al., 1992; Knapp et al., 1994; Rogers et al., 1998; Raskind et al., 1999; Wilkinson and Murray, 2001; Munoz-Torrero, 2008). Several factors have limited this therapeutic approach, the first being that AChE inhibitors increase levels of ACh not only in the CNS but in the periphery. This leads to a host of adverse side effects mediated primarily by peripheral mAChRs. The most prominent adverse effects of AChE inhibitors are mediated by activation of peripheral M₂ and M₃ mAChRs and include bradycardia, GI distress, excessive salivation, and sweating (Krejci and Tucek, 2002; Bymaster et al., 2003c; Bymaster et al., 2003a; Unno et al., 2005).

An alternative therapeutic strategy involves the used and development of cholinergic agonists that activate mAChRs directly and would replace the deficiency in endogenous acetylcholine signaling. This approach would circumvent one of the limitations of AChE inhibitors in that those drugs rely on intact ACh release; as discussed above, one of the prominent pathologies underlying AD and the cholinergic hypothesis is the degeneration of cholinergic inputs. Direct acting agonists therefore would not rely on presynaptic cholinergic projections to be intact and functional.

The M₁ receptor subtype has been viewed as the most likely candidate for mediating the beneficial effects of cholinergic therapies on cognition, attention mechanisms, and sensory processing. Because of this, considerable effort has been focused on developing selective M₁ agonists for treatment of AD (Fisher, 1997; Korczyn, 2000; Messer et al., 2000; Greenlee et al., 2001; Fisher et al., 2002; Messer, 2002a). The development and use of compounds such as AF102B and AF267B, talsaclidine and xanomeline (Pittel et al., 1996; Bodick et al., 1997b; Nitsch et al., 2000; Fisher et al., 2002; Messer, 2002a; Shekhar et al., 2008) have provided important proof of concept evidence that this is a viable approach. Treatment with these compounds caused a modest improvement in cognitive impairments measured by the AD assessment scale; however, these efforts were limited because cholinergic side effects similar to those seen with AChE inhibitors were seen. These findings indicate that despite claims of M₁ selectivity *in vitro*, these compounds are not selective for M₁ *in vivo*. Differences in receptor expression levels in recombinant systems and the use of varying functional readouts of receptor activation does lead to discrepancies in selectivity profiles of many compounds when characterized by different research groups. Our lab and others have found that AF267B (Fisher et al., 2002; Caccamo et al., 2009), also activates M₃ and M₅ receptor subtypes (Jones et al., 2008; Langmead et al., 2008b). Furthermore, we and others have found that xanomeline not only activates M₁ and M₄ but M₂, M₃, and M₅ in recombinant cell lines (Langmead et al., 2008b).

Xanomeline

Of the mAChR agonists to date, xanomeline has progressed furthest in clinical development. In an early large multicenter trial, it had a modest effect on cognitive function in AD patients that barely reached significance (Bodick et al., 1997b; Bodick et al., 1997a). Although the cognition-enhancing effects of this compound in Phase III trials were somewhat disappointing, the most exciting and surprising finding in the xanomeline trial was that this agonist had robust therapeutic effects on psychotic symptoms and behavioral disturbances such as vocal outbursts, suspiciousness, delusions, agitation, and hallucinations that are associated with AD (Bodick et al., 1997a). These data indicate that activation of mAChRs could be a therapeutic strategy for treatment of psychosis and behavioral disturbances in patients suffering from a broad range of disorders including schizophrenia, AD and other neurodegenerative disorders (Felder et al., 2000; Bymaster et al., 2002; Mirza et al., 2003; Langmead et al., 2008a; Conn et al., 2009b). Indeed, initial clinical findings from a small-scale double-blind, placebo-controlled study testing the efficacy of xanomeline in treating the various positive, negative, and cognitive symptoms in twenty subjects with schizophrenia, significant improvements in positive and negative symptoms occurred with treatment compared to placebo. Subjects in the xanomeline group also showed improvements in cognitive measures of verbal learning and short-term memory function. Together, these studies provide strong clinical validation of mAChR agonists as novel therapeutic agents used for the treatment of psychosis and behavioral disturbances in patients suffering from a broad range of disorders including schizophrenia, AD and other neurodegenerative disorders. Unfortunately, because xanomeline lacks true M₁/M₄ specificity and has significant affinity and efficacy at M₂, M₃, and M₅ (Jakubik et

al., 2006; Langmead et al., 2008b; Noetzel et al., 2009) and is also poorly brain penetrable so that high plasma concentrations are required to achieve sufficient brain levels for M₁ activation, it suffers from the same peripheral side effects as those of AChE inhibitors. This dose-limiting toxicity prevented determination of whether higher doses would have induced a more robust effect on cognition (Bodick et al., 1997b; Bodick et al., 1997a; Shekhar et al., 2008).

mAChR subtypes involved in the therapeutic efficacy of xanomeline

Although the exact mAChR subtype responsible for the effects of xanomeline in schizophrenia patients agents is not certain, xanomeline is an M₁/M₄-preferring agonist and multiple animal studies indicate that one or both of these mAChR subtypes is likely to be responsible for the clinical efficacy of this compound (Felder et al., 2001; Gerber et al., 2001; Miyakawa et al., 2001; Bymaster et al., 2002; Marino and Conn, 2002; Anagnostaras et al., 2003; Tzavara et al., 2004; Langmead et al., 2008a). Thus, it will be important to rigorously evaluate the potential roles of both of these receptor subtypes in animal models that predict efficacy in the different symptom clusters associated with schizophrenia (i.e. positive, negative and cognitive symptoms). Interestingly, the M₁-selective allosteric agonist TBPB has activity in multiple animal models used to predict the efficacy in treatment of positive symptoms of schizophrenia. These include the reversal of amphetamine-induced hyperlocomotor activity and disruption of prepulse inhibition, in addition to changes in c-fos expression that are almost identical to changes induced by atypical antipsychotic agents (Jones et al., 2008). Furthermore, the M₁-selective allosteric agonist 77-LH-28-1 increases hippocampal pyramidal cell firing and initiates gamma

frequency network oscillations in slices and increased pyramidal cell firing in rat hippocampus *in vivo* (Langmead et al., 2008b). Our studies show that the selective M₁ PAM BQCA increases spontaneous EPSCs and firing rate of mPFC neurons in slices and *in vivo* and acute administration of this compound also reverses impairments in reversal learning in an animal model of AD (Shirey et al., 2009). BQCA also increases *c-fos* expression and ERK phosphorylation in rodent cortex and hippocampus in addition to dose-dependently reversing scopolamine-induced memory deficits in contextual fear conditioning, a measure of hippocampal-dependent memory (Ma et al., 2009). Despite data from M₁ knockout mice showing a lack of major impairments in hippocampal-dependent learning in behavioral paradigms (Anagnostaras et al., 2003) current data employing selective pharmacological activation of M₁ strongly support the hypothesis that is a promising therapeutic target for psychosis and cognitive impairment.

The dopamine hypothesis of schizophrenia

Another neurotransmitter system involved in the etiology of schizophrenia is the dopaminergic system. Clinically relevant antipsychotic drugs block dopamine D₂ receptors, and drugs such as amphetamine and cocaine that cause increases in DA levels are psychotomimetics that can mimic positive symptoms of schizophrenia in healthy individuals (Bymaster and Felder, 2002; Raedler et al., 2007). The dopamine hypothesis of schizophrenia (Kapur et al., 2005) also suggests that hyperactivity of the mesolimbic dopaminergic pathway underlies the positive symptoms and that hypoactivity of the mesocortical dopaminergic pathways causes the negative and cognitive symptoms of the disease. Typical and atypical antipsychotics do not possess efficacy in treatment of many

of the negative and cognitive symptoms, however, implying that dopaminergic dysfunction cannot fully account for the array of symptoms seen in this patient population (Gold, 2004). In addition, these therapies also are often poorly tolerated because of numerous side effects including sedation, weight gain, sexual dysfunction, diabetes, and Parkinson's disease-like symptoms related to DAR blockade. Furthermore, greater than 25% of schizophrenia patients do not respond to these dopamine-based therapies (Hirsch and Barnes, 1995). Thus, although it is evident that dopamine does play a prominent role in the pathogenesis and treatment of schizophrenia, the dopamine hyperfunction hypothesis of schizophrenia fails to account for all aspects of this disorder, and it is increasingly evident that other neurotransmitter systems are probably involved. Interestingly, M₁ and M₄ knockout mice both display significantly elevated dopamine neurotransmission in basal ganglia structures, increased basal locomotor activity, and increased responsiveness to the stimulatory effects of amphetamine (Gerber et al., 2001; Tzavara et al., 2004). M₄ knockout animals also showed elevated basal levels and stimulated dopamine efflux and metabolites in the nucleus accumbens compared to wild-types; basal levels of ACh in the midbrain were also significantly increased (Tzavara et al., 2004). These data indicate that M₄ controls ACh release from cholinergic projections to the midbrain and also controls mAChR-regulated dopamine release. It has been speculated that selective activation of M₄ may alleviate mid-brain dopamine hyperactivity that is attributed to the psychosis observed in schizophrenia (Langmead et al., 2008a). Growing data supporting this hypothesis includes the finding that the selective M₄ PAM LY2033298 potentiates oxotremorine-stimulated dopamine release in the PFC but not in nucleus accumbens; when the compound was administered subcutaneously, it attenuated conditioned avoidance responding and apomorphine-induced

disruption of prepulse inhibition of the acoustic startle reflex when co-administered with a subthreshold dose of oxotremorine, two preclinical animal models predictive of antipsychotic efficacy (Chan et al., 2008). Additionally, as described in this thesis, we found that the related M₄ PAMs VU0152100 and VU0152099 reversed amphetamine-induced hyperlocomotion without affecting baseline levels of motor performance as assessed by the rotorod test (Brady et al., 2008).

Therapeutic promise of mAChR ligands: conclusions

In summary, abundant and burgeoning preclinical and clinical data bolster the theory that selective activation of either or both M₁ and M₄ receptors represents an exciting and promising approach to the treatment of numerous CNS disorders including AD and schizophrenia, bringing together the potential for both cognitive improvements via M₁ and dopaminergic imbalances via M₄. New tools described in this thesis including BQCA and VU0152100 provide an exciting opportunity to activate M₁ and M₄ receptors *in vivo* with exquisite selectivity. It remains to be seen if selective activation of either receptor alone will be enough to replicate and improve upon the antipsychotic efficacy and cognitive-improving effects of xanomeline without inducing undesirable, dose-limiting cholinergic side effects.

CHAPTER II

METHODS

Compounds and Materials

Commercially available test compounds from the M₄ PAM analog structure similarity database mining search were purchased from ChemBridge Research Laboratories (San Diego, CA). Probenecid, dimethyl sulfoxide (DMSO), acetylcholine chloride (ACh), adenosine-5'-triphosphate (ATP), guanosine 5'-[γ -thio]triphosphate (GTP γ S), guanosine 5'-diphosphate (GDP) and atropine were purchased from Sigma-Aldrich (St. Louis, MO), and glutamate was purchased from Tocris Cookson (Ellisville, MO). All tissue culture reagents as well as fluo-4 AM were purchased from Invitrogen (Carlsbad, CA). BioCoat poly-D-lysine 384-well culture plates were obtained from Becton Dickinson Biosciences Discovery Labware (Bedford, MA); Greiner optical bottom TC-treated 384-well culture plates and Axygen polypropylene 96-well deep well plates were obtained from VWR Scientific Products (Sewanee, GA). *l*-[N-methyl-³H]scopolamine was purchased from GE Healthcare (Little Chalfont, Buckinghamshire, UK); [³⁵S]GTP γ S, Unifilter-96 GF/B plates and MicroScint-20 were obtained from PerkinElmer Life and Analytical Sciences (Boston, MA).

Chemical Database Mining for M₄ PAM LY2033298 Analogs: Chapter IIIa

Substructures searches were performed using ChemFinder (CambridgeSoft Corp., Cambridge, MA) to search the commercially available database of ChemBridge Corp.

(San Diego, CA). The thienopyridine-2-carboxamide core of LY2033298 (Chan et al., 2008) was used to search the library yielding approximately 500 substructure hits. The set of compounds was then limited by properties such as molecular weight, polar surface area, rotatable bonds and number of hydrogen bond donor/acceptors to provide a library of 232 compounds.

General procedure for the synthesis of compounds VU10001-VU10010: Chapter IIIa

2-bromo-N-(4-chlorobenzyl)acetamide: To a solution of 4-chlorobenzylamine (12.0 g, 85.1 mmol) in CH₂Cl₂ (300 mL) at 0 °C was added Et₃N (14.32 g, 141.8 mmol, 1.7 equiv) and bromoacetyl bromide (21.49 g, 106.4 mmol, 1.25 equiv). The reaction was stirred for 2 h. The reaction was quenched with the addition of water (400 mL) and mixture was extracted with CH₂Cl₂ (3 x 300 mL). The combined organic layers were dried (MgSO₄), filtered, and concentrated under reduced pressure to afford the bromoamide. (22.3g, quant.) as a light brown solid. ¹H-NMR (400 MHz, CDCl₃) δ 7.35 (d, J = 8.5 Hz, 2H), 7.25 (d, J = 8.5 Hz, 2H), 6.80 (s, 1H), 4.47 (d, J = 6 Hz, 2H), 3.96 (s, 2H). MS (*m/z*): calcd for (C₉H₉BrClNO+H)⁺, 262; found, 262.

3-amino-N-(4-chlorobenzyl)-4,6-dimethylthieno[2,3-b]pyridine-2-carboxamide

(M₄ PAM VU10010) synthesis: To a solution of mercaptopyridine (5.0 g, 30.48 mmol) in DMF (100 mL) was added bromo amide (11.95 g, 45.73 mmol, 1.5 equiv) followed by KOH (6.82 g, 121.9 mmol, 5 equiv) and water (4 mL). The reaction was stirred at room temperature for 15 h and then heated to 50 °C for 24 h. The reaction mixture was diluted with water (500 mL) and extracted with EtOAc (2 x 400 mL). The combined organic layers were washed with brine (300 mL), dried (MgSO₄), filtered, and concentrated

under reduced pressure to afford the free amine title compound (6.75 g, 64%) as a light brown solid. The free amine was suspended in acetonitrile (30 mL) and water (5 mL) and TFA was added (2 mL). The mixture was filtered and the filtrate was concentrated to give the title compound as the mono TFA salt.

VU10001: $^1\text{H-NMR}$ (400 MHz, DMSO- d_6): δ 7.68 (t, $J = 6.0$ Hz, 1H), 7.01 (s, 1H), 3.01 (t, $J = 6$ Hz, 2H), 2.70 (s, 3H), 2.50 (s, 3H), 1.89-1.77 (m, 1H), 0.85 (d, $J = 6$ Hz, 6H). $^{13}\text{C-NMR}$ (100 MHz, DMSO- d_6): δ 165.6, 158.7, 158.6, 147.8, 145.0, 122.2, 98.2, 46.7, 28.5, 24.1, 20.6, 20.1. HRMS (m/z): calcd for $(\text{C}_{14}\text{H}_{19}\text{ClN}_3\text{OS}+\text{H})^+$, 278.1327; found, 278.1324.

VU10002: $^1\text{H-NMR}$ (400 MHz, DMSO- d_6): δ 7.66 (t, $J = 6.0$ Hz, 1H), 7.00 (s, 1H), 3.19-3.10 (m, 2H), 2.70 (s, 3H), 2.50 (s, 3H), 1.56-1.41 (m, 2H), 0.85 (t, $J = 7$ Hz, 3H). $^{13}\text{C-NMR}$ (100 MHz, DMSO- d_6): δ 165.2, 158.5, 158.3, 147.4, 144.4, 123.2, 121.7, 97.7, 40.6, 23.7, 22.6, 19.7, 11.4. HRMS (m/z): calcd for $(\text{C}_{13}\text{H}_{17}\text{N}_3\text{OS}+\text{H})^+$, 264.1171; found, 264.1173.

VU10003: $^1\text{H-NMR}$ (400 MHz, DMSO- d_6): δ 7.02 (s, 1H), 2.71 (s, 3H), 2.50 (s, 3H), 1.37 (s, 9H). $^{13}\text{C-NMR}$ (100 MHz, DMSO- d_6): δ 165.8, 158.5, 158.3, 147.6, 145.1, 123.8, 122.2, 99.1, 51.6, 29.1, 24.0, 20.2. HRMS (m/z): calcd for $(\text{C}_{14}\text{H}_{19}\text{N}_3\text{OS}+\text{H})^+$, 278.1327; found, 278.1330.

VU10004: $^1\text{H-NMR}$ (400 MHz, DMSO- d_6): δ 7.72-7.66 (m, 1H), 7.99 (s, 1H), 2.80-2.72 (m, 1H), 2.69 (s, 3H), 2.47 (s, 3H), 0.67-0.52 (m, 4H). $^{13}\text{C-NMR}$ (100 MHz, DMSO- d_6): δ 167.0, 158.9, 158.7, 148.0, 144.9, 123.5, 122.1, 97.7, 24.1, 23.3, 20.1, 6.2. HRMS (m/z): calcd for $(\text{C}_{13}\text{H}_{15}\text{N}_3\text{OS}+\text{H})^+$, 262.1014; found, 262.1015.

VU10005: $^1\text{H-NMR}$ (400 MHz, DMSO- d_6): δ 8.28 (t, $J = 6.0$ Hz, 1H), 7.37-7.30 (m, 2H), 7.17-7.09 (m, 2H), 7.03 (s, 1H), 4.37 (d, $J = 6$ Hz, 2H), 2.70 (s, 3H), 2.50 (s, 3H). $^{13}\text{C-NMR}$ (100 MHz, DMSO- d_6): δ 165.6, 158.7, 158.5, 148.3, 145.1, 136.6, 129.6, 123.6, 122.2, 115.4, 115.2, 97.6, 42.0, 24.1, 20.1. HRMS (m/z): calcd for $(\text{C}_{17}\text{H}_{16}\text{FN}_3\text{OS}+\text{H})^+$, 330.1076; found, 330.1078.

VU10006: $^1\text{H-NMR}$ (400 MHz, DMSO- d_6): δ 8.01 (d, $J = 6.0$ Hz, 1H), 7.42-7.16 (m, 5H), 7.01 (s, 1H), 5.19-5.10 (m, 1H), 2.70 (s, 3H), 2.50 (s, 3H), 1.46 (d, $J = 8$ Hz, 3H). $^{13}\text{C-NMR}$ (100 MHz, DMSO- d_6): δ 165.0, 158.9, 158.7, 148.3, 145.4, 145.0, 128.5, 126.9, 126.5, 123.6, 122.2, 97.8, 48.6, 24.1, 22.2, 20.2. HRMS (m/z): calcd for $(\text{C}_{18}\text{H}_{19}\text{N}_3\text{OS}+\text{H})^+$, 326.1327, found, 326.1330.

VU10007: $^1\text{H-NMR}$ (400 MHz, DMSO- d_6): δ 8.01 (d, $J = 6.0$ Hz, 1H), 7.42-7.16 (m, 5H), 7.01 (s, 1H), 5.19-5.10 (m, 1H), 2.70 (s, 3H), 2.50 (s, 3H), 1.46 (d, $J = 8$ Hz, 3H). $^{13}\text{C-NMR}$ (100 MHz, DMSO- d_6): δ 165.0, 158.9, 158.7, 148.3, 145.4, 145.0, 128.5, 126.9, 126.5, 123.6, 122.2, 97.8, 48.6, 24.1, 22.2, 20.2. HRMS (m/z): calcd for $(\text{C}_{18}\text{H}_{19}\text{N}_3\text{OS}+\text{H})^+$, 326.1327; found, 326.1329.

VU10008: $^1\text{H-NMR}$ (400 MHz, DMSO- d_6): δ 8.36 (t, $J = 6.0$ Hz, 1H), 7.68 (d, $J = 8$ Hz, 2H), 7.51, (d, $J = 8$ Hz, 2H), 7.03 (s, 1H), 4.46 (d, $J = 6$ Hz, 2H), 2.70 (s, 3H), 2.50 (s, 3H). $^{13}\text{C-NMR}$ (100 MHz, DMSO- d_6): δ 165.8, 158.9, 158.8, 148.4, 145.3, 145.2, 128.2, 125.6, 125.5, 123.6, 122.3, 97.3, 42.4, 24.1, 20.1. HRMS (m/z): calcd for $(\text{C}_{18}\text{H}_{16}\text{F}_3\text{N}_3\text{OS}+\text{H})^+$, 380.1044; found, 380.1051.

VU10009: $^1\text{H-NMR}$ (400 MHz, DMSO- d_6): δ 7.73-7.64 (t, $J = 6.0$ Hz, 1H), 7.01 (s, 1H), 3.28-3.16 (m, 2H), 2.70 (s, 3H), 2.50 (s, 3H), 1.08 (t, $J = 8$ Hz, 3H). $^{13}\text{C-NMR}$ (100 MHz,

DMSO-d6): δ 165.4, 158.6, 158.5, 147.8, 145.0, 123.7, 122.2, 98.2, 34.1, 24.1, 20.1, 15.4. HRMS (m/z): calcd for $(C_{12}H_{15}N_3OS+H)^+$, 250.1014; found, 250.1019.

VU10010: 1H -NMR (300 MHz, DMSO-d6): δ 8.30 (t, $J = 6.0$ Hz, 1H), 7.39 (d, $J = 8.5$ Hz, 2H), 7.33 (d, $J = 8.5$ Hz, 2H), 7.05 (s, 1H), 4.38 (d, $J = 6$ Hz, 2H), 2.72 (s, 3H), 2.50 (s, 3H). ^{13}C -NMR (100 MHz, DMSO-d6): δ 166.1, 159.3, 159.2, 148.8, 145.6, 140.0, 132.0, 130.0, 129.0, 124.1, 122.7, 98.0, 42.6, 24.5, 20.6. MS (m/z): calcd for $(C_{17}H_{16}ClN_3OS+H)^+$, 346; found, 346. Analysis (calcd, found for $C_{19}H_{17}ClF_3N_3O_3S$): C (49.62, 49.96), H (3.73, 3.72), N (9.14, 8.94).

General Medicinal Chemistry Methods: Chapter IIIb

All NMR spectra were recorded on a 400-MHz Bruker NMR. 1H chemical shifts were reported in δ values in parts per million down-field from tetramethylsilane as the internal standard in DMSO. Data are reported as follows: chemical shift, multiplicity (s = singlet, d = doublet, t = triplet, q = quartet, br = broad, and m = multiplet), integration, and coupling constant (in Hertz). ^{13}C chemical shifts are reported in δ values in parts per million with the DMSO carbon peak set to 39.5 ppm. Low resolution mass spectra were obtained on an Agilent 1200 LC/MS with electrospray ionization (Agilent Technologies, Santa Clara, CA). High-resolution mass spectra were recorded on a Quadrupole Time of Flight (Q-ToF)-API-US plus Acquity system (Waters, Milford, MA). Analytical thin-layer chromatography was performed on 250- μ m Silica Gel 60 F₂₅₄ plates. Analytical HPLC was performed on an Agilent 1200 analytical LC/MS with UV detection at 214 and 254 nm along with ELSD detection. Preparative purification was performed on a custom Agilent 1200 preparative LC/MS with collection triggered by mass detection.

Solvents for extraction, washing, and chromatography were of HPLC grade. All reagents were purchased from Aldrich Chemical Co. (Milwaukee, WI), Maybridge Chemicals (Trevillet, UK), ChemBridge Corporation (San Diego, CA), and SPECS Technologies Corporation (Sarasota, FL) and were used without purification. All polymer-supported reagents were purchased from Biotage AB (Uppsala, Sweden).

General Procedure for M₄ PAM Library Synthesis of Analogs 7: Each of the 31 glass vials containing 3 ml of CH₂Cl₂ was loaded with *N,N*-diisopropylethylamine (0.3 ml, 1.70 mmol), AM-807/25050004 (50 mg, 0.225 mmol; SPECS Technologies Corporation), 1-hydroxybenzotriazole hydrate (30.4 mg, 0.225 mmol, 1.0 equivalents), polystyrene-bound *N*-cyclohexylcarbodiimide (317 mg, 0.450 mmol, 1.42 mmol/g, 2.0 equivalents), and one of 31 amines (0.225 mmol, 1.0 equivalents). The reactions were stirred for 48 h at room temperature. Macroporous triethylammonium methylpolystyrene carbonate (145 mg, 0.225 mmol, 3.11 mmol/g, 2.0 equivalents) was added, and the reactions were stirred for an additional 3 h at room temperature. Then, the reactions were filtered and concentrated on a heat-air block to afford 84 to 99% pure products. Those <99% pure were purified by mass-directed HPLC.

M₄ PAM VU0152099 Synthesis: The following components were added to a stirred solution of 3-amino-4,6-dimethylthioenol[2,3-*b*]-pyridine-2-carboxylic acid (3.0 g, 13.51 mmol; ChemBridge Corporation) in CH₂Cl₂ (90 ml) at 25°C under room atmosphere: *N,N*-diisopropylethylamine (10 ml, 56.66 mmol); 1-hydroxybenzotriazole hydrate (1.83 g, 13.51 mmol, 1.0 equivalents); 4-methoxybenzylamine (2.04 g, 14.86 mmol, 1.1 equivalents); and *N*-(3-dimethylaminopropyl)-*N'*-ethyl-carbodiimide hydrochloride (5.18 g, 27.02 mmol, 2.0 equivalents). After 48 h, macroporous triethylammonium

methylpolystyrene carbonate (4.4 g, 13.51 mmol, 3.077 mmol/g, 1.0 equivalents) was added to the solution, which was then stirred for 3 h at 25°C under room atmosphere. The solution was vacuum-filtered next, and the filtrate was separated with citric acid (1.0 M in water) and CH₂Cl₂. The organics were dried over MgSO₄ and concentrated in vacuo to produce a dark yellow solid. The solid was purified by column chromatography (silica gel, fixed 1:2 EtOAc/hexanes) to afford 2.5 g (7.33 mmol, 54%) of the title compound as a bright yellow solid. Analytical LC/MS (J-Sphere80-S4, 3.0 x 50 mm, 4.0-min gradient, 5%[CH₃CN]: 95%[0.1% trifluoroacetic acid/H₂O] to 100%[CH₃CN]): 2.773 min, >99% (214 nm and ELSD), M + 1 peak *m/e* 342.12; ¹H NMR (400 MHz, DMSO-*d*₆) δ 7.27 (d, *J* = 8.8 Hz, 2H), 6.89 (s, 1H), 6.86 (d, *J* = 8.8 Hz, 2H), 6.34 (br s, 2H), 5.80 (s, 1H), 4.53 (d, *J* = 6.0 Hz, 2H), 3.79 (s, 3H), 2.73 (s, 3H), 2.57 (s, 3H); ¹³C NMR (100 MHz, DMSO-*d*₆) δ 165.9, 159.3, 159.2, 147.7, 143.9, 130.7, 129.3, 123.7, 122.4, 114.4, 98.5, 55.5, 43.3, 24.5, 20.4; high-resolution mass spectroscopy (Q-ToF): *m/z* calc for C₁₈H₁₉N₃O₂S[M + H]: 342.1198; found, 342.1276.

M₄ PAM VU0152100 Synthesis: The following components were added to a stirred solution of 3-amino-4,6-dimethylthioenol[2,3-*b*]-pyridine-2-carboxylic acid (2.50 g, 11.26 mmol; ChemBridge Corporation) in CH₂Cl₂ (90 ml) at 25°C under room atmosphere: *N,N*-diisopropylethylamine (10 ml, 56.66 mmol); 1-hydroxybenzotriazole hydrate (1.52 g, 11.26 mmol, 1.0 equivalents); piperonylamine (1.87 g, 12.38 mmol, 1.1 equivalents); and *N*-(3-dimethylaminopropyl)-*N'*-ethyl-carbodiimide hydrochloride (4.32 g, 22.52 mmol, 2 equivalents). After 48 h, macroporous triethylammonium methylpolystyrene carbonate (3.66 g, 11.26 mmol, 3.077 mmol/g, 1.0 equivalents) was added to the solution, which was then stirred for 3 h at 25°C under room atmosphere. The

solution was vacuum-filtered next, and the filtrate was separated with citric acid (1.0 M in water) and CH₂Cl₂. The organics were dried over MgSO₄ and concentrated in vacuo to produce a dark yellow solid. The solid was purified by column chromatography (silica gel, fixed 1:2 EtOAc/hexanes) to afford 2.0 g (5.63 mmol, 50%) of the title compound as a yellow solid. Analytical LC/MS (J-Sphere80-S4, 3.0 x 50 mm, 4.0 min gradient, 5%[CH₃CN]: 95%[0.1% trifluoroacetic acid/H₂O] to 100%[CH₃CN]): 2.740 min, >99% (214 nm and ELSD), M + 1 peak *m/e* 356.10; ¹H NMR (400 MHz, DMSO-d₆) δ 8.38 (s, 1H), 7.18 (s, 1H), 6.88 (s, 1H), 6.84 (d, *J* = 8.0 Hz, 1H), 6.78 (d, *J* = 8.0 Hz, 1H), 5.98 (br s, 2H), 5.97 (s, 2H), 4.30 (d, *J* = 5.2 Hz, 2H), 2.77 (s, 3H), 2.57 (s, 3H); ¹³CNMR (100 MHz, DMSO-d₆) δ 179.9, 164.8, 161.7, 158.0, 153.4, 147.4, 133.8, 122.4, 121.9, 120.5, 108.0, 107.9, 100.8, 92.8, 42.1, 22.4, 20.0; high-resolution mass spectroscopy (Q-ToF): *m/z* calc for C₁₈H₁₇N₃O₃S[M + H]: 356.0991; found, 356.1069.

General Medicinal Chemistry Methods: Chapter IV

All NMR spectra were recorded on a 400 MHz Bruker NMR. ¹H chemical shifts are reported in δ values in ppm downfield from TMS as the internal standard in DMSO. Data are reported as follows: chemical shift, multiplicity (s = singlet, d = doublet, t = triplet, q = quartet, br = broad, m = multiplet), integration, coupling constant (Hz). ¹³C chemical shifts are reported in δ values in ppm with the DMSO carbon peak set to 39.5 ppm. Low resolution mass spectra were obtained on an Agilent 1200 LCMS with electrospray ionization. High resolution mass spectra were recorded on a Waters QToF-API-US Plus Acquity system. Analytical thin layer chromatography was performed on 250 mM silica gel 60 F₂₅₄ plates. Analytical HPLC was performed on an Agilent 1200

analytical LCMS with UV detection at 214 nm and 254 nm along with ELSD detection. Preparative purification was performed on a custom Agilent 1200 preparative LCMS with collection triggered by mass detection. Solvents for extraction, washing and chromatography were HPLC grade. All reagents were purchased from Aldrich Chemical Co., Ryan Scientific, Maybridge, and BioBlocks, and were used without purification. All polymer-supported reagents were purchased from Biotage, Inc.

General Procedure for M₁ PAM Library I Synthesis: Each of seven glass vials containing 2 mL of DMF were loaded with ethyl 8-fluoro-4-oxo-1,4-dihydroquinoline-3-carboxylate (25 mg, 0.106 mmol, Maybridge BTB02003EA), K₂CO₃ (30 mg, 0.212 mmol, 2.0 equivalents), KI (2 mg, 0.011 mmol, 0.1 equivalents), and one of seven benzyl bromides (0.319 mmol, 3.0 equivalents). The reactions were stirred for 24 hours at room temperature before receiving polystyrene-bound thiophenol (0.159 mmol, 1.5 equivalents) each, and then stirred for an additional 3 hours. The reactions were then judged complete by LCMS, filtered, and separated into CH₂Cl₂ and H₂O. The organics were washed with brine, dried over MgSO₄, filtered, and concentrated *in vacuo* yielding seven benzyl-substituted ethyl 8-fluoro-4-oxo-1,4-dihydroquinoline-3-carboxylates confirmed by analytical LCMS. Next, crude products (0.1 mmol) and LiOH (8 mg, 0.3 mmol, 3.0 equivalents) were dissolved in 3 mL of THF:H₂O (9:1) in glass vials. The reactions were microwave irradiated at 120°C for 10 minutes and then separated into EtOAc and H₂O, which was acidified to pH 4 drop-wise using 1N HCl. Organics were dried over MgSO₄, filtered, and concentrated *in vacuo* yielding seven benzyl-substituted 8-fluoro-4-oxo-1,4-dihydroquinoline-3-carboxylic acids confirmed by LCMS.

Purification using mass-directed HPLC afforded the seven compounds (25-85% total yield) as TFA salts with >98% purity.

General Procedure for M₁ PAM Library II Synthesis: Each of seven glass vials containing 2 mL of DMF were loaded with ethyl 4-oxo-1,4-dihydroquinoline-3-carboxylate (25 mg, 0.115 mmol, Ryan Scientific 6J-050), K₂CO₃ (32 mg, 0.230 mmol, 2.0 equivalents), KI (2 mg, 0.012 mmol, 0.1 equivalents), and one of seven benzyl bromides (0.345 mmol, 3.0 equivalents). The reactions were stirred for 24 hours at room temperature before receiving polystyrene-bound thiophenol (0.173 mmol, 1.5 equivalents) each, and then stirred for an additional 3 hours. The reactions were then judged complete by LCMS, filtered, and separated into CH₂Cl₂ and H₂O. The organics were washed with brine, dried over MgSO₄, filtered, and concentrated *in vacuo* yielding seven benzyl-substituted ethyl 4-oxo-1,4-dihydroquinoline-3-carboxylates confirmed by analytical LCMS. Next, crude products (0.1 mmol) and LiOH (8 mg, 0.3 mmol, 3.0 equivalents) were dissolved in 3 mL of THF:H₂O (9:1) in glass vials. The reactions were microwave irradiated at 120°C for 10 minutes and then separated into EtOAc and H₂O, which was acidified to pH 4 drop-wise using 1N HCl. Organics were dried over MgSO₄, filtered, and concentrated *in vacuo* yielding seven benzyl-substituted 4-oxo-1,4-dihydroquinoline-3-carboxylic acids confirmed by LCMS. Purification using mass-directed HPLC afforded the seven compounds (25-85% total yield) as TFA salts with >98% purity.

General Procedure for M₁ PAM Library III Synthesis: Each of seven glass vials containing 2 mL of DMF were loaded with ethyl 5,8-difluoro-4-oxo-1,4-dihydroquinoline-3-carboxylate (25 mg, 0.099 mmol, Ryan Scientific 6J-020), K₂CO₃

(27 mg, 0.198 mmol, 2.0 equivalents), KI (2 mg, 0.099 mmol, 0.1 equivalents), and one of seven benzyl bromides (0.297 mmol, 3.0 equivalents). The reactions were stirred for 24 hours at room temperature and atmosphere before receiving polystyrene-bound thiophenol (0.149 mmol, 1.5 equivalents) each, and then stirred for an additional 3 hours. The reactions were then judged complete by LCMS, filtered, and separated into CH₂Cl₂ and H₂O. The organics were washed with brine, dried over MgSO₄, and concentrated *in vacuo* yielding seven benzyl-substituted ethyl 5,8-difluoro-4-oxo-1,4-dihydroquinoline-3-carboxylates confirmed by analytical LCMS. Next, crude products (0.1 mmol) and LiOH (8 mg, 0.3 mmol, 3.0 equivalents) were dissolved in 3 mL of THF:H₂O (9:1) in glass vials. The reactions were microwave irradiated at 120°C for 10 minutes and then separated into EtOAc and H₂O, which was acidified to pH 4 drop-wise using 1N HCl. Organics were dried over MgSO₄ and concentrated *in vacuo* yielding seven benzyl-substituted 5,8-difluoro-4-oxo-1,4-dihydroquinoline-3-carboxylic acids confirmed by LCMS. Purification using mass-directed HPLC afforded the seven compounds (25-85% total yield) as TFA salts with >98% purity.

Sodium 1-(4-methoxybenzyl)-4-oxo-1,4-dihydroquinoline-3-carboxylate (BQCA)

synthesis: To stirred solution of 200 mL DMF in a glass flask was added ethyl 4-oxo-1,4-dihydroquinoline-3-carboxylate (3.40 g, 15.66 mmol, Ryan Scientific 6J-050), K₂CO₃ (4.33 g, 31.32 mmol, 2.0 equivalents), KI (260 mg, 1.57 mmol, 0.1 equivalents), and 4-methoxybenzyl bromide (4.70 g, 23.49 mmol, 1.5 equivalents). After 48 hours of stirring at room temperature and atmosphere, the reaction was monitored by LCMS and judged complete. The reaction was then partitioned into CH₂Cl₂ and H₂O, and the organics were washed with brine, dried over MgSO₄, and concentrated *in vacuo*. Purification by diethyl

ether washing (6 x 50 mL) afforded the intermediate product ethyl 1-(4-methoxybenzyl)-4-oxo-1,4-dihydroquinoline-3-carboxylate (4.99 g, 14.83 mmol, 95%) as an off-white solid at >98% purity by LCMS. To a glass vial containing ethyl 1-(4-methoxybenzyl)-4-oxo-1,4-dihydroquinoline-3-carboxylate (4.99 g, 14.83 mmol) in 90 mL THF:H₂O (5:1) was added LiOH (1.07 g, 44.49 mmol, 3.0 equivalents). The reaction was microwave irradiated at 120°C for 10 minutes and then partitioned into CH₂Cl₂ and H₂O. The solution was re-acidified to pH 5 drop-wise using 2N HCl. The organics were dried over MgSO₄, filtered, concentrated *in vacuo*, and analyzed by LCMS. The crude product was purified by diethyl ether washing (6 x 50 mL) and additional H₂O wash (1 x 100 mL) to afford the intermediate product 1-(4-methoxybenzyl)-4-oxo-1,4-dihydroquinoline-3-carboxylic acid (3.20 g, 10.35 mmol, 70%) as an off-white crystalline solid at >98% purity by LCMS. To a stirred solution of 1-(4-methoxybenzyl)-4-oxo-1,4-dihydroquinoline-3-carboxylic acid (1.89 g, 6.11 mmol) in 25 mL DMF in a glass flask at 0°C was added NaH (143 mg, 5.99 mmol, 0.98 equivalents). The reaction was allowed to warm to room temperature and stirred for 1 hour before concentration *in vacuo*. The crude product was washed with diethyl ether (3 x 30 mL) to afford the title compound (1.80 g, 5.44 mmol, 89%) as a white solid at >98% purity by LCMS. ¹H NMR (400 MHz, D₂O): δ = 9.07 (s, 1H), 8.25 (d, *J* = 8.0 Hz, 1H), 7.53 (t, *J* = 8.4 Hz, 1H), 7.45 (d, *J* = 8.4 Hz, 1H), 7.39 (t, *J* = 8.0 Hz, 1H), 7.11 (d, *J* = 8.8 Hz, 2H), 6.79 (d, *J* = 8.8 Hz, 2H), 5.35 (s, 2H), 3.67 (s, 3H). ¹³C NMR (100 MHz, D₂O, externally referenced to DMSO-*d*₆): δ = 176.3, 172.2, 158.0, 147.4, 138.5, 132.3, 127.5, 127.2, 126.9, 125.5, 124.5, 117.5, 116.9, 113.8, 55.8, 54.7. HRMS calcd for C₁₈H₁₄NO₄Na₂ [M + 2Na] 354.0718, found 354.0716.

JetMilling

M₄ PAMS VU0152099 and VU0152100 as well as M₁ PAM BQCA were Jet-milled, to afford uniform nanoparticles, before vehicle formulation and *in vivo* studies employing a Model 00 Jet-O-Mizer with a High-Yield® Collection Module from Fluid Energy Processing & Equipment Company.

Stable Recombinant Cell Line Establishment and Cell Culture

Chinese hamster ovary (CHO) cells stably expressing rat M₁ were purchased from the American Type Culture Collection (ATCC) and cultured following their recommendations. CHO cells stably expressing human M₂ (hM₂), human M₃ (hM₃), and human M₅ (hM₅) were generously provided by A. Levey (Emory Medical School, Atlanta, GA); rat M₄ (rM₄) cDNA provided by T.I. Bonner (National Institutes of Health, Bethesda, MD) was used to stably transfect CHO-K1 cells purchased from the ATCC using Lipofectamine 2000 reagent according to manufacturer protocol. To make stable hM₂ and rM₄ cell lines for use in calcium mobilization assays, these cells were also stably co-transfected with a chimeric G protein, Gq_{i5} (Coward et al., 1999), obtained from Bruce Conklin at the University of California using Lipofectamine 2000. Gq_{i5} is a Gq_α protein containing the five c-terminal amino acid residues corresponding to those of Gi_α (EYNLV → DCGLF) and was expressed in a pcDNA3.1 vector containing a hygromycin resistance cassette. Large quantities of Gq_{i5} DNA were made by transforming DH5α *E. coli* cells with the construct, plating bacteria for individual colonies and expanding a single colony in liquid growth medium (LB containing hygromycin and tetracycline). A Qiagen MaxiPrep kit was used to isolate DNA from the bacterial culture. rM₁, hM₃, and

hM₅ cells were grown in Ham's F-12 medium containing 10% heat-inactivated fetal bovine serum (FBS), 2 mM GlutaMax I, 20 mM HEPES, and 50 µg ml⁻¹ G418 sulfate. hM₂-Gq_{i5} cells were grown in the same medium also containing 500 µg ml⁻¹ Hygromycin B. Stable rM₄ cells lacking the Gq_{i5} construct were grown in Dulbecco's modified Eagle's medium (DMEM) containing 10% heat-inactivated FBS, 2 mM GlutaMax I, 1 mM sodium pyruvate, 0.1 mM nonessential amino acids, 20 mM HEPES, and 400 µg ml⁻¹ G418 sulfate; rM₄-Gq_{i5} cells were grown in the same medium also containing 500 µg ml⁻¹ Hygromycin B. Parental untransfected CHO-K1 cells were cultured in Dulbecco's modified Eagle's medium (DMEM) containing 10% heat-inactivated FBS, 2 mM GlutaMax I, 1 mM sodium pyruvate, 0.1 mM nonessential amino acids, and 20 mM HEPES. Human embryonic kidney (HEK) 293A cells stably expressing rat mGluR5a were grown in DMEM containing 10% heat-inactivated FBS, 2 mM GlutaMax I, 0.1 mM nonessential amino acids, 20 mM HEPES, and 500 µg ml⁻¹ G418 sulfate.

Calcium Mobilization Assays

For experiments in **Chapter III**, recombinant muscarinic cell lines were plated at a seeding density of 3 to 5 x 10⁵ cells per well in Greiner clear-bottomed, TC-treated 384-well plates (VWR Scientific, Suwanee, GA) in antibiotic-free growth medium and incubated overnight at 37°C in 5% CO₂. Rat mGluR5a HEK cells were plated in an identical manner in clear-bottomed, poly-D-lysine-coated 96-well plates in glutamate-glutamine-free medium for growth overnight. For experiments in **Chapter IV**, all recombinant Chinese Hamster Ovary (CHO-K1) cell lines stably expressing rM₁, hM₃, or hM₅ receptors were plated at a seeding density of 50,000 cells/100µl/well in Greiner

clear-bottomed, TC-treated 384-well plates. CHO-K1 cells stably co-expressing hM₂-Gq_{i5} and rM₄-Gq_{i5} were plated at a seeding density of 60,000 cells/100µl per well. Cells were incubated in antibiotic-free medium overnight at 37°C/5% CO₂ and assayed the following day. The following day, medium was replaced with 2 µM calcium indicator dye, fluo-4 AM, for 1 h at 37°C. Dye was removed and replaced with 20 µl per well assay buffer containing 1x Hanks balanced salt solution (Invitrogen, Carlsbad, CA), 20 mM HEPES, and 2.5 mM probenecid, pH 7.4.

For experiments in **Chapter IIIa/b**, cell plates were then loaded into the Functional Drug Screening System 2000 (FDSS 6000, Hamamatsu, Japan), and cells were preincubated with either vehicle or test compound for 5 min before a 1 min incubation with agonists (i.e., ACh, glutamate, or ATP). All test compounds were dissolved and diluted in 100% DMSO and then serially diluted into assay buffer for a 2.5x stock in 0.25% DMSO; stock compounds were then added to the assay for a final DMSO concentration of 0.1%. ACh, ATP, and Glu were prepared as 5x stock solutions in assay buffer before addition to the assay plate. Calcium mobilization was measured using the FDSS 6000 and data recorded as fold over basal fluorescence; raw data was then normalized to the maximal response to agonist in the presence of vehicle for each receptor type.

For experiments in **Chapter IV**, all compounds were serially diluted in assay buffer for a final 2X stock in 0.6% DMSO. This stock was then added to the assay plate for a final DMSO concentration of 0.3%. ACh (EC₂₀ concentration or full dose-response curve) was prepared at a 10X stock solution in assay buffer prior to addition to assay plates. Calcium mobilization was measured at 25°C using a FLEXstation II (Molecular

Devices, Sunnyvale, CA). Cells were preincubated with test compound (or vehicle) for 1.5 min prior to the addition of the agonist, ACh. Cells were then stimulated for 50 sec with a submaximal concentration (EC_{20}) or a full dose-response curve of ACh. The signal amplitude was first normalized to baseline and then as a percentage of the maximal response to ACh.

GIRK-Mediated Thallium Flux Assay

Because the M_4 receptor couples to Gi/o G proteins, we were able to use a novel functional assay recently developed in our lab that takes advantage of the ability of endogenous Gi/o $\beta\gamma$ subunits of Gi/o-coupled GPCRs to alter the kinetics of G-protein regulated inwardly rectifying K^+ (GIRK) channels to conduct the ion, thallium (Niswender et al., 2008). For these studies, HEK293 cells stably co-expressing heteromeric GIRK1/2 channels and the hM_4 muscarinic receptor were pre-incubated with test compound and then stimulated with agonist (ACh) in the presence of thallium ion. Cells were incubated with 80 μ l/well of 1.7 μ M benzothiazole coumarin-acetoxymethyl ester indicator dye [prepared as a stock in DMSO and mixed in a 1:1 ratio with 10% Pluronic acid F-127 in assay buffer (1x Hanks' balanced salt solution supplemented with 20 mM HEPES)] for 1 h at room temperature in the dark. The dye was then replaced with 40 μ l of assay buffer. Test compounds were prepared as described above. Acetylcholine (EC_{20} concentration or full dose-response curve) was prepared as a 5x stock solution in thallium buffer (pH 7.3, 12 mM thallium sulfate, 1 mM $MgSO_4$, 1.8 mM $CaSO_4$, 5 mM glucose, and 10 mM HEPES) to which 125 mM $NaHCO_3$ was added immediately before use. Thallium flux was measured at 25°C using the FLEXstation II,

as described above for calcium mobilization assays. The slope of the fluorescence increase was obtained over a 10-s window beginning at 5 s after agonist/thallium addition. The signal amplitude was first normalized to baseline and then as a percentage of the maximal response to acetylcholine.

Ancillary Pharmacology Assays

Before conducting *in vivo* experiments, M₄ PAMs VU0152099 and VU0152100 were submitted to MDS Pharma Services (King of Prussia, PA) and evaluated in the LeadProfiling Screen, a radioligand binding assay panel employing 68 GPCRs, ion channels, transporters, and enzymes, to ensure a clean ancillary pharmacology profile. VU0152099 was also submitted to GPCR Profiler Service (Millipore Corporation, Billerica, MA) where it was evaluated for agonist, antagonist, and allosteric potentiator activity against a panel of 16 GPCRs in a functional screening paradigm. M₁ PAM BQCA was also submitted to Millipore's GPCR Profiler™.

Equilibrium Radioligand Binding Assays

To prepare membranes from CHO-K1 cells stably expressing rM₁, hM₂, hM₃, rM₄, or hM₅, cells were washed once with ice-cold phosphate-buffered saline, pH 7.4. Cells were then harvested with a cell scraper, resuspended in ice-cold buffer (20 mM HEPES, 100 mM NaCl, 10 mM MgCl₂, pH 7.4), and homogenized using a glass homogenizer (Dounce). The homogenate was centrifuged at 20,000xg for 20 min at 4°C. This final step was repeated twice more with homogenization between centrifugations, and the final pellets were resuspended and homogenized in ice-cold buffer in aliquots at a

final protein concentration of 1-3 mg ml⁻¹ and stored at -80°C until use. Protein concentrations were measured using the Bio-Rad Protein Assay Kit (Bio-Rad, Hercules, CA) with serum albumin (Pierce Chemical, Rockford, IL) as the standard. For each binding experiment, membranes were resuspended and homogenized in ice-cold buffer. Non-specific binding, calculated in the presence of 1 μM atropine, was never greater than 10% of total binding; in both saturation and competition binding experiments, bound radioligand did not exceed 10%.

For competition binding experiments in **Chapter IIIa/b and IV**, VU10010, BQCA and atropine were dissolved in 100% DMSO, diluted in assay buffer to make a 3x stock, and then added to the assay plate for a final maximum DMSO concentration of 0.3% for VU10010 and 0.01% for atropine. Vehicle for each condition was DMSO-matched control made in binding buffer. For ACh competition experiments, VU10010 was diluted in binding buffer to make a 5x stock and then added to the assay plate for a maximum final DMSO concentration of 0.1%. Binding reactions were incubated at room temperature for 2 h on a Titer Plate Shaker (Lab-Line Instruments, Melrose, IL), and equilibrium binding was terminated by rapid filtration through Unifilter-96 GF/B filter plates presoaked for at least 2 h with 0.1% polyethylenimine (PEI, Sigma). Filter plates were washed three times with ice-cold harvesting buffer (50 mM Tris-HCl, 150 mM NaCl, pH 7.4) using a 96-well Brandel harvester (Brandel Inc., Gaithersburg, MD). Plates were then dried overnight and 35 μl MicroScint-20 was added to each well the following day. Radioactivity was counted using a TopCount NXT microplate scintillation and luminescence counter (PerkinElmer Life and Analytical Sciences, Downers Grove, IL). All binding reactions were carried out in 1 ml volumes containing

12-25 μg membrane protein, and non-specific binding was determined in the presence of 1 μM atropine. [^3H]NMS saturation binding was performed to calculate the B_{max} and NMS K_d for each mAChR-expressing cell line using GraphPad Prizm software. Competition binding reactions contained membrane protein, appropriate concentrations of test compounds or vehicle, and 0.1 nM [^3H]NMS in 96-well deep well plates. Counts were normalized to maximal specific binding in the presence of vehicle.

[^{35}S]GTP γ S Binding Assays

Membranes were prepared from rM $_4$ -CHO cells that were not transfected with the G $_{\text{q}15}$ construct as described above for [^3H]NMS binding. After thawing, membranes were diluted and homogenized in ice-cold assay buffer containing 20 mM HEPES, 150 mM NaCl, 10 mM MgCl $_2$, and 1 mM EDTA, pH 7.4, and 5 μM GDP. Assay reactions contained 25 μg membrane protein, 10 μM VU10010 or vehicle, ACh, and 0.1 nM [^{35}S]GTP γ S in a total volume of 100 μl ; samples were incubated in a 96-well deep well plate for 1 h at room temperature. Nonspecific binding in each experiment was determined in the presence of 10 μM unlabeled GTP γ S. Equilibrium binding was terminated and radioactivity counted as described above. Counts were normalized to maximal specific binding in the presence of vehicle and 100 μM ACh.

Animals: Slice Electrophysiology in Chapter IIIa/b and IV, behavior in Chapter III

All experiments were conducted in accordance with the National Institutes of Health regulations of animal care covered in *Principles of Laboratory Animal Care* (National Institutes of Health publication 85-23, revised 1985) and were approved by the

Institutional Animal Care and Use Committee. Subjects were housed in groups of four to five per cage in a large colony room under a 12-h light/dark cycle (lights on at 6:00 a.m.) with food and water provided ad libitum. Animals were housed in an Association for Assessment and Accreditation of Laboratory Animal Care (AALAC) approved, and all efforts were made to minimize animal suffering and to reduce the number of animals used.

Brain Slice Electrophysiology: Chapter IIIa

All whole-cell recordings were carried out using hippocampal slices prepared from 16- to 23-day old Sprague Dawley rats (Charles River Laboratories, MA, USA) or 15- to 23-day WT and M₄ knockout (KO). Animals were anesthetized with isoflurane and decapitated. The brain was rapidly removed from the skull and submerged in ice-cold modified artificial cerebrospinal fluid (ACSF), which was oxygenated with 95% O₂ and 5% CO₂ and was composed of (in mM) 230 sucrose, 2.5 KCl, 0.5 CaCl₂, 10 MgSO₄, 1.25 NaH₂PO₄, 26 NaHCO₃, and 10 D-glucose. The brain was then blocked in the horizontal plane, glued to the stage of a vibratome (Vibratome, St. Louis, MO, USA) that was filled with ice-cold modified ACSF, and cut at a thickness of 300 μm for rat hippocampal slices and 275-280 μm for mice. Slices were then incubated in oxygenated normal ACSF (in mM, 126 NaCl, 2.5 KCl, 2 CaCl₂, 2 MgSO₄, 1.25 NaH₂PO₄, 26 NaHCO₃, and 10 D-glucose) at 31-32°C for 1 h and maintained at room temperature afterward until transferred individually to a recording chamber, which was continuously perfused with oxygenated ACSF at 31-32°C. Whole-cell recordings were made from visually identified hippocampal CA1 pyramidal neuron soma under an Olympus BX50WI upright

microscope (Olympus, Lake Success, NY, USA). A low-power objective (4x) was used to identify CA1 region of the hippocampus, and a 40x water immersion objective coupled with Hoffman optics and infrared video was used to visualize individual pyramidal cells. A MultiClamp amplifier (Molecular devices, Union City, CA) was used for current- and voltage-clamp recordings. Patch pipettes (2-3 M Ω) were prepared from borosilicate glass (World Precision Instrument, Sarasota, FL, USA) using a Narashige vertical patch pipette puller (Narashige, Japan). Excitatory or inhibitory postsynaptic currents (EPSCs or IPSCs) were evoked in CA1 pyramidal cells by electrical stimulation of Schaffer collaterals using a concentric bipolar stimulating electrode (FHC, Bowdoinham, ME, USA) in the presence of the GABA_A receptor antagonist bicuculine (20 μ M) or ionotropic glutamate receptor antagonists CNQX (10 μ M) and AP-5 (50 μ M), respectively. For recordings of EPSCs, the recording pipette solution contained (in mM) 123 K-gluconate, 7 KCl, 1 MgCl₂, 0.025 CaCl₂, 10 HEPES, and 0.1 EGTA, 2 Mg-ATP, and 0.2 Na-GTP. For recordings of IPSCs, the recording pipette solution contained (in mM) 65 K-gluconate, 65 CsCl, 3.5 NaCl, 1 MgCl₂, 0.025 CaCl₂, 10 HEPES, 0.1 EGTA, 2 Mg-ATP, and 0.2 Na-GTP. The pH of the pipette solutions were adjusted to 7.3 with 1 M KOH, and osmolarity was adjusted to ~295 mOsm. All drugs were bath applied. Cells were typically voltage-clamped at -60 mV. IPSCs were inward currents in such recording conditions because the calculated Cl⁻ equilibrium potential was approximately -20 mV. The access resistance was continuously monitored, and only recordings that had access resistance less than 20 M Ω with < 15% change were used for further analysis. Data analysis was performed using a PC computer equipped with pClamp data acquisition and analysis system (Molecular Devices, Union City, CA).

Statistical analysis: Electrophysiology data was analyzed using the nonparametric Wilcoxon matched-pairs signed-ranks test or Mann-Whitney U test, and p-values less than 0.05 ($P < 0.05$) were considered to be statistically significant. All cell-based, binding, and electrophysiological data are presented as mean \pm S.E.M.

Brain Slice Electrophysiology: Chapter IV

Brain slices were prepared from Sprague-Dawley rats (Charles River, Wilmington, MA), wild-type C57Bl/6Hsd (Harlan, Indianapolis, IN) or M₁ receptor KO mice (Taconic, Cambridge City, IN with permission from J. Wess); all animals were postnatal day 16-26. Animals were anesthetized with isoflurane. Brains were rapidly removed and submerged in ice-cold modified oxygenated artificial cerebrospinal fluid (ACSF) composed of 126 mM choline chloride, 2.5 mM KCl, 8 mM MgSO₄, 1.3 mM MgCl, 1.2 mM NaH₂PO₄, 26 mM NaHCO₃, 10 mM D-glucose, 5 μ M glutathione, and 0.5 mM sodium pyruvate. Coronal brain slices (295-300 μ m) containing the mPFC were made using a Leica VT1000S or 3000 vibratome (St. Louis, MO). Slices were incubated in oxygenated ACSF at 32°C for 30-60 min and then maintained at 20-22°C (room temperature) for 1-6 hr until they were transferred to a recording chamber. The recording chamber was continuously perfused at 30 \pm 0.2°C with oxygenated ACSF containing 126 mM NaCl, 2.5 mM KCl, 3.0 mM CaCl₂, 2.0 mM MgSO₄, 1.25 mM NaH₂PO₄, 26 mM NaHCO₃, and 10 mM D-glucose. Spontaneous and miniature EPSCs were recorded from layer V pyramidal cells in whole-cell voltage-clamp mode using either an Axon Multiclamp 700B amplifier (Molecular Devices, Sunnyvale, CA) or a Warner 501A amplifier (Warner Instruments, Hamden, CT) and visualized with an Olympus BX50WI

upright microscope (Olympus, Lake Success, NY) coupled with a 40x water immersion objective and Hoffman optics. Borosilicate glass (World Precision Instruments, Sarasota, FL) patch pipettes were prepared using a Flaming-Brown micropipette puller (Model P-97; Sutter Instruments, Novato, CA) and filled with 123 mM potassium gluconate, 7 mM KCl, 1 mM MgCl₂, 0.025 mM CaCl₂, 10 mM HEPES, 0.1 mM EGTA, 2 mM ATP, and 0.2 mM GTP at a pH of 7.3 and osmolarity of 285-295 mOsM. Filled patch pipettes had resistances of 2 to 4 MΩ. EPSCs were recorded at a holding potential of -70 mV; GABA_A receptor-mediated inhibitory currents were undetectable under these conditions. The voltage-clamp signal was low-pass-filtered at 5 kHz, digitized at 10 kHz, and acquired using a Clampex9.2/DigiData1332 system (Molecular Devices, Sunnyvale, CA). All drugs were bath-applied. Compounds were made in a 100X or 1000X stock in either purified water or 100% DMSO and diluted in oxygenated ACSF immediately before use. After a stable baseline was recorded for 5 – 10 min, the effect of each compound on baseline sEPSC or mEPSC amplitude and frequency was examined. Miniature EPSCs and inward currents were recorded in the presence of 1 μM tetrodotoxin, a concentration which completely blocked action potential firing upon depolarizing current injections in current clamp mode.

Statistical analysis: EPSCs were analyzed using the Mini Analysis Program (Synaptosoft, Decatur, GA). The peak amplitude and inter-event interval of sEPSCs and mEPSCs from 2-min episodes during control and drug application were used to generate cumulative probability plots. The mean values of EPSC amplitude and inter-event interval from the 2-min episode were grouped (mean ± S.E.M.) and compared using a paired *t*-test. Inward current data analysis was performed using Clampfit software (v9.2,

Molecular Devices, Sunnyvale, CA). All electrophysiology data was quantified and graphed using GraphPad Prism (GraphPad Software Inc, San Diego, CA) and Excel (Microsoft Corp., Redmond, WA). Cumulative probability plots were made using Origin (v6, Microcal Origin, Northampton, MA). Statistical analysis was performed using the student's paired or unpaired *t*-test, and statistical significance was set at $P < 0.05$. Averaged data are presented as mean \pm standard error of the mean (S.E.M.).

***In vivo* mPFC Unit Activity Recordings**

Multichannel single unit recordings were obtained from extracellular electrode arrays (NeuroLinc, Corp., New York, NY) chronically implanted in the medial prefrontal cortex (mPFC) of 300-400g Sprague-Dawley rats performing an auditory detection task for food reward. For recording sessions, animals were fitted with a HST/16V-G20 miniature headstage 20x pre-amplifier (Plexon Corp., Dallas, TX) and spike event data (1.1 ms data window) was captured by a Cheetah 32-channel acquisition system (Neuralynx, Bozeman, MT) for offline processing. Individual data sessions consisted of a 30-minute pre-injection baseline followed by three 30-minute post-injection (vehicle or BQCA, 20mg/kg) epochs. Single neurons were isolated offline using a manual spike sorter (Mclust; A.D. Redish). A sorted file was only considered to emanate from the activity of a single neuron if bins within ± 1.1 ms (considered absolute refractory period) of the autocorrelogram contained counts $< 1\%$ of the overall mean of the autocorrelogram. In addition, cells with properties characteristic of fast-spiking interneurons (spike width < 250 ms and firing rate > 6 Hz) were eliminated from analysis. Following offline clustering, the mean firing rate for each neuron within an epoch was calculated by

averaging rates across all 10-s pre-tone intervals within an epoch (approximately 50 tone presentations / 30 minute epoch). The average firing rate in an epoch was expressed as a percent of the pre-injection baseline rate and data were compared across treatment conditions with respect to changes in mean rate across the three 30-minute post-injection epochs.

Brain and Plasma Exposure Pharmacokinetic Profiling of M₄ PAMs

Male Sprague-Dawley rats (Harlan Sprague-Dawley, Inc., Indianapolis, IN) weighing 225 to 250 grams were fasted overnight before dosing. Compounds were dissolved at a concentration of 56.6 mg/ml in 10% Tween 80 and double deionized water, with the pH adjusted to approximately 7.0 using 1 N NaOH, and sonicated until a uniform homogenous solution was obtained. The dose was administered *i.p.* at 56.6 mg/kg per compound. Three animals were used for each time point. The rat blood and brain were collected at 0.5, 1, 2, and 4 h. Animals were euthanized and decapitated, and the brains were removed and frozen on dry ice. Trunk blood was collected in EDTA vacutainer tubes, and plasma was separated by centrifugation and stored at -80°C until analysis. For the brain sample preparation, frozen whole-rat brains were weighed (1.5–1.8 g) and placed in 3 ml of ice-cold solution of acetonitrile and methanol (1:1, volume) with a synthetic internal standard (50 ng/ml) and homogenized using a Sonic Dismembrator model 100 (Thermo Fisher Scientific, Waltham, MA) at maximal speed for 2 min. A 1-ml aliquot of each homogenate was placed next into 1.5-ml centrifuge tubes and centrifuged at 16,000 rpm for 5 min. Finally, 100 µl of supernatant was injected into LC-MS-MS.

Plasma samples (100 μ l) were combined with 200 μ l of ice-cold solution of the internal standard (100 ng/ml) in acetonitrile with 0.1% formic acid. After vortexing for 1 min, the mixture was centrifuged at 16,000 rpm for 5 min in a bench-top Spectrafuge 16M Microcentrifuge (Labnet, Woodbridge, NJ). The supernatant (100 μ l) was injected again into LC-MS-MS.

For the LC-MS-MS analysis, the LC separation was carried out on a Luna ODS column (5 μ m, 2.1 mm x 5 cm; Phenomenex, Torrance, CA) at a flow rate of 0.3 ml/min. The gradient started with 80% solvent A (0.1% formic acid in water) and 20% solvent B (0.1% formic acid in CH₃CN), held for 1 min, increased to 100% B in 4 min, and held for 1 min. Mass spectrometry was carried out using a ThermoFinnigan TSQ Quantum Ultra (Thermo Fisher Scientific, Waltham, MA) mass spectrometer in positive ion mode. The software Xcalibur version 2.0 was used to control the instrument and collect data. The electrospray ionization source was fitted with a stainless steel capillary (100 μ m i.d.). Nitrogen was used as both the sheath gas and the auxiliary gas. The ion transfer tube temperature was 300°C. The spray voltage, tube lens voltage, and pressure of sheath gas and auxiliary gas were optimized to achieve maximal response using the test compounds mixing with the mobile phase A (50%) and B (50%) at a flow rate of 0.3 ml/min. Collision-induced dissociation was performed on the test compounds and internal standards under 1.0 mTorr of argon. Selected reaction monitoring was carried out using the transitions from m/z 356 to 205 at 30 eV for VU0152099, m/z 342 to 205 at 27 eV for VU0152100, and m/z 310 to 223 at 25 eV for our internal standard. The calibration curves were constructed by spiking known amounts of test compounds in blank brain homogenates and plasma. The samples went through the same extraction steps as

described above. A linear response was achieved from 50 ng/ml to 100 µg/ml in both matrices. Compound exposure following administration was determined by calculating $AUC_{0-\infty}$ using the trapezoidal method.

Pharmacokinetics and Brain /Plasma Exposure Profiling of M₁ PAM, BQCA

Male Sprague-Dawley rats (Harlan, Indianapolis, USA) weighing 225-250 g, were injected *i.p.* with the micro-suspension (containing 10% tween 80) of BQCA at the dose of 10 mg/kg. The blood and whole brain tissue samples were collected at 0.5, 1, 2, 4 and 8 hours post-injection. Blood samples were collected through cardiac puncture in EDTA vacutainer tubes. The plasma was separated by centrifugation and stored at -80°C until analysis. The animals were decapitated and the whole brain tissue were removed and immediately frozen on dry ice.

Brain tissue was weighed and homogenized in 5 ml of ice-cold phosphate buffered saline using a Sonic Dismembrator Model 100 (Fisher Scientific) at maximal speed for 2 min. Five hundred µL of the homogenate samples were treated with 2.0 mL of an ice-cold solution of acetonitrile containing 0.1% formic acid and VU178 (internal standard), 100 ng/mL, and vortexed for 1 min. Plasma samples (100 µl) were combined with 500 µl of ice-cold solution of the internal standard (100 ng/ml) in acetonitrile with 0.1% formic acid and vortexed. The samples were centrifuged at 14,000 rpm for 5 min using a Spectrafuge 16M Microcentrifuge (Labnet, Woodbridge, NJ). The supernatants were evaporated and the residues were reconstituted in 100 µl of 80:20 acetonitrile/water, filtered through 0.2 µm nylon filter and injected onto LC-MS-MS.

LC separation was carried out on Waters Acquity UPLC[®] BEH C18 (1.7 μm 1.0 x 50 mm) column at a flow rate of 0.6 ml/min flow rate. The gradient started with 80% solvent A (0.1% formic acid in water) and 20% solvent B (0.1% formic acid in acetonitrile), and held for 1 min. The mobile phase composition was increased to 100% B by 2 min. and held for 1 min., before it was returned to the initial conditions. The samples were analyzed in a run time of 6 min. Mass spectrometry was carried out using a ThermoFinnigan TSQ Quantum Ultra (Thermo Scientific, Waltham, MA) mass spectrometer in positive ion mode. Xcalibur (version 2.0) software was used for instrument control and data collection. The ESI source was fitted with a stainless steel capillary (100 μm i.d.). Nitrogen was used as both the sheath gas and the auxiliary gas. The ion- transfer capillary tube temperature was 300°C. The spray voltage, tube lens voltage, pressure of sheath gas and auxiliary gas were optimized to achieve maximal response using the test compounds infused with the mobile phase A (50%) and B (50%) at a flow rate of 0.6 ml/min. Collision-induced dissociation (CID) was performed on the test compounds and internal standards under 1.0 mTorr of argon. Selected reaction monitoring (SRM) was carried out using the transitions from m/z 310 to 121 @ 17 eV for BQCA and m/z 310 to 223 @ 25 eV for the internal standard. The unknown concentrations were determined against calibration curves constructed by spiking known amounts of test compounds into the blank brain homogenate and plasma samples. A linear response was achieved from 10 ng/ml to 2 $\mu\text{g/ml}$ in plasma and 10 ng/ml to 1 $\mu\text{g/ml}$ in brain homogenates. PK parameters were calculated by non-compartmental analysis of individual concentration-time data using WinNonLin, version 5.2.1 (Pharsight Corporation, Mountain View, CA).

Amphetamine-Induced Hyperlocomotion: Chapter IIIb

All behavioral studies were conducted using male Sprague-Dawley rats (Harlan Sprague-Dawley, Inc., Indianapolis, IN) weighing 270 to 300 g. Subjects were housed in pairs in a large colony room under a 12-h light/12-h dark cycle (lights on at 6:00 AM) with food and water provided ad libitum. Test sessions were performed between 6:00 AM and 6:00 PM. Dose groups consisted of 8 to 16 rats per dose group. All doses of M₄ PAMs VU0152099 and VU0152100 refer to the salt form and were injected in a 1.0 ml/kg volume. Each compound was dissolved in 10% Tween 80 and double deionized water with the pH adjusted to approximately 7.0 using 1 N NaOH.

Apparatus: Amphetamine-induced hyperlocomotor activity studies were conducted using a SmartFrame Open Field System (Kinder Scientific., San Diego, CA) equipped with 32 horizontal (*x*- and *y*-axes) infrared photobeams located 1 cm above the floor of the chamber. Changes in ambulation or locomotor activity were measured as the number of total photobeam breaks, expressed in 5-min intervals, and were recorded with a Pentium I computer equipped with the Motor Monitor System software (Kinder Scientific).

Procedure: Rats were placed in the open-field chambers for a 30-min habituation interval (data not shown), followed by a pretreatment with vehicle or a 56.6 mg/kg i.p. dose of either M₄ PAM VU0152099 or M₄ PAM VU0152100 for an additional 30 min. Next, all rats received an injection of 1 mg/kg s.c. amphetamine, and locomotor activity was measured for an additional 60 min. Data were analyzed by a one-way ANOVA with comparison with the vehicle + amphetamine control group using Dunnett's test.

Calculations were performed using JMP version 5.1.2 (SAS Institute Inc., Cary, NC) statistical software.

Rotorod Test: The effects of M₄ PAM VU0152100 on motor performance were evaluated using a rotorod (Columbus Instruments, Columbus, OH). All rats were given an initial training trial of 120 s, followed by two additional training trials of 85 s, approximately 10 min apart, using a rotorod (7.5 cm in diameter) rotating at a constant speed of 20 revolutions per min. After initial training trials, a baseline trial of 85 s was conducted, and any rats that did not reach the 85-s criteria were excluded from the study. Rats were then pretreated for 30 min i.p. with vehicle or dose of M₄ PAM VU0152100, specifically 30, 56.6, or 100 mg/kg, and then the time each animal remained on the rotorod was recorded; animals not falling off of the rotorod were given a maximal score of 85 s. Data were analyzed by a one-way ANOVA, with comparison to the vehicle control group using Dunnett's test. Calculations were performed using JMP version 5.1.2 (SAS Institute Inc.) statistical software.

Reversal Learning: Chapter IV

Forty Tg2576 mice on the 129S6 background were obtained when they were 10 to 12 weeks of age from Taconic (Hudson, NY, USA). Tg2576 APP^{sw} mice over-expressed a 695 amino acid splice form (Swedish mutation K670N M671L) of the human amyloid precursor protein (APP₆₉₅) that results in a five-fold increase in A β 1–40 and a 14-fold increase in A β 1–42 with increasing age (Hsiao et al., 1996). In this study, 10 hemizygous males and 12 of their wild type male littermates and 9 hemizygous females and 9 of their wild type female litter mates were individually housed, maintained on a 12

hour light:dark cycle (lights on at 8:00 a.m), with *ad libitum* food and water. At approximately 12 months of age evaluation of reversal learning began. The mice were divided into groups and counter-balanced for genotype and treatment type, either BQCA or vehicle. Experiments were performed during the light cycle. Before the start of testing, subjects were placed on a restricted food diet of approximately 1 to 2 grams of food per day, contingent on their performance on the food motivated tasks. A weight basis of 85% of their pre-food deprivation weight was used as a guideline to avoid excessive weight loss. Water was available *ad libitum* during all phases of testing. All experimental procedures were approved by the Wake Forest University School of Medicine Animal Care and Use Committee and were conducted in compliance with guidelines set forth in the NIH Guide for Care and Use of Laboratory Animals.

Apparatus: The reversal-learning test was adapted from a rat set-shifting paradigm. Subjects were trained to dig in identical terra cotta pots to retrieve a food reward. A 1/20th piece of a Reese's Peanut Butter Chip (The Hershey Company) was the food reward. Pots were 1 3/4" in diameter and 1 1/2" deep. A square of vinyl window screen was glued inside the pot to form a cavity underneath the pot in which to place a food reward that was unobtainable by the subject to serve as a control for odor. Essential Oils (New Directions Aromatics, San Ramon, CA) were applied to the rim of the pot to produce a long-lasting odor and media placed inside the pots to a depth that produced vigorous digging for the subject to reach the food reward. Each odor had unique pots assigned to it and the pots were filled with the corresponding media and placed in a plastic sealable container where they were returned after each use.

Testing was carried out in the subject's home cage placed inside an ordinary 24" (length) x 16" (width) x 16" (depth) cardboard box to shield the subject from seeing movement within the room. A plexiglass holder was fabricated to insert and remove two pots at a time from the testing cage. The two pots were separated by a plexiglass partition. A 1000 ml plastic beaker was painted black and placed over the subject at the end of the cage closest to the experimenter to create a holding area. When the holder with the two pots was placed at the opposite end of the cage, the subject was then released from the black beaker. Upon completion of the dig, the subject was recovered to the holding area with the black beaker. Between all discriminations, the inter-discrimination delay was approximately three minutes.

Habituation and Shaping: After three days of food deprivation, subjects in their home cages were habituated to the test apparatus (holding beaker and pot holder) and then shaped to dig a reward after release from the holding beaker. Two pots were filled with Alpha-Dri (Shepherd Specialty Papers) and a reward was randomly placed at the very bottom of either pot to encourage the subject to dig vigorously to find it. The subjects were released from the holding area and allowed to dig in the pots. When the reward was found, the subject was recovered to the holding area using the black beaker. A pot was re-baited randomly and the trial re-run until a total of ten digs was recorded. If the subject did not reach ten digs, this habituation procedure was repeated the following day. No subject required more than two days of habituation.

Testing Paradigm: The reversal learning digging task was used previously in Tg2576 mice (Zhuo et al., 2007; Zhuo et al., 2008). The reversal learning testing was performed with olfactory discriminations as this has proven, in our hands, to be the more difficult of

discriminations compared to using media as the stimulus. One hour before testing, BQCA or vehicle was administered *s.c.* to the subjects at 30 mg/kg. The first four trials of the discriminations (exploratory trials) allowed the subject to explore both pots to find the reward. If the reward was found, a correct response was recorded and the subject recovered to the beaker. If digging first occurred in the non-reward pot, an error was recorded and the subject was allowed to search the other pot for the reward. If the subject remained motionless for one minute, a “no dig” was recorded, the trial discontinued and the next trial started. In the subsequent trials after the initial four, a correct dig was recorded when the subject retrieved the reward and an incorrect dig “error” was recorded if the subject dug vigorously in the incorrect pot. Vigorous digging was defined as the subject having its head and shoulders within the pot and using its paws to vigorously move the media. The subject was limited to 40 trials to reach criteria. No subjects were eliminated due to the 40 trial limit. Analysis was based on the total number of trials the subject took to reach the criteria of six correct trials in a row including the first four exploratory trials but not counting correct trials within the exploratory trials as part of the six correct trials.

Media and odor for the compound discriminations were established in pairs to reduce the degrees of freedom (see **Table 1**). For example, in a simple discrimination (SD) using odor as the relevant dimension, aniseed odor would always be on one pot while benzoin odor would always be on the other pot. Alpha-Dri medium was always used as the irrelevant dimension in both pots in the simple discriminations. In the compound discrimination (CD), two separate pairs of pots were used and presented to the subjects in pairs in a random order. For example, the first pair of pots would have the

exemplar, jamaroosa root, paired with soft sorbent in one pot and myrrh paired with soft snow in the other. The second pair of pots would have the exemplar, jamaroosa root, paired with soft snow in one pot and myrrh paired with soft sorbents in the other.

Two shaping SD's were run the first day of testing. Each subject was allowed one discrimination with medium as the relevant dimension and one discrimination with odor as the relevant dimension. Once a pair of dimensions had been used during the shaping SD's, they were not presented to the subjects again in the testing paradigm (for an example of experimental design, see **Table 2**).

On the second day of testing, simple odor discrimination was performed first. Upon reaching criteria for the SD, a simple discrimination reversal (SDR) was performed so that the pot with the odor that was not rewarded now became the rewarded pot. Following that, a compound discrimination was performed. An irrelevant dimension (different media) was added at this point that had no predictive power on the location of the reward. Upon reaching criteria on the compound discrimination, a compound discrimination reversal (CDR) was performed so that the pot with the odor that was not rewarded now became the pot with the odor with the reward.

Statistical analysis: Data for each phase of the digging test (*e.g.*, simple discrimination, compound discrimination) were analyzed using a chi-square analysis and subsequent odds ratio calculation to identify the relative likelihood of choice errors on the discrimination tests in the presence of BQCA within the two groups. Each task phase was analyzed independently. Since most subjects had excellent performance with no errors, only those subjects making 1 or more errors were selected for analysis.

Table 1. Media and Odor Pairings for reversal learning with exemplars in bold.

Media Pairs		Odor Pairs	
M1A = CUT FOAM	M1B = CUT MOSS	O1A = ANISEED	O1B = BENZOIN
		O2A = VANILLA	O2B = ORANGE
M3A= SOFT SORBENT	M3B = SOFT SNOW	O3A = JAMAROOSA ROOT	O3B = MYRRH

Table 2. Example of Experimental Design for reversal learning with exemplars in bold.

Discriminations	Dimensions		Exemplar Combinations	
	Relevant	Irrelevant	+	-
<u>Day 1 Shaping</u>				
SD1	Odor		O1A	O1B
SD2	Media		M1A	M1B
<u>Day 2 Testing</u>				
SD3	Odor	Medium	O2A	O2B
SDR	Odor	Medium	O2B	O2A
CD	Odor	Medium	O3A/M3A	O3B/M3B
CDR	Odor	Medium	O3B/M3B	O3A/M3A

Amyloid precursor protein (APP) processing

PC12 N21 cells (a gift from Dr. Richard Burry, Ohio State University, Columbus, OH) were maintained in DMEM containing 10% horse serum, 5% fetal clone, 100 U/ml penicillin, and 100 µg/ml streptomycin at 37°C and 5% CO₂. A humanized amyloid precursor protein sequence bearing the Swedish mutation (KM670/671/NL) was cloned in place of green fluorescent protein (GFP) in the FUGW backbone. High titer virus (~1 x 10⁹ infectious particles/ml) was used to transduce PC12 N21 cells. The amyloid precursor protein (APP)-infected cells were subsequently infected with a lentivirus in which GFP was replaced by the human M₁ muscarinic receptor sequence. For amyloid processing experiments, cells were plated at 50,000 in 12-well trays 3-4 days before the experiment. On the day of the experiment, the culture medium was replaced with 450 µL of Dulbecco's Modified Eagle's Medium (DMEM) containing the indicated concentration of BQCA or DMSO. Following a 10 min pre-treatment, CCh was added in 50 µL DMEM to the indicated final concentrations, and the medium was conditioned for 4 hr at 37°C. Conditioned medium was collected and centrifuged at 17,000 x g for 5 min to remove any cellular debris. Cells were placed on ice, rinsed with cold PBS, and harvested in PBS containing protease inhibitor cocktail (Roche Diagnostics). Primary antibodies included 6E10 (APP Aβ domain; Signet) and C8 (APP C terminus; a gift from Dr. Dennis Selkoe, Center for Neurologic Diseases, Harvard Medical School, Boston, MA). Amyloid-β₄₀ (Aβ₄₀) levels were measured using the hAmyloid β40 ELISA (HS) kit (The Genetics Company) according to the instructions of the manufacturer. Plates were read at 450 nm on a Spectra Max Plus plate reader (Molecular Devices). For Western blots, a total of 50 µg of protein from cell extracts or 15 µl of conditioned medium was

prepared in Laemmli's sample buffer, separated by SDS-PAGE, and transferred to Immobilon-P membranes (Millipore, Bedford, MA). Membranes were blocked at room temperature for 30 min and incubated with primary antibodies overnight at 4°C. Blots were rinsed and incubated with fluorophore-conjugated secondary antibodies (Invitrogen and Rockland) for 1 h at room temperature. Blots were imaged, and band intensities were quantified using an Odyssey Image Station (LI-COR). Statistical analysis was performed using Graphpad Prism 4.0 software.

CHAPTER IIIA

AN ALLOSTERIC POTENTIATOR OF M₄ mAChR MODULATES HIPPOCAMPAL SYNAPTIC TRANSMISSION

Introduction

One of the most important neuromodulatory systems responsible for regulation of multiple aspects of central nervous system (CNS) function is a widespread network of neurons that employ ACh as the primary neurotransmitter. Cholinergic projections from the basal forebrain provide major modulatory inputs to the cortex and hippocampus (Brown and Zador, 1990) and play a critical role in memory and attention mechanisms (Drachman and Leavitt, 1974; Bartus et al., 1982; Fibiger, 1991). Furthermore, abundant evidence suggests that the clinical syndrome associated with Alzheimer's disease (AD) results, at least in part, from failed neurotransmission at cholinergic synapses in the hippocampus and neocortex. There are also a number of other critical cholinergic systems in the central nervous system, including cholinergic interneurons in the striatum and other midbrain regions, as well as cholinergic projection neurons in various brain stem regions (Brown and Zador, 1990; Cooper and Sofroniew, 1996). Together, these cholinergic pathways have been implicated in a wide variety of CNS functions including nociception, regulation of sleep/wake cycles, motor control, and arousal. Agents that regulate cholinergic transmission have been proposed to have potential efficacy in a wide variety of CNS and neurodegenerative disorders including chronic and neuropathic pain, sleep disorders, epilepsy, schizophrenia, Alzheimer's disease, and Parkinson's disease

(Hartvig et al., 1989; Eglen et al., 1999; Bymaster et al., 2003a; Katzenschlager et al., 2003).

Based on this broad influence of cholinergic systems in the CNS, it is surprising that there have not been greater advances in development of therapeutic agents that target cholinergic signaling. Efforts to develop agents that enhance cholinergic transmission for ameliorating the loss of cognitive function in patients with AD and other memory disorders have been partially successful, and clinical trials with tacrine and other acetylcholinesterase (AChE) inhibitors have established dose-related improvements in measures of cognitive performance and quality of life (Davis et al., 1992; Rogers et al., 1998; Raskind et al., 1999; Wilkinson and Murray, 2001). More recently, cholinergic agents have been shown to reduce behavioral disturbances and psychotic symptoms in patients suffering from AD as well as a variety of other neurodegenerative disorders including Lewy body dementia, Parkinson's disease dementia, vascular dementia, and schizophrenia (Kaufer et al., 1998; Bullock and Cameron, 2002; Feldman, 2002; Rosler, 2002; Mirza et al., 2003). However, while this clinical validation of the efficacy of cholinergic agents is exciting, all cholinergic agents developed thus far have dose limiting adverse effects that prevent widespread use in the clinic. These adverse effects are primarily due to activation of muscarinic acetylcholine receptors (mAChRs) in the periphery. To take advantage of the therapeutic potential of manipulating cholinergic systems, it will be critical to develop new approaches for selectively regulating cholinergic signaling in central circuits involved in CNS disorders while avoiding the peripheral adverse effects associated with currently available treatments.

Evidence suggests that cholinergic transmission in many of the most critical CNS circuits is mediated primarily by mAChRs (Brown and Zador, 1990). Of the five mAChR subtypes that have been identified (termed M₁ – M₅), M₁ and M₄ are most heavily expressed in the CNS and are the most likely candidates for mediating the effects on cognition, attention mechanisms, and sensory processing (Marino et al., 1998; Rouse et al., 1999; Rouse et al., 2000b). In contrast, the most prominent adverse effects of cholinergic agents (bradycardia, GI distress, salivation, and sweating) are mediated by activation of peripheral M₂ and M₃ mAChRs (Okamoto et al., 2002; Bymaster et al., 2003b; Bymaster et al., 2003a). To attempt to avoid these peripheral side effects, considerable effort has been focused on developing subtype-selective agonists for treatment of AD and other CNS disorders (Messer, 2002a). Unfortunately, these efforts have been largely unsuccessful because of an inability to develop compounds that are highly selective for a single mAChR relative to other mAChR subtypes (Caulfield and Birdsall, 1998; Felder et al., 2000).

The difficulty in developing mAChR subtype-selective compounds is likely due to the high level of conservation of the ACh binding site (Wess, 1996). In recent years, we have been very successful in developing highly selective allosteric potentiators of metabotropic glutamate receptors (mGluRs) (Marino et al., 2003; O'Brien et al., 2003; Kinney et al., 2005; Galici et al., 2006), which are members of the family III/C GPCRs. These compounds do not activate the receptor directly but interact with an allosteric site to potentiate responses to activation of the receptor by traditional agonists. These compounds provide unprecedented selectivity for the intended receptor and can have behavioral effects *in vivo* that are very similar to those of direct acting agonists.

Interestingly, the strychnine analog, brucine, is a weak allosteric potentiator of M₁ (Lazareno et al., 1998), and thiochrome has been reported as an M₄ allosteric potentiator (Lazareno et al., 2004). These findings suggest that this approach can also be applied to mAChRs. More recently, a report showed that a novel compound, LY2033298 (**Fig. 2**), is a robust allosteric potentiator highly selective for the human M₄ mAChR subtype (Chan et al., 2008). We used this structure to initiate cheminformatics and medicinal chemistry studies in which we have now identified a series of highly selective, robust allosteric potentiators of rat M₄ (rM₄). Using these compounds along with M₄ KO mice, we now report that M₄ is one of the primary mAChR subtypes responsible for regulating excitatory but not inhibitory synaptic transmission at a key synapse in the hippocampal formation that is thought to be important for cholinergic regulation of certain aspects of cognitive function.

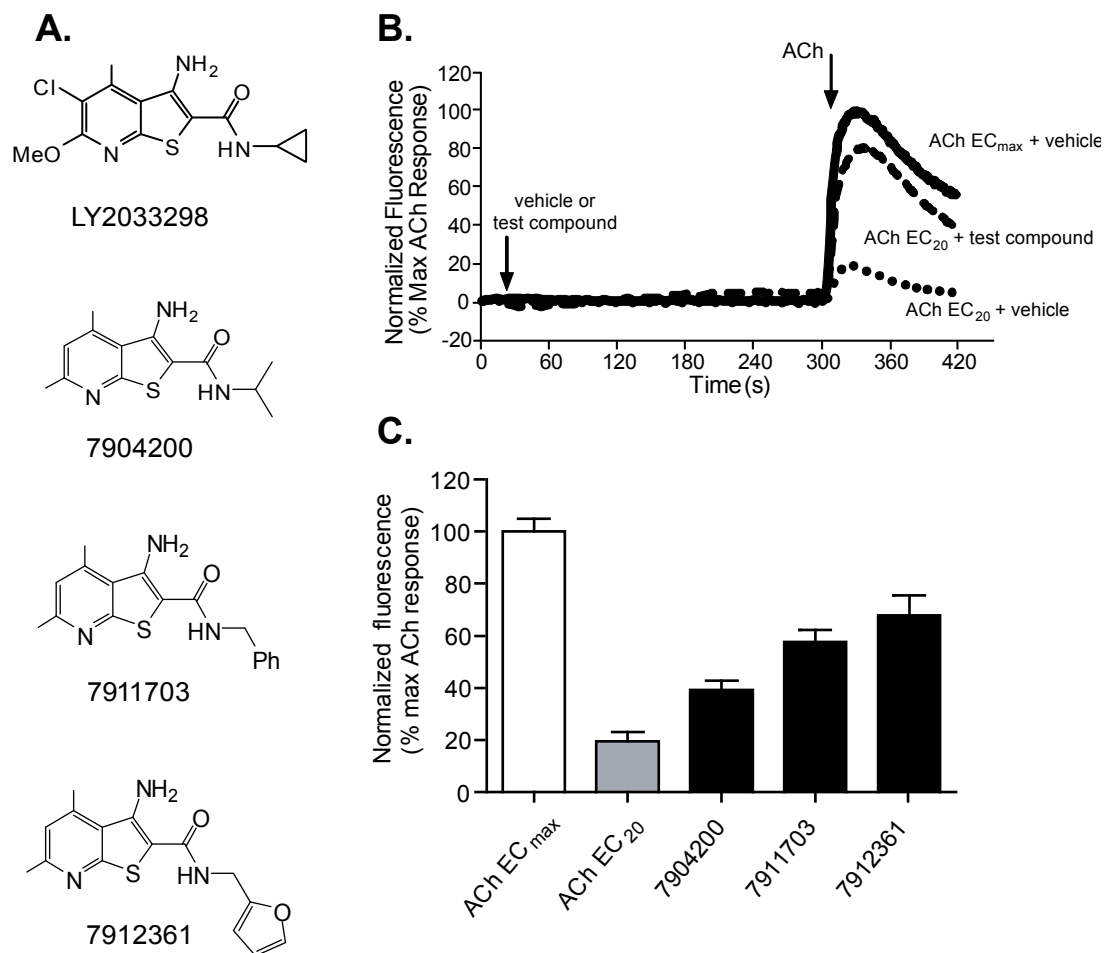


Figure 2. Database mining yields a series of compounds from the ChemBridge library with allosteric potentiator activity at the rat M_4 receptor. **A.** Chemical structures of LY2033298 and test compounds 7904200, 7911703, and 7912361. **B.** Effect of a representative allosteric potentiator hit on the rat M_4 calcium mobilization response to an EC_{20} concentration of ACh (15 nM). The responses to an EC_{20} concentration of ACh in the presence of vehicle (\bullet) and test compound 7912361 (10 μ M, ---) are shown. Also shown is the response to a maximally effective concentration of ACh (10 μ M, —). Traces are from one representative experiment. **C.** The activity of the most robust allosteric potentiators from the ChemBridge series is shown (black bars); responses were normalized as percentage of the maximum response to 10 μ M ACh after preincubation with vehicle (white bar) and compared to the EC_{20} response in the presence of vehicle (grey bar); bars represent the mean \pm S.E.M. from four independent experiments, each performed in singlicate. Database mining performed by A. Rodriguez.

Results

Database mining of the ChemBridge chemical library yields a focused library of 232 compounds with possible M₄ PAM activity

The structure of the novel M₄ mAChR allosteric potentiator, LY2033298 (Chan et al., 2008), is shown in **Fig. 2**. We performed a search of compounds contained within the chemical database of ChemBridge Corp. (San Diego, CA) for compounds containing a core structure similar to this compound. This search yielded a set of 232 compounds whose chemical ID numbers are listed in **Table 3**. These compounds were purchased and tested for activity as allosteric potentiators of M₄ in Chinese hamster ovary (CHO) cells stably expressing rM₄ and the chimeric G-protein, G_{qi5} (Coward et al., 1999). Activation of rM₄ was assessed using a functional fluorescence-based calcium assay. To identify compounds that potentiated agonist activation of rM₄, we determined the response to an EC₂₀ concentration of acetylcholine (ACh, 15 nM) in the absence and presence of test compound. Representative calcium fluorescence traces illustrating the effects of EC₂₀ (15 nM, ●) and EC₁₀₀ (10 μM, —) concentrations of ACh after pre-incubation with vehicle are shown in **Fig. 2**. In addition, the effect of a representative test compound that potentiated the effect of 15 nM ACh is shown (—). Compounds that increased the response to 15 nM ACh at least 2 standard deviations above the vehicle control in at least three of four independent experiments were defined as putative allosteric potentiators of the receptor. Compounds that met this criterion are highlighted in bold within **Table 3**. Secondary assays were performed to confirm initial hits, and compounds 7904200, 7911703, and 7912361 were found to be the most robust potentiators in this collection; the activity of these compounds is shown in **Fig. 3**, and the structures of these three lead

compounds are shown in **Fig. 2**. These compounds had no effect on M₄ alone but increased the functional response to a sub-maximal concentration of ACh when compared to vehicle control.

Table 3. Identification numbers of compounds and hits from the ChemBridge library.

5169108	6387497	7870176	7412870	6659786	7904152
5212048	7490526	7870578	7414550	6660698	7904200
5231589	7494270	7854487	7424915	6662916	7904411
5240462	7498365	7857288	6388075	6663230	7904463
5240467	7499445	7859283	6389172	7870944	7911696
5251219	7506534	7863792	6392658	7871282	7911698
5255524	7512235	7866797	6394090	7872987	7911699
5271808	7514919	7867196	6394713	7874317	7911700
5275133	7530053	7870176	6395313	7874468	7911703
5276901	7535026	7870578	6397197	7875849	7911705
5277323	7535375	6684242	6399377	7878578	7911706
5277481	7538140	6686650	6399865	7879850	7912361
5278619	7542163	6688345	6403645	7880651	7932590
5280655	7543470	6688888	6406928	7880971	7936360
5280786	7549000	6691423	6410109	7881499	7938195
5282186	7562976	6792256	6417144	7903663	7940724
5282257	7566498	6801885	6418448	7903681	7940923
5282377	7613501	6816325	6419303	7903683	7950152
5285006	7659652	6819140	6419575	7903694	7951001
5377101	7673326	6830908	6420481	7903706	7953070
5468907	7674625	6837167	6422275	7903729	7954474
5474303	7674750	6851361	6422766	7903731	7957062
5716785	7745085	6867990	6426854	7903735	7958103
5728212	7746407	6933087	6626765	7903737	7959199
5788658	7753203	6946842	6631832	7903799	7964860
5835275	7832304	6955524	6632612	7903810	7980513
5835470	7845204	6975540	6638434	7903841	7981803
5835633	7845460	6976958	6640339	7903867	7993127
5919559	7847172	6983578	6640650	7903947	7993539
6034849	7847589	7084505	6642571	7903960	7993727
6043941	7850005	7139207	6643255	7903986	7995223
6045083	7852383	7139699	6645298	7904013	7997155
6047710	7852850	7149817	6646017	7904046	9000975
6048642	7854487	7191812	6646204	7904047	9003285
6157275	7857288	7210223	6646749	7904048	9003877
6244219	7859283	7354970	6648211	7904049	9004590
6342131	7863792	7358962	6652559	7904064	5809177
6350328	7866797	7403247	6653720	7904095	
6362515	7867196	7410242	6656495	7904104	

Compounds that potentiated the rM₄ response to ACh at least 2 standard deviations above the mean EC₂₀ response compared to vehicle in at least three of four independent experiments are shown in bold.

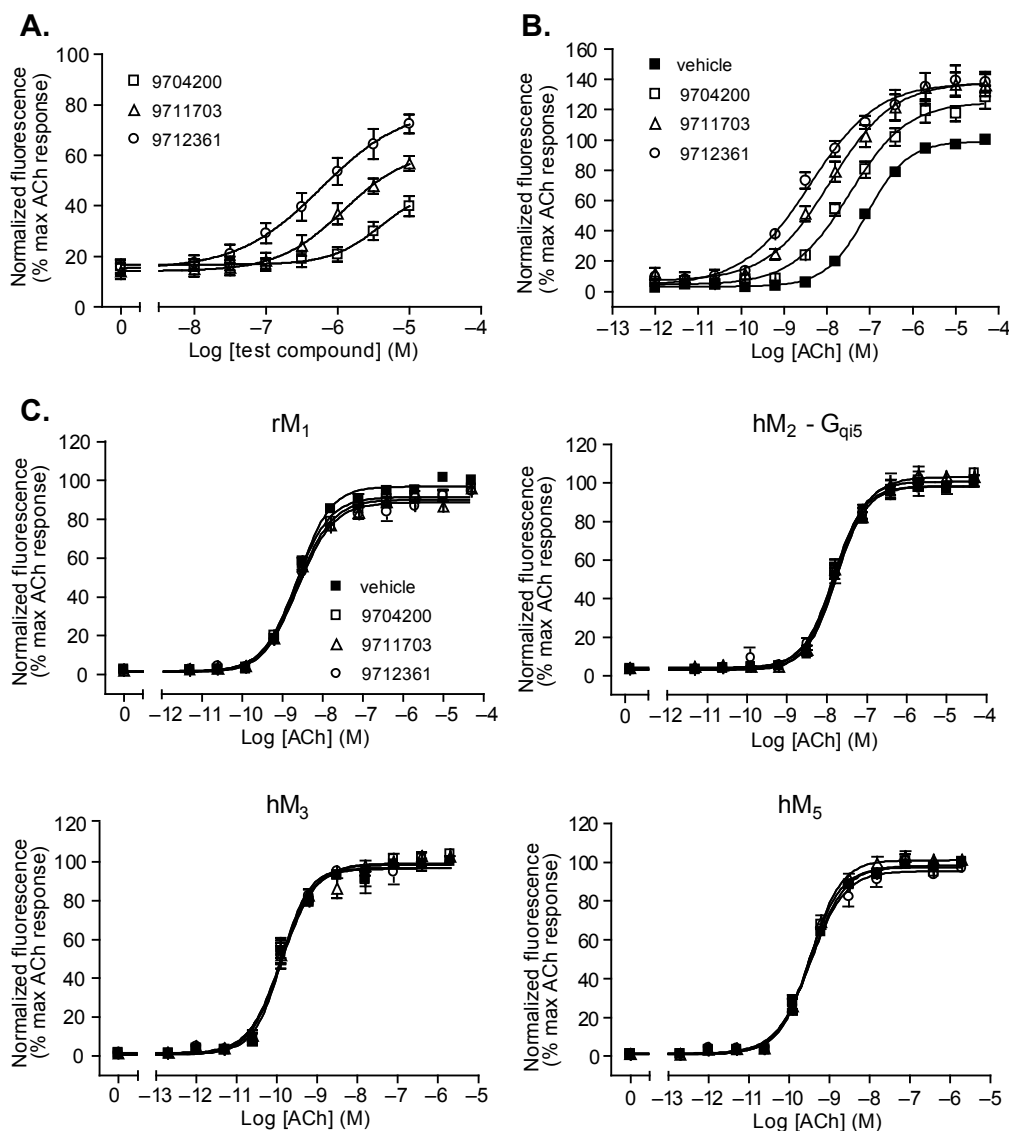


Figure 3. Lead compounds robustly potentiate M₄-mediated calcium mobilization and are selective for M₄ relative to other mAChR subtypes. **A.** CRCs of each compound were performed in the presence of an EC₂₀ concentration (15 nM) of ACh. Data were normalized to the maximum M₄ response to 10 μM ACh. Points represent the mean of three independent experiments performed in triplicate, and error bars represent S.E.M. **B.** The CRC of ACh in the presence of 10 μM compound 7904200 (□), 7911703 (△), or 7912361 (○) is shifted leftward when compared to vehicle control, and the leftward shift is accompanied by an increase in the maximal M₄ response. Points represent the mean of five experiments performed in triplicate, and error bars represent S.E.M. **C.** There was no significant change in the ACh EC₅₀ in cells expressing rM₁, hM₂ and G_{q15}, hM₃, or hM₅ after pre-incubation with either vehicle or 10 μM test compound as shown by overlapping ACh CRCs. Data were normalized as percent maximum response to 10 μM ACh; points represent mean ± S.E.M (*n* = 3).

Primary screening hits are robust, subtype selective allosteric potentiators of rat M₄

The potency of each compound was determined by pre-incubating cells with vehicle or increasing concentrations of test compound followed by the addition of an EC₂₀ concentration (15 nM) of ACh to yield concentration-response curves (CRCs) as shown in **Fig. 3**. The responses to these compounds did not reach a clear plateau in the concentration range used, and solubility limits prevented further increases in concentrations. However, in the concentration ranges tested, compound 7912361 was the most potent with an EC₅₀ of 395 ± 28 nM, while compounds 7904200 and 7911703 had EC₅₀ values of 6 ± 0.28 μ M and 1.3 ± 0.28 μ M, respectively.

We next determined the effects of maximal concentrations of each compound on the CRC of ACh. Cells were pre-incubated with a fixed concentration (10 μ M) of test compound and subsequently stimulated with increasing concentrations of ACh. Each compound induced a leftward shift of the ACh CRC and increased the maximal response to ACh (**Fig 3**). The EC₅₀ value for ACh in the presence of vehicle was 87 ± 12 nM, whereas the EC₅₀ values were 34, 12, and 4 nM in the presence of compounds 7904200, 7911703, and 7912361, respectively. Thus, compound 7912361 proved to be the most robust potentiator causing a 21-fold leftward shift in the ACh CRC (**Fig. 3**).

Experiments were then performed to assess the functional selectivity of our three lead compounds at potentiating M₄ responses relative to other mAChRs. Cells expressing rM₁, rM₂-G_qi5, rM₃, or rM₅ were incubated first with 10 μ M test compound or vehicle, then with increasing concentrations of ACh to test whether these potentiators would have any effect on functional mAChR responses in these cell lines. As shown in **Fig. 3**, among the five muscarinic receptor subtypes, these three novel compounds

possess perfect functional subtype selectivity for M₄ as shown by their lack of effect on any other mAChR in the absence or presence of ACh. Because the experimental protocol measures real-time calcium mobilization during a pre-incubation with each test compound, any agonist or antagonist as well as allosteric modulator activity is detected. The ACh CRCs for rM₁, rM₂, rM₃, and rM₅ in the presence of vehicle or 10 μM test compound are virtually overlapping with no effect on the functional ACh EC₅₀.

Chemical optimization of primary M₄ allosteric potentiator hits

The results from the 232 compound screen were analyzed to understand the structure activity relationship of the compounds. The top three lead compounds had a dimethyl substitution on the pyridine ring, and most compounds that had larger substitutions lost all activity. Substitution of the primary amine was mostly tolerated but resulted in loss of some activity. We chose to keep the primary amine and substitute the amide functionality with side chains related to compounds 7904200 and 7912361. A collection of 10 amines were acylated with bromoacetyl bromide to give the corresponding bromo amides (**Fig. 4**). Subsequent ‘one-pot’ alkylation and cyclization of mercaptopyridine with the bromo amides using KOH provided compounds VU10001-VU10010 (**Fig. 4**) as yellow solids after conversion to their TFA salts.

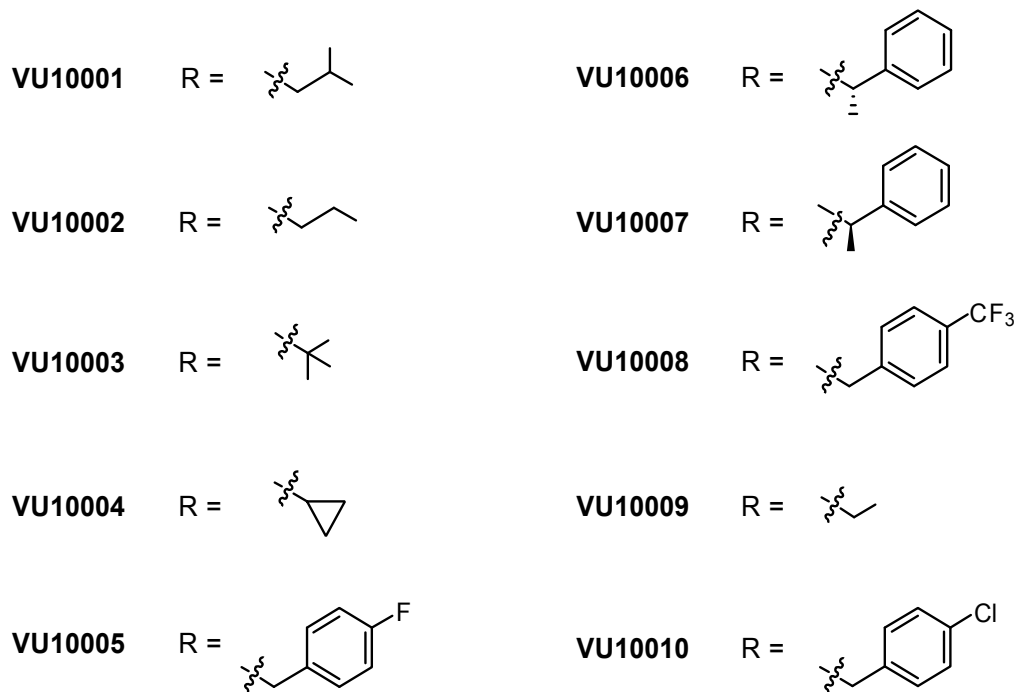
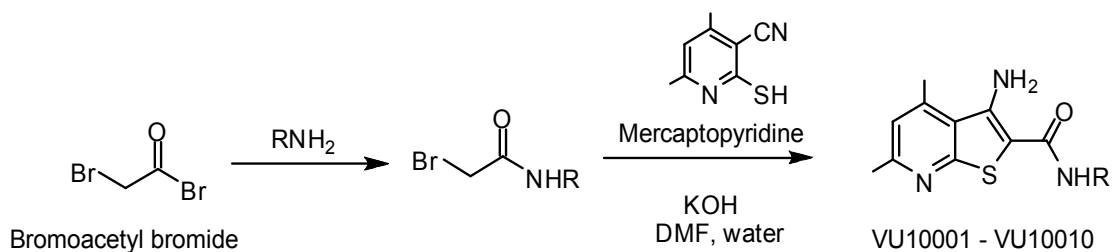


Figure 4. Synthesis of compounds in the VU10000 series. A collection of 10 amines were acylated with bromoacetyl bromide to give the corresponding bromo amides. Subsequent alkylation and cyclization of mercaptopyridine with the bromo amides using KOH provided compounds VU10001-VU10010. Syntheses performed by D. Orton and R. Williams.

Characterization of novel compounds in the VU10000 series

To test this small library of ten compounds for rM4 allosteric potentiator activity, functional experiments identical to the ones described above were performed. **Fig. 5** shows the response of cells expressing rM4 and Gqi5 to an EC₂₀ concentration of ACh in the presence of either vehicle (EC₂₀ grey bar) or test compound (black bars) as compared to the maximum response to 10 μM ACh after pre-incubation with vehicle (white bar). All compounds except VU10007 showed allosteric potentiator activity; VU10005, VU10008, and VU10010 caused the largest potentiation of the EC₂₀ response and these compounds were selected for further testing. CRCs of these potentiators showed that all three compounds have submicromolar potencies; compounds VU10005, VU10008, and VU10010 have EC₅₀ values of 300 ± 75 nM, 715 ± 160 nM, and 400 ± 100 nM, respectively (**Fig. 5b**). When comparing the rM4 ACh CRC in the presence of either vehicle or 10 μM test compound, we found VU10010 to be the most robust allosteric potentiator as is shown by the 47-fold shift in the ACh EC₅₀ (**Fig. 5c**). The EC₅₀ value of ACh was 33 ± 9 nM in the absence of VU10010 and 0.7 ± 0.2 nM in the presence of this compound. All three lead compounds in the VU10000 series produced greater leftward shifts in the functional rM₄ response to ACh than the best lead compound from the ChemBridge library, compound 7912361, which induced a 21-fold increase in ACh potency (**Fig. 3 and 5**). Compounds VU10005 and VU10008 produced 30- and 37-fold leftward shifts in the curve, respectively. From these data, we concluded that VU10010 had the best combination of potency and efficacy of all compounds tested, and we chose this allosteric potentiator for use in all subsequent experiments. The next critical step

was to confirm that VU10010 maintained the high degree of subtype selectivity that was shown for compounds in the ChemBridge series.

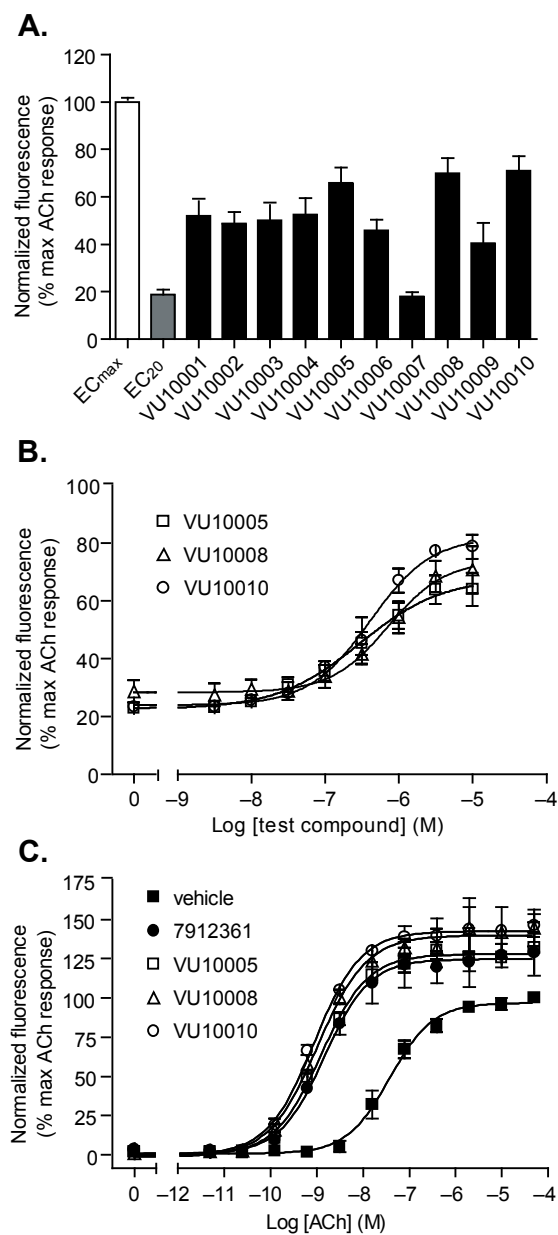


Figure 5. Chemical optimization generates compounds that potentiate M₄-mediated calcium mobilization with greater efficacy than lead compound 7912361. **A.** Nine of the ten compounds synthesized and tested showed allosteric potentiator activity (black bars) compared to the ACh EC₂₀ control (grey bar). Data were normalized to the maximal response to 10 μM ACh (white bar). Bars represent the mean ± S.E.M. of five independent experiments, each performed in triplicate. **B.** The three compounds that showed the highest degree of potentiation in panel (A.) were further characterized to determine their potencies. As shown by their CRCs, all three compounds have potencies in the submicromolar range. **C.** When compared to compound 7912361, all three lead compounds in this series induced a more robust leftward shift in the rM₄ ACh CRC as well as a larger increase in the maximal response. Points represent mean ± S.E.M. (*n* = 3).

Figure 6 shows that the response to ACh in cell lines expressing each of the other mAChR subtypes is unaffected in the presence of a maximal (10 μ M) concentration of VU10010 when compared to vehicle control. To further investigate the functional selectivity of this allosteric potentiator, we performed parallel experiments with cells expressing two unrelated receptors. The family I/A GPCR P2Y1 is a $G\alpha_q$ -coupled receptor endogenously expressed in rM₄-CHO cells that, when activated by ATP, stimulates intracellular calcium mobilization. The family III/C GPCR mGluR5 also activates PLC β via $G\alpha_q$ to cause calcium release from intracellular stores upon stimulation by glutamate. VU10010 (10 μ M) had no agonist, antagonist, or allosteric potentiator activity at P2Y1R or mGluR5 (**Fig. 7**).

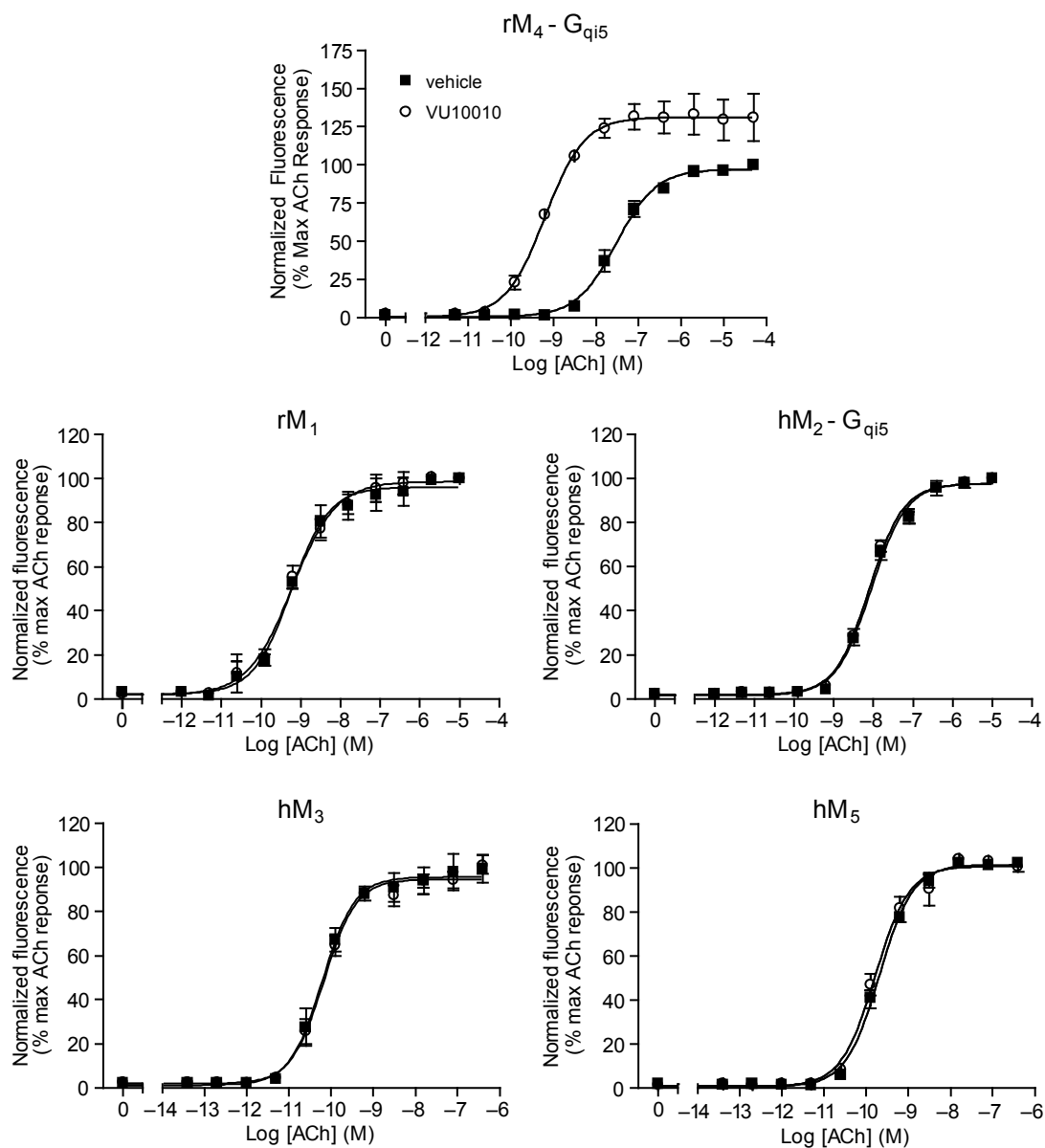


Figure 6. VU10010 is selective for the rM₄ receptor relative to the other mAChRs. VU10010 showed no activity at rM₁, hM₂, hM₃, or hM₅ compared to the robust potentiation of rM₄ where preincubation with 10 μ M VU10010 (\circ) causes a 47-fold decrease in the ACh EC₅₀. Points represent mean \pm S.E.M. ($n = 3$).

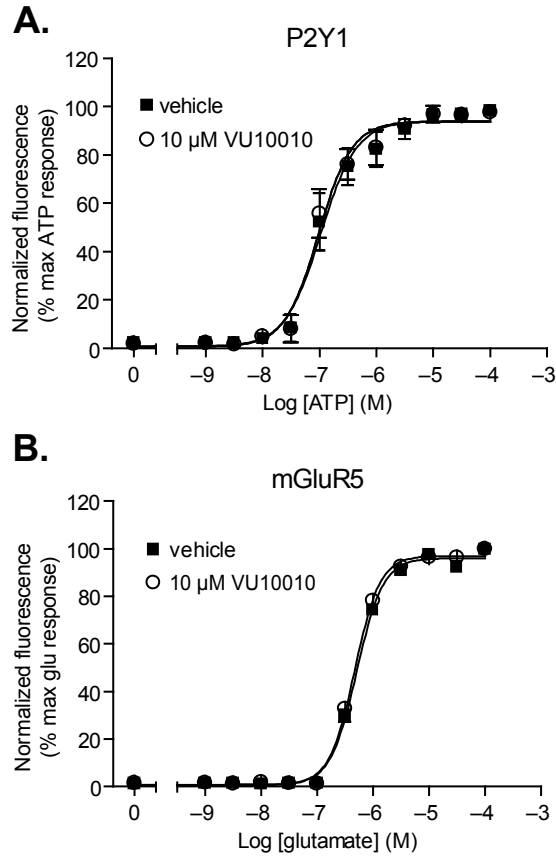


Figure 7. VU10010 showed no agonist, antagonist, or potentiator activity at two GPCRs unrelated to m_4 mAChR. Agonist CRCs from cells expressing the ATP receptor, P2Y1 (**A.**), or the metabotropic glutamate receptor, mGluR5 (**B.**), were overlapping in the presence of 10 μ M VU10010 (\circ) compared to vehicle control. Data points represent mean \pm S.E.M. ($n = 3$).

VU10010 binds allosterically and increases M₄ receptor affinity for ACh

In order to determine the effects of VU10010 on orthosteric binding and to further confirm an allosteric mechanism of binding, we performed equilibrium radioligand binding studies. Membranes prepared from cells expressing rM₄ were incubated with a non-saturating concentration of the orthosteric site antagonist [³H]NMS (0.1 nM) in the absence or presence of increasing concentrations of either atropine or VU10010. Consistent with atropine's high affinity at the orthosteric site, this compound displaced [³H]NMS binding with an K_i value of 0.52 ± 0.23 nM. In contrast, VU10010 did not displace [³H]NMS binding at concentrations up to 30 μM, which is 75 times the EC₅₀ value of this compound at potentiating responses to ACh (**Fig. 8**). While this finding does not exclude the possibility that VU10010 could alter [³H]NMS binding under some conditions, it provides strong support for the functional data and further suggests that VU10010 acts at a site on the M₄ receptor that is distinct from the orthosteric antagonist/agonist binding site. To further confirm that VU10010 is selective for M₄ relative to other mAChRs, we performed parallel binding experiments using membranes from cell lines expressing rM₁, rM₂, rM₃, and rM₅. As shown in **Fig. 9**, this compound does not displace [³H]NMS binding at any mAChR subtype. The [³H]NMS K_d, B_{max}, and atropine K_i values for each mAChR from saturation and competition binding experiments are listed in **Table 4**.

Table 4. Radioligand binding parameters for mAChR-expressing cell lines.

	[³H]NMS K_d (nM)	B_{max} (fmol/mg)	Atropine K_i (nM)
rM₁	0.131 ± 0.004	509 ± 12	0.79 ± 0.14
hM₂	0.296 ± 0.018	892 ± 60	1.45 ± 0.18
hM₃	0.109 ± 0.004	2313 ± 57	0.80 ± 0.07
rM₄	0.046 ± 0.004	247 ± 15	0.52 ± 0.23
hM₅	0.264 ± 0.006	968 ± 32	0.86 ± 0.07

[³H]NMS K_d and B_{max} for each receptor subtype were determined from saturation binding experiments. K_i values for atropine were determined based on competition with 0.1 nM [³H]NMS at each mAChR. Values are mean ± S.E.M (*n* = 3).

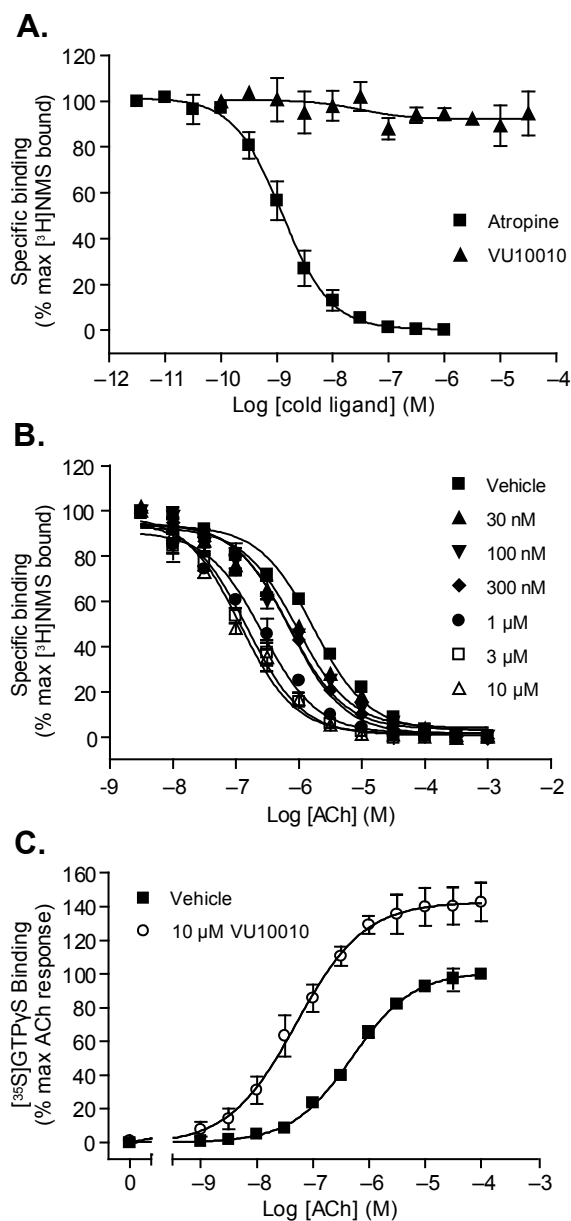


Figure 8. Compound VU10010 binds to an allosteric site on M₄ mAChR and causes an increase in affinity for ACh and M₄-mediated [³⁵S]GTPγS binding. **A.** Binding of 0.1 nM [³H]NMS was displaced by atropine (■, K_i = 0.52 ± 0.23 nM) but not by VU10010 (▲). Data are from three independent experiments performed in triplicate. Error bars are S.E.M. **B.** In a dose-dependent manner, VU10010 shifted the ACh competition curve leftward causing a 14-fold decrease in the K_i at maximal concentration of 10 μM (Δ). Data are mean ± S.E.M. (n = 3). **C.** VU10010 potentiates the response to ACh in membranes from cells expressing rM₄. VU10010 (○, 10 μM) induced a 10-fold decrease in the ACh EC₅₀ when compared to vehicle control (■). The leftward shift in the CRC was also accompanied by a 43 ± 12% increase in the maximal response. Data represent mean ± S.E.M. (n = 3).

One possible mechanism by which a compound could enhance receptor activation by an agonist is by increasing the receptor's affinity for that agonist (Christopoulos and Kenakin, 2002). As shown in **Fig. 8**, compound VU10010 does in fact induce a concentration-dependent shift in the potency of ACh at displacing rM₄ [³H]NMS binding. At 10 μM, a concentration that causes maximal potentiation, VU10010 increased the apparent affinity of ACh 14-fold. Thus, the K_i value for ACh at the orthosteric site decreased from 540 ± 72 nM in the absence of VU10010 to 39 ± 7 nM in the presence of 10 μM VU10010. These data suggest that this compound binds to an allosteric site on M₄ mAChR and shifts the receptor into a conformation that has higher affinity for ACh.

VU10010 enhances M₄ coupling to downstream effector proteins

The finding that VU10010 increases affinity of ACh for the orthosteric site suggests that this contributes to the ability of this compound to potentiate responses to ACh. However, the magnitude of this shift (14-fold) is not sufficient to account for the magnitude of the shift in the ACh potency at increasing calcium mobilization (47-fold). Also, the shift in agonist potency was also accompanied by an increase in agonist maximal response which cannot be explained by an increase in affinity alone. Thus, we examined the effect of VU10010 on the ability of M₄ to increase activation of G proteins by measuring effects of this compound on ACh-induced increases in guanosine 5'-O-(3-[³⁵S]thiotriphosphate ([³⁵S]GTPγS) binding. To assess this, the effect of increasing concentrations of ACh on [³⁵S]GTPγS binding to membranes from rM₄-CHO cells was measured in the absence and presence 10 μM compound VU10010. Compound VU10010 shifted the CRC of ACh at increasing [³⁵S]GTPγS binding to the left and also

increased maximal [³⁵S]GTPγS binding by roughly 50% (**Fig. 8**). Thus, the EC₅₀ value for ACh was 514 ± 82 nM in the absence of VU10010 and 51 ± 11 nM in the presence of this compound. These data are consistent with the hypothesis that the allosteric potentiator not only increases affinity of the receptor for agonist but also increases coupling efficiency and efficacy.

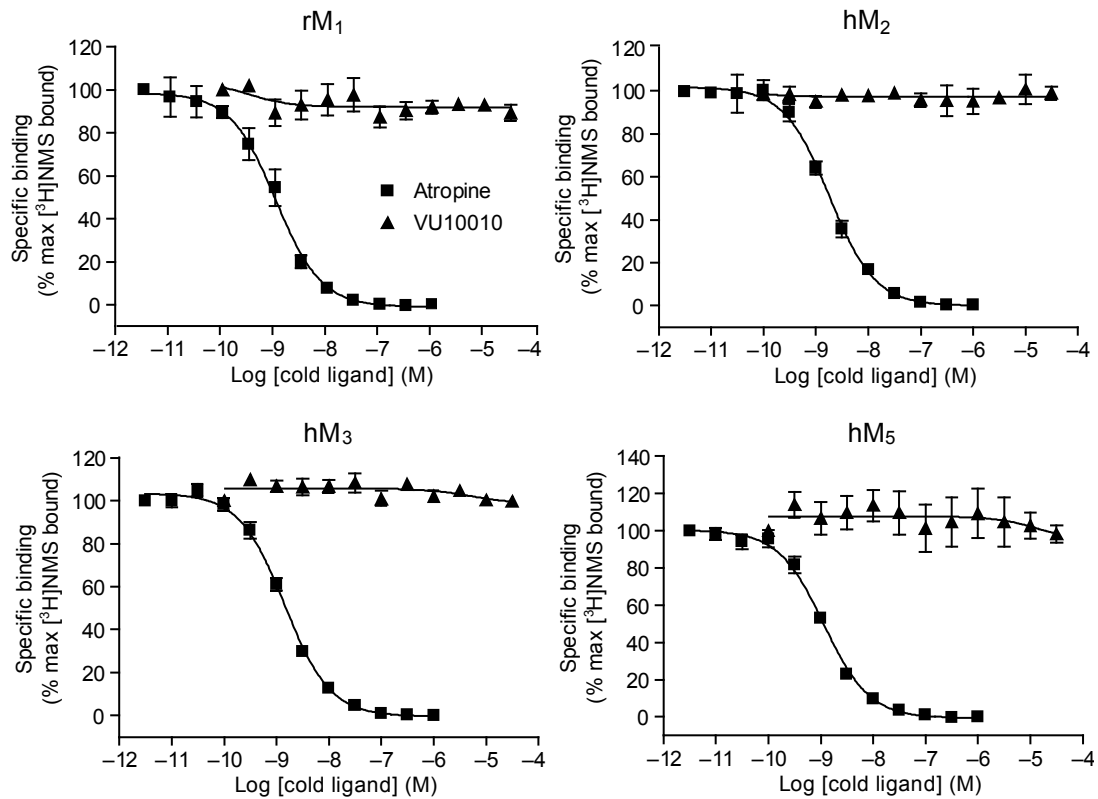


Figure 9. VU10010 does not compete for binding at rat M₁, M₂, M₃, or M₅. Binding of 0.1 nM [³H]NMS was displaced by atropine (■) but not by VU10010 (▲). Data are from three independent experiments performed in triplicate, and error bars are S.E.M.

VU10010 enhances muscarinic depression of excitatory post synaptic currents in hippocampal CA1 pyramidal cells

Discovery of novel highly selective and potent allosteric potentiators of M₄ provides an unprecedented opportunity to begin functional studies aimed at determining the physiological roles of this receptor subtype in native preparations. One of the most prominent effects of mAChR activation that is seen in a variety of forebrain and cortical regions is depression of transmission at excitatory glutamatergic synapses; in addition, muscarinic agonists can reduce transmission at inhibitory GABAergic synapses in these same circuits (Valentino and Dingledine, 1981; Bilkey and Goddard, 1985; Sheridan and Sutor, 1990; Pitler and Alger, 1994; Qian and Saggau, 1997; Fernandez de Sevilla and Buno, 2003). However, the lack of subtype-selective ligands for specific mAChR subtypes has made it impossible to definitively determine which mAChR subtypes mediate each of these effects. Thus, we determined the effect of VU10010 on the ability of the non-selective mAChR agonist, carbachol (CCh), to reduce excitatory and inhibitory transmission at the Schaffer collateral-CA1 synapse in the rat hippocampus. Consistent with previous findings, CCh reversibly inhibited evoked EPSCs at Schaffer-collateral-CA1 synapses in a concentration-dependent manner (**Fig. 10**). CCh at 100 μ M caused a marked reduction of EPSCs (16.1 ± 4.0 % of control value, $n = 5$, **Fig. 10**), whereas at a sub-maximal concentration of 1 μ M, CCh induced a relatively small reduction of EPSCs (60.5 ± 4.1 % of control value, $n = 15$; **Fig. 10**). In contrast, VU10010 (5 μ M) had no effect on excitatory transmission at this synapse when added alone (EPSC amplitude 107.9 ± 5.2 % of the control, $P = 0.16$, $n = 7$; **Fig. 10**). However, when VU10010 (5 μ M) was co-applied with a sub-maximal concentration of CCh (1 μ M), this compound increased the CCh-induced reduction of EPSCs (36.9 ± 5.7 % of control, $n = 7$,

Fig. 10) when compared to the effect of 1 μM CCh alone ($60.5 \pm 4.1\%$ of control value, $n = 15$; $P = 0.0038$, **Fig. 10**). Thus, VU10010 potentiates CCh-induced inhibition of excitatory synaptic transmission at this critical synapse in the hippocampus. As a negative control, we used VU10007, a closely related analog of VU10010 that is completely inactive as an allosteric potentiator of M_4 in cell-based assays (see **Fig. 5**). VU10007 (5 μM) had no effect on the CCh-induced reduction of EPSCs ($61.6 \pm 5.0\%$ of control value, $n = 7$, **Fig. 10**); compared to $60.5 \pm 4.1\%$ of control value by CCh alone, $n = 15$; $P = 1$). These results suggest that M_4 is one of the mAChRs involved in the regulation of excitatory synaptic transmission at Schaffer collateral-CA1 synapses.

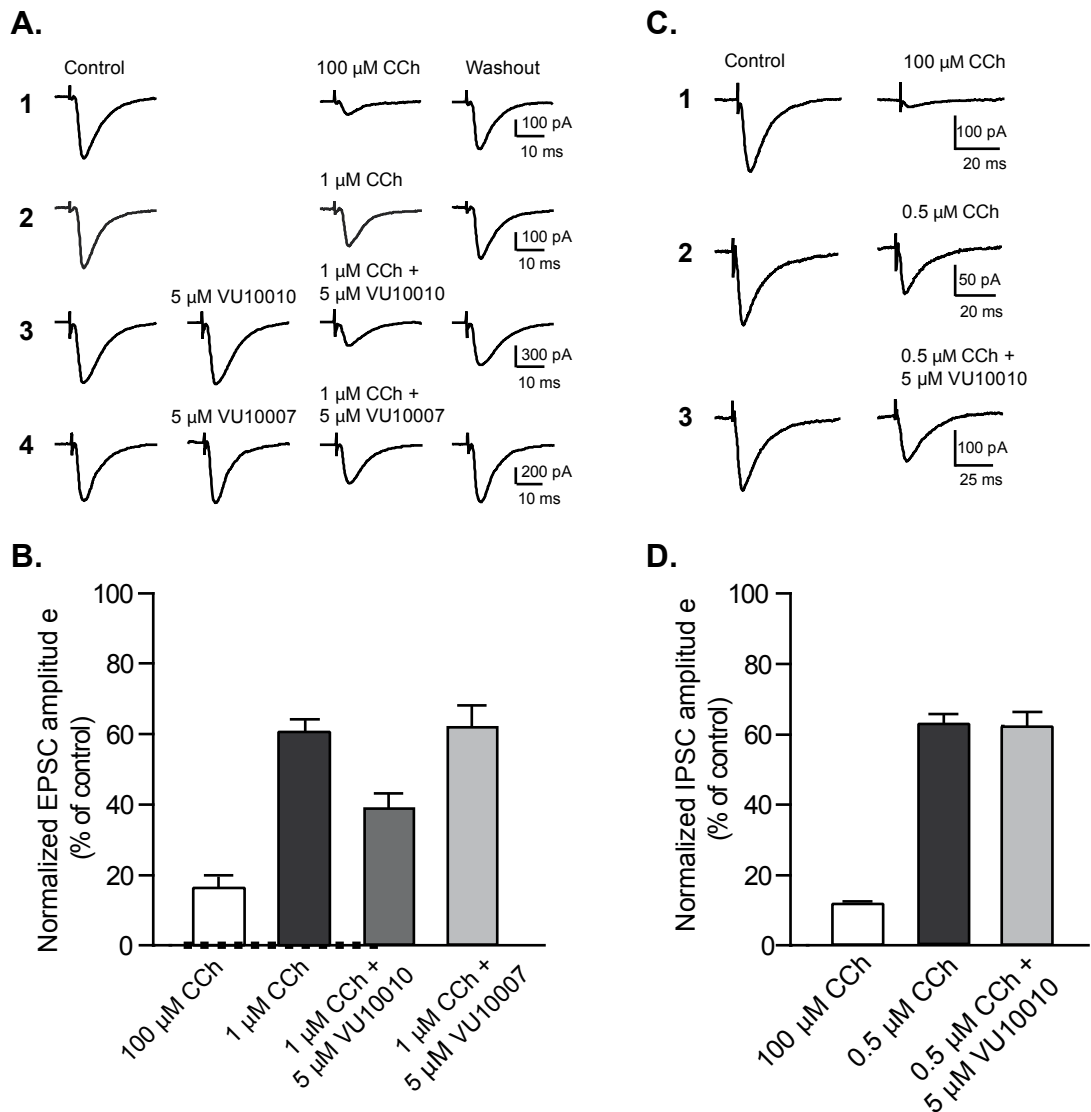


Figure 10. VU10010 potentiates CCh-induced reduction of EPSCs but not IPSCs at rat hippocampal Shaffer collateral-CA1 synapses. **A.** Averaged EPSCs obtained from experiments in which the effects of the following reagents on EPSC amplitude were examined: 100 μ M CCh (**A1**), 1 μ M CCh (**A2**), 1 μ M CCh with 5 μ M VU10010 (**A3**), 1 μ M CCh with 5 μ M VU10007 (an inactive analog of VU10010, **A4**). **B.** Bar graph summarizing the potentiation effect of VU10010 on CCh-induced reduction of EPSCs. Data represent mean \pm S.E.M. **C.** Averaged IPSCs obtained from experiments in which the effects of the following reagents on IPSC amplitude were examined: 100 μ M CCh (**C1**), 0.5 μ M CCh (**C2**) and 0.5 μ M CCh with 5 μ M VU10010 (**C3**). **D.** Bar graph summarizing the effect of VU10010 on CCh-induced reduction of IPSCs in CA1 pyramidal cells. Data are shown as mean \pm S.E.M. Experiments performed by Z. Xiang.

Muscarinic depression of inhibitory post synaptic currents is not affected by M₄ potentiation

Muscarinic receptors also play a role in regulating inhibitory synaptic transmission in hippocampal CA1 pyramidal cells (Valentino and Dingledine, 1981; Pitler and Alger, 1994). Consistent with previous studies, we found that application of 100 μ M CCh greatly reduced monosynaptic IPSC amplitude to $10.9 \pm 0.9\%$ of control value ($n = 3$, **Fig. 10**), and a sub-maximal concentration of CCh (0.5 μ M) caused a smaller reduction of IPSC amplitude ($62.2 \pm 3.5\%$ of control, $n = 6$, **Fig. 10**). Application of the M₄ potentiator VU10010 (5 μ M) alone had no effect on IPSC amplitude (98.5 ± 1.7 of control, $n = 4$, $P = 0.875$). Furthermore, VU10010 (5 μ M) had no effect on the depression of IPSCs induced by 0.5 μ M CCh ($61.7 \pm 3.9\%$ with CCh and VU10010, $n = 6$, versus $62.2 \pm 3.5\%$ with CCh alone, $n = 6$, $P = 0.82$; **Fig. 10**). These results indicate that M₄ mAChRs are probably not involved in muscarinic modulation of inhibitory synaptic transmission in CA1 pyramidal cells. To further test this hypothesis, we compared the effect of sub-maximal concentration of CCh on IPSCs in hippocampal CA1 pyramidal cells in M₄ knockout and WT mice. At 2 μ M, CCh caused a reduction of IPSCs with a comparable magnitude in both WT and M₄ KO mice ($56.0 \pm 4.6\%$ and $60.2 \pm 2.7\%$ of control values, $n = 6$ and $n = 6$, respectively; $P = 0.48$, **Fig. 11**). While these data do not completely rule out a role for M₄ in regulating IPSCs in WT animals, the data are consistent the hypothesis that M₄ mAChRs are not involved in modulation of inhibitory synaptic transmission in CA1 pyramidal cells.

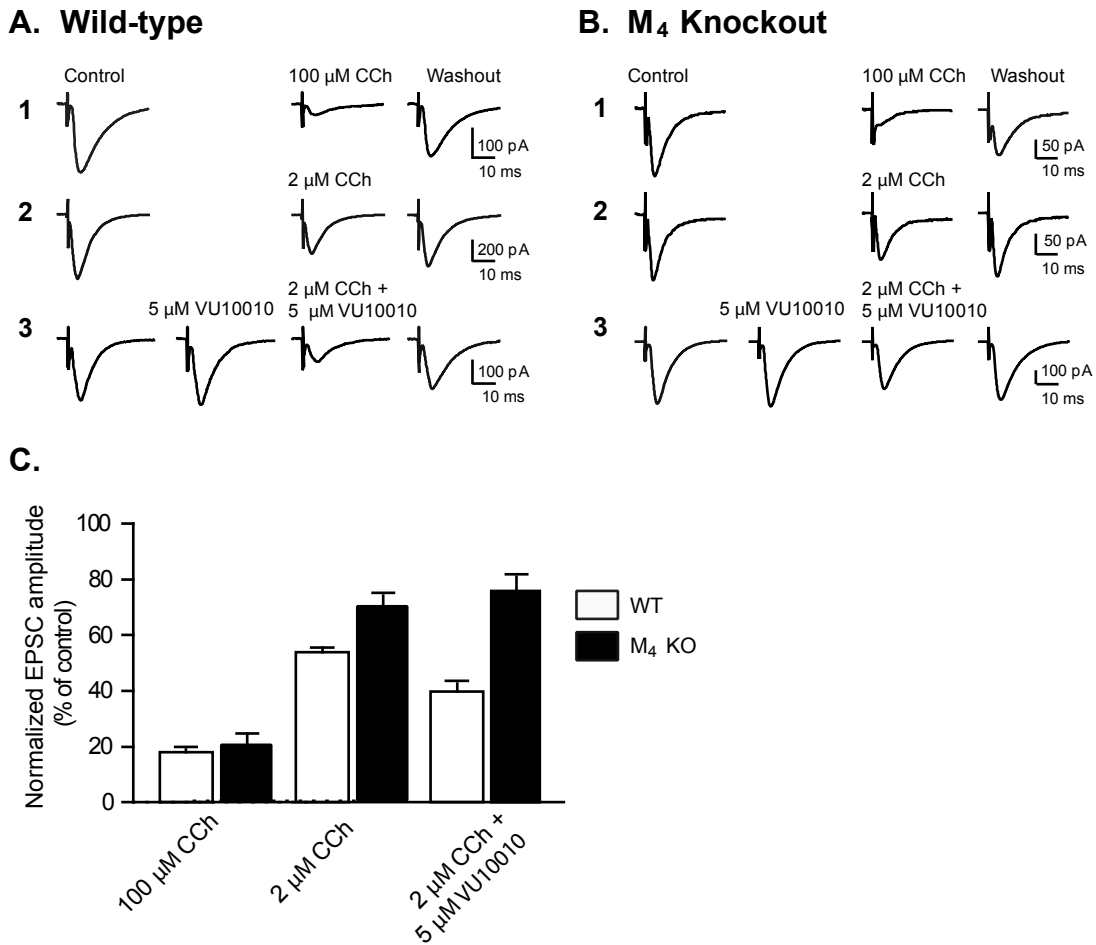


Figure 11. VU10010 potentiates CCh-induced reduction of EPSCs in wild-type (WT) but not in M₄ KO mice. **A.** Averaged EPSCs obtained from experiments in which the effects of the following reagents on EPSC amplitude in WT mice were examined: 100 μM CCh (**A1**), 2 μM CCh (**A2**), and 2 μM CCh with 5 μM VU10010 (**A3**). **B.** Averaged EPSCs obtained from experiments in which the effects of the same reagents on EPSC amplitude in M₄ KO mice were examined: 100 μM CCh (**B1**), 2 μM CCh (**B2**), and 2 μM CCh with 5 μM VU10010 (**B3**). **(C)** Bar graph summarizing the effect of VU10010 on CCh-induced reduction of EPSCs in WT mice (white bars) and M₄ KO mice (black bars). Data represent mean ± S.E.M. Experiments performed by Z. Xiang and J.E. Ayala.

VU10010 potentiates CCh-induced reduction of EPSCs in wild-type (WT) but not in M₄ knockout (KO) mice

To confirm that the potentiation effect of VU10010 on CCh-induced reduction of EPSCs was due to its action on M₄ receptors, we examined the effect of VU10010 in M₄ KO mice (Gomez et al., 1999). As a control, we first assessed the effect of VU10010 in WT mice of the same mixed genetic background as the M₄ KO mice. Similar to the result obtained from rats, CCh at 100 μ M caused a sizable reduction of EPSCs at Schaffer collateral-CA1 synapses in WT mice (18.0 ± 0.9 % of control value, $n = 6$, **Fig. 11**), whereas at a sub-maximal concentration of 2 μ M, CCh induced a smaller inhibition of EPSCs (53.7 ± 1.4 % of control, $n = 6$; **Fig. 11**). Compound VU10010 (5 μ M) had no effect on excitatory transmission at this synapse when added alone (EPSC amplitude 102.5 ± 3.8 % of the control, $P = 0.31$, $n = 5$; **Fig. 11**). However, when co-applied with 2 μ M CCh, VU10010 (5 μ M) significantly enhanced the CCh-induced reduction of EPSCs (39.8 ± 2.7 % of the control, $n = 5$, **Fig. 11**) when compared to the effect of 2 μ M CCh alone (54.7 ± 1.1 % of control, $n = 5$; $P = 0.0079$, **Fig. 11**).

In M₄ KO mice, application of 100 μ M CCh decreased the EPSC amplitude to 21.1 ± 3.8 % of control value ($n = 6$, **Fig. 11**), whereas at the sub-maximal concentration of 2 μ M, CCh induced a relatively small suppression of EPSCs (70.8 ± 3.6 % of control value, $n = 9$; **Fig. 11**), which was significantly different than the reduction of EPSCs caused by 2 μ M CCh in WT mice (53.7 ± 1.4 % of control, $n = 6$; $P = 0.0076$, **Fig. 11**). Furthermore, when compound VU10010 was co-applied with 2 μ M CCh, it failed to potentiate the CCh-induced reduction of EPSCs in M₄ KO mice (77.5 ± 4.6 % of control value, $n = 7$, **Fig. 11**) when compared to the effect of 2 μ M CCh alone (70.8 ± 3.6 % of control value, $n = 9$; $P = 0.14$, **Fig. 11**). These data support the conclusion that the

potentiation of CCh-induced reduction of EPSCs by VU10010 is solely due to its action on M₄ receptors and that M₄ participates in the muscarinic modulation of these synaptic responses.

Discussion

Over the past two decades, major attention has been focused on developing highly selective agonists of specific mAChR subtypes to use as research tools in order to achieve a better understanding of the roles of each subtype in specific organ systems and also to develop therapeutic agents that lack the adverse effects of AChE inhibitors and nonselective muscarinic agents. However, the muscarinic receptor agonists developed to date lack true specificity for individual muscarinic receptor subtypes. This thesis chapter reports the discovery of a novel series of compounds that act as robust positive allosteric modulators (allosteric potentiators) of the M₄ mAChR subtype. These compounds are highly selective for M₄ and have no detectable activity at any other mAChR subtype. As with previously discovered allosteric potentiators of metabotropic glutamate receptors (mGluRs), the novel positive allosteric modulators of M₄ reported here have no detectable affinity for the orthosteric site on M₄. The action of these compounds at a site that is distinct from the highly conserved orthosteric ACh binding site is likely to be critical for achieving this high degree of subtype selectivity.

Interestingly, the M₄ allosteric potentiator reported here increases affinity of ACh for the orthosteric site. This is similar to previous reports of allosteric modulators of GPCRs acting by altering affinity of ligands at the orthosteric site; the magnitude of binding cooperativity or the shift in orthosteric agonist affinity is referred to as the alpha

factor (Christopoulos and Kenakin, 2002). However, while VU10010 apparently acts in part by increasing ACh affinity, the magnitude of this effect was only a 14-fold increase in ACh affinity whereas VU10010 induced an almost 50-fold shift in the ACh concentration response curve for activating calcium mobilization. Thus, effects on agonist binding cannot fully account for the allosteric potentiator activity measured in the functional assay; potentiation by this compound must also increase efficacy and coupling to downstream effectors. The present data suggest that VU10010 acts by both increasing ACh affinity and also through a positively cooperative interaction with ACh for activation of G proteins and downstream signaling pathways. Studies of the effects of VU10010 on [³⁵S]GTPγS binding revealed a 10-fold shift in ACh potency; this value is close to the calculated shift in ACh affinity at the orthosteric site, suggesting that the increase in ACh affinity could account for the shift in ACh potency at increasing G protein activation. However, VU10010 also increased the maximal ACh-induced [³⁵S]GTPγS binding response, suggesting that this potentiator increases the efficiency of M₄ coupling to G proteins. These two factors together likely contribute to the robust shift in ACh potency for inducing calcium mobilization relative to more modest shift observed in ACh affinity.

Discovery of a highly selective allosteric modulator of M₄ provides an unprecedented opportunity to selectively increase activity of this receptor and develop a more detailed understanding of the functional roles of M₄ in brain circuits that are heavily modulated by cholinergic innervation. One of the most important roles of cholinergic systems in the CNS is modulation of transmission through the hippocampal formation, a limbic cortical structure that plays a critical role in learning and memory and is thought to

be important for cholinergic regulation of cognitive function. Activation of mAChRs in the hippocampus induces a marked reduction of transmission at both excitatory glutamatergic and inhibitory GABAergic synapses by presynaptic reduction of neurotransmitter release (Valentino and Dingledine, 1981; Bilkey and Goddard, 1985; Fernandez de Sevilla and Buno, 2003). Multiple mAChR subtypes are expressed in the hippocampus, and evidence suggests that both M_2 and M_4 are localized in presynaptic terminals where they could regulate excitatory and inhibitory synaptic transmission (Levey et al., 1995; Rouse et al., 1999; Rouse et al., 2000a). In addition, evidence suggests that activation of postsynaptic mAChRs on hippocampal pyramidal cells where M_1 and M_4 are expressed could reduce synaptic transmission in the hippocampus by inducing release of endocannabinoids that activate presynaptic CB1 cannabinoid receptors (Ohno-Shosaku et al., 2003). Thus, the specific mAChR subtypes involved in regulating transmission at these important synapses has not been clear. The present finding that VU10010 potentiates effects of mAChR agonists on excitatory but not inhibitory synaptic transmission provides strong evidence that M_4 is one of the mAChR subtypes responsible for regulating transmission at glutamatergic synapses in the hippocampus but is not likely to be involved in regulation of transmission at inhibitory synapses in this brain region. This selective regulation of excitatory synaptic transmission is a first critical step in developing a detailed understanding of the roles of M_4 in modulating hippocampal function. In future studies, it will be important to take advantage of this novel class of allosteric potentiators to further investigate the roles of M_4 in hippocampus as well as other cortical and basal ganglia structures where this receptor has been postulated to play a critical neuromodulatory role. Also, it will be

important to further optimize these compounds for use as tools that will provide a path for developing an understanding of the impact of selectively increasing M₄ activation *in vivo*.

CHAPTER IIIB

CENTRALLY ACTIVE ALLOSTERIC POTENTIATORS OF THE M₄ MUSCARINIC ACETYLCHOLINE RECEPTOR REVERSE AMPHETAMINE-INDUCED HYPERLOCOMOTOR ACTIVITY IN RATS

Introduction

To date, five muscarinic acetylcholine receptor (mAChR) subtypes have been identified (M₁-M₅) and play important roles in mediating the actions of ACh in the peripheral and central nervous systems (Wess, 1996). Of these, M₁ and M₄ are the most heavily expressed in the CNS and represent attractive therapeutic targets for cognition, Alzheimer's disease (AD) and schizophrenia (Bymaster et al., 2002; Messer, 2002; Raedler et al., 2007). In contrast, the adverse effects of cholinergic agents are thought to be primarily due to activation of peripheral M₂ and M₃ mAChRs (Bymaster et al., 2003b; Bymaster et al., 2003a). Due to the high sequence homology and conservation of the orthosteric ACh binding site among the mAChR subtypes, development of chemical agents that are selective for a single subtype has been largely unsuccessful, and in the absence of highly selective activators of M₄, it has been impossible to test the role of selective M₄ activation. Clinical trials with xanomeline (**Fig. 12**), an M₁/M₄ preferring orthosteric agonist, demonstrated efficacy as both a cognition enhancing agent, and as an antipsychotic agent (Bodick et al., 1997b; Shekhar et al., 2001; Shekhar et al., 2008). In follow-up studies in rats, xanomeline displayed an antipsychotic-like profile comparable to clozapine (Stanhope et al., 2001). However, a long standing question concerned whether or not the antipsychotic efficacy or antipsychotic-like activity in animal models

is mediated by activation of M₁, M₄, or a combination of both receptors. Data from mAChR knock-out mice led to the suggestion that a selective M₁ agonist would be beneficial for cognition, whereas an M₄ agonist would provide antipsychotic activity for the treatment of schizophrenia (Felder et al., 2001; Bymaster et al., 2003b; Bymaster et al., 2003a). This proposal is further supported by recent studies demonstrating that M₄ receptors modulate the dynamics of cholinergic and dopaminergic neurotransmission and that loss of M₄ function results in a state of dopamine hyperfunction (Tzavara et al., 2004). These data, coupled with findings that schizophrenic patients have altered hippocampal M₄, but not M₁, receptor expression (Scarr et al., 2007) suggest that selective activators of M₄ may provide a novel treatment strategy for schizophrenia patients. However, multiple studies suggest that M₁ may also play an important role in the antipsychotic effects of mAChR agonists and the relative contributions of M₁ and M₄ to the antipsychotic efficacy of xanomeline or antipsychotic-like effects of this compound in animal models are not known. Unfortunately, the lack of highly selective, systemically active activators of M₁ and M₄ has made it difficult to fully evaluate the effects of activation of these mAChR subtypes in animal models.

Recently, we reported discovery of a number of positive allosteric modulators for class C GPCRs that bind to allosteric sites, provide high levels of subtype selectivity and display behavioral effects *in vivo* comparable to direct acting agonists (O'Brien et al., 2003; Lindsley et al., 2004; O'Brien et al., 2004; Kinney et al., 2005; Galici et al., 2006; Hemstapat et al., 2006; Marino and Conn, 2006; Zhao et al., 2007). In addition, we identified a highly selective positive allosteric modulator of M₄ termed VU10010 (**Fig. 12**) (Shirey et al., 2008). This compound induces a 47-fold potentiation of the M₄ ACh

concentration response curve (CRC), possesses an EC₅₀ in the 400 nM range and causes no activation of the other mAChR subtypes. Additional *in vitro* pharmacological characterization studies suggested that VU10010 binds to an allosteric site on the M₄ receptor to increase affinity for ACh and coupling to G proteins (Shirey et al., 2008). Subsequent studies with VU10010 revealed that selective potentiation of M₄ increased carbachol (CCh)-induced depression at excitatory, but not inhibitory, synapses and that the effect on excitatory currents was not mimicked by an inactive analog of VU10010 or in M₄ knock-out mice (Shirey et al., 2008).

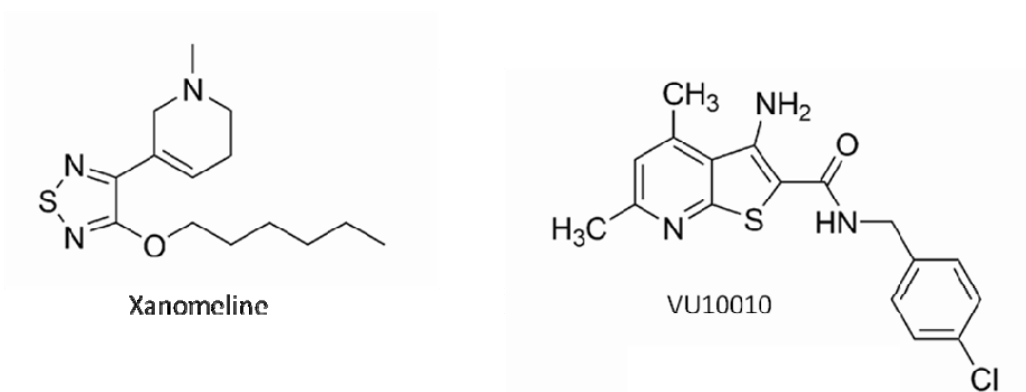


Figure 12. Chemical structures of Xanomeline [3-[3-hexyloxy-1,2,5-thiadiazol-4-yl]-1,2,5,6-tetrahydro-1-methylpyridine] and VU10010 [3-amino-*N*-(4-chlorobenzyl)-4,6-dimethylthieno[2,3-*b*]pyridine-2-carboxamide].

Despite this notable advance, VU10010 suffered from poor physicochemical properties ($\log P \sim 4.5$) and *in vivo* studies proved infeasible because we were unable to formulate VU10010 into a homogeneous solution in any acceptable vehicle, regardless of salt form or particle size. Several suspensions were prepared and dosed *i.p.*, but VU10010 was not found to be centrally active. In order to evaluate the role of selective

M₄ activation *in vivo*, VU10010 would require further chemical optimization. Here we report the development and characterization of two novel analogs of VU10010 that are CNS penetrant following systemic administration.

Results

Chemical Lead Optimization

For the chemical optimization of VU10010, we undertook a diversity-oriented synthesis (DOS) approach to explore Structure-Activity-Relationships (SAR) with a variety of hypothesis-driven, structural changes to the lead compound. The rationale for this approach for the optimization of VU10010 is that SAR for allosteric ligands is often ‘flat’ or ‘shallow’, with subtle structural modifications leading to a complete loss of activity, and often only one portion of an allosteric ligand is amenable to change. Therefore, a multi-dimensional, DOS library approach provides the best opportunity to quickly identify productive SAR as opposed to a lead optimization strategy based on classical, single compound synthesis (Lindsley et al., 2004; Zhao et al., 2007). One explanation for the lack of central activity observed with VU10010 could be the result of the poor physicochemical properties alone, or in combination with P-glycoprotein (P-gp) efflux. P-gp is an efflux transporter with broad substrate specificity present on the luminal membrane of epithelial cells comprising the blood-brain barrier, which is known to impair the brain penetrability of a number of drugs. The β -aminoamide motif 3 present in VU10010 represents a potential P-gp liability, which could be removed by cyclization to analogs such as **2** (**Fig. 13A**). Alternatively, P-gp susceptibility could also be

diminished by electronically attenuating the basicity of the amine moieties by the incorporation of distal fluorine atoms. Utilizing solution phase parallel synthesis (**Fig. 13B**), we synthesized small, 12- to 24-member focused libraries around each of the 10 scaffolds **4, 5-13** (**Fig. 13C**) which were then purified by mass-directed preparative HPLC to analytical purity (>98%). This collection of VU10010 analogs incorporated CF₃ moieties (scaffolds **7** and **8**) to electronically attenuate potential P-gp susceptibility, deletion of the β-amino moiety (scaffold **12**), or replacement of the β-amino moiety with an isosteric methyl group (scaffold **11**). Other scaffolds explored the deletion of substituents on the pyridine nucleus (**9**), incorporation of an additional nitrogen atom to afford a pyrimidine nucleus (**10**) or removal of the pyridine nitrogen atom in VU10010 (**13**). Finally, library **5** focused on maintaining the core structure of VU10010, but explored alternative amides, selected to improve physiochemical properties and lower the logP value.

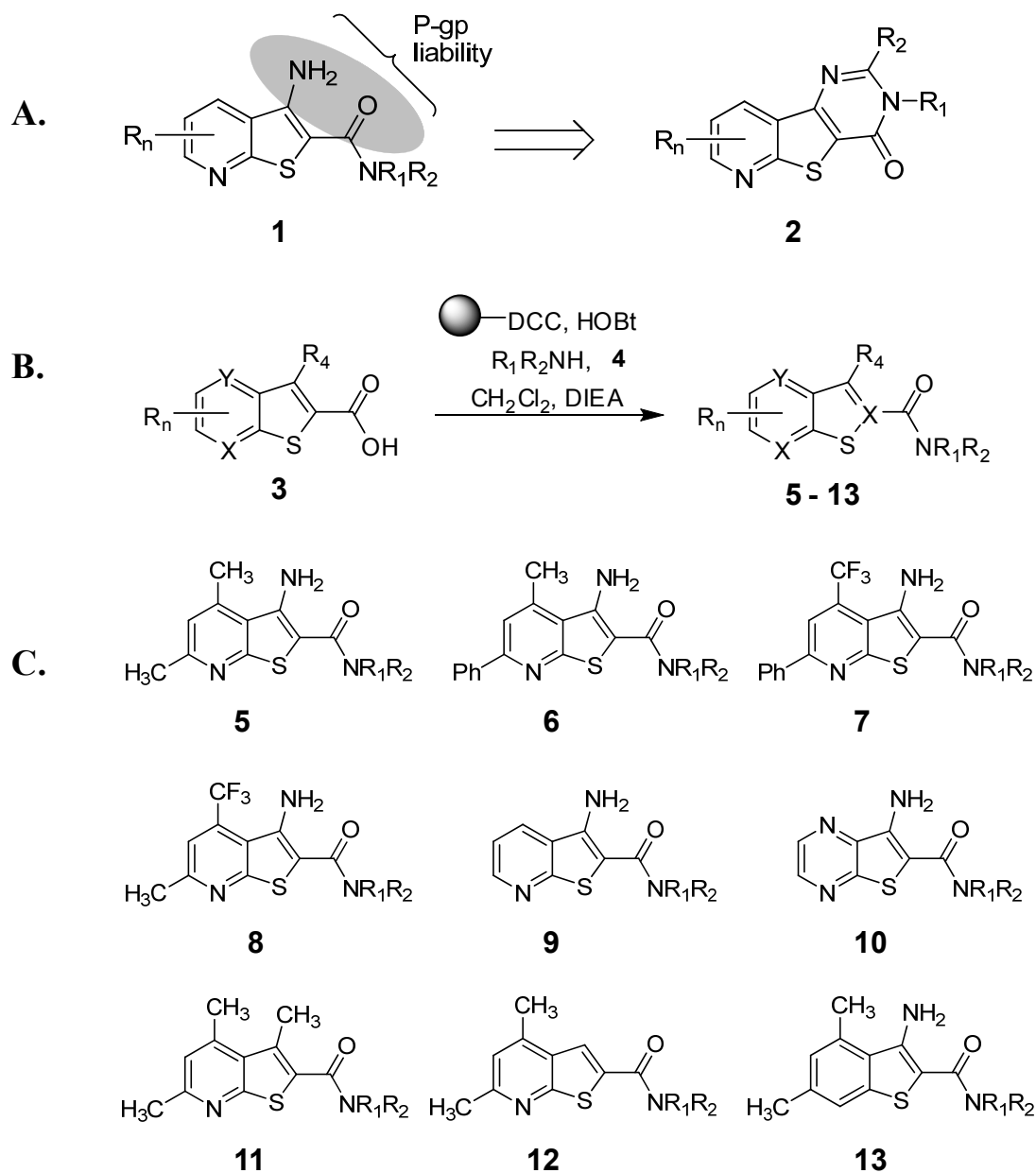


Figure 13. Chemical optimization of VU10010 using a diversity-oriented approach to achieve soluble, centrally penetrant M₄ positive allosteric modulators. **A.** β -aminoamide as a potential P-gp liability in series **1** and cyclization strategy to diminish this liability in series **2**. **B.** Solution phase parallel synthesis of libraries of VU10010 analogs. Commercial heterocyclic carboxylic acids **3** (X, Y = C or N) were coupled to 12 different amines (HNR₁R₂, **4**) to afford focused VU10010 analog libraries **5-13** in yields ranging from 15% to 99%. **C.** Generic structures of analogs of VU10010 evaluated in the chemical lead optimization program in an effort to develop soluble, centrally penetrant M₄ positive allosteric modulators. Syntheses performed by T.M. Bridges and J.P. Kennedy.

Screening Paradigm for Analog Libraries

As observed with positive allosteric modulators of Class C GPCRs, SAR around VU10010 was relatively flat, possibly due to a shallow binding pocket (Lindsley et al., 2004; Zhao et al., 2007). An EC₂₀ triage screen, employing a functional, fluorescence-based Ca²⁺ assay in CHO-K1 cells stably co-expressing the rat M₄ mACh receptor and the chimeric G protein, G_{qi5}, (**Fig. 14**) quickly eliminated all VU10010 analogs except those in library **5**. Within library **5**, all aliphatic and non-benzyl amides were inactive, and only benzyl and heteroaryl methyl congeners of VU10010, **5a-5p**, retained M₄ PAM activity (**Table 5**). Analogs were synthesized as described in the methods section (Chapter II). To identify compounds that potentiated agonist activation of M₄, we determined the response to an EC₂₀ concentration of ACh in the absence and presence of test compound. The potency of each compound was determined by pre-incubating cells with vehicle or increasing concentrations of test compound followed by the addition of an EC₂₀ concentration of ACh to yield concentration-response curves (CRCs). Subtle substitution changes on the arene ring lost activity 5-10-fold in terms of M₄ EC₅₀ and/or fold-shift of the ACh CRC (**Table 5**). For instance, **5d**, in which the 4-Cl moiety of VU10010 is moved to the 3-position results in a loss in potency of over 9-fold (EC₅₀ = 3.7 μM). Similarly, the unsubstituted phenyl congener **5a** retains M₄ PAM activity (EC₅₀ = 630 nM), but the fold-shift diminishes to 8.6-fold, *versus* the 47-fold shift observed for VU10010 (Shirey et al., 2008). In general, functionalized benzyl amides and pyridyl methyl congeners (**5f** and **5g**) were well tolerated, providing selective M₄ PAMs with EC₅₀ values ranging from 380 nM to 3.7 μM and with fold-shifts of the ACh dose-response curve from 8.6- to 70-fold (**Table 5**).

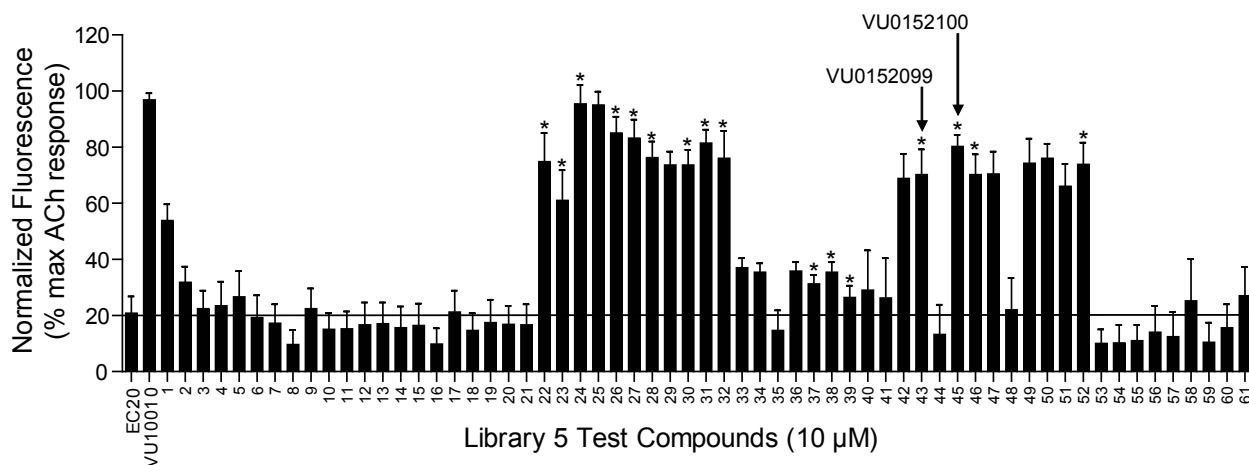
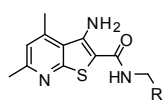
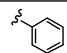
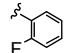
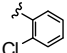
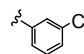
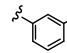
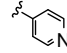
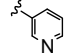
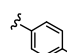
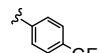
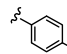
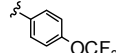
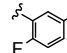
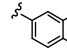
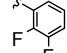
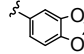
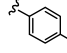


Figure 14. Screening paradigm for analog libraries 5-13 allowing for the rapid triage of inactive analogs. A representative library of 61 analogs from library 5 (Fig. 13C) were tested at a single concentration (10 μ M) for their ability to potentiate an EC₂₀ concentration of ACh in CHO-K1 cells stably co-expressing the rM₄ mAChR and the chimeric G protein, G_{qi5}. Calcium mobilization was measured using a Flexstation II, as described in Methods (Chapter II). Of those tested, 16 compounds (denoted by an asterisk) were selected for further evaluation. The response to an EC₂₀ concentration of ACh alone is shown in the bar on the far left and this level of activity is indicated by the solid line spanning the panel. Thus, test compounds increasing the % max ACh response above this level were considered potentiators of the rM₄ mAChR. VU10010 was included as a positive control. Bars represent the mean \pm S.E.M. of 3 or more determinations, each performed in duplicate. Experiments performed by A.E. Brady.

Table 5. Structures, activities, and ACh CRC fold-shifts of M₄ PAM library 5 analogs.



Library 5

Compound	R	rat M4 EC ₅₀ (μM)	rat M4 ACh fold-shift
5a		0.63	8.6
5b		0.83	11.8
5c		1.83	ND
5d		3.70	ND
5e		2.63	ND
5e		2.04	ND
5f		2.88	ND
5g		1.44	ND
5h		1.80	ND
5i		2.96	ND
5j		3.04	ND
5k		0.88	ND
5l		1.12	ND
5m		0.72	13.7
5n		0.40	29.7
5o		0.38	70.1

EC₅₀s and fold-shifts are an average of at least 3 determinations; ND, not determined.

Subtle substitution changes on the arene ring lost 5-10-fold in terms of M₄ EC₅₀ and/or fold-shift of the ACh CRC. For instance, **5d**, in which the 4-Cl moiety of VU100010 is moved to the 3-position results in a loss in potency of over 9-fold (EC₅₀ = 3.7 μM). Similarly, the unsubstituted phenyl congener **5a** retains M₄ PAM activity (EC₅₀ = 630 nM), but the fold-shift diminishes to 8.6-fold, *versus* the 47-fold shift observed for VU10010 (Shirey et al., 2008). Compounds **5o** (VU0152099) and **5p** (VU0152100) retained M₄ PAM activity comparable to VU10010 (EC₅₀ values of 403 ± 117 nM and 380 ± 93 nM, respectively).

VU0152099 and VU0152100 are Potent Positive Allosteric Modulators of M₄ in two independent *in vitro* assays

Two compounds were selected for further evaluation of their ability to potentiate the M₄-mediated calcium response. VU0152099 (**5o**, **Fig. 15A**) and VU0152100 (**5p**, **Fig. 15D**) retained M₄ PAM activity (EC₅₀ values of 403 ± 117 nM and 380 ± 93 nM, respectively) comparable to VU10010, and in the absence of an ACh EC₂₀, neither VU0152099 nor VU0152100 elicited a response (**Fig. 15B, E**). We next determined the effects of maximal concentrations of each compound on the CRC of ACh. Cells were pre-incubated with a fixed concentration (0.1 - 30 μM) of test compound and subsequently stimulated with increasing concentrations of ACh. Both VU0152099 and VU0152100 induced a dose-dependent leftward shift of the ACh CRC with maximal shifts of 30-fold observed with 30 μM VU0152099 (**Fig. 15C**) and 70-fold observed with 10 μM VU0152100 (**Fig. 15F**).

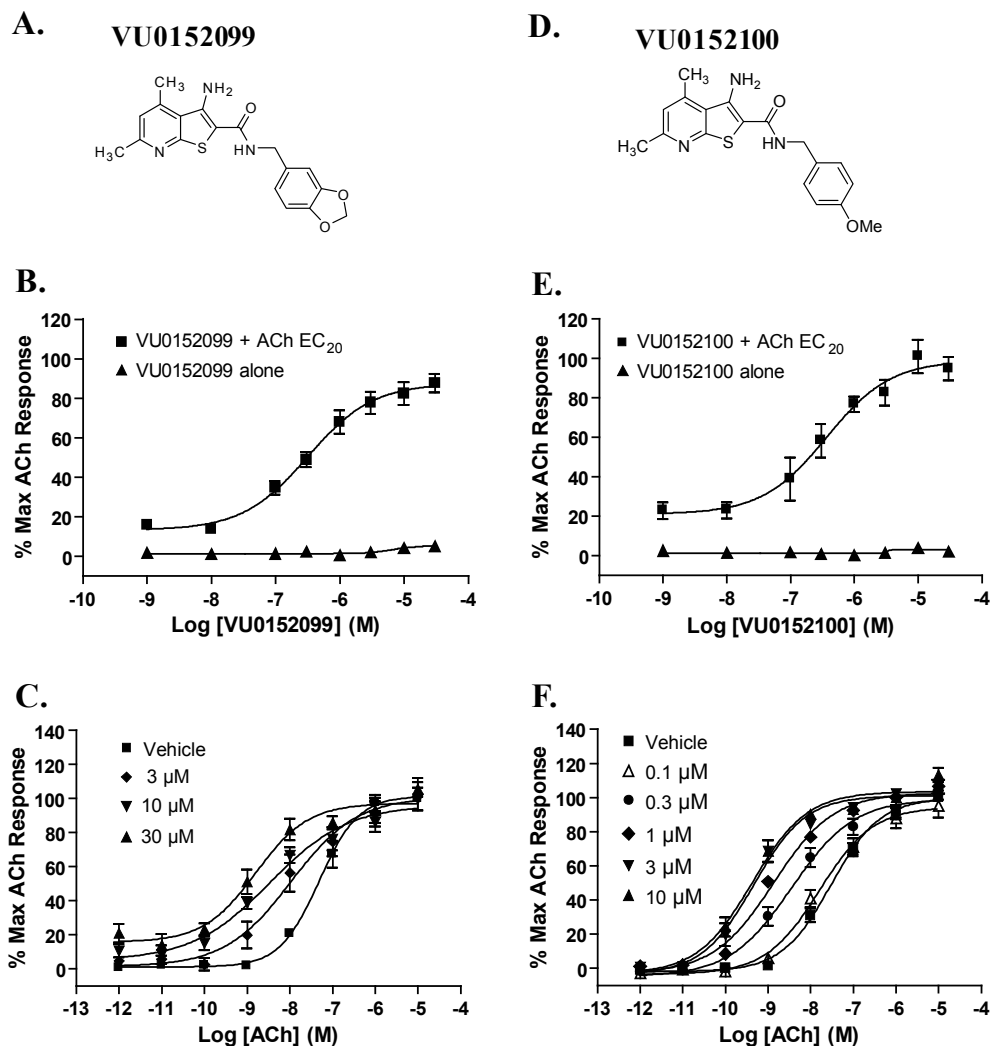


Figure 15. VU0152099 and VU0152100 are potent positive allosteric modulators of rM_4 *in vitro*. Chemical structures of VU0152099 (A.) and VU0152100 (D.). B.,E. Potency of VU0152099 (403 ± 117 nM, B.) and VU0152100 (380 ± 93 nM, E.) was evaluated at the rM_4 receptor by measuring calcium mobilization in Chinese hamster ovary (CHO) cells stably expressing rM_4 and the chimeric G-protein, G_{qi5} . A range of concentrations of test compound was added to cells, followed 1.5 minutes later by addition of an EC_{20} concentration of ACh. In the absence of an EC_{20} concentration of ACh, neither test compound elicited a response. Data were normalized as a percent of the maximal response to $10 \mu\text{M}$ ACh and represent the mean \pm S.E.M. of three independent experiments. C.,F. VU0152099 (C.) and VU0152100 (F.) potentiate the response of rM_4 to ACh, as manifest by a dose-dependent leftward shift in the ACh CRC. At the highest concentrations tested, VU0152099 ($30 \mu\text{M}$) induced a 30-fold shift and VU0152100 ($10 \mu\text{M}$) induced a 70-fold shift in the ACh CRC. Data were normalized as a percent of the maximal response to $10 \mu\text{M}$ ACh and represent the mean \pm S.E.M. of 3-5 independent experiments. Experiments performed by A.E. Brady.

Using calcium mobilization to assess the functional activity of VU0152099 and VU0152100 at the M₄ receptor requires co-expression of the chimeric G protein, G_{qi5}, in order to link the G_{i/o}-coupled M₄ receptor to the PLCβ/Ca²⁺ pathway. As an alternative approach to measure M₄ PAM activity, we chose to take advantage of a novel functional assay recently developed in our lab that takes advantage of the ability of endogenous G_{βγ} subunits of G_{i/o}-coupled GPCRs to alter the kinetics of G-protein regulated inwardly rectifying K⁺ (GIRK) channels to conduct the ion, thallium (Niswender et al., 2008). For these studies, HEK293 cells stably co-expressing heteromeric GIRK1/2 channels and the human M₄ muscarinic receptor were pre-incubated with test compound and then stimulated with agonist (ACh) in the presence of thallium ion. Both VU0152099 and VU0152100 dose-dependently potentiated the response to an EC₂₀ concentration of ACh with EC₅₀ values of 1.2 ± 0.3 μM and 1.9 ± 0.2 μM, respectively, and increased the maximal response to ACh to approximately 130 % (**Fig 16A**). As observed in the calcium mobilization assays described above, both VU0152099 and VU0152100 (10 μM) also enhanced the potency of ACh to induce GIRK-mediated thallium flux, as manifest by a robust (~30-fold) leftward shift in the ACh CRC from 77 ± 1.2 nM to 2.09 ± 0.3 nM and 2.35 ± 0.5 nM, respectively (**Fig 16B**). Taken together, these *in vitro* studies suggest that VU0152099 and VU0152100 are potent positive allosteric modulators that enhance the response of the M₄ receptor to the endogenous agonist, ACh.

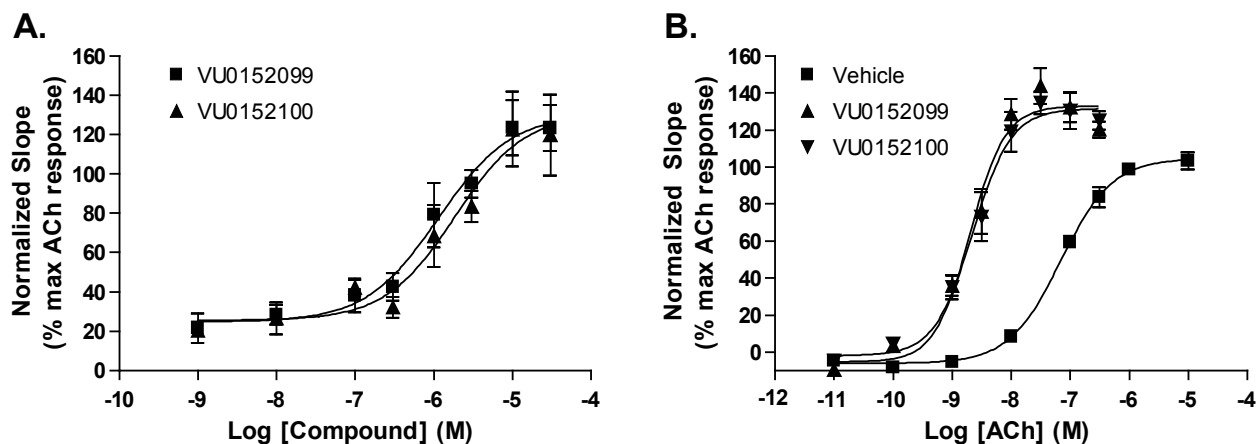


Figure 16. VU0152099 and VU0152100 potentiate GIRK-mediated thallium flux in response to ACh in HEK cells expressing the human M₄ receptor. **A.** Both VU0152099 (■) and VU0152100 (▲) potentiate hM₄-induced GIRK-mediated thallium flux in response to an EC₂₀ concentration of ACh with potencies of 1.2 ± 0.3 μM and 1.9 ± 0.2 μM, respectively. **B.** In the presence of 10 μM VU0152099 (▲) and VU0152100 (▼), the ACh CRC for induction of GIRK-mediated thallium flux was leftward shifted (≈30-fold) from 77 ± 1.2 nM (■ Veh) to 2.09 ± 0.3 nM (▲, VU0152099) and 2.35 ± 0.5 nM (▼, VU0152100). Data were normalized as a percent of the maximal response to 10 μM ACh and represent the mean ± S.E.M. of 3-4 independent experiments performed in quadruplicate. Experiments performed by A.E. Brady.

VU0152099 and VU0152100 are selective for M₄ relative to other mAChR subtypes

We next evaluated VU0152099 and VU0152100 in calcium mobilization assays for effects at all mAChR subtypes to determine whether these compounds are selective for M₄. Both VU0152099 and VU0152100 were selective for M₄ relative to M₁, M₂, M₃ and M₅. Thus, neither VU0152099 (**Fig. 17A**) nor VU0152100 (**Fig. 17B**) had any effect on the ACh dose-response curves at these other mAChR subtypes at concentrations up to 30 μ M. To further assess selectivity of these compounds for M₄ relative to other potential targets, the activity of VU0152099 and VU0152100 also were evaluated in radioligand binding assays against a large panel of 68 discrete GPCRs, ion channels, transporters and enzymes (**Table 6**). These compounds were largely inactive at each of the targets in this panel screen. At concentrations of 10 μ M, both compounds were completely inactive at most targets and induced less than 50% displacement of binding for all targets tested, with the single exception of GABA_A receptors (assessed by flunitrazepam binding), where VU0152099 displayed 51% displacement. This suggests that VU0152099 may interact with the flunitrazepam site with an IC₅₀ value of approximately 10 μ M, which still provides high selectivity for M₄ relative to GABA_A receptors.

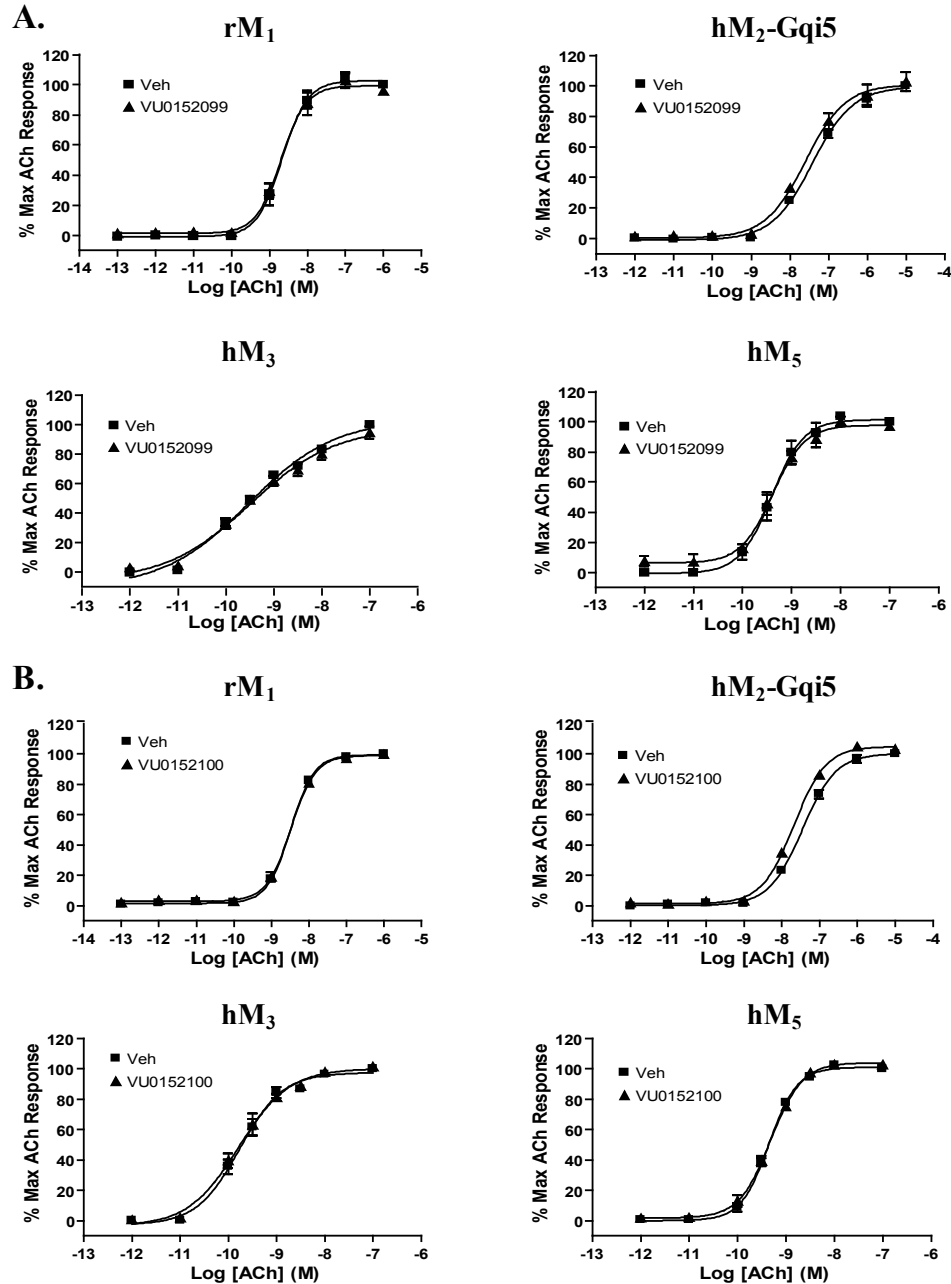


Figure 17. VU152099 (A.) and VU152100 (B.) are functionally selective for the M₄ mAChR subtype relative to other mAChRs. No shift in the ACh CRC was observed in the presence of 30 μ M test compound at CHO-K1 cells stably expressing rM₁, hM₂-Gqi₅, hM₃, or hM₅. Calcium mobilization was measured in response to increasing concentrations of ACh following preincubation with either vehicle or test compound (30 μ M), as described in Methods. Assays of rM₁, hM₃, and hM₅, took advantage of endogenous coupling to G_q proteins, and for hM₂, cells co-expressing the chimeric G protein, G_{qi5}, to allow coupling of this receptor to calcium mobilization. Points represent the mean \pm S.E.M. of three independent experiments. Experiments performed by A.E. Brady.

Table 6. Selectivity of VU0152099 and VU0152100 determination in radioligand binding assays in the LeadProfilingScreen® by MDS Pharma.

Target	Species	% Inhibition		Target	Species	% Inhibition	
		VU0152099	VU0152100			VU0152099	VU0152100
Adenosine A1	human	28	-1	Histamine H ₃	human	10	9
Adenosine A2	human	46	43	Imidazoline I ₂ , Central	rat	7	8
Adenosine A3	human	28	40	Interleukin IL-1	mouse	-19	-4
Adrenergic α _{1A}	rat	10	9	Leukotriene, Cysteinyl CysLT ₁	human	-4	-6
Adrenergic α _{1B}	rat	-7	-7	Melatonin MT ₁	human	15	20
Adrenergic α _{1D}	human	1	1	Muscarinic M ₁	human	-3	0
Adrenergic α _{2A}	human	7	17	Muscarinic M ₂	human	-1	-4
Adrenergic β ₁	human	17	17	Muscarinic M ₃	human	-1	-2
Adrenergic β ₂	human	30	35	Neuropeptide Y Y ₁	human	2	9
Androgen (testosterone)AR	rat	6	6	Neuropeptide Y Y ₂	human	-2	2
Bradykinin B ₁	human	13	1	Nicotinic Acetylcholine	human	6	-6
Bradykinin B ₂	human	-5	-9	Nicotinic Acetylcholine α ₁ , Bungarotoxin	human	-10	-4
Calcium channel L-type, benzothiazepine	rat	13	7	Opiate δ (OP1, DOP)	human	2	-13
Calcium channel L-type, dihydropyridine	rat	21	17	Opiate κ (OP2, KOP)	human	5	2
Calcium channel N-type	rat	-8	-4	Opiate μ (OP3, MOP)	human	2	-2
Dopamine D ₁	human	6	7	Phorbol Ester	mouse	2	4
Dopamine D _{2S}	human	2	0	Platelet Activating Factor (PAF)	human	13	22
Dopamine D ₃	human	-1	5	Potassium Channel [K _{ATP}]	hamster	3	6
Dopamine D _{4,2}	human	-13	-11	Potassium Channel hERG	human	5	5
Endothelin ET _A	human	-8	-8	Prostanoid EP ₄	human	15	7
Endothelin ET _B	human	2	-4	Purinergic P _{2X}	rabbit	6	-4
Epidermal Growth Factor (EGF)	human	9	-5	Purinergic P _{2Y}	rat	15	14
Estrogen ERα	human	-1	-1	Rolipram	rat	36	29
G protein-coupled receptor GPR103	human	-3	-4	Serotonin (5-Hydroxytryptamine) 5-HT _{1A}	human	2	2
GABA _A Flunitrazepam, central	rat	51	43	Serotonin (5-Hydroxytryptamine) 5-HT ₃	human	-2	14
GABA _A Muscimol, central	rat	6	9	Sigma σ ₁	human	2	6
GABA _{B1A}	human	-7	12	Sigma σ ₂	rat	-8	-3
Glucocorticoid	human	-3	8	Sodium Channel, Site 2	rat	11	20
Glutamate, Kainate	rat	3	-15	Tachykinin NK ₁	human	-15	-18
Glutamate, NMDA, Agonism	rat	17	22	Thyroid Hormone	rat	-1	0
Glutamate, NMDA, Glycine	rat	3	2	Transporter, Dopamine (DAT)	human	27	46
Glutamate, NMDA, Phencyclidine	rat	2	3	Transporter, GABA	rat	26	13
Histamine H ₁	human	14	7	Transporter, Norepinephrine (NET)	human	34	22
Histamine H ₂	human	7	10	Transporter, Serotonin (5-Hydroxytryptamine) (SERT)	human	0	4

VU0152099 and VU0152100 were tested at 10 μM for orthosteric radioligand displacement against a large panel of 68 GPCRs, ion channels, transporters and enzymes to ensure a clean ancillary pharmacology profile.

Since VU0152099 and VU0152100 are allosteric modulators of M₄, it is possible that they have activity at similar allosteric sites on other GPCRs. If so, this would not be apparent in the radioligand binding assays discussed above. The finding that these compounds are completely inactive at other mAChR subtypes makes this less likely since M₄ is more closely related to the other mAChR subtypes than to other GPCRs. However, to further evaluate the selectivity of VU0152099 for M₄ relative to other family A GPCRs, we contracted with Millipore Corp. (St. Charles, MO) to determine the effects of these compounds on functional responses of a panel of 15 other GPCRs to activation by their respective agonists. For these studies, we chose family A GPCR subtypes that are among the closest relatives of mAChRs. We first determined the effects of VU0152099 alone on each receptor and found that these compounds had no agonist activity at any receptor studied. We then determined the effects of VU0152099 on full concentration response curves of agonists of each of these receptors. This allows unambiguous evaluation of whether the compounds possess antagonist activity (either allosteric or orthosteric) or allosteric potentiator activity at these other GPCRs. Consistent with our internal studies, VU0152099 induced a robust potentiation of ACh-induced activation of M₄, but had no potentiator activity at M₁ (**Figure 18**). In addition, VU0152099 had no allosteric potentiator activity at any of the other GPCR subtypes tested (**Figure 18**). The only significant activity detected for VU0152099 in this functional panel screen was weak antagonist activity at the serotonin 5HT_{2B} receptor (**Figure 18**). Together, these data suggest that VU0152099 and VU0152100 possess clean ancillary pharmacology profiles, which would allow us to pursue the behavioral effects of selective M₄ activation *in vivo*.

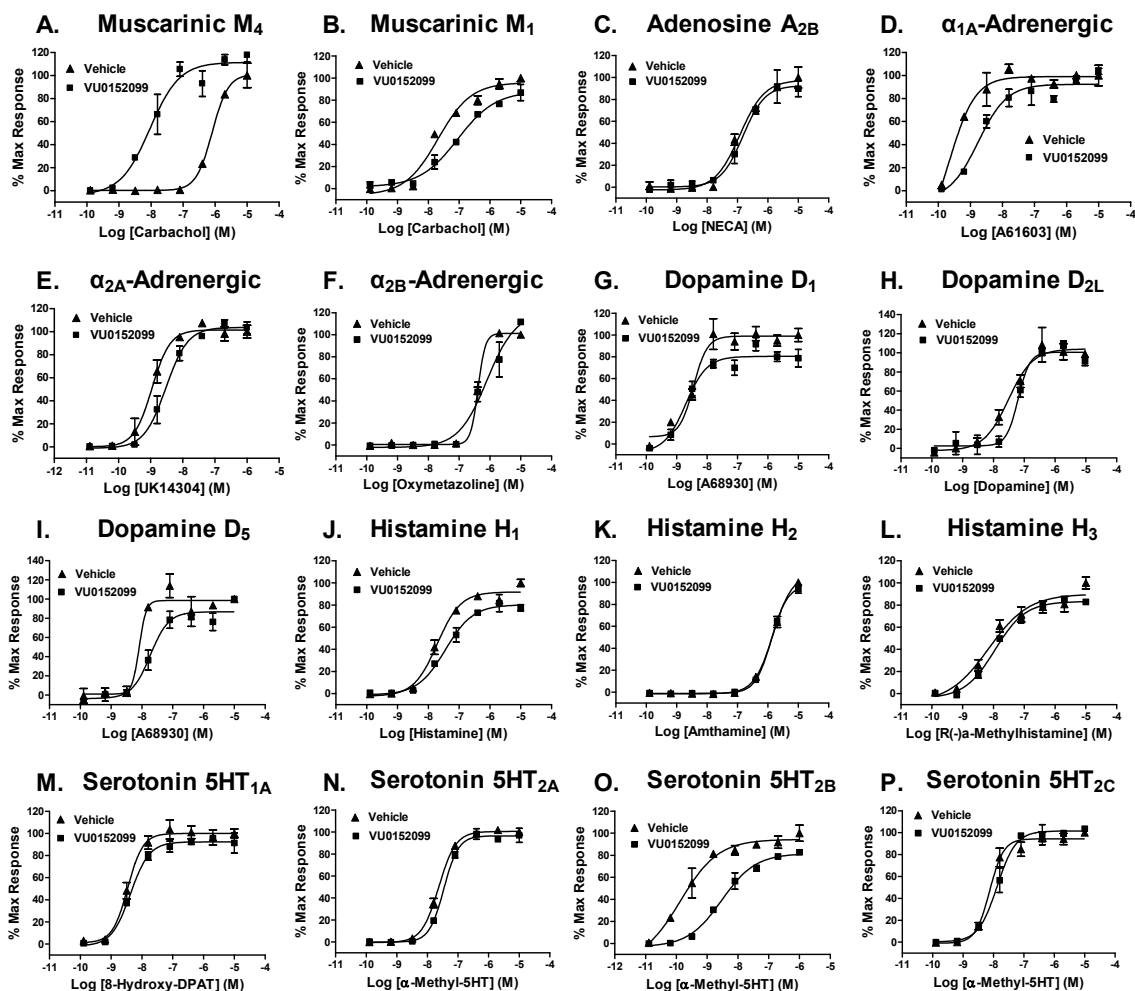


Fig 18. Millipore GPCR Profiler™ Functional Screen. Because of the potential liability for off-target activity at other class A GPCRs, VU0152099 was evaluated in Millipore's GPCR Profiler™ screen for activity at 16 GPCR targets using a Fluorimetric Imaging Plate Reader (FLIPR^{Tetra}, Molecular Device Corp). This cell-based assay relies on endogenous expression of the promiscuous G protein, $G\alpha_{15/16}$, to couple recombinant receptors to calcium mobilization, and uses a two addition protocol to assess agonist, antagonist, and allosteric modulator activity. VU0152099 exhibited no agonist activity at any of the targets tested and was found to possess antagonist activity only at the 5HT_{2B} receptor (as indicated by an ≈ 16 fold rightward shift in the agonist CRC in the presence of VU0152099). Potentiator activity was assessed by performing agonist CRCs in the absence (vehicle, ▲) or presence (VU0152099, ■) of 10 μ M VU0152099. **A.** At the human M₄ mAChR, 10 μ M VU0152099 elicits a robust ≈ 80 -fold leftward shift in the carbachol CRC (EC₅₀ values: CCh alone ≈ 800 nM, CCh + 10 μ M VU0152099 ≈ 10 nM). **B-P.** Similar CRC curves were generated for additional GPCRs: Muscarinic M₁ (**B.**), Adenosine A_{2B} (**C.**), α_{1A} -, α_{2A} -, α_{2B} -Adrenergic (**D-F.**), Dopamine D₁, D_{2L}, D₅ (**G-I.**), Histamine H₁, H₂, H₃ (**J-L.**), and Serotonin 5HT_{1A}, 2A, 2B, 2C (**M-P.**), with no substantial shift observed at any other target tested. All data represent the mean of duplicate determinations. Experiments performed at Millipore.

VU0152099 and VU0152100 bind allosterically and increase ACh affinity

To further confirm an allosteric mechanism of action by the novel M₄ PAMs, we evaluated the effect of VU0152099 and VU0152100 on equilibrium radioligand binding studies using membranes prepared from cells expressing the rM₄ receptor. We first assessed the ability of increasing concentrations of the two M₄ PAMs to displace the orthosteric radioligand, [³H]NMS (0.1 nM). Unlike the orthosteric antagonist, atropine, which potently inhibited [³H]NMS binding ($K_i = 0.54 \pm 0.1$ nM), neither M₄ PAM displaced [³H]NMS at concentrations up to 30 μ M (**Fig. 19A**), strongly suggesting that VU0152099 and VU0152100 act at a site on the M₄ receptor that is distinct from the orthosteric binding site.

In addition, we evaluated the effect of VU0152099 and VU0152100 on the affinity of ACh for the M₄ receptor by assessing the ability of an increasing concentration of ACh to displace [³H]NMS (0.1 nM) binding in the absence or presence of the M₄ potentiators. VU0152099 and VU0152100 were found to induce a 20-25 fold leftward shift in the potency of ACh to displace [³H]-NMS binding to M₄ as manifest by a reduction in the ACh K_i from 252 ± 17.9 nM (veh) to 10.4 ± 0.91 nM (VU0152099) and 12.2 ± 0.49 nM (VU0152100) (**Fig. 19B**). These data present a possible mechanism whereby these compounds could enhance receptor activation by increasing the affinity of M₄ for acetylcholine, and are in agreement with data previously determined for VU10010, where a 14-fold decrease in the ACh K_i was reported (Shirey et al., 2008).

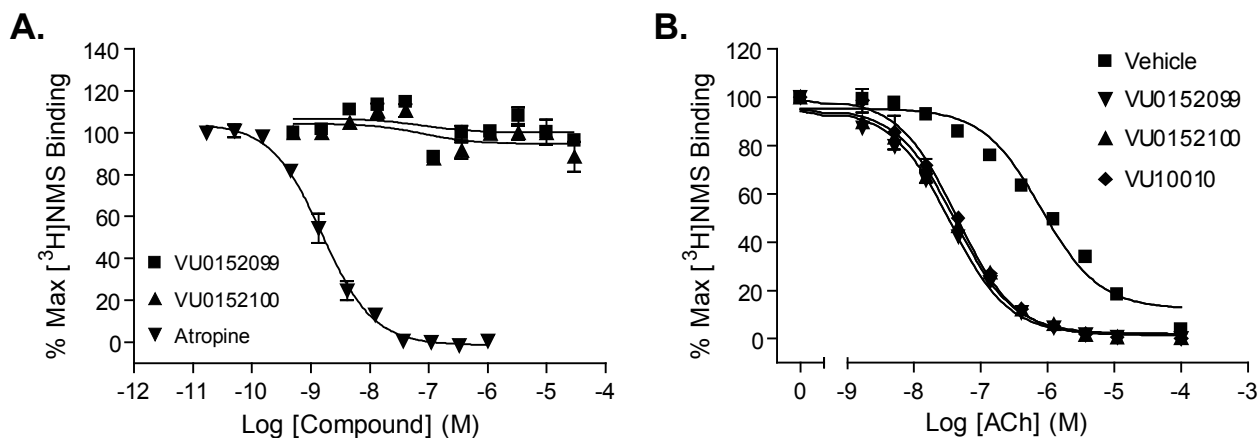


Figure 19. VU0152099 and VU0152100 bind allosterically and increase ACh affinity at rM₄. **A.** In competition binding studies, neither VU0152099 (■) nor VU0152100 (▲) displaced the orthosteric radioligand, [³H]NMS (0.1 nM), at concentrations up to 30 μM. However, the orthosteric antagonist, atropine (▼), potently inhibited [³H]NMS binding with a K_i of 0.54 ± 0.1 nM. **B.** In the presence of vehicle alone, an increasing concentration of ACh displaces [³H]NMS (0.1 nM) binding with a K_i of 252 ± 17.9 nM (■). In the presence of a fixed concentration (10 μM) of VU0152099 or VU0152100, the potency of ACh to displace [³H]NMS binding is shifted leftward, yielding K_i values of 10.4 ± 0.91 nM (▼, VU0152099) and 12.2 ± 0.49 nM (▲, VU0152100), which represent a 25-fold and 21-fold shift in ACh potency, respectively. Data represent the mean ± S.E.M. of 3 independent experiments, performed in duplicate. Experiments performed by A.E. Brady.

VU0152099 and VU0152100 Exhibit Improved Physiochemical and Pharmacokinetic Properties

Prior to conducting *in vivo* studies with VU0152099 and VU0152100, pharmacokinetic studies were undertaken to assess brain/plasma ratios following systemic dosing of these compounds. In contrast, to the high logP of VU10010 (4.5), both VU0152099 and VU0152100 possessed logPs of 3.65 and 3.6, respectively, a full order of magnitude less lipophilic than VU10010 (Shirey et al., 2008). As a consequence, both VU0152099 and VU0152100 displayed improved physiochemical properties and afforded homogeneous dosing solutions in multiple vehicles acceptable for *in vivo* studies. Further, we conducted *in vivo* exposure (brain and plasma) studies in rats at the dose of 56.6 mg/kg, *i.p.* Both compounds exhibited substantial systemic absorption and brain penetration (**Fig. 20**). After 56.6 mg/kg *ip* administration, peak brain concentrations for both the compounds were in the range of 3-5 µg/ml. VU0152100 (**Fig. 20B**) was far superior to VU0152099 (**Fig. 20A**) in terms of brain penetration, as evident from AUC (0-∞) values (**Table 7**). The AUC brain/AUC plasma ratio, which is an estimate of CNS bioavailability, for VU0152099 was calculated to be 0.39 ± 0.01 , while the ratio for VU0152100 was determined to be 0.86 ± 0.08 (**Table 7**). The half-life of the compounds in the brain was 1.25 ± 0.02 h (VU0152099) and 1.12 ± 0.01 h (VU0152100) (**Table 7**). Therefore, our earlier concern of P-glycoprotein (P-gp) transport susceptibility within this series was likely unwarranted, and the lack of central activity for VU10010 was most likely due solely to physiochemical properties.

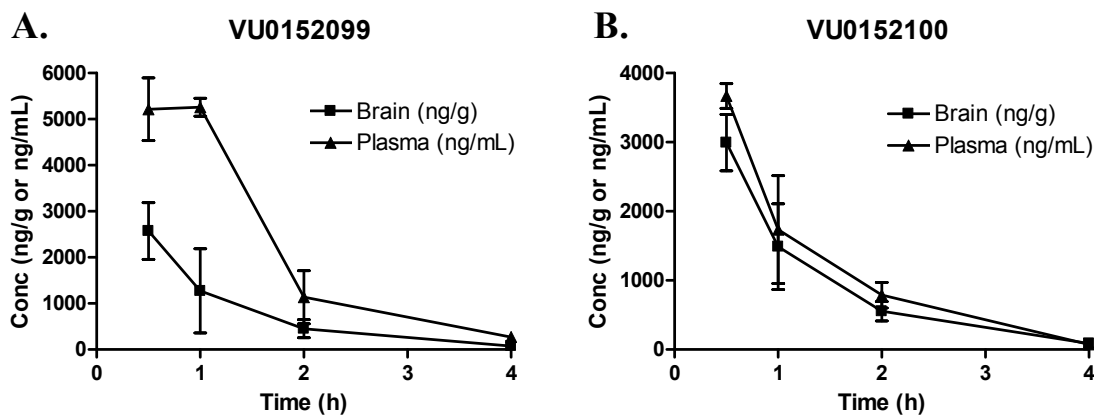


Figure 20. Pharmacokinetic profiling of VU0152099 and VU0152100 in rats. Concentration-time profile of VU152099 (A.) and VU152100 (B.) in brain (■) and plasma (▲) of male Sprague Dawley rats following a 56.6 mg/kg *ip* administration of each compound. Blood and brain tissue were collected at 0.5, 1, 2 and 4h after injection. Samples were extracted as described in Methods and analyzed by LC-MS-MS. Each time point represents the mean determination \pm S.E.M. of three rats. Experiments performed by S.B. Jadhav and H. Yin.

Table 7. Pharmacokinetic analysis of VU0152099 and VU0152100.

PK Parameter	VU0152099	VU0152100
Mean AUC (0- ∞) brain (ng.h/g)	4751.80 \pm 666.17	5726.35 \pm 694.68
Mean AUC(0- ∞) plasma (ng.h/ml)	11928.00 \pm 1472.36	6570.35 \pm 235.87
AUC brain / AUC plasma	0.39 \pm 0.01	0.86 \pm 0.08
$t_{1/2}$ plasma (h)	1.66 \pm 0.39	1.62 \pm 0.69
$t_{1/2}$ brain (h)	1.25 \pm 0.023	1.12 \pm 0.01

AUC(0- ∞) and $t_{1/2}$ values of VU0152099 and VU0152100 in exposure studies in male rats after 56.6 mg/kg intraperitoneal administration are shown. Values represent mean \pm SEM ($n = 3$ rats).

VU0152099 and VU0152100 exhibit *in vivo* activity in rat

Previous studies using the M₁/M₄-preferring muscarinic agonist xanomeline produced robust effects in several preclinical models predictive of antipsychotic-like activity, including reversal of amphetamine-induced hyperlocomotion in rats (Stanhope et al., 2001). Based on our initial pharmacokinetic studies suggesting that systemic administration of VU0152099 and VU0152100 provides robust brain levels of these compounds, the effects of VU0152099 and VU0152100 were evaluated in reversing amphetamine-induced hyperlocomotion using a dose of 56.6 mg/kg *i.p.* for each compound with a 30 min pretreatment interval. As shown in **Fig. 21A**, both VU0152099 and VU0152100 produced robust decreases in amphetamine-induced hyperlocomotion over the time course tested. In addition, to provide further confirmation that the M₄ PAMs have no effect on baseline levels of motor performance which could complicate the interpretation of the amphetamine-induced hyperlocomotion data, we evaluated the effects of one of the M₄ PAMs, specifically VU0152100, after administration alone on performance in the rotorod test (**Fig. 21B**). As shown, VU0152100 had no effect on performance in the rotorod test, even when tested at a dose of 100mg/kg, which was higher than that required to observe reversal of amphetamine-induced hyperlocomotion.

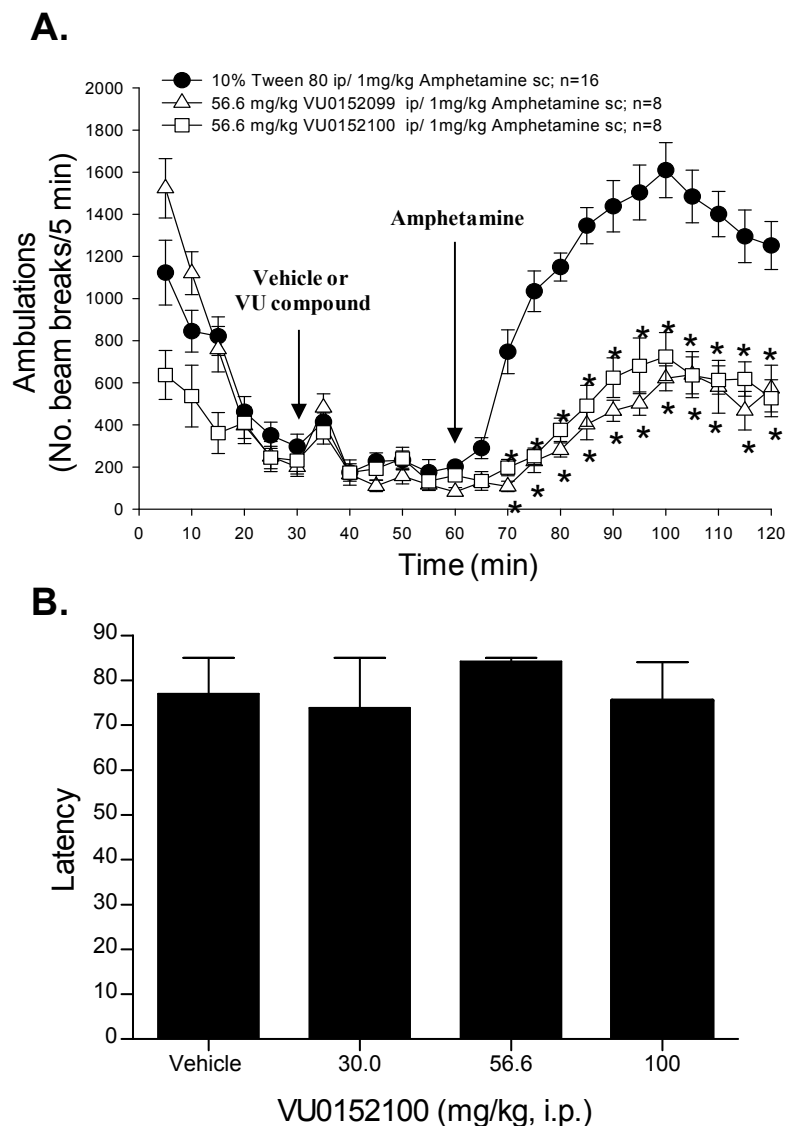


Figure 21. VU0152099 and VU0152100 inhibit amphetamine-induced hyperlocomotor activity in rats without causing sedation. **(A.)** Rats were pretreated for 30 min with vehicle or a 56.6 mg/kg dose of either VU0152099 or VU0152100 *i.p.* Next, all rats received an injection of 1 mg/kg *s.c.* of amphetamine and locomotor activity was measured for an additional 60 min. Each point represents the mean of eight-sixteen rats. The error bars represent \pm S.E.M. and are absent when less than the size of the point. Abscissa, time in minutes; ordinate, ambulations or total beam breaks per 5 min intervals; *, $P < 0.05$ versus veh+amphetamine control group, Dunnett's test. **(B.)** Lack of effect of VU0152100 on motor performance on the rotorod. After initial training trials, rats were pretreated for 30 minutes *i.p.* with vehicle or a dose of VU0152100, specifically 30, 56.6 or 100 mg/kg, and then the time each animal remained on the rotorod was recorded; animals not falling off the rotorod were given a maximum score of 85 s. Abscissa, dose of VU0152100 in milligrams per kilogram; ordinate, time spent on the rotorod in sec. Each bar graph represents the mean of eight-ten rats. The error bars represent \pm S.E.M. Experiments performed by C.K. Jones, A.D. Thompson, and J.U. Heiman.

Discussion

In recent years, the mAChRs have emerged as potential novel targets for the treatment of schizophrenia. This is based on clinical studies demonstrating efficacy of mAChR agonists in treatment of positive symptoms in schizophrenia patients, as well as multiple animal studies suggesting that mAChR agonists could be useful in treatment of cognitive dysfunction in schizophrenia patients (Bymaster et al., 2002). Furthermore, a growing body of evidence from clinical and animal studies involving pharmacological manipulations, post mortem tissue analysis, and brain imaging is consistent with this hypothesis (Raedler et al., 2007). While recent advances suggesting potential utility of mAChR activators in treatment of schizophrenia have been exciting, there have been few selective pharmacological tools available to fully explore this emerging muscarinic hypothesis of schizophrenia. Unfortunately, previous attempts to develop traditional orthosteric agonists that are highly selective for individual mAChR subtypes have been unsuccessful.

The current discovery and optimization of VU0152099 and VU0152100 as highly selective positive allosteric modulators of M₄ provides a major advance in establishing a new approach for developing highly selective activators of these receptors. The data presented provide further support for the ability to achieve high subtype selectivity by targeting allosteric sites and provide exciting new data demonstrating that highly selective M₄ PAMs have robust activity in at least one animal model that is similar to effects previously described for the non-selective orthosteric mAChR agonist, xanomeline (Stanhope et al., 2001). The finding that VU0152099 and VU0152100 mimic effects of xanomeline in an animal model that has been used to predict

antipsychotic activity of new compounds is especially exciting in light of clinical studies demonstrating the clinical efficacy of xanomeline in schizophrenia patients. This raises the exciting possibility that selective activation of M₄ may provide a novel approach for the treatment of some symptoms associated with schizophrenia. Furthermore, the discovery of systemically active M₄ PAMs suggests that this will be a viable approach for developing selective activators of M₁ and other mAChR subtypes.

While the *in vitro* data for VU0152099 and VU0152100 indicate high pharmacologic selectivity for M₄ relative to any other mAChR subtypes or closely related GPCRs, the possibility exists that the observed behavioral effects may be due to an off-target activity not yet identified. In future studies, it will be critical to further validate that the effects of VU0152099 and VU0152100 observed *in vivo* are mediated by activation of M₄ using other tools, including structurally distinct M₄ PAMs or selective M₄ antagonists, as they become available, and/or M₄ knockout mice. Unfortunately, studies in M₄ knockout mice will be complex since these mice display fundamentally different responses to psychomotor stimulants and compounds will need to be optimized for appropriate pharmacokinetic properties in mice. Also, several behavioral parameters are substantially altered in the M₄ knockout mice, including increases in baseline locomotor activity, altered responses to amphetamine, and altered dopamine release in the mesolimbic dopamine circuitry (Gomez et al., 1999; Gomez et al., 2001; Tzavara et al., 2004). These factors will complicate interpretation of studies with M₄ knockout mice. However, while it is not possible to definitively establish an exclusive role for M₄ in mediating the behavioral effects observed here, previous studies have established similar effects of structurally distinct mAChR agonists (Stanhope et al., 2001). This, coupled

with the high selectivities of VU0152099 and VU0152100 for M₄ relative to any other mAChR subtype, suggests that M₄ is a likely candidate for mediating these effects. Also, extensive profiling of VU0152099 and VU0152100 showed no functional effects on responses to other closely related family A GPCRs and no significant off-target activity at any of 68 other GPCRs, ion channels, or enzymes. Thus, while it is impossible to entirely rule out unknown off-target activity, these compounds appear to be much more highly selective for the targeted receptor than is typical for most orthosteric GPCR ligands. As new tools become available for targeting M₄ and other mAChR subtypes, they will provide the means to develop a more complete understanding of the roles of each of the individual mAChR subtypes in regulating CNS function.

In addition to suggesting the potential roles of M₄ *in vivo*, these data have important implications related to the molecular pharmacology of allosteric modulators of GPCRs. One of the most promising properties of allosteric modulators of GPCRs has been that it is often possible to achieve high selectivity for a targeted GPCR subtype relative to closely related family members (Marino et al., 2003; O'Brien et al., 2003; Kinney et al., 2005; Galici et al., 2006). However, discovery of these compounds also raises the question of whether allosteric modulators may have broad activity across other GPCRs by interacting at potentially promiscuous allosteric sites. The present finding that VU0152099 and VU0152100 had no major activities across multiple targets in a large panel radioligand binding screen was encouraging in suggesting the high selectivity of these compounds, but does not address this critical question. However, the finding that these compounds had no allosteric modulator activity across a panel of 15 other family A GPCR subtypes is exciting and suggests that they are not likely to have activity at a site

that is shared across multiple GPCRs. While it is impossible to rule out activity at other unidentified targets that were not tested, these data suggest that it may be possible to achieve higher subtype selectivity across a range of receptors than has been possible with many orthosteric ligands.

CHAPTER IV

A SELECTIVE ALLOSTERIC POTENTIATOR OF THE M₁ MUSCARINIC ACETYLCHOLINE RECEPTOR INCREASES ACTIVITY OF MEDIAL PREFRONTAL CORTICAL NEURONS AND RESTORES IMPAIRMENTS IN REVERSAL LEARNING

Introduction

The muscarinic acetylcholine (ACh) receptors (mAChRs) play important roles in regulating higher cognitive function. Non-selective mAChR antagonists induce profound attention and memory deficits (Aigner et al., 1991; Fibiger, 1991; Miller and Desimone, 1993) and degeneration of forebrain cholinergic neurons is one of the earliest pathological changes observed in AD (Bartus et al., 1982; Bartus, 2000). Furthermore, acetylcholinesterase inhibitors (AChEIs) have established efficacy in the treatment of AD symptoms (Birks, 2006; Munoz-Torrero, 2008).

Of the five mAChR subtypes, the M₁ receptor is viewed as the most important subtype for memory and attention mechanisms (Levey et al., 1991; Felder et al., 2000). Based on this, selective activators of M₁ have been proposed as having potential utility in treatment of AD (Bodick et al., 1997b; Bodick et al., 1997a; Gu et al., 2003; Caccamo et al., 2006; Jones et al., 2008; Caccamo et al., 2009). However, recent studies revealed that genetic deletion of M₁ does not alter mAChR excitatory effects on hippocampal pyramidal cells (Rouse et al., 2000a), impair hippocampal-dependent learning, or alter cognition-impairing effects of mAChR antagonists (Miyakawa et al., 2001; Anagnostaras et al., 2003). Interestingly, while hippocampal-dependent learning was intact, M₁ receptor knockout mice had specific deficits in forms of learning and memory that

require activation of the prefrontal cortex (PFC) (Anagnostaras et al., 2003). Thus, M₁ may play a role in regulating PFC function, and M₁ receptor-selective activators could improve deficits in PFC-dependent learning in patients suffering from AD.

Unfortunately, lack of highly selective activators and antagonists of the M₁ receptor has prevented detailed studies of the functional consequences of selective M₁ receptor activation. The difficulty in developing highly selective M₁ agonists is due to the high sequence homology among the orthosteric binding sites of mAChR subtypes. However, an alternative strategy for achieving high subtype selectivity is targeting allosteric binding sites that are distinct from the ACh binding site (Conn et al., 2009a; Conn et al., 2009b). We recently reported discovery of multiple positive allosteric modulators (PAMs) of M₁ (Marlo et al., 2009). Furthermore, Ma and colleagues (Ma et al., 2009) report evidence that BQCA is a potent and highly selective PAM at the human M₁ receptor. Based on these preliminary findings, we synthesized a series of molecules related to BQCA and report that BQCA and related compounds are highly selective rat M₁ PAMs. These compounds do not interact with the ACh site, but dramatically increase the affinity of the M₁ receptor for ACh and potentiate the response to orthosteric agonist. In addition, activation of the M₁ receptor induces an inward current and increases excitatory synaptic currents in mPFC layer V pyramidal cells. Consistent with this, BQCA increases firing of mPFC neurons *in vivo*. Finally, BQCA reverses deficits in a PFC-dependent form of learning and memory in a transgenic mouse model of AD and promotes non-amyloidogenic APP processing *in vitro*. Together, these data suggest that the M₁ receptor plays an important role in regulating excitatory drive to the PFC and that

selective potentiation of activity at this receptor can reverse deficits in PFC-dependent cognitive function.

Results

A panel of 21 compounds related to BQCA has a range of activities as allosteric potentiators at the rat M₁ mAChR

Ma et al., (2008) recently reported BQCA as a selective positive allosteric modulator (PAM) of the human M₁ muscarinic receptor (hM₁). However, GPCR PAMs can display species specificity, and the effects of BQCA were not extensively evaluated on the rat M₁ receptor (rM₁). Thus, in order to determine whether BQCA and related compounds have properties needed for use in rodent studies, we synthesized BQCA and a panel of 20 structurally related analogs to identify compounds that can act as selective PAMs for the rM₁ receptor. Effects of BQCA and related compounds were evaluated by measuring effects on calcium mobilization elicited by a submaximal concentration (EC₂₀) of ACh (**Fig. 22**). Libraries **I**, **II**, and **III** each consisted of seven compounds possessing the same *N*-benzyl substitutions based on either an 8-fluorinated quinolone carboxylic acid (**Ia-Ig**), a quinolone carboxylic acid (**IIa-IIg**, including BQCA), or a 5,8-difluorinated quinolone carboxylic acid (**IIIa-IIIg**) template, respectively (**Fig. 22A**). The activity of test compounds was initially assessed by incubating CHO-K1 cells stably expressing the rM₁ receptor with fixed concentrations of each compound at 10, 1, or 0.3 μM (**Fig. 22B-D**) for 1.5 min prior to the addition of an EC₂₀ concentration of ACh. From the panel, four compounds that exhibited robust potentiator activity at 0.3 μM were selected for further evaluation based on their structural diversity. As can be seen in the

representative trace, 1 μ M BQCA has no effect when added alone, but greatly enhances the response to an EC₂₀ concentration of ACh when compared to vehicle. A maximal response to ACh is also shown for comparison (**Fig. 22E**). To determine the potency of each of these compounds, full concentration response curves (CRCs) were generated by pre-incubating rM₁ CHO-K1 cells with increasing concentrations of test compound, followed 1.5 min later by the addition of an EC₂₀ concentration of ACh (**Fig. 23A**). All four compounds had similar potencies at rM₁ with EC₅₀ values in the 200-400 nM range. As a second measure of their ability to potentiate the rM₁ receptor-mediated calcium response to ACh, rM₁ receptor expressing CHO-K1 cells were pre-incubated with a fixed concentration (3 μ M) of the test compound (or vehicle) and then stimulated with increasing concentrations of ACh to generate a series of ACh CRCs. Each of the four test compounds elicited a robust potentiation of the ACh response, as manifest by a leftward shift in the ACh CRC (9.5- to 18.6-fold shift, **Fig. 23B**).

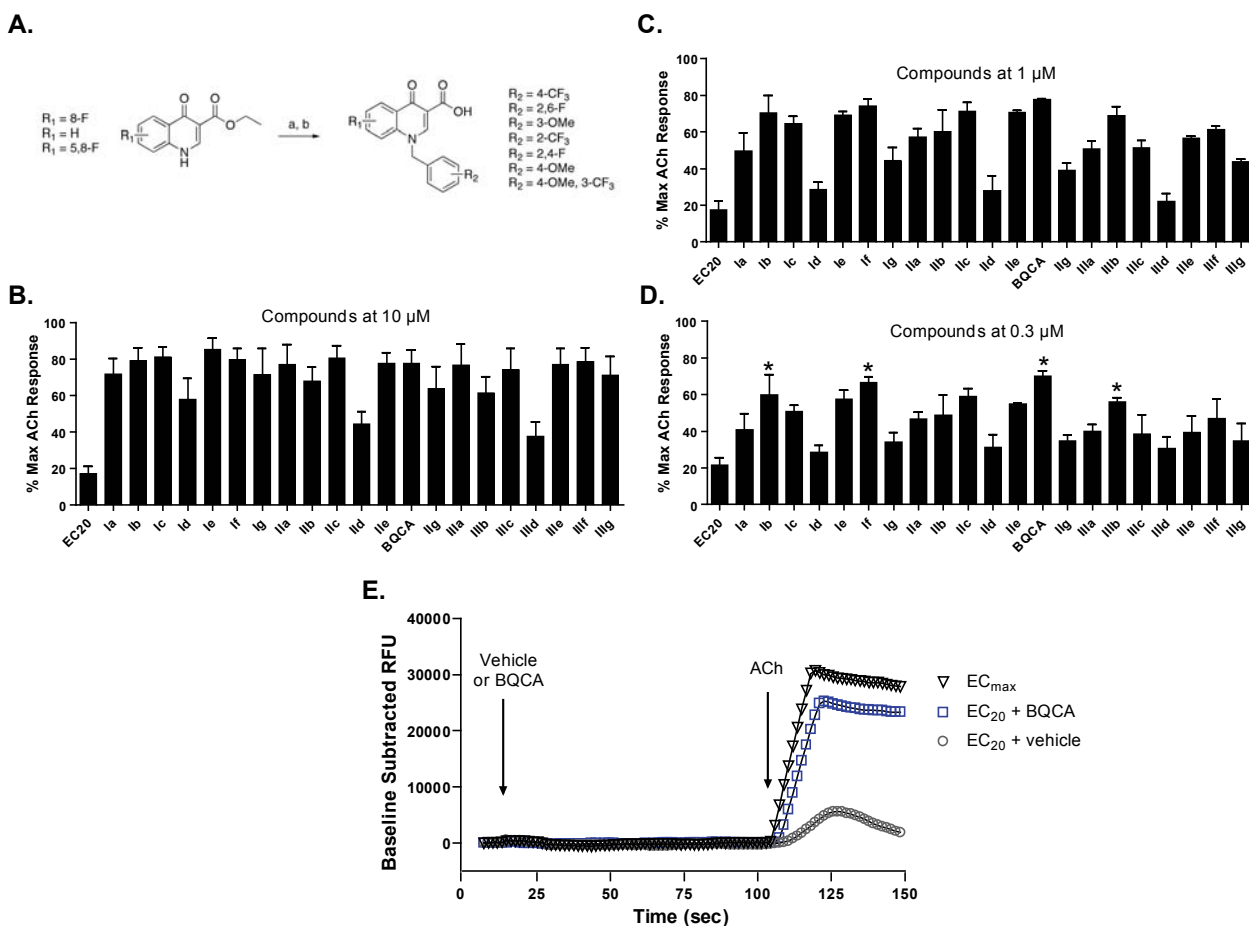


Figure 22. Twenty-one putative M_1 receptor PAMs were synthesized and evaluated at the r M_1 mAChR for their ability to potentiate an EC_{20} concentration of ACh. **A.** Synthesis: a. K_2CO_3 , KI, R-Br, DMF, 24 hr. at r.t., b. LiOH, 9:1 THF:H₂O 10 min 120°C μ wave. Calcium mobilization was measured using a Flexstation II, as described in Methods. Test compounds were evaluated at fixed concentrations of 10 μ M (**B.**), 1 μ M (**C.**), or 0.3 μ M (**D.**) in the presence of an EC_{20} concentration of ACh. Four compounds, denoted by an asterisk (*) in panel **D.**, were selected for further evaluation based on their structural diversity and ability to potentiate an EC_{20} concentration of ACh at 0.3 μ M. Data were normalized as a percent of the maximal response to 10 μ M ACh and represent the mean \pm S.E.M. of 3 independent experiments. **D.** A representative calcium trace from one experiment shows the effect of 1 μ M BQCA on the r M_1 receptor response to an EC_{20} concentration of ACh; the response to an EC_{20} and EC_{max} concentration of ACh in the presence of vehicle are also shown for comparison. Experiments performed by A.E. Brady.

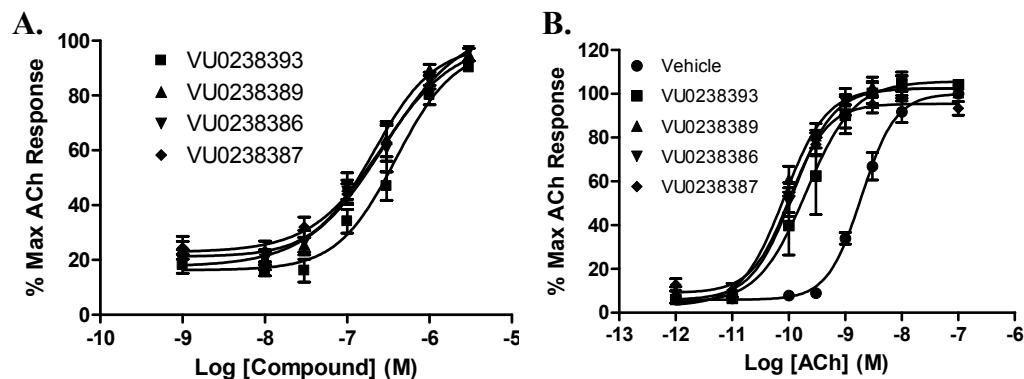


Figure 23. Four of the compounds initially identified as robust M_1 potentiators of the calcium response were further characterized *in vitro* at the rM_1 mAChR. **A.** Potency of each test compound was determined based on its ability to potentiate an EC_{20} concentration of ACh, yielding EC_{50} values of 404 ± 59 nM, VU0238393 (■), 187 ± 39 nM, VU0238389 (▲), 316 ± 102 nM, VU0238386 (BQCA, ▼) and 284 ± 32 nM VU0238387 (◆). **B.** Test compounds were then evaluated at a fixed concentration of $3 \mu\text{M}$ for their ability to shift the potency of an ACh concentration response curve. ACh alone stimulated calcium mobilization with an EC_{50} value of 2.09 ± 0.43 nM (●). In the presence of each of the four test compounds, a robust leftward shift in the ACh CRC was induced resulting in the following EC_{50} values and fold shift in the ACh curve (in parentheses): 0.280 ± 0.164 nM (9.5X), VU0238393 (■), 0.039 ± 0.017 nM (23.2X), VU0238389 (▲), 0.142 ± 0.007 nM (16.4X), VU0238386 (BQCA, ▼) and 0.107 ± 0.003 nM (18.6X), VU0238387 (◆). Data were normalized as a percent of the maximal response to $10 \mu\text{M}$ ACh and represent the mean \pm S.E.M. of 3 independent experiments. Experiments performed by Ashley Brady.

BQCA is a potent and selective positive allosteric modulator of the rat M₁ receptor *in vitro*

Of the molecules tested in this panel screen, BQCA was among the most potent and efficacious at potentiating rM₁ receptor-mediated responses. This is consistent with its activity at the human receptor (Ma et al., 2009). Based on this and its favorable physiochemical properties, we chose to pursue studies focusing exclusively on BQCA. First, we evaluated the potency of BQCA as a positive allosteric modulator of the rM₁ receptor by measuring calcium mobilization in CHO-K1 cells stably expressing this receptor. Cells were incubated with increasing concentrations of BQCA for 1.5 min prior to the addition of an EC₂₀ concentration of ACh, yielding a concentration response curve for BQCA with an EC₅₀ value of 267 ± 31 nM (**Fig. 24A**). We next determined the effect of increasing fixed concentrations of BQCA on the ACh CRC. Rat M₁ CHO-K1 cells were pre-incubated with a fixed concentration (0.3, 1, and 3 μ M) of BQCA and subsequently stimulated with increasing concentrations of ACh. BQCA induced a dose-dependent leftward shift in the ACh CRC with a maximal shift of 21-fold observed with 3 μ M BQCA (**Fig. 24B**).

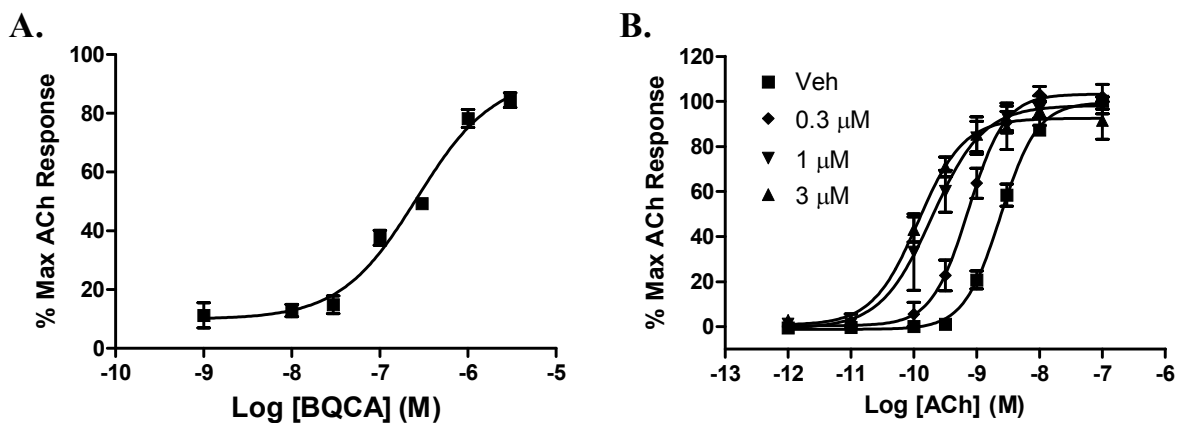


Figure 24. BQCA is a potent positive allosteric modulator of the rM₁ receptor *in vitro*. **A.** The potency of BQCA was evaluated at the rM₁ receptor by measuring calcium mobilization in Chinese Hamster Ovary (CHO-K1) cells stably expressing the rM₁ receptor. Increasing concentrations of test compound was added to cells, followed 1.5 minutes later by addition of an EC₂₀ concentration of ACh. BQCA robustly potentiated the response to ACh with an EC₅₀ value of 267 ± 31 nM. **B.** The ability of BQCA to potentiate the response of the rM₁ receptor to ACh is also manifest by a dose-dependent leftward shift in the ACh CRC. ACh alone stimulated calcium mobilization with an EC₅₀ value of 2.42 ± 0.337 nM (■). In the presence of increasing fixed concentrations of BQCA (0.3 - 3 μM), a robust leftward shift in the ACh CRC was induced, resulting in the following EC₅₀ values (fold shift in the ACh curve is shown in parentheses); 0.3 μM (◆) = 0.762 ± 0.56 nM (3.3-fold), 1.0 μM (▼) = 0.221 ± 0.079 nM (12-fold), 3 μM (▲) = 0.123 ± 0.026 nM (21-fold). Data were normalized as a percent of the maximal response to 10 μM ACh and represent the mean \pm S.E.M. of 3-4 independent experiments. Experiments performed by A.E. Brady.

BQCA is functionally selective for the M₁ mAChR subtype

One of the primary difficulties in developing novel selective ligands for muscarinic receptors has been the failure to identify compounds that can distinguish between the highly conserved orthosteric binding site shared by the five members of this GPCR subfamily. Development of ligands that bind to allosteric sites, both potentiators and direct acting agonists, has proven to be a practical way to circumvent this issue (Conn et al., 2009a; Conn et al., 2009b). Thus, it was important to determine whether BQCA is selective for the M₁ mAChR relative to other mAChR subtypes. We evaluated the effect of BQCA on the ACh CRC in calcium mobilization assays at each of the other mAChR subtypes. As shown in **Fig. 24B**, pre-incubation of rM₁ receptor-expressing CHO-K1 cells with 3 μM BQCA results in a robust leftward shift in the CRC for ACh. However, at this same concentration, BQCA had no effect on the ACh concentration response curves generated in CHO-K1 cells stably expressing the hM₂, hM₃, rM₄, or hM₅ receptors (**Fig. 25A-D**). To further assess selectivity of BQCA for the M₁ receptor relative to other class A GPCR targets that may also harbor similar allosteric sites, we took advantage of the GPCR Profiler™ service offered by Millipore Corp. (St. Charles, MO) to determine the effect of this compound on the functional response of 15 other closely related GPCRs (**Fig. 26**). A two-addition protocol afforded the ability to detect potential agonist, potentiator, and antagonist activity of BQCA at these other GPCR subtypes. Consistent with our internal studies, BQCA induced robust potentiation at the hM₁ receptor, but had no activity in this assay at the hM₄ receptor. Moreover, BQCA had no effect at any of the other GPCRs tested (**Fig. 26A-P**). This included a lack of PAM activity or antagonist activity (either allosteric or orthosteric) at any of these other

GPCRs, which would have resulted in a rightward shift in the concentration response curve. Together, these data suggest that BQCA is highly selective for the M₁ mAChR subtype and has no detectable activity at closely related family A GPCRs that were tested.

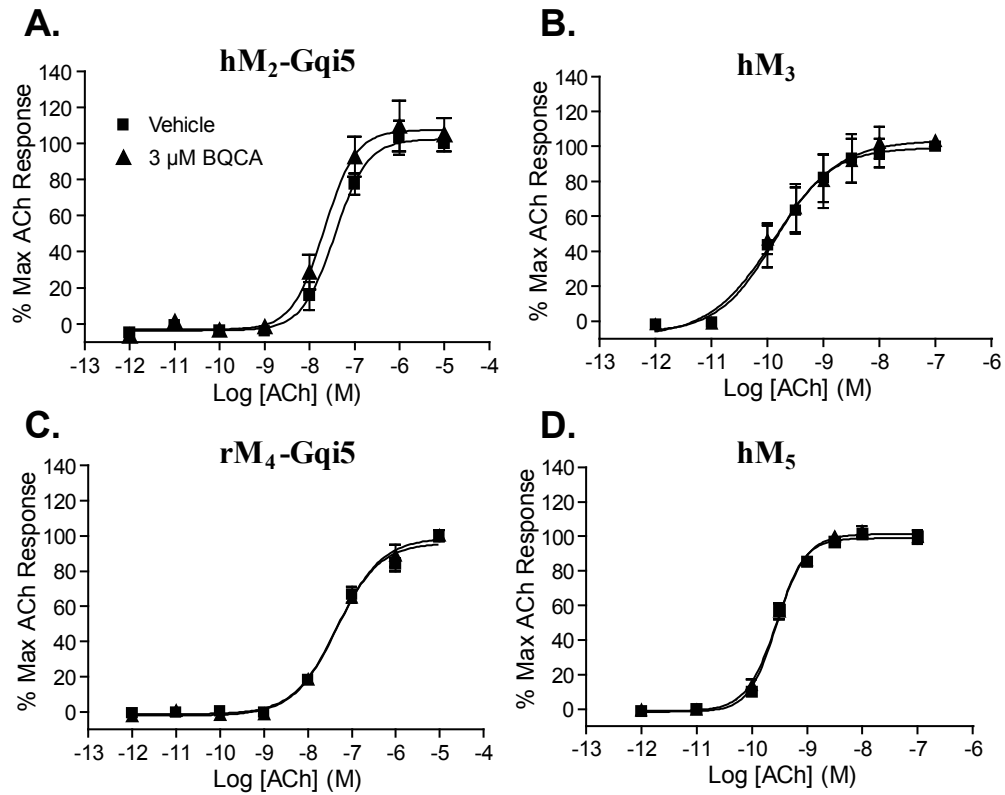


Figure 25. The presence of BQCA has no effect on the ACh concentration-response curve at any other mAChR subtype. No shift in the ACh CRC was observed in the presence of 3 μ M BQCA in CHO-K1 cells stably expressing M₂-Gqi5 (A.), M₃ (B.), M₄-Gqi5 (C.), or M₅ receptors (D.). Calcium mobilization was measured in response to increasing concentrations of ACh following preincubation of cells with either vehicle (■) or 3 μ M BQCA (▲), as described in Methods. Data represent the mean \pm S.E.M. of three independent experiments. Experiments performed by A.E. Brady.

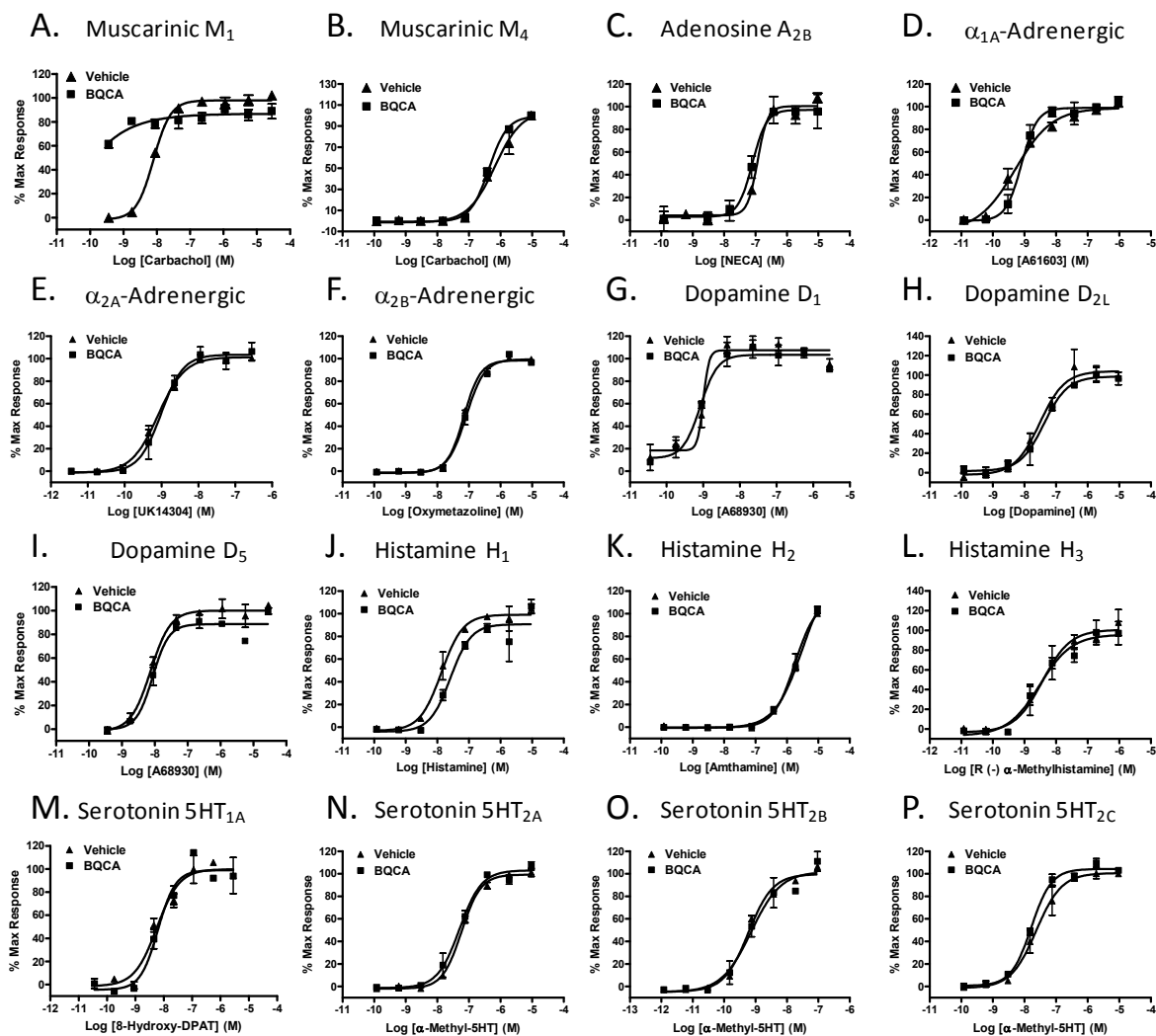


Figure 26. Millipore GPCR Profiler BQCA selectivity data. To confirm that BQCA retains selectivity at M₁ when assayed at non-mAChR GPCRs, it was evaluated in Millipore’s GPCR Profiler™ screen for activity at 15 additional Class A GPCR targets. A Fluorimetric Imaging Plate Reader (FLIPR^{Tetra}), (Molecular Device Corp), was used to measure calcium mobilization in response to agonist stimulation in a proprietary cell line that relies on endogenous expression of the promiscuous G protein, G $\alpha_{15/16}$, to couple recombinant receptors to the PLC β /Ca²⁺ pathway. This assay takes advantage of a two addition protocol such that it was possible to detect any agonist, antagonist, or allosteric potentiator activity. BQCA exhibited no agonist or antagonist activity at any of the targets tested. Allosteric potentiator activity was assessed by performing agonist concentration response curves in the absence (vehicle, ▲) or presence of 10 μ M test compound (BQCA, ■). **A.** At the human M₁ mAChR, 10 μ M BQCA elicits a robust leftward shift in the carbachol concentration-response curve. **B-P.** Similar CRC curves were generated for additional GPCRs: Muscarinic M₄ (**B.**), Adenosine A_{2B} (**C.**), α_{1A} -, α_{2A} -, α_{2B} -Adrenergic (**D-F.**), Dopamine D₁, D_{2L}, D₅ (**G-I.**), Histamine H₁, H₂, H₃ (**J-L.**), and Serotonin 5HT_{1A}, 2A, 2B, 2C (**M-P.**), with no detectable leftward shift in the agonist concentration-response-curve observed at any other target tested. All data represent the mean of duplicate determinations.

BQCA does not compete for orthosteric antagonist binding and it induces a robust leftward shift in ACh affinity at the rM₁ receptor

We previously reported that novel selective PAMs of the rM₄ receptor, exemplified by VU10010 and VU152100, have no detectable affinity at the orthosteric ACh binding site of the rM₄ receptor but allosterically increase affinity of ACh for the rM₄ receptor (Brady et al., 2008; Shirey et al., 2008). To determine whether BQCA shares this property with the rM₄ PAMs, we assessed the ability of this compound to compete for binding with the orthosteric radioligand, [³H]-NMS (0.1 nM) to the orthosteric site using membranes prepared from cells expressing the rM₁ receptor. BQCA had little effect on [³H]-NMS binding, with no displacement of radioligand observed at concentrations up to 10 μM (**Fig. 27A**). In contrast, the orthosteric antagonist, atropine, potently inhibited [³H]-NMS binding with a K_i value of 1.35 ± 0.022 nM (**Fig. 27A**). The effect of BQCA on the affinity of ACh for the rM₁ receptor was also evaluated by assessing the ability of increasing concentrations of ACh to displace [³H]-NMS (0.1 nM) binding in the absence or presence of fixed concentrations of the M₁ receptor potentiator (0.3, 1.0, and 3.0 μM). BQCA induced a robust concentration-dependent leftward shift in the concentration response curve of ACh-induced displacement of [³H]-NMS binding to the rM₁ receptor, with a 30-fold shift observed at the highest concentration tested (3.0 μM). This shift reveals that BQCA induces a reduction in the ACh K_i from 1700 ± 96.4 nM (vehicle) to 348 ± 43.4 nM (0.3 μM), 163 ± 22.9 nM (1.0 μM), and 56.1 ± 4.99 nM (3.0 μM), respectively (**Fig. 27B**). Taken together, these data strongly suggest that BQCA acts at a site on the rM₁ receptor that is distinct from the orthosteric binding site and that it may enhance M₁ receptor activation by increasing the affinity for ACh.

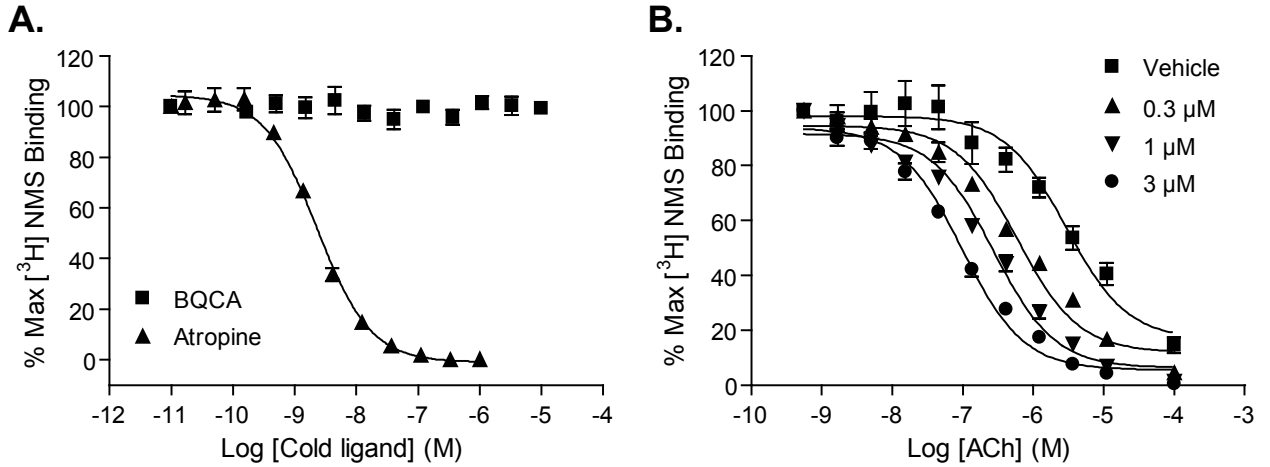


Fig 27. BQCA does not compete for orthosteric antagonist binding and it induces a robust leftward shift in ACh affinity at the rM₁ receptor. **A.** At concentrations up to 10 μM, BQCA (■) did not displace the orthosteric radioligand, [³H]-NMS (0.1 nM) in competition binding studies. However, the orthosteric antagonist, atropine (▲), potently inhibited [³H]-NMS binding with a K_i of 1.35 ± 0.022 nM. **B.** In the presence of vehicle alone, an increasing concentration of ACh displaces [³H]-NMS (0.1 nM) binding with a K_i of 1700 ± 96.4 nM (■). In the presence of increasing fixed concentrations (0.3 - 3.0 μM) of BQCA, the potency of ACh to displace [³H]-NMS binding is shifted leftward, yielding K_i values of 348 ± 43.4 nM (0.3 μM, ▲), 163 ± 22.9 nM (1.0 μM, ▼), and 56.1 ± 4.99 nM (3.0 μM, ●), which represent 5-fold, 10.6-fold and 30.6-fold shifts in ACh potency, respectively. Data represent the mean ± S.E.M. of 3 independent experiments performed in duplicate. Experiments performed by A.E. Brady.

Activation of the M₁ receptor induces an inward current in rat mPFC layer V pyramidal cells and this effect is potentiated by BQCA

Prefrontal cortical function is required for higher executive function, memory storage and retrieval, and cognition (Miller and Cohen, 2001). Recent studies suggest that M₁ receptor signaling may play an important role in activation of the prefrontal cortex by lower brain regions (Anagnostaras et al., 2003). Based on this, it was postulated that activation of the M₁ receptor could increase excitability of mPFC pyramidal cells or increase excitatory synaptic drive to these neurons. In order to examine the effects of M₁ receptor activation on mPFC pyramidal cells, layer V pyramidal neurons were visually identified and membrane currents measured using patch clamp recordings in acute coronal slices. Cell type was confirmed by examining firing properties upon depolarizing current injection. Typical resting membrane potentials of these pyramidal neurons were -55 to -65 mV under the conditions used. Holding current was measured in cells voltage clamped at -70 mV during baseline recording, drug application, and wash. Bath application of CCh induced a robust, concentration-dependent inward current as shown in **Fig. 28** (10 μM CCh, 16.55 ± 1.93 pA, *n* = 4; 100 μM CCh, 53.14 ± 5.92 pA, *n* = 4). Although this CCh-induced inward current is in agreement with previously reported studies, it is not known whether this response is mediated by the M₁ receptor or another mAChR subtype (Krnjevic, 2004; Carr and Surmeier, 2007). However, previous studies suggest that the M₁ receptor may not be responsible for induction of inward currents in hippocampal CA1 pyramidal cells (Rouse et al., 2000a). Before evaluating the effect of BQCA on this current, we determined the effect of VU0255035, the first highly selective M₁ receptor antagonist that was recently reported (Sheffler et al., 2009), on the CCh-induced inward current. The M₁ receptor

antagonist, VU0255035 (10 μ M), had no effect on holding current alone but significantly blocked the current induced by 100 μ M CCh ($P = 0.0202$, unpaired t -test). These results suggest that the CCh-induced inward current in rat mPFC layer V pyramidal cells is largely mediated by activation of the M_1 receptor. If this is the case, we would predict that the M_1 receptor PAM BQCA should potentiate the CCh-induced inward current. Interestingly, BQCA induced a small change in holding current when applied alone (21.54 ± 2.42 pA, $n = 5$, **Fig. 28**). In addition, BQCA significantly increased the inward current induced by 10 μ M CCh (55.07 ± 6.28 pA upon co-application, $n = 5$, compared to 10 μ M CCh alone, $P = 0.0210$). These data are consistent with the hypothesis that activation of the M_1 receptor induces an inward current in mPFC layer V pyramidal cells and that M_1 receptor PAMs can induce a marked potentiation of this response.

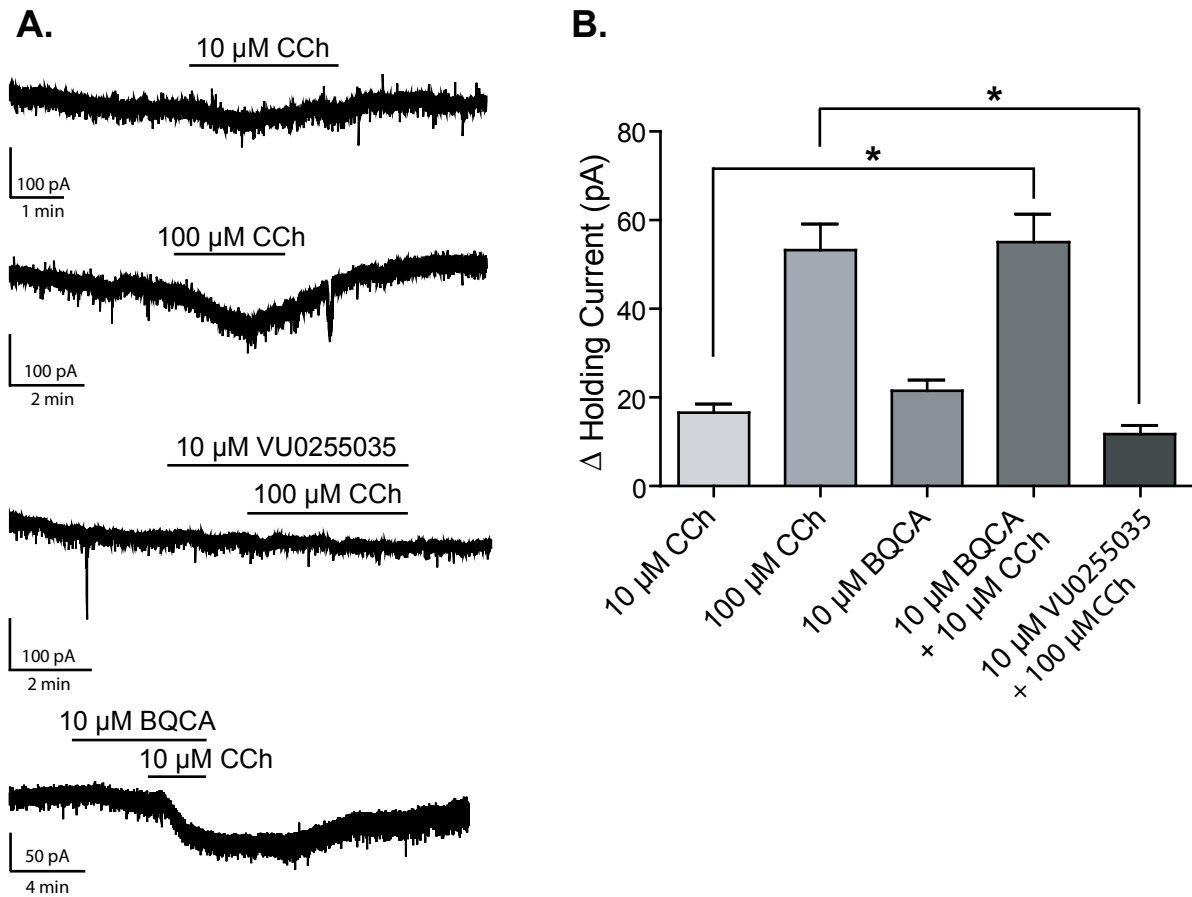


Figure 28. CCh-induced inward current in mPFC layer V pyramidal cells is reduced by M_1 receptor antagonist VU0255035 and potentiated by BQCA. **A.** Sample traces from single experiments showing the change in holding currents upon drug treatments. **B.** Activation of mAChRs by CCh causes a dose-dependent inward current as measured in voltage clamp mode as a change in holding current (16.55 ± 1.93 pA in the presence of $10 \mu\text{M}$ CCh, $n = 4$; 53.14 ± 5.92 pA with $100 \mu\text{M}$ CCh, $n = 4$). M_1 receptor PAM BQCA also caused an inward current when applied alone, and significantly increased the effect of $10 \mu\text{M}$ CCh (21.54 ± 2.42 pA change with $10 \mu\text{M}$ BQCA, $n = 5$; 55.07 ± 6.28 pA when BQCA was co-applied with $10 \mu\text{M}$ CCh, $n = 5$, as compared to $10 \mu\text{M}$ CCh alone, $P = 0.0210$). The effect of $100 \mu\text{M}$ CCh was also significantly inhibited by $10 \mu\text{M}$ M_1 receptor antagonist VU0255035 (11.78 ± 1.90 pA in the presence of antagonist, $n = 3$, compared to $100 \mu\text{M}$ CCh alone, $P = 0.0202$). Sample traces represent experiments from single cells, and bars show duration of drug exposure. All changes in holding current were compared to baseline control and are represented as mean \pm S.E.M. Asterisks indicate significant differences from control (*, $P < 0.05$; unpaired t -test).

BQCA does not potentiate CCh-mediated inward currents in M₁ knockout mice

Application of CCh caused a dose-dependent inward current in mPFC layer V pyramidal cells in slices from wild-type (3 μ M CCh, 24.0 ± 3.9 pA; 30 μ M CCh, 34.4 ± 5.8 pA; **Fig. 29A**) and M₁ knockout mice (3 μ M CCh, 2.1 ± 1.2 pA; 30 μ M CCh, 6.1 ± 2.0 pA; 100 μ M CCh, 42.0 ± 10.5 pA **Fig. 29B**) but had much lower potency in slices from knockout animals. While BQCA alone (10 μ M) induced a slight inward current in wildtype cells (17.9 ± 6.0 pA), it induced a much smaller change in holding current in M₁ knockout cells (9.1 ± 1.9 pA); co-application of BQCA with 3 μ M CCh increased the inward current induced by this low concentration of CCh (35.2 ± 9.9 pA). In contrast, BQCA did not potentiate the response to 30 μ M CCh in M₁ knockout slices (3.5 ± 1.2 pA). Because of the limited availability of knockout animals during this time, experiments testing the ability of atropine or the M₁ antagonist, VU0255035, to block the inward current caused by 100 μ M CCh were not performed. While this critical control is necessary for conclusive interpretation of these data, trends in the dose response to CCh between wildtype and M₁ knockout animals imply that the M₁ subtype mediates, at least in part, the CCh-induced inward current. While the slight response to BQCA (**Fig. 29B**) in knockout animals is somewhat worrisome, holding current stability throughout the duration of these experiments is highly variable and further controls to test the significance of this response will be required.

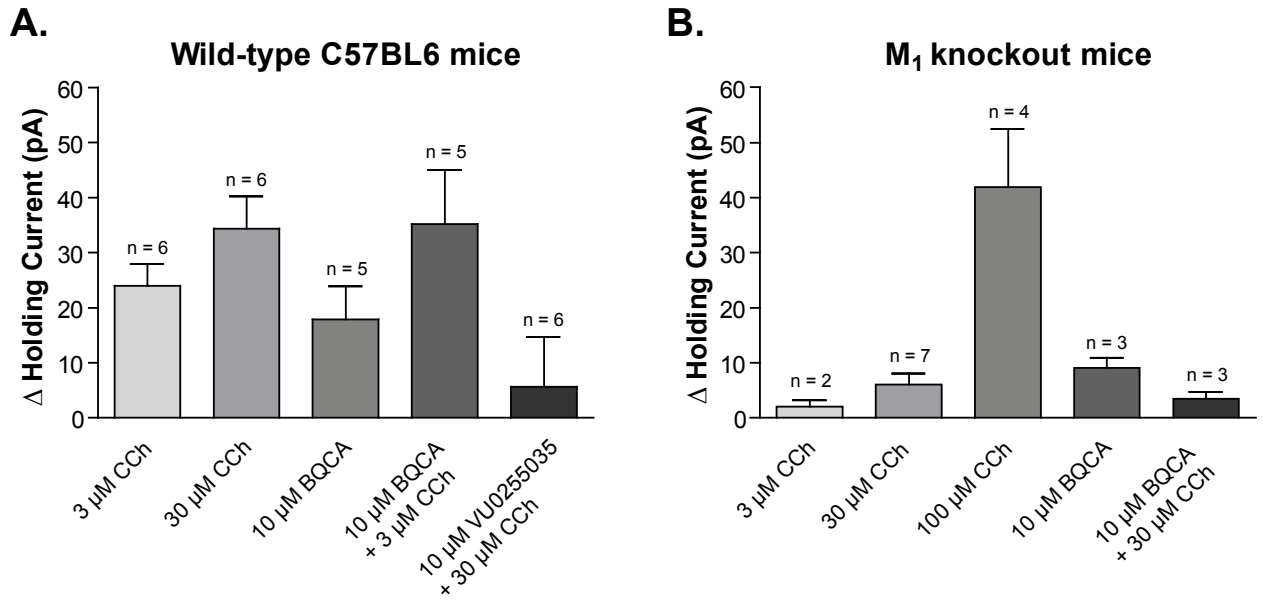


Figure 29. BQCA does not potentiate CCh-mediated inward currents in M₁ knockout mice. Application of CCh caused a dose-dependent inward current in mPFC layer V pyramidal cells in slices from wild-type (3 μM CCh, 24.0 ± 3.9 pA; 30 μM CCh, 34.4 ± 5.8 pA) and M₁ knockout mice (3 μM CCh, 2.1 ± 1.2 pA; 30 μM CCh, 6.1 ± 2.0 pA; 100 μM CCh, 42.0 ± 10.5 pA) but had much lower potency in slices from knockout animals. While BQCA alone (10 μM) induced a slight inward current in wildtype cells (17.9 ± 6.0 pA), it induced a much smaller change in holding current in M₁ knockout cells (9.1 ± 1.9 pA); co-application of BQCA with 3 μM CCh increased the inward current induced by this low concentration of CCh (35.2 ± 9.9 pA). In contrast, BQCA did not potentiate the response to 30 μM CCh in M₁ knockout slices (3.5 ± 1.2 pA).

mAChR activation increases mPFC spontaneous EPSC amplitude and frequency

It is also possible that activation of the M_1 receptor could increase activity of excitatory synaptic inputs to the mPFC and that this could contribute to the postulated role of this receptor in increasing PFC activity from *in vivo* studies in M_1 receptor knockout mice (Anagnostaras et al., 2003). Thus, we determined the effect of mAChR activation on spontaneous excitatory postsynaptic currents (sEPSCs) in mPFC pyramidal cells. Application of CCh caused a dramatic, concentration-dependent increase in the frequency of spontaneous EPSCs; the effect of a maximal concentration of 100 μ M CCh on one representative cell is shown in **Fig. 30A**. Cumulative probability plots of amplitude and inter-event interval from the same cell demonstrate significant shifts in the presence of 100 μ M CCh that are reversible upon wash (**Fig. 30B**). The concentration-response relationships for CCh effects on sEPSC amplitude and frequency are shown in **Fig. 30C**. A concentration of 10 μ M CCh was without effect ($97.5 \pm 4.4\%$ control for amplitude, $90.1 \pm 12.4\%$ control for frequency, $n = 6$); however, 30 and 100 μ M CCh increased both amplitude and frequency (30 μ M amplitude, $108.3 \pm 3.9\%$, frequency, $455.0 \pm 101.9\%$ control, $n = 7$; 100 μ M amplitude, $154.3 \pm 46.2\%$, $887.6 \pm 268.5\%$ control for frequency, $n = 5$). The effects of 30 μ M CCh on both amplitude and frequency were completely blocked by the non-selective muscarinic antagonist, atropine (5 μ M, $102.9 \pm 7.8\%$ and $104.4 \pm 19.6\%$ control, respectively, $n = 3$) indicating that the effect of CCh was due to activation of mAChRs.

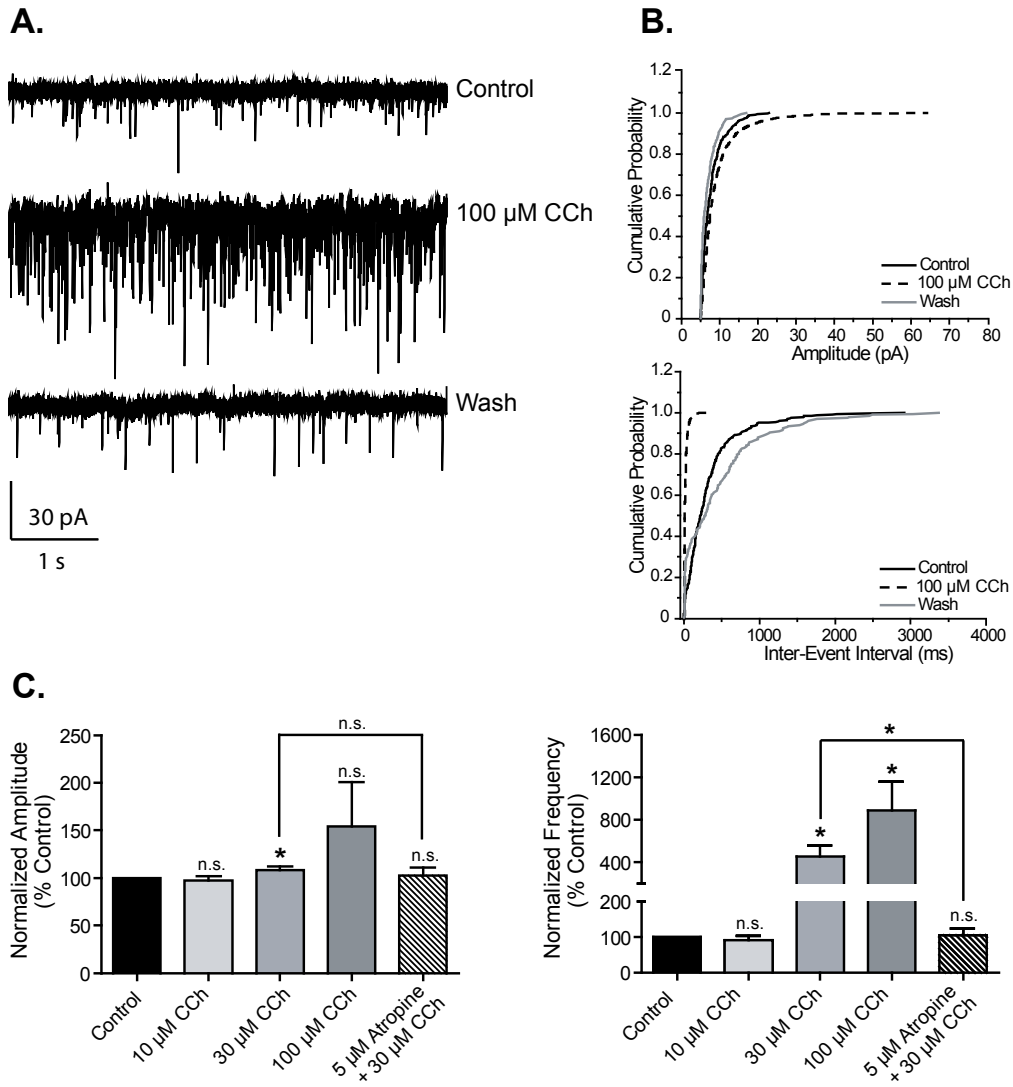


Figure 30. Muscarinic receptor activation increases mPFC spontaneous EPSC amplitude and frequency. **A.** Representative traces from one cell showing the effect of a maximal concentration of 100 μM CCh. **B.** Change in cumulative probability plots of sEPSC amplitude (top panel) and inter-event interval (bottom panel) upon addition and wash of 100 μM CCh from one representative cell. **C.** Averaged amplitude and frequency show that CCh treatment induces a dose-dependent increase in both sEPSC amplitude and frequency which is reversible upon washout and is inhibited by 5 μM atropine (amplitudes, 10 μM CCh, $97.5 \pm 4.4\%$, $n = 6$, $P = 0.2727$; 30 μM CCh, $108.3 \pm 3.9\%$, $n = 7$, $P = 0.0498$; 100 μM CCh, $154.3 \pm 46.2\%$, $n = 5$, $P = 0.2393$; 5 μM atropine/30 μM CCh, $102.9 \pm 7.8\%$ of control, $n = 3$, $P = 0.5365$. 30 μM CCh vs. 5 μM atropine/30 μM CCh, $P = 0.4478$; frequencies, 10 μM CCh, $90.1 \pm 12.4\%$, $P = 0.9364$; 30 μM CCh, $455.0 \pm 101.9\%$, $P = 0.0139$; 100 μM CCh, $887.6 \pm 268.5\%$, $P = 0.0314$; 5 μM atropine/30 μM CCh, $104.4 \pm 19.6\%$ of control, $P = 0.6260$. 30 μM CCh vs. 5 μM atropine/30 μM CCh, $P = 0.0458$). All changes in amplitude and frequency were compared to baseline control and are represented as mean \pm S.E.M. Asterisks indicate significant differences from control or between conditions ($*P < 0.05$; paired or unpaired t -test).

The effect of CCh on sEPSC amplitude and frequency is inhibited by VU0255035

To further evaluate the role of the M₁ receptor in the effect of CCh on sEPSCs, slices were treated with the selective M₁ receptor antagonist VU0255035 (5 μM) for 2 min. prior to addition of 30 μM CCh (**Fig. 31A, B**). VU0255035 alone decreased sEPSC amplitude ($92.9 \pm 3.4\%$ control, $n = 11$), and amplitude was further decreased by co-application with 30 μM CCh ($87.1 \pm 3.5\%$ control, **Fig. 31C**). Antagonist alone had no effect of sEPSC frequency ($114.1 \pm 25.8\%$ control) but caused a significant decrease in frequency in the presence of CCh ($62.5 \pm 10.1\%$ control, **Fig. 31C**). These data suggest that the CCh-induced increase in sEPSC amplitude and frequency is mediated by activation of the M₁ receptor. The reversal of the CCh effect on sEPSC frequency in the presence of the M₁ receptor antagonist suggests that blocking the M₁ receptor unmasks an inhibitory action of CCh that may be mediated by another mAChR subtype, possibly M₂ or M₄ receptors.

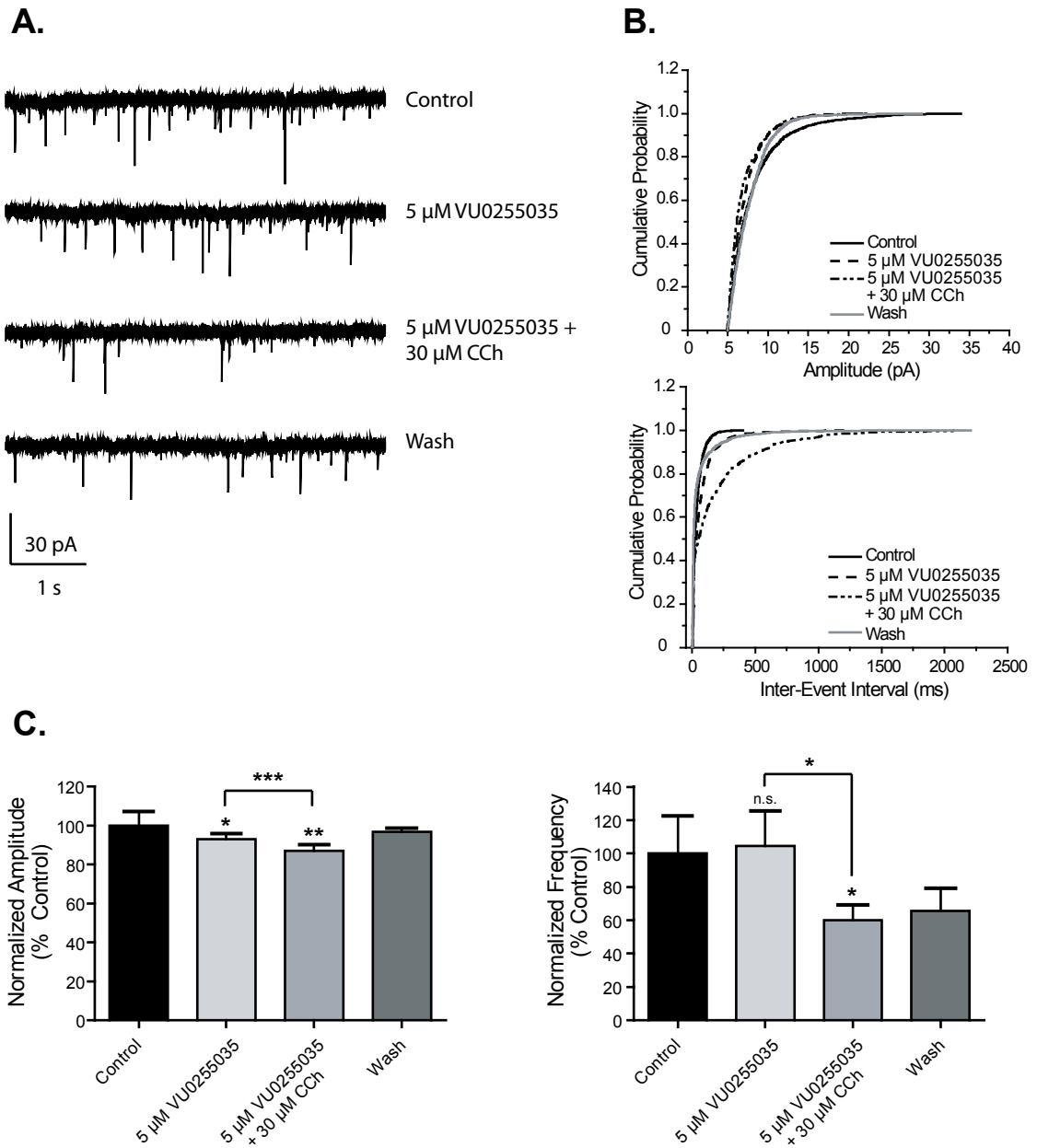


Figure 31. The effect of CCh on sEPSC amplitude and frequency is inhibited by VU0255035. **A.** Sample traces from one cell showing lack of effect of 30 μM CCh in the presence of the M_1 receptor antagonist VU0255035. **B.** Cumulative probability plots of sEPSC amplitude and frequency from the same cell. **C.** Averaged ($n = 11$) amplitude and frequency. The increase in sEPSC amplitude and frequency induced by 30 μM CCh was reversed by 5 μM VU0255035 (amplitudes, 5 μM VU0255035, $92.9 \pm 3.4\%$, $P = 0.0338$; 5 μM VU0255035 + 30 μM CCh, $87.1 \pm 3.5\%$, $P = 0.0026$; antagonist alone vs. with CCh, $P = 0.0350$; frequencies, 5 μM VU0255035, $114.1 \pm 25.8\%$, $P = 0.4543$; 5 μM VU0255035 + 30 μM CCh $62.5 \pm 10.1\%$ of control, $P = 0.0357$; antagonist alone vs. with 30 μM CCh, $P = 0.0161$). All changes in amplitude and frequency were compared to baseline control and are represented as mean \pm S.E.M. Asterisks indicate significant differences from control or between drug conditions (*, $P < 0.05$; **, $P < 0.01$; ***, $P < 0.0001$; paired or unpaired t -test).

BQCA increases sEPSCs and potentiates the effect of a sub-threshold concentration of CCh on sEPSC frequency

Our results thus far suggest that the M_1 receptor is responsible for the CCh-induced increase in sEPSC frequency; therefore, this response should be potentiated by BQCA. To test this hypothesis, slices were treated with BQCA alone for 2 min. (10 μ M) prior to addition of 10 μ M CCh. Sample traces and cumulative probability plots are shown in **Fig. 32A and 32B**. Treatment with BQCA alone did not significantly affect sEPSC amplitude, but increased the frequency of events ($108.3 \pm 6.6\%$ control, $277.0 \pm 97.7\%$ control, respectively, $n = 11$, **Fig. 32C**). Co-application of BQCA and 10 μ M CCh induced a further increase in sEPSC frequency ($994.5 \pm 301.5\%$ control), which differed significantly from the effect of 10 μ M CCh ($P = 0.0045$, unpaired t -test) (see **Fig. 30C**) or BQCA alone ($P = 0.0116$, paired t -test).

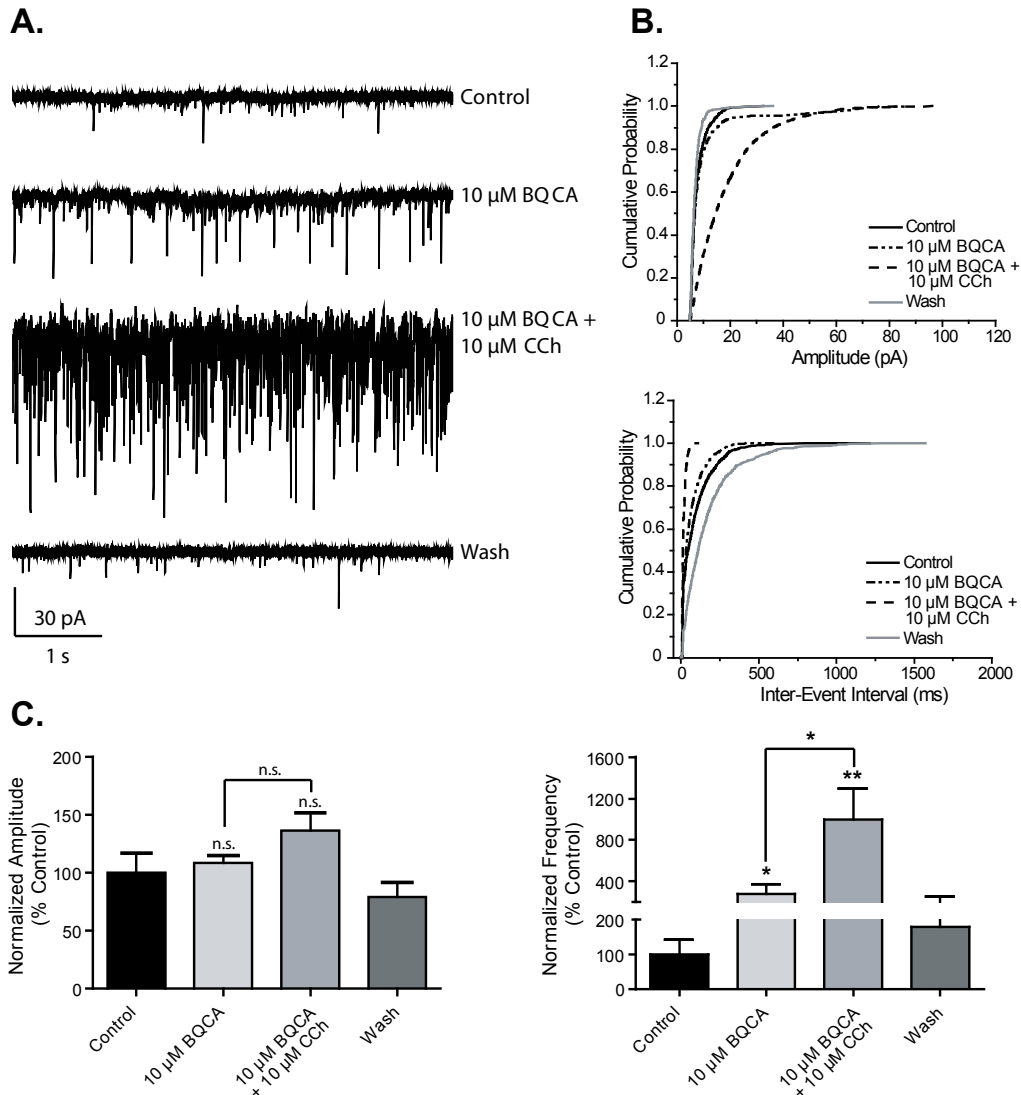


Figure 32. BQCA increases sEPSCs and potentiates a sub-threshold concentration of CCh to increase sEPSC frequency. **A.** Representative traces from one cell showing the effect of 10 μM BQCA alone and in the presence of 10 μM CCh. This concentration of CCh had no significant effect on sEPSC amplitude or frequency when applied alone. **B.** Change in cumulative probability plots from one representative cell of sEPSC amplitude (top panel) and inter-event interval (bottom panel) upon addition of 10 μM BQCA with and without 10 μM CCh. **C.** Averaged ($n = 11$) amplitude and frequency. Neither drug condition elicited a significant effect on sEPSC amplitude (10 μM BQCA, $108.3 \pm 6.6\%$, $P = 0.5013$; 10 μM BQCA/10 μM CCh, $136.0 \pm 15.3\%$ control, $P = 0.0524$) but significantly increased frequency (10 μM BQCA, $277.0 \pm 97.7\%$, $P = 0.0229$; 10 μM BQCA/10 μM CCh, $994.5 \pm 301.5\%$ control, $P = 0.0045$; the effect of combined drug treatment vs. 10 μM BQCA alone was significantly different, $P = 0.0116$). The effect of 10 μM CCh on frequency in the absence and presence of BQCA was also significantly different ($P = 0.0177$). All changes in amplitude and frequency were compared to baseline control and are represented as mean \pm S.E.M. Asterisks indicate significant differences from control or between drug conditions (*, $P < 0.05$; **, $P < 0.01$; paired or unpaired t -test).

CCh and BQCA have no effect on miniature EPSC amplitude and frequency in rat mPFC layer V pyramidal cells

To determine whether the actions of CCh and BQCA require action potential-dependent EPSCs, we determined the effects of these compounds on miniature EPSCs (mEPSCs). mEPSCs were recorded in voltage clamp mode at a holding potential of -70 mV and in the presence of 1 μ M tetrodotoxin (TTX) to block voltage-gated sodium channels. At this concentration, TTX completely eliminates action potential firing and action potential-mediated synaptic activity (Morisset and Urban, 2001). Under these conditions, neither CCh nor BQCA elicited any effect on mEPSC amplitude or frequency. Sample traces from one cell in a slice to which 100 μ M CCh was applied in the presence of TTX show a clear lack of effect (**Fig. 33A**). Cumulative probability plots of amplitude and frequency during control, CCh treatment, and wash from the same cell overlap (**Fig. 33B**). Pooled amplitude and frequency for all drug treatments are quantified in **Fig. 33C** (10 μ M CCh, $n = 5$; 100 μ M CCh, $n = 4$; 10 μ M BQCA with and without 10 μ M CCh, $n = 4$). The only significant effect was that of 10 μ M CCh, which slightly decreased mEPSC amplitude ($88.6 \pm 3.8\%$ control). The effects of M_1 receptor activation on spontaneous EPSCs thus require action potential firing.

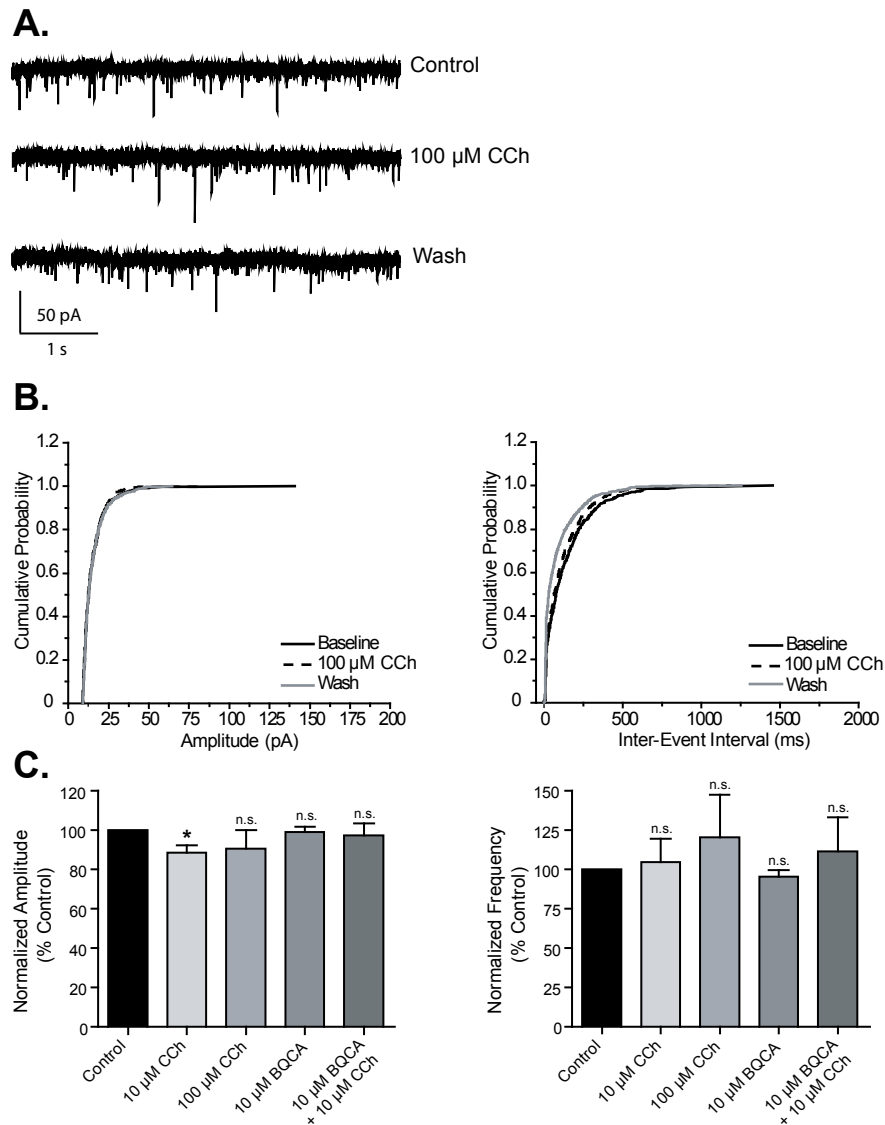


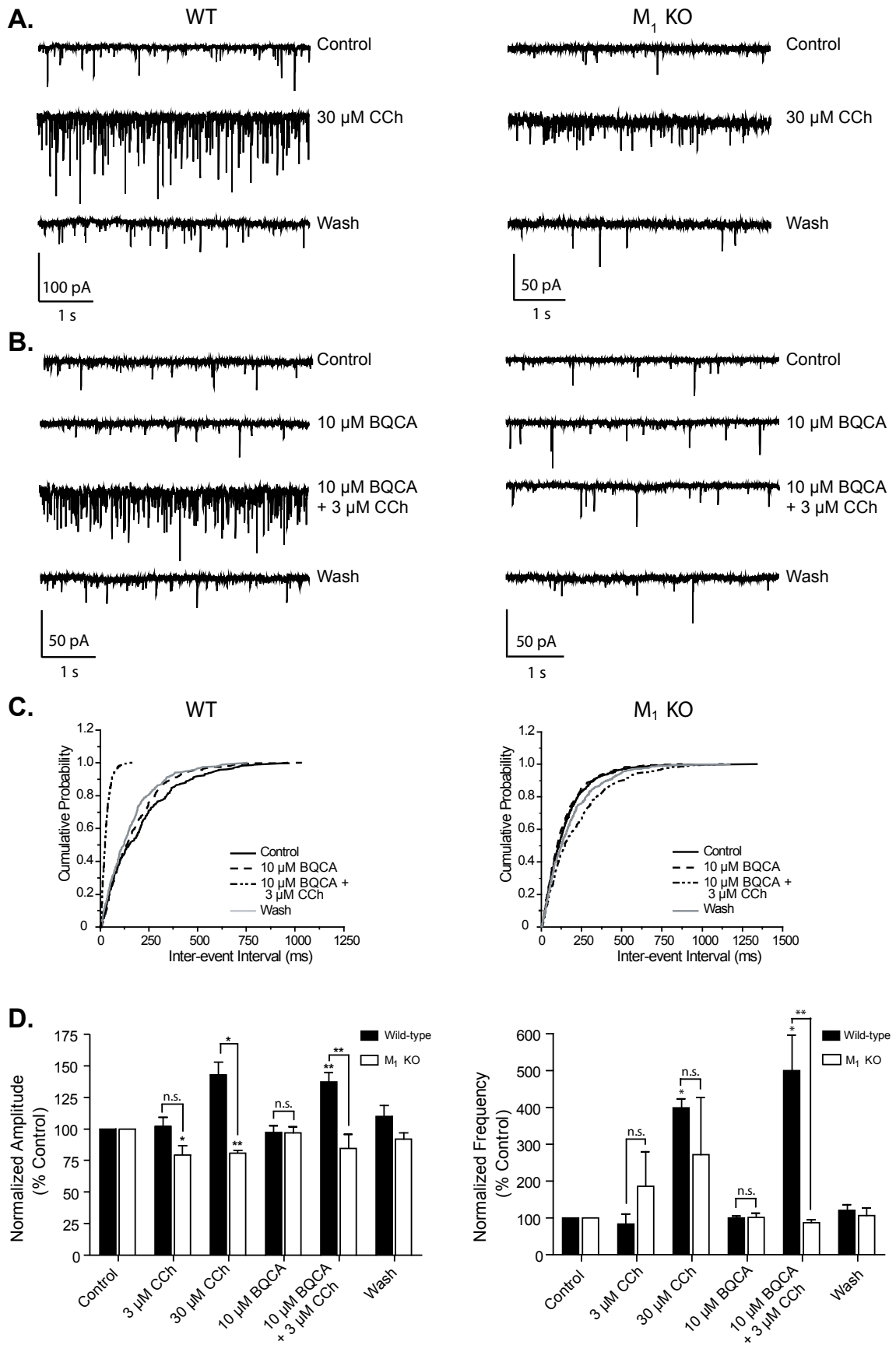
Figure 33. CCh and BQCA have no effect on miniature EPSC amplitude and frequency in rat mPFC layer V pyramidal cells. **A.** Sample traces from one cell showing the lack of 100 μM CCh on mEPSCs in the presence of 1 μM TTX. **B.** Cumulative probability plots for amplitude and frequency of miniature excitatory events from the representative cell shown in **A.** **C.** Averaged amplitude and frequency (10 μM CCh, $n = 5$; 100 μM CCh, $n = 4$; 10 μM BQCA alone and with 10 μM CCh, $n = 4$) of mEPSCs recorded in rat slices. No increase in either amplitude or frequency of events occurred in the presence of low or high CCh, BQCA, or BQCA co-applied with CCh (amplitudes, 10 μM CCh, $88.6 \pm 3.8\%$, $P = 0.0475$; 100 μM CCh, $90.8 \pm 9.4\%$, $P = 0.2592$; 10 μM BQCA, $99.1 \pm 2.8\%$, $P = 0.9562$; 10 μM BQCA/10 μM CCh, $97.6 \pm 5.8\%$, $P = 0.7334$; frequencies: 10 μM CCh, $104.6 \pm 14.9\%$, $P = 0.8883$; 100 μM CCh, $120.4 \pm 27.1\%$, $P = 0.8174$; 10 μM BQCA, $95.3 \pm 4.3\%$, $P = 0.2105$; 10 μM BQCA/10 μM CCh, $111.5 \pm 21.6\%$, $P = 0.6445$). All changes in amplitude and frequency were compared to baseline control and are represented as mean \pm S.E.M. Asterisks indicate significant differences from control or between drug conditions (*, $P < 0.05$; **, $P < 0.01$; ***, $P < 0.0001$; paired t -test).

BQCA has no effect on sEPSCs in slices from M₁ receptor KO mice

In order to confirm that the actions of BQCA were mediated by M₁ receptor activation, recordings of sEPSCs in mPFC layer V neurons were made using slices from mice lacking the M₁ receptor and compared to wild-type (WT) controls. Consistent with our studies in rat slices, CCh caused a concentration-dependent increase in sEPSC amplitude and frequency in WT mice (**Fig. 34A left panel, 34D black bars**). While 3 μ M CCh had no effect on amplitude or frequency, 30 μ M CCh significantly increased both parameters (amplitudes, 3 μ M CCh, $102.6 \pm 11.7\%$ of control, $n = 3$; 30 μ M CCh, $143.1 \pm 22.0\%$, $n = 5$; frequencies: 3 μ M CCh, $83.2 \pm 47.1\%$, 30 μ M CCh, $398.3 \pm 56.2\%$). In contrast to effects in rat slices, BQCA had no effect alone in WT slices (10 μ M BQCA, $97.3 \pm 11.3\%$ control amplitude, $99.8 \pm 11.3\%$ control frequency, $n = 5$), but induced robust increases in both amplitude and frequency when co-applied with 3 μ M CCh ($137.2 \pm 16.7\%$ control amplitude, $500.5 \pm 212.3\%$ control frequency). In slices from M₁ receptor KO mice, the response to CCh was markedly reduced. In M₁ KO mice, CCh decreased sEPSC amplitude at both concentrations tested and induced a more modest increase in sEPSC frequency that did not achieve statistical significance (amplitudes, 3 μ M CCh, $79.4 \pm 14.9\%$, $n = 4$; 30 μ M CCh, $80.7 \pm 5.2\%$, $n = 4$; frequencies, 3 μ M CCh, $186.3 \pm 187.4\%$, 30 μ M CCh, $271.7 \pm 310.4\%$). Importantly, the response to BQCA was completely absent in slices from M₁ receptor KO mice. Thus, BQCA had no effect when applied alone or when co-applied with 3 μ M CCh (amplitudes, 10 μ M BQCA, $96.9 \pm 10.6\%$; BQCA/CCh, $84.5 \pm 25.3\%$, $n = 5$; frequencies, 10 μ M BQCA, $101.3 \pm 26.1\%$; BQCA/CCh, $86.6 \pm 17.3\%$). Responses to co-application of BQCA and CCh differed significantly between WT and M₁ receptor

KO for both sEPSC amplitude and frequency ($P = 0.0046$ for amplitude; $P = 0.0025$ for frequency, unpaired t -test). These results confirmed that the actions of BQCA in WT mice and rats are due to its action at M_1 receptors.

Figure 34. BQCA has no effect and does not potentiate the CCh effect on sEPSCs in M_1 receptor KO mice. **A.** Sample traces from individual cells in slices made from wild-type (left panels) and M_1 receptor KO mice (right panels) showing the robust effects of 30 μ M CCh on both sEPSC amplitude in frequency compared to the milder effect in the M_1 receptor KO slice (top panels). **B.** Bottom panels illustrate the lack of effect of 10 μ M BQCA in both the WT and M_1 receptor KO and contrast the increase in amplitude and frequency with the addition of BQCA and 10 μ M CCh to the lack of effect in the M_1 receptor KO. **C.** Cumulative probability plots of the inter-event intervals from the two cells shown in bottom panels above. **D.** Averaged amplitude and frequency of sEPSCs measured in wild-type (black bars: 3 μ M CCh, $n = 3$; 30 μ M CCh, $n = 5$; 10 μ M BQCA and 10 μ M BQCA + 3 μ M CCh, $n = 5$) and M_1 receptor KO slices (white bars: 3 μ M CCh, $n = 4$; 30 μ M CCh, $n = 4$; 10 μ M BQCA and 10 μ M BQCA + 3 μ M CCh, $n = 5$). In **wild-type slices**, 3 μ M CCh had no significant effect on amplitude or frequency ($102.6 \pm 11.7\%$, $P = 0.6381$ and $83.2 \pm 47.1\%$ of control, $P = 0.4423$, respectively) whereas 30 μ M CCh increased both ($143.1 \pm 22.0\%$, $P = 0.0306$ for amplitude, $398.3 \pm 56.2\%$, $P = 0.0342$ for frequency). BQCA had no effect on amplitude or frequency but potentiated the response to 3 μ M CCh (amplitudes, 10 μ M BQCA, $97.3 \pm 11.3\%$, $P = 0.7642$ compared to control; 10 μ M BQCA/3 μ M CCh, $137.2 \pm 16.7\%$, $P = 0.0052$ compared to control; frequencies, 10 μ M BQCA, $99.8 \pm 11.3\%$, $P = 0.7261$ compared to control; 10 μ M BQCA/3 μ M CCh, $500.5 \pm 212.3\%$, $P = 0.0209$ compared to control). In **M_1 receptor KO slices**, 3 μ M CCh decreased amplitude but had no significant effect on frequency ($79.4 \pm 14.9\%$, $P = 0.0490$ and $186.3 \pm 187.4\%$ of control, $P = 0.7656$, respectively). 30 μ M CCh also significantly decreased amplitude and increased frequency although the effect on frequency was less dramatic than that seen in WT controls ($80.7 \pm 5.2\%$, $P = 0.0092$ for amplitude, $271.7 \pm 310.4\%$, $P = 0.6010$ for frequency). While the difference between the 30 μ M CCh effect on amplitude was significant between genotypes ($P = 0.0229$), the effect on frequency was not ($P = 0.4756$). BQCA had no effect alone in KO slices (amplitude, $96.9 \pm 10.6\%$, $P = 0.4925$; frequency, $101.3 \pm 26.1\%$, $P = 0.7286$) and there was no difference in this lack of effect between genotypes (amplitude, $P = 0.9596$; frequency, $P = 0.9133$). When applied with 3 μ M CCh, BQCA had no significant effect on amplitude or frequency (amplitude, $84.5 \pm 25.3\%$, $P = 0.3383$; frequency, $86.6 \pm 17.3\%$, $P = 0.1388$ compared to KO control), and both effects were significantly different those in WT slices ($P = 0.0046$ for amplitude, $P = 0.0025$ for frequency). All changes in amplitude and frequency were compared to baseline control and are represented as mean \pm S.E.M. Asterisks indicate significant differences from control or between drug conditions (*, $P < 0.05$; **, $P < 0.01$; ***, $P < 0.0001$; paired or unpaired t -test).



BQCA achieves brain penetration after systemic administration

The studies outlined above suggest that BQCA could be an excellent tool for probing M₁ receptor function. Furthermore, based on these and previous studies, it is possible that BQCA could enhance mPFC activity and enhance PFC-dependent cognitive function. However, before using BQCA for *in vivo* studies, it was critical to determine whether this compound had a pharmacokinetic (PK) profile suitable from systemic dosing and whether it crossed the blood brain barrier. Thus, we performed a PK analysis of BQCA after systemic dosing. BQCA was measured at multiple time points in both plasma and brain after *i.p.* injection in rats (**Fig. 35 and Table 8**). BQCA is slowly but very significantly absorbed into systemic circulation with maximum concentration (~10 µg/ml) being achieved 2 h after *i.p.* administration. The compound is rapidly taken up into the brain and achieves a maximal brain concentration between 30 min and 1 hr after dosing. Furthermore the brain concentration is maintained at a stable level for approximately 4 hr. While the brain concentrations are significantly lower when compared to plasma concentrations (**Fig. 35 and Table 8**), BQCA possesses an acceptable PK profile and brain penetration to allow use for *in vivo* studies of effects this compound on CNS function.

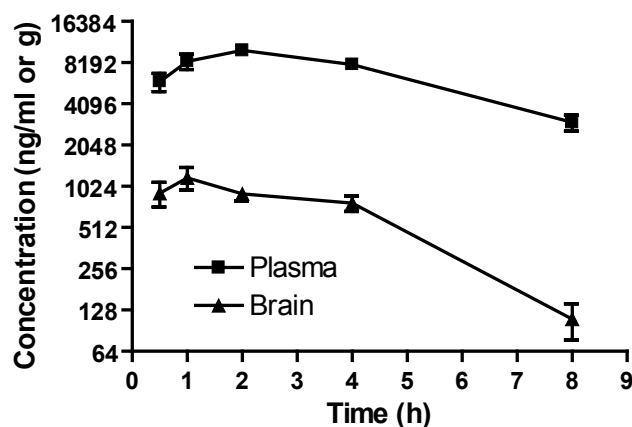


Figure 35. Pharmacokinetic profiling of BQCA in rats. Concentration-time profile of BQCA in brain and plasma of male Sprague Dawley rats following 10 mg/kg *ip* administration. Blood and brain tissue were collected at 0.5, 1, 2, 4 and 8 h after dosing. Samples were extracted as described in Methods and analyzed by LC-MS-MS (**Chapter II**). BQCA is characterized by significant absorption into and slow elimination from systemic circulation after intraperitoneal administration. Although the compound is rapidly and significantly taken up into the brain, the brain concentrations are rapidly eliminated when compared to plasma concentrations. Each time point represents the mean determination \pm S.D. of three rats. Experiments performed by S.B. Jadhav and U. Menon.

Table 8. Pharmacokinetic Analysis of BQCA

PK Parameter	Plasma	Brain
C_{max} (ng/mL)	10017.31 \pm 1562.77	1181.65 \pm 224.43
T_{max} (h)	2	1
Elimination $T_{1/2}$ (h)	3.33	2.04
AUC ₍₀₋₈₎ (ng.h/mL)	52344.03 \pm 2382.63	4797.28 \pm 388.81
V/F (L/kg)	0.72	n.d.
V _{ss} /F (L/Kg)	0.83	n.d.
Cl/F (L/h/kg)	0.149	n.d.

The pharmacokinetic parameters of BQCA in exposure studies in male rats after 10.0 mg/kg intraperitoneal administration are shown. AUC (0-8) Brain/AUC (0-8) Plasma = 0.091. Values represent mean \pm S.E.M. (n = 3 rats). (n.d., not determined).

BQCA increases the firing rate of mPFC neurons *in vivo* in rats

Having established the PK profile and CNS penetration of BQCA, we performed *in vivo* electrophysiology studies to test the hypothesis that the electrophysiological effects observed on mPFC neurons *in vitro* can lead to increases in activity of mPFC neurons in behaving animals. To accomplish this, multiple single-unit recordings were obtained from the mPFC of rats trained to perform an auditory detection task for food reward. A total of 57 cells (vehicle, $n = 20$; BQCA, $n = 37$) with waveform and firing rate characteristics consistent with those of putative pyramidal cells were obtained from 6 rats in the presence of either vehicle or drug (20 mg/kg). **Figure 36** shows the average percentage change, relative to a thirty-minute pre-injection epoch, in the spontaneous firing rate of mPFC cells following drug or vehicle administration. Consistent with the acute cortical slice data, BQCA caused an elevation in spontaneous firing rate significantly different from vehicle (2-way anova: drug vs. vehicle, $P < 0.005$). Significant elevations in firing rate were observed within the first thirty-minute epoch following injection and were maintained across the entire hour and a half recording period.

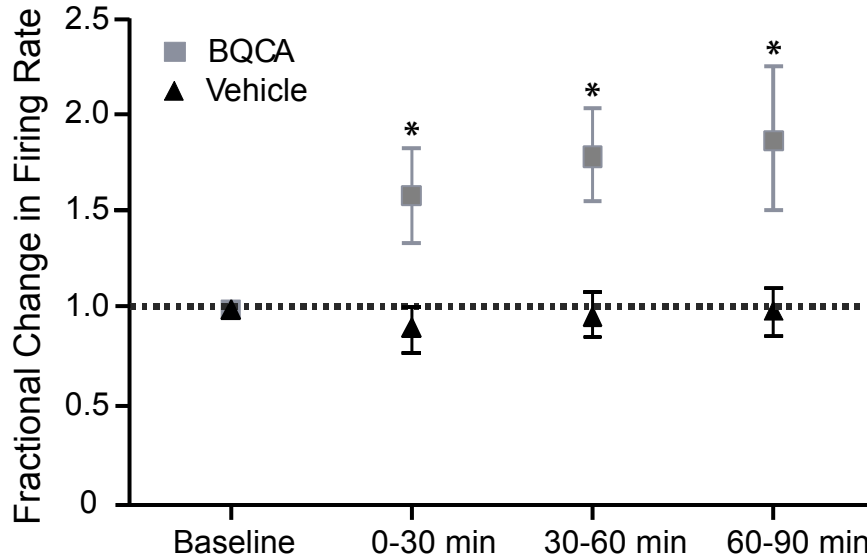


Figure 36. BQCA increases the firing rate of mPFC neurons *in vivo* in rats. Multiple single-unit recordings were obtained from the medial prefrontal cortex of conscious, freely moving rats. A total of 57 cells (vehicle, $n = 20$, BQCA, $n = 37$) with waveform and firing rate characteristics consistent with those of putative pyramidal cells were obtained from 6 rats in the presence of either vehicle or drug (20 mg/kg). The mean firing rate for each neuron within an epoch was calculated as a percent of the pre-injection baseline rate. Treatment with BQCA (■) resulted in an elevation in spontaneous firing rate that was significantly different from vehicle (▲) (2-way anova; BQCA vs. vehicle; $P < 0.005$) within the first 30 min epoch and was maintained across the entire trial period. Experiments performed by E.P. Christian, J.J. Doherty, M.C. Quirk, and D.H. Snyder at AstraZeneca Pharmaceuticals.

Acute administration of BQCA restores impairment in reversal learning in Tg2576 mice

Recent studies have revealed that mice over-expressing a familial AD mutant form of the amyloid precursor protein (Tg2576 mice) are impaired on compound discrimination reversal learning compared to littermate controls (Zhuo et al., 2007; Zhuo et al., 2008). Interestingly, reversal learning is a PFC-dependent form of learning, suggesting that this mouse model of AD leads to disruption of at least one form of PFC-dependent cognition. Based on the finding that M₁ receptor KO mice have deficits in PFC function (Anagnostaras et al., 2003) and that BQCA increases PFC activity, it is possible that this M₁ receptor-selective PAM could reverse deficits in compound discrimination reversal learning observed in Tg2576 mice. In agreement with previously published reports, we found that Tg2576 mice exhibit impaired performance in a compound discrimination reversal learning task (**Fig. 37**). Acute administration of BQCA improved the performance of the Tg2576 mice on the compound discrimination and the compound discrimination reversal task by reducing the odds that errors would be committed, $\chi^2 = 23.19$ and $\chi^2 = 13.03$, 1, respectively ($P < 0.001$, **Table 9, Fig. 37C-D**). On the compound discrimination, the odds that vehicle-treated Tg2576 mice made errors were 6.89 times greater than the BQCA-treated Tg2576 mice. Similarly, on the compound discrimination reversal, the odds of the vehicle-treated Tg2576 mice to make errors were 3.22 times greater than the BQCA-treated Tg2576 mice. There prevalence of errors on the simple discrimination or the simple discrimination reversal tasks did not significantly differ across groups or treatments. Overall, the results indicate that BQCA improves compound reversal learning which is consistent with hypothesis that M₁

activation may enhance PFC-dependent cognitive function. Additionally, BQCA may also have more widespread effects on cognition, indicated by the reduction of errors on the compound discrimination in BQCA-treated Tg2576 mice, and may be of even broader utility in enhancing other domains of cognitive function.

Table 9. BQCA reverses impairments in discrimination learning in Tg2576 mice

Group	Simple Discrimination	Simple Discrimination Reversal	Compound Discrimination*	Compound Discrimination Reversal**
Wild-type + Vehicle	2/9 (22%)	5/9 (55%)	4/9 (44%)	3/9 (33%)
Wild-type + BQCA	3/12 (25%)	6/12 (50%)	5/12 (42%)	4/12 (33%)
Tg2576 + Vehicle	1/8 (12%)	4/8 (50%)	5/8 (62%)	7/8 (87%)
Tg2576 + BQCA	2/11 (18%)	5/11 (45%)	1/11 (9%)	3/11 (27%)

* $\chi^2 = 23.19, P < 0.0001$

** $\chi^2 = 13.03, P < 0.001$

The frequency of errors on discrimination learning between wild-type and Tg2576 mice in the presence of vehicle or BQCA (number of subjects with errors ≥ 1 /total number of subjects in group expressed as a percentage).

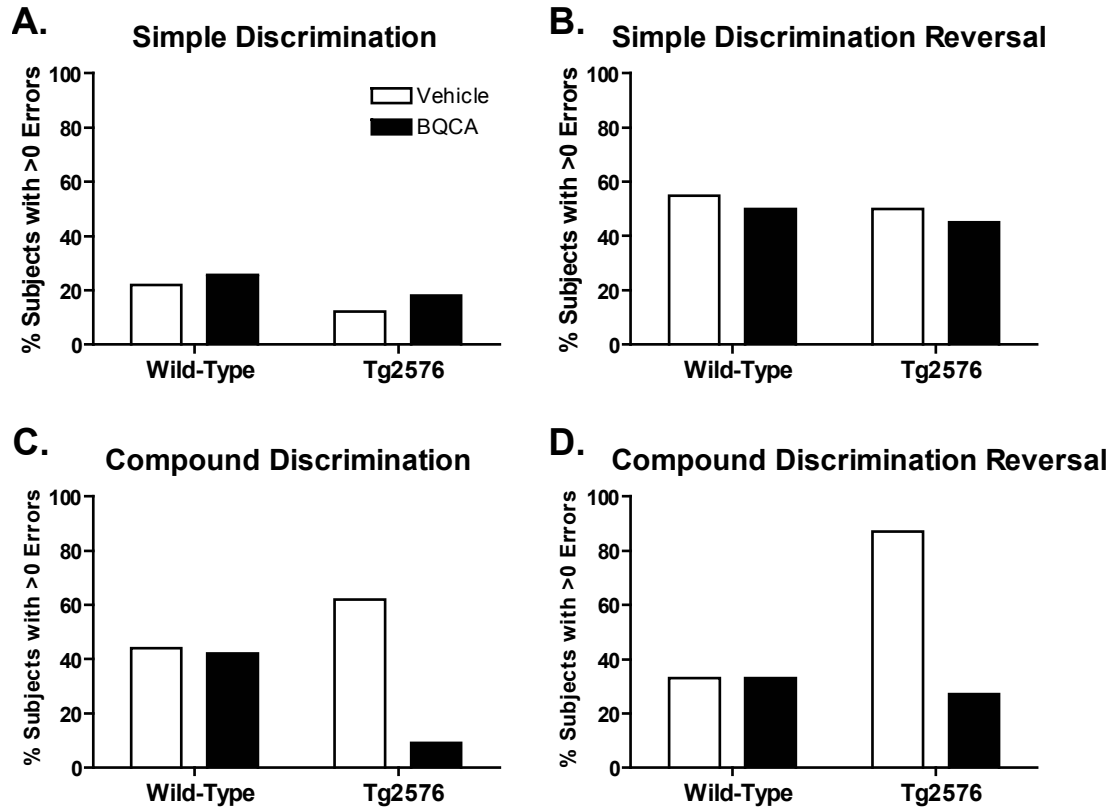


Figure 37. Effects of acute administration of BQCA on discrimination learning in Tg2576 mice. Errors to reach criterion on a discrimination task were assessed in wild-type and Tg2576 mice at 12 months of age. Mice were injected *s.c.* one hour before testing with either saline vehicle or 30 mg/kg BQCA. Shown are the frequency of errors on discrimination learning between wild-type and Tg2576 mice in the presence or absence of BQCA. Data are expressed as the number of subjects with errors > 0/total number of subjects in the group and expressed as a percentage. BQCA significantly reduced the odds of Tg2576 mice making errors on the compound discrimination and the compound discrimination reversal. Chi-square, $P < .001$ for both compound discrimination and compound discrimination reversal. Experiments performed by Michelle Nicolle and Mona Watson, Wake Forest University.

BQCA regulates non-amyloidogenic APP processing

The data presented above suggest that BQCA has efficacy in improving at least one form of cognitive function in an animal model of AD. In addition to providing symptomatic relief, it has been postulated that increasing M₁ receptor activity could also have disease modifying effects in AD patients (Fisher, 2008; Caccamo et al., 2009). The amyloid precursor protein (APP) undergoes proteolytic cleavage in two competing pathways (Thinakaran and Koo, 2008). In the amyloidogenic pathway, sequential cleavage by β -secretase and γ -secretase releases the A β peptide which forms the core of amyloid plaques found in AD and is implicated in numerous models of neurotoxicity. Alternatively, in the non-amyloidogenic pathway, APP is cleaved by α -secretase within the A β sequence, preventing A β generation. Interestingly, previous studies suggest that activation of M₁ promotes APP processing through the non-amyloidogenic pathway (Caccamo et al., 2006; Jones et al., 2008). If BQCA can promote non-amyloidogenic processing of APP, this could provide a mechanism for slowing accumulation of A β and potentially slow progression of AD.

In order to determine whether BQCA can potentiate the APP processing effect of a low concentration of the mAChR agonist CCh, we treated PC12 cells overexpressing human APP and the M₁ receptor with an approximate EC₂₀ concentration (50 nM) of CCh in the presence of increasing concentrations of BQCA and measured the levels of APP metabolites in the conditioned media and cell extracts. BQCA caused a dose-dependent increase in the shedding of APP α , the amino-terminal ectodomain of APP released by α -secretase cleavage (**Fig. 38A-B**). The highest concentration of BQCA

tested (30 μ M) increased APPs α levels to 244% of vehicle-treated cells ($P < 0.05$). BQCA treatment also resulted in the accumulation of CTF α (C83), the corresponding carboxy-terminal fragment generated by α -secretase (**Fig. 38A, C**; increased to 245% of vehicle, $P < 0.05$). Finally, consistent with the observed increases in non-amyloidogenic APP fragments, 30 μ M BQCA treatment resulted in a 30% decrease ($P < 0.01$) in the secretion of the β -secretase derived A β_{40} peptide (**Fig. 38D**). Taken together, these results indicate that BQCA can effectively regulate non-amyloidogenic APP processing, suggesting that M₁ receptor PAMs have the potential to provide both symptomatic and disease modifying effects in AD patients.

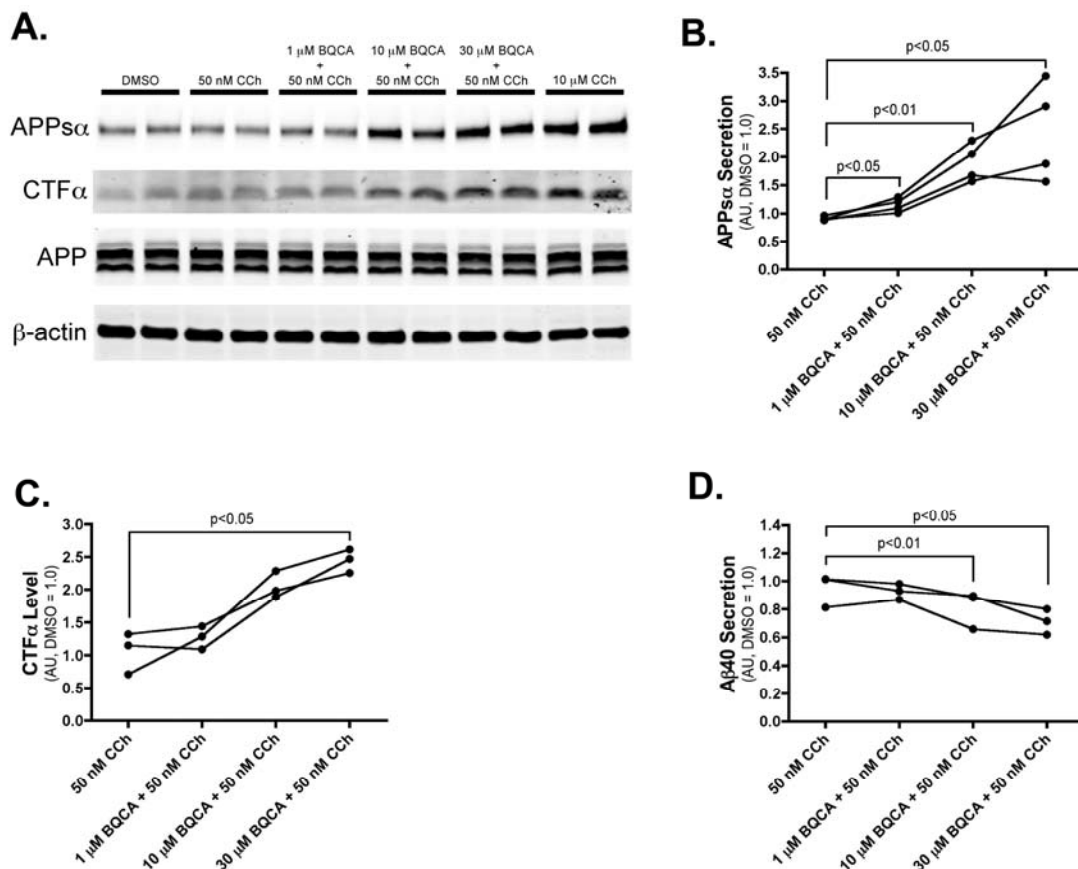


Figure 38. BQCA regulates non-amyloidogenic APP processing. **A.** Western blot analysis of APP metabolites from conditioned media and cell lysates demonstrates increased generation of APPs α and CTF α with increasing concentrations of BQCA as compared to the submaximal concentration of 50 nM CCh. 10 μ M CCh is shown as a maximum concentration. β -actin is shown as a loading control. **B.** Quantitation of APPs α band intensity from conditioned media demonstrates a dose-dependent effect of BQCA on the shedding of APPs α (repeated measures ANOVA, $P = 0.0271$), and pairwise comparisons revealed significant differences at all concentrations of BQCA compared to 50 nM CCh alone (P -values for paired t -tests are shown). **C.** Quantitation of CTF α band intensity from cell lysates shows a dose-dependent effect of BQCA on the production of CTF α (repeated measures ANOVA, $P = 0.0017$) and a significant difference (paired t -test) between 30 μ M BQCA plus 50 nM CCh as compared to 50 nM CCh alone. **D.** ELISA measurements from conditioned media demonstrate that BQCA decreases the secretion of A β ₄₀ peptide in a dose-dependent manner (repeated measures ANOVA, $P = 0.0019$), with significant differences between 50 nM CCh alone and the two highest concentrations of BQCA (paired t -tests). Mean values are shown from three or four independent experiments performed in duplicate. All values are normalized to vehicle-treated cells. Experiments performed by Albert Davis, Emory University.

Discussion

The M₁ receptor has long been viewed as an exciting potential target for increasing cognitive function in patients suffering from AD and other CNS disorders (Wess et al., 2007; Fisher, 2008; Langmead et al., 2008a; Caccamo et al., 2009). Despite major efforts to develop highly selective M₁ agonists over the past two decades, this receptor has proven intractable using traditional approaches, thus preventing M₁ agonists from advancing to clinical use for treatment of AD and other disorders. Also, lack of agents that selectively activate this receptor has made it impossible to develop a full understanding of the functional effects of selectively increasing M₁ receptor activity in the CNS. Discovery and characterization of BQCA and its structural analogs provide a major advance in establishing the utility of M₁ receptor PAMs as an alternative approach to increasing activity of this receptor in a highly subtype-selective manner.

Studies with BQCA, along with the new M₁ receptor- selective antagonist VU0255035, provide important support for the hypothesis that the M₁ receptor may increase activation of the PFC and may enhance PFC-dependent cognitive function (Anagnostaras et al., 2003). Non-selective mAChR agonists, such as CCh, induce an inward current in PFC pyramidal cells, and the present data provide strong evidence that this response is mediated by activation of the M₁ receptor. In addition, activation of the M₁ receptor increases the frequency of spontaneous excitatory synaptic events in mPFC layer V pyramidal cells. While the source of glutamatergic afferents giving rise to these sEPSCs has not been established, this is consistent with the hypothesis that the M₁ receptor plays an important role in increasing excitability and excitatory drive to mPFC pyramidal cells.

One of the most important implications of these studies is that they raise the possibility that highly selective M₁ receptor PAMs may provide a novel approach for treatment of AD and other CNS disorders that may involve impaired cholinergic signaling. Clinical studies using both direct and indirect-acting muscarinic agonists have reported improvements in both cognitive function and behavioral disturbances (*i.e.* hallucinations, delusions, outbursts, and paranoia) observed in AD patients (Bodick et al., 1997b; Cummings et al., 2001). If M₁ receptor activation is responsible for, or plays an important role in, these effects of nonselective cholinergic agents, M₁ receptor PAMs could provide a viable approach to symptomatic treatment of AD. Furthermore, in addition to potential efficacy in reducing symptoms in AD patients, recent studies suggest that mAChR activation could reduce accumulation of toxic A β protein, thereby also providing disease modifying effects. For instance, the muscarinic agonist AF102B was shown to decrease production of the amyloidogenic peptide A β 42 in the cerebral spinal fluid of AD patients (Nitsch et al., 2000). Furthermore, preclinical studies with a related mAChR agonist, AF267B suggest that mAChR activation increases non-amyloidogenic processing and prevents A β formation (Caccamo et al., 2006). While these earlier mAChR agonists are not selective for the M₁ receptor relative to other mAChR subtypes, more recent studies revealed that the M₁ receptor-selective agonist, TBPB, has similar effects in PC12 cells (Jones et al., 2008).

Lastly, it is important to note that recent clinical and animal studies raise the possibility that mAChR agonists may also provide a novel approach for treatment of schizophrenia (Felder et al., 2001; Langmead et al., 2008a; Conn et al., 2009b). For instance, Shekhar and colleagues (Shekhar et al., 2008) recently reported that the M₁/M₄

receptor–preferring agonist xanomeline induced a robust improvement in positive and negative symptoms, as well as some measures of cognitive function, in schizophrenic patients. Based on animal studies, it is likely that both M₁ and M₄ receptors may be important for clinical efficacy in this patient population (Felder et al., 2001; Brady et al., 2008; Chan et al., 2008; Jones et al., 2008; Langmead et al., 2008b; Langmead et al., 2008a; Conn et al., 2009b). Availability of BQCA, along with the new systemically active M₄ receptor- selective PAM, VU0152100 (Brady et al., 2008) should make it possible to evaluate the effects of selective activation of each of these mAChR subtypes as well as co-administration of both BQCA and VU0152100 in a range of animal models that may be relevant to the antipsychotic effects of xanomeline.

CHAPTER V

DISCUSSION AND FUTURE DIRECTIONS

Over the past two decades, major attention has been focused on developing highly selective agonists of specific mAChR subtypes to use as research tools in order to achieve a better understanding of the roles of each subtype in specific organ systems and also to develop therapeutic agents that lack the adverse effects of AChE inhibitors and nonselective muscarinic agents. We now report the discovery of a novel series of compounds that act as robust positive allosteric modulators (allosteric potentiators) of the M₄ and M₁ mAChR subtypes. Unlike traditional agonists, these small molecules do not bind to the orthosteric ACh binding site, but instead act at a distinct site to potentiate activation of the receptor by its natural ligand, ACh. This is directly analogous to the use of benzodiazepines as selective GABA receptor PAMs, which provide an effective and safe approach to the treatment of anxiety and sleep disorders without inducing the potentially lethal effects of direct-acting GABA_A receptor agonists (Mohler et al., 2002). While allosteric modulators of ion channels are well established as research tools and therapeutic agents, they have not been a traditional focus of drug discovery efforts for GPCRs. The discovery of VU10010 and related M₄ PAMS as well as M₁ PAM BQCA adds to recent major advances in developing highly selective allosteric modulators of mAChRs (Chan et al., 2008; Ma et al., 2009; Marlo et al., 2009) and other GPCRs (May et al., 2007; Conn et al., 2009a). These compounds are highly selective for each targeted receptor subtype with no detectable functional activity at other mAChRs. As with

previously discovered allosteric potentiators of metabotropic glutamate receptors (mGluRs), the novel PAMs of M₁ and M₄ receptors reported here have no detectable affinity for the orthosteric site when examined in competition radioligand studies at equilibrium (Brady et al., 2008; Shirey et al., 2008; Shirey et al., 2009). The action of these compounds at a site that is distinct from the highly conserved orthosteric ACh binding site is likely to be critical for achieving this high degree of subtype selectivity.

In addition to providing advantages in terms of achieving high selectivity for an individual mAChR subtype, it is possible that the mechanism of action of these compounds could provide other properties that are ultimately advantageous for developing therapeutic agents. Positive allosteric modulators of M₁ and M₄ mAChRs described here do not activate the receptor directly but induce a dramatic potentiation of the response to activation by ACh. This could provide an advantage to traditional agonists by amplifying endogenous cholinergic signaling for a specific mAChR subtype and thereby maintaining a level of activity dependence of receptor activation. Interestingly, the majority of clinically useful drugs that activate other neuromodulatory systems exert more subtle actions rather than serving as direct-acting receptor agonists. For instance, serotonin reuptake inhibitors have been highly successful in treatment of depression, whereas highly effective serotonin receptor agonists have not been successfully developed. For anxiety disorders, it is likely that direct acting GABA_A receptor agonists would have a narrow therapeutic window and would be lethal. In contrast, benzodiazepines are selective allosteric potentiators of GABA_A receptor chloride channels and are safe and highly effective in the clinic. Dopamine receptor agonists are used but exert more profound acute adverse effects than indirect acting

agents such as L-DOPA, amphetamine, and methylphenidate (Ritalin). Interestingly, highly selective allosteric potentiators of different mGluR subtypes have robust effects in animal models used to predict efficacy in treatment of multiple CNS disorders, including schizophrenia, anxiety disorders and Parkinson's disease (Marino et al., 2003; Kinney et al., 2005; Galici et al., 2006). Furthermore, a highly selective allosteric potentiator of the calcium-sensing receptor (a family III/C GPCR), termed Sensipar, has now received FDA approval for use in treatment of hyperparathyroidism (Dong, 2005). As with the current M₁ and M₄-selective allosteric potentiators, the key to achieving high selectivity for these receptors has been the targeting of sites that are distinct from the highly conserved orthosteric neurotransmitter binding site. These advances with allosteric potentiators of family III/C GPCRs along with the present findings raise the possibility that discovery of highly selective and robust allosteric modulators of specific mAChR subtypes and other family I/A GPCRs will provide an exciting new approach for the discovery and development of novel research tools and therapeutic agents that target this important class of signaling proteins. However, discovery of these compounds also raises the question of whether allosteric modulators may have broad activity across other GPCRs by interacting at potentially promiscuous allosteric sites. The present finding that novel mAChR PAMs have no major activities across multiple targets in a large panel radioligand binding screen was encouraging, but does not address this critical question. The finding that these compounds had no allosteric modulator activity across a panel of other family A GPCR subtypes is exciting and suggests that they are not likely to have activity at a site that is shared across multiple GPCRs. While it is impossible to rule out activity at other unidentified targets, these data suggest that it may be possible to achieve higher subtype

selectivity across a range of receptors than has been possible with many orthosteric ligands.

Interestingly, the M₁ and M₄ PAMs reported here increase affinity of ACh for the orthosteric site. This is similar to previous reports of allosteric modulators of GPCRs acting by altering affinity of ligands at the orthosteric site; the magnitude of binding cooperativity or the shift in orthosteric agonist affinity is referred to as the alpha factor (Christopoulos and Kenakin, 2002). However, while M₄ PAM VU10010 apparently acts in part by increasing ACh affinity, the magnitude of this effect was only a 14-fold increase in ACh affinity whereas VU10010 induced an almost 50-fold shift in the ACh concentration response curve for activating calcium mobilization, **Chapter IIIA** (Shirey et al., 2008). Thus, effects on agonist binding cannot fully account for the allosteric potentiator activity measured in the functional assay; potentiation by this compound must also increase efficacy and coupling to downstream effectors. The present data suggest that VU10010 acts by both increasing ACh affinity and activation of G proteins and downstream signaling pathways. Studies of the effects of VU10010 on [³⁵S]GTPγS binding in cells expressing rat M₄ revealed a 10-fold shift in ACh potency; this value is close to the calculated shift in ACh affinity at the orthosteric site, suggesting that the increase in ACh affinity could account for the shift in ACh potency by increasing G protein activation. However, VU10010 also increased the maximal ACh-induced [³⁵S]GTPγS binding response, suggesting that this potentiator increases the efficiency of M₄ coupling to G proteins. These two factors together likely contribute to the robust shift in ACh potency for inducing calcium mobilization relative to more modest shift observed in ACh affinity. In contrast, radioligand binding studies examining the effect of BQCA

on M₁ receptor affinity for ACh revealed that the fold-shift decrease in ACh K_i induced by BQCA was around 30-fold, whereas the shift in the functional calcium response was 21-fold (Shirey et al., 2009). The increase in affinity for agonist could therefore fully account for the potentiation of calcium mobilization by M₁. This demonstrates the possibility that different allosteric modulators may induce varying degrees of receptor affinity for orthosteric agonists and downstream effector signaling.

A notion that complicates interpretation of selectivity data as discussed above is the possibility of binding of an allosteric modulator to an off-target GPCR without a detectable functional consequence. Because radioligands that bind to allosteric sites of mAChRs and other GPCRs have not yet been developed (with the exception of mGluR5), it is difficult to assess binding at these sites using traditional equilibrium experiments. It is possible, however to determine if allosteric ligands affect the affinity of orthosteric site ligands. For example, VU10010 and BQCA did not compete for orthosteric [³H]-NMS binding but induced a leftward shift in the ACh competition curve (**Chapters IIIA and IV**, (Shirey et al., 2008)). While VU10010 did not compete for [³H]-NMS binding in membranes from cells expressing any mAChR subtype, its effects on ACh affinity at off-target receptor subtypes were not determined. This will be one critical experiment that should be performed with novel allosteric modulators to assess their binding to off-target receptors. Another related experimental approach that may be useful in screening for compounds that only bind to a targeted mAChR or other GPCR involves examining neutral allosteric binding to off-target receptors or receptor subtypes. With the newly available panel of allosteric modulators (and in the case of M₁, allosteric agonists such as TBPB) of mAChRs, it is now possible to detect neutral allosteric binding to these

receptors. This is an important area of exploration as no neutral allosteric modulators have been reported for mAChRs to date.

Discovery of selective allosteric modulators of mAChRs provides an unprecedented opportunity to develop a more detailed understanding of the functional roles of these receptors in neural circuits that are heavily modulated by cholinergic innervation. One of the most important roles of cholinergic systems in the CNS is modulation of transmission through the hippocampal formation, a limbic structure that plays a critical role in learning and memory that is thought to be important for cholinergic regulation of cognitive function. Activation of mAChRs in the hippocampus induces a marked reduction of transmission at both excitatory glutamatergic and inhibitory GABAergic synapses by presynaptic reduction of neurotransmitter release (Valentino and Dingledine, 1981; Bilkey and Goddard, 1985; Fernandez de Sevilla and Buno, 2003). Multiple mAChR subtypes are expressed in the hippocampus, and evidence suggests that both M_2 and M_4 are localized in presynaptic terminals where they could regulate excitatory and inhibitory synaptic transmission (Levey et al., 1995; Rouse et al., 1999; Rouse et al., 2000a). In addition, evidence suggests that activation of postsynaptic mAChRs on hippocampal pyramidal cells that express M_1 and M_4 could reduce synaptic transmission in the hippocampus by inducing release of endocannabinoids that activate presynaptic CB1 cannabinoid receptors (Ohno-Shosaku et al., 2003). Thus, the specific mAChR subtypes involved in regulating transmission at these important synapses is not clear. The finding that VU10010 potentiates effects of mAChR agonists on excitatory but not inhibitory synaptic transmission provides strong evidence that M_4 is one of the mAChR subtypes responsible for regulating transmission at glutamatergic synapses in the

hippocampus but is not likely to be involved in regulation of transmission at inhibitory synapses in this brain region (**Chapter IIIA**, (Shirey et al., 2008)). This selective regulation of excitatory synaptic transmission is a first critical step in developing a detailed understanding of the roles of M₄ in modulating hippocampal function. Although a growing body of literature implicates M₁ receptors in many of the excitatory postsynaptic effects of mAChR activation and in long-term plasticity (both LTP and LTD) in the hippocampus and cortex, many of these studies have relied on compounds that are not subtype selective or on studies employing knockout mice where compensatory mechanisms can complicate data interpretation. In future studies, it will be critical to take advantage of these novel selective allosteric potentiators to further investigate the roles of M₁ and M₄ in hippocampus as well as other cortical and basal ganglia structures where mAChRs have been postulated to play a critical neuromodulatory role. For instance, if the M₁ receptor subtype does mediate the excitatory postsynaptic effects of muscarinic agonists (depolarization, blockade of spike frequency adaptation and afterhyperpolarization currents, etc.), these effects of CCh should be blocked by the selective M₁ antagonist VU0255035 and should be mimicked by M₁ agonists. Likewise, M₁ agonists and PAMs should induce or modulate hippocampal LTP and LTD if this receptor subtype is responsible for the effects of CCh and ACh on these forms of long-term plasticity.

The M₁ receptor has long been viewed as an exciting potential target for increasing cognitive function in patients suffering from AD and other CNS disorders (Wess et al., 2007; Fisher, 2008; Langmead et al., 2008a; Caccamo et al., 2009). Despite major efforts to develop highly selective M₁ orthosteric agonists over the past two

decades, this receptor has proven intractable using traditional approaches, thus preventing M₁ agonists from advancing to clinical use for treatment of AD and other disorders. Also, lack of agents that selectively activate this receptor has made it impossible to develop a full understanding of the functional effects of selectively increasing M₁ receptor activity in the CNS. Studies with BQCA, along with the new M₁-selective antagonist VU0255035 (Sheffler et al., 2009), provide important support for the hypothesis that the M₁ receptor may increase activation of the PFC and may enhance PFC-dependent cognitive function (Anagnostaras et al., 2003). Non-selective mAChR agonists, such as CCh, induce an inward current in PFC pyramidal cells, and the present data (**Chapter IV**) provide strong evidence that this response is mediated by activation of the M₁ receptor. In addition, activation of the M₁ receptor increases the frequency of spontaneous excitatory synaptic events in mPFC layer V pyramidal cells. While the source of glutamatergic afferents giving rise to these sEPSCs has not been established, this is consistent with the hypothesis that the M₁ receptor plays an important role in increasing excitability and excitatory drive to mPFC pyramidal cells. It is also unclear thus far whether depolarization of glutamatergic pyramidal cells in cortical circuits underlies the increase in sEPSCs induced by CCh, or if these are two separate and unrelated phenomena.

Interestingly, mAChR activation induces direct excitatory effects in hippocampal CA1 pyramidal cells that are similar to those observed in mPFC pyramidal cells. However, while CA1 pyramidal cells express high levels of the M₁ receptor (Levey et al., 1991), previous studies suggest that the M₁ receptor is not the mAChR subtype responsible for some of the excitatory effects on these cells (Rouse et al., 2000a). Thus,

the precise physiological roles of the M₁ receptor are likely to vary in different brain regions and neuronal populations. The finding that M₁ receptor activation has excitatory effects and increases excitatory synaptic activity in mPFC pyramidal cells is interesting in the context of the recent finding that M₁ receptor knockout mice display clear deficits in PFC-dependent learning (Anagnostaras et al., 2003), whereas hippocampal-dependent learning is largely unaffected in M₁ receptor knockout mice (Anagnostaras et al., 2003) and in animals treated with the M₁ receptor- selective antagonist VU0255035 (Sheffler et al., 2009).

One of the most important implications of these studies is that they raise the possibility that highly selective M₁ receptor PAMs may provide a novel approach for treatment of AD and other CNS disorders that involve impaired cholinergic signaling. Clinical studies using both direct and indirect-acting muscarinic agonists have reported improvements in both cognitive function and behavioral disturbances (*i.e.* hallucinations, delusions, outbursts, and paranoia) observed in AD patients (Bodick et al., 1997b; Cummings et al., 2001). If M₁ receptor activation is responsible for, or plays an important role in, these effects of nonselective cholinergic agents, M₁ receptor PAMs could provide a viable approach to symptomatic treatment of AD. Furthermore, in addition to potential efficacy in reducing symptoms in AD patients, recent studies suggest that mAChR activation could reduce accumulation of toxic A β protein, thereby providing additional disease modifying effects. For instance, the muscarinic agonist AF102B was shown to decrease production of the amyloidogenic peptide A β 42 in the cerebral spinal fluid of AD patients (Nitsch et al., 2000). Furthermore, preclinical studies with a related mAChR agonist, AF267B suggest that mAChR activation increases non-amyloidogenic

processing and prevents A β formation (Caccamo et al., 2006). While these earlier mAChR agonists are not selective for the M₁ receptor relative to other mAChR subtypes, more recent studies revealed that the M₁ receptor-selective agonist, TBPB, has similar effects in PC12 cells (Jones et al., 2008).

The present finding that BQCA reverses deficits in compound discrimination reversal learning in a transgenic mouse model of AD provides exciting support for the hypothesis that highly selective M₁ receptor PAMs may provide efficacy in treatment of at least some domains of cognitive function in AD (**Chapter IV**). Furthermore, the finding that BQCA promotes non-amyloidogenic APP processing suggests that these agents could also reduce amyloid burden. In future studies, it will be important to fully explore the effects of BQCA in animal models that reflect other domains of cognitive function that are impaired in AD patients. For instance it is possible that M₁ receptor-selective PAMs will have robust efficacy in improving PFC-dependent learning, but have lesser effects on hippocampal-dependent learning. A mouse model of AD with impairments in hippocampal-dependent memory tasks could be used to test whether BQCA could restore performance in the Morris water maze or in other forms of spatial memory that require intact hippocampal functioning. Also, other types of cognitive function may involve different mAChR subtypes and be differentially affected by selective activators of the M₁ receptor *versus* selective PAMs of other mAChR subtypes, such as the recently reported M₄ and M₅ receptor-selective PAMs (Brady 2008; Chan 2008; Shirey 2008; Bridges 2009). Interestingly, the high subtype-selectivity of BQCA may prove to be important for achieving maximal effects in increasing non-amyloidogenic APP processing. Previous studies suggest that activation of M₂ and/or M₄

mAChR subtypes may have an antagonistic effect on the non-amyloidogenic APP processing shown to be promoted by M₁ receptor activation (Farber et al., 1995). Thus, in addition to reducing the adverse effect profile, it is possible that selective activation of the M₁ receptor may provide greater efficacy in regulating APP processing.

In addition to implications for AD, the electrophysiology studies reveal interesting findings that may provide important insights related to the potential roles of mAChRs in regulating PFC function. For instance, when added alone, BQCA induced a slight inward current and a slight increase in sEPSC frequency (**Chapter IV**, (Shirey et al., 2009)). This suggests that there may be a low tonic level of M₁ receptor activity or a low level of endogenous acetylcholine in slices that can be potentiated by BQCA. Furthermore, it was interesting to find that CCh induced a small reduction in sEPSC frequency when added in the presence of a saturating concentration of the selective M₁ antagonist, VU0255035. This suggests that activation of another mAChR subtype can reduce sEPSC frequency and that this effect is unmasked when the M₁ receptor is selectively blocked. To test the hypothesis that this inhibitory effect is mediated by the M₄ receptor subtype, the selective M₄ PAM, VU0152100, could be used alone and in combination with a low concentration of CCh. If this hypothesis were correct, I would expect to see a decrease in sEPSCs in the presence of VU0152100 and CCh. Interestingly, while effects of CCh on sEPSC frequency were dramatically reduced in M₁ receptor knockout mice, CCh did induce a small effect in slices from these animals. This suggests that another mAChR subtype may be capable of eliciting this response and could partially compensate for genetic deletion of the M₁ receptor. Importantly, the effect of the highly selective M₁ receptor PAM, BQCA, was eliminated in M₁ receptor

knockout mice, suggesting that the effects of this compound are fully dependent on activation of the M₁ receptor. Discovery of new mAChR subtype-selective ligands for multiple mAChR subtypes over the last year will allow for a better understanding of the roles of mAChR subtypes in regulating PFC function.

Recent clinical and animal studies raise the possibility that mAChR agonists may provide a novel approach for treatment of schizophrenia (Felder et al., 2001; Langmead et al., 2008a; Conn et al., 2009b). For decades, the prevailing theory behind the etiology of schizophrenia has been that excessive dopaminergic neurotransmission in the central nervous system is the major contributing factor underlying this severe psychiatric illness. This so-called dopamine hyperfunction hypothesis is based primarily on the observation that stimulation of the endogenous dopamine system (*e.g.* with amphetamine or cocaine) often leads to transient psychotic symptoms in healthy individuals (Bymaster et al., 2002; Raedler et al., 2007). Furthermore, all clinically relevant antipsychotic drugs, both typical and atypical, possess significant antagonist activity at D₂ dopamine receptors (D₂Rs) (Carlsson, 1988; Bymaster et al., 2002; Raedler et al., 2007). Thus, the majority of the efforts to discover novel therapeutic agents for the treatment of schizophrenia have been aimed at developing therapies that result in some level of D₂R blockade or a combination of blockade of D₂Rs and other monoamine receptors. Nevertheless, D₂R antagonists are only partially effective in treating schizophrenia, in that they only improve the positive symptoms associated with the disease, despite the fact that the negative and cognitive symptoms also markedly impact the quality of life for schizophrenic patients. In addition, these therapies also are often poorly tolerated because of numerous side effects including sedation, weight gain, sexual dysfunction,

diabetes and Parkinson's disease-like symptoms. Furthermore, greater than 25% of schizophrenia patients do not respond to these dopamine-based therapies. Thus, while it is evident that dopamine does play a prominent role in the pathogenesis and treatment of schizophrenia, the dopamine hyperfunction hypothesis of schizophrenia fails to account for all aspects of this disorder. It is increasingly evident that other neurotransmitter systems are likely involved. Based on this, it is unlikely that exclusive focus on discovery and development of antagonists of D₂Rs and other monoamine receptors will provide fundamental breakthroughs in the standard of treatment of schizophrenia patients relative to current therapies.

In recent years the mAChRs, namely M₁ and M₄, have emerged as potential novel targets for the treatment of schizophrenia. This is based on clinical studies demonstrating efficacy of mAChR agonists in treatment of positive symptoms in schizophrenia patients, as well as multiple animal studies suggesting that mAChR agonists could be useful in treatment of cognitive dysfunction in schizophrenia patients (Bymaster et al., 2002). A growing body of evidence from clinical and animal studies involving pharmacological manipulations, post mortem tissue analysis, and brain imaging is consistent with this hypothesis (Raedler et al., 2007). Furthermore, Shekhar and colleagues (Shekhar et al., 2008) recently reported that the M₁/M₄ receptor-preferring agonist xanomeline induced a robust improvement in positive and negative symptoms, as well as some measures of cognitive function, in schizophrenic patients. While recent advances suggesting potential utility of mAChR activators in treatment of schizophrenia have been exciting, there have been few selective pharmacological tools available to fully explore this emerging muscarinic hypothesis of schizophrenia. Unfortunately, previous attempts to develop

traditional orthosteric agonists that are highly selective for individual mAChR subtypes have been unsuccessful.

The recent discovery and optimization of highly selective positive allosteric modulators of M₁ and M₄ provides a major advance in establishing a new approach for developing highly selective activators of these receptors. The data presented provide further support for the ability to achieve high subtype selectivity by targeting allosteric sites and provide exciting new data demonstrating that highly selective M₄ PAMs have robust activity in at least one animal model that is similar to effects previously described for the non-selective orthosteric mAChR agonist, xanomeline (Stanhope et al., 2001). The finding that VU0152099 and VU0152100 mimic effects of xanomeline in an animal model that has been used to predict antipsychotic activity (Brady et al., 2008) is especially promising in light of clinical studies demonstrating the clinical efficacy of xanomeline in schizophrenia patients. This raises the exciting possibility that selective activation of M₄ may provide a novel approach for the treatment of some symptoms associated with schizophrenia. Based on animal studies, it is likely that both M₁ and M₄ receptors may be important for clinical efficacy in this patient population (Felder et al., 2001; Gerber et al., 2001; Miyakawa et al., 2001; Marino and Conn, 2002; Messer, 2002b; Anagnostaras et al., 2003; Bymaster et al., 2003b; Tzavara et al., 2004; Brady et al., 2008; Langmead et al., 2008a; Shirey et al., 2008). Availability of BQCA along with the systemically active M₄ receptor-selective PAM, VU0152100, should make it possible to evaluate the effects of selective activation of each of these mAChR subtypes as well as co-administration of both BQCA and VU0152100 in a range of animal models that may be relevant to the antipsychotic effects of xanomeline.

In addition to their potential relevance for schizophrenia, mAChRs also are thought to regulate motor function by exerting effects on dopaminergic transmission in the basal ganglia (Pisani et al., 2007; Raedler et al., 2007). For instance, multiple electrophysiology studies with M₄ knockout mice have led to the suggestion that activation of the M₄ mAChR may oppose some actions of dopaminergic neurons on striatal motor function (Calabresi et al., 1998; Sanchez-Lemus and Arias-Montano, 2006). Again, the lack of highly selective activators of M₄ has made it impossible to test this hypothesis directly. Also, previous studies with traditional orthosteric muscarinic agonists bypass the action of endogenous ACh in the basal ganglia and do not provide information about the effects of endogenous acetylcholine on motor activity. The finding that highly selective M₄ potentiators reverse amphetamine-induced hyperlocomotor activity in rats provides exciting new evidence in support of the hypothesis that endogenous ACh plays an important role in regulating dopaminergic control of motor function. Because these compounds do not activate M₄ directly, but selectively increase responses of M₄ to endogenous ACh, this provides direct evidence that this response can be modulated by endogenous ACh acting on M₄ receptors. In addition, this raises the possibility that selective M₄ modulators could provide a novel approach to treatment of other disorders involving altered dopaminergic function in the basal ganglia, including Parkinson's disease and dystonia. Ongoing studies in the Conn lab are in fact examining the efficacy of M₄ PAMS in animal models of these diseases.

In conclusion, the recent development of compounds that selectively activate or modulate individual mAChRs provides an exciting new opportunity to begin to answer questions about the role of these receptors in normal and pathological CNS function.

These tools will also allow the further validation of individual mAChR subtypes as therapeutic targets for a variety of disorders including AD and schizophrenia. One important aspect of research will include the elucidation of various signaling cascades activated by different classes of orthosteric and allosteric ligands. Preliminary data from our lab and others suggests that allosteric agonists of the M₁ receptor like TBPB (Jones et al., 2008) do not induce β -arrestin recruitment or activate mPFC neurons in the same manner as CCh; it will be important to determine whether specific signaling pathways like these and ERK1/2 activation are necessary for the therapeutically beneficial effects of mAChR activation. One way to assess the involvement of β -arrestin recruitment in the CCh-induced activation of mPFC neurons would be to perform recordings of sEPSCs in the presence of CCh using mice lacking the β -arrestin protein. If this signaling molecule is required for the muscarinic activation of mPFC layer V neurons, this effect would likely be absent or altered in the β -arrestin knockout mice. An alternate strategy could involve the use of a β -arrestin blocking peptide or antibody in the recording pipet in experiments with wildtype mice or rats. Likewise, a selective, cell permeable MEK inhibitor could be used in the recording bath to determine if ERK1/2 phosphorylation is required for CCh-induced increase in sEPSCs. If these experiments yielded data that support the involvement of these signaling proteins, this would be one possible explanation for the lack of effect of M₁ allosteric agonists like TBPB and VU0184670 on mPFC neurons since these compounds do not appear to induce β -arrestin recruitment.

It will also be interesting to examine the efficacy of PAMs in animal models of diseases that involve degeneration of cholinergic nuclei. Because postsynaptic mAChR expression remains largely intact despite the loss of cholinergic input, it has been

hypothesized that activation of these remaining postsynaptic receptors will alleviate many of the cognitive impairments associated with cholinergic decline (Caccamo et al., 2009). While this may be true for direct-acting agonists, it may not be possible to achieve therapeutic efficacy using allosteric potentiators that do not directly activate mAChRs. Depending on the level of disease progression and cholinergic degeneration, allosteric compounds could display a varying array of efficacies. The recent development of selective M₁ activators that are suitable for use in clinical trials with patients suffering from AD will also allow researchers and clinicians to determine the disease-modifying potential of these compounds. Although initial studies indicating that the M₁-preferring agonist AF102B decreased levels of A β in CSF of AD patients (Nitsch et al., 2000), it remains to be seen if sustained, selective M₁ activation will have any effect on disease progression or pathology in brain tissue of this patient population.

Because the M₁/M₄-preferring agonist xanomeline lacked true subtype selectivity and caused dose-limiting side effect associated with activation of peripheral M₃ receptors (Shekhar et al., 2008), clinical trial assessing the ability of this drug to significantly improve the symptoms of schizophrenia were somewhat limited. However, a growing body of literature including studies using knockout mice and initial studies with VU0152100, TBPB, and BQCA support the hypothesis that M₁ and M₄ receptors show great promise as therapeutic targets for diseases involving cognitive impairment such as AD and schizophrenia. Whether drugs that selectively activate these receptors will provide a more tolerable side-effect profile than that of AChE inhibitors or xanomeline remains to be seen. It will also be critical to determine if selective activation of M₁ or M₄

alone will be sufficient to improve symptoms of schizophrenia in the same manner as xanomeline.

REFERENCES

- Abe K, Nakata A, Mizutani A, Saito H (1994) Facilitatory but nonessential role of the muscarinic cholinergic system in the generation of long-term potentiation of population spikes in the dentate gyrus in vivo. *Neuropharmacology* 33:847-852.
- Anagnostaras SG, Murphy GG, Hamilton SE, Mitchell SL, Rahnama NP, Nathanson NM, Silva AJ (2003) Selective cognitive dysfunction in acetylcholine M1 muscarinic receptor mutant mice. *Nat Neurosci* 6:51-58.
- Andrade R (1991) Cell excitation enhances muscarinic cholinergic responses in rat association cortex. *Brain Res* 548:81-93.
- Arendt T, Bigl V, Arendt A, Tennstedt A (1983) Loss of neurons in the nucleus basalis of Meynert in Alzheimer's disease, paralysis agitans and Korsakoff's Disease. *Acta Neuropathol* 61:101-108.
- Auerbach JM, Segal M (1994) A novel cholinergic induction of long-term potentiation in rat hippocampus. *J Neurophysiol* 72:2034-2040.
- Auerbach JM, Segal M (1996) Muscarinic receptors mediating depression and long-term potentiation in rat hippocampus. *J Physiol* 492 (Pt 2):479-493.
- Auld DS, Kornecook TJ, Bastianetto S, Quirion R (2002) Alzheimer's disease and the basal forebrain cholinergic system: relations to beta-amyloid peptides, cognition, and treatment strategies. *Prog Neurobiol* 68:209-245.
- Bartus RT, Dean RL, 3rd, Beer B, Lippa AS (1982) The cholinergic hypothesis of geriatric memory dysfunction. *Science* 217:408-414.
- Basile AS, Fedorova I, Zapata A, Liu X, Shippenberg T, Duttaroy A, Yamada M, Wess J (2002) Deletion of the M5 muscarinic acetylcholine receptor attenuates morphine reinforcement and withdrawal but not morphine analgesia. *Proc Natl Acad Sci U S A* 99:11452-11457.
- Behrends JC, ten Bruggencate G (1993) Cholinergic modulation of synaptic inhibition in the guinea pig hippocampus in vitro: excitation of GABAergic interneurons and inhibition of GABA-release. *J Neurophysiol* 69:626-629.
- Benardo LS, Prince DA (1982) Ionic mechanisms of cholinergic excitation in mammalian hippocampal pyramidal cells. *Brain Res* 249:333-344.
- Berkeley JL, Gomez J, Wess J, Hamilton SE, Nathanson NM, Levey AI (2001) M1 muscarinic acetylcholine receptors activate extracellular signal-regulated kinase in CA1 pyramidal neurons in mouse hippocampal slices. *Mol Cell Neurosci* 18:512-524.
- Berntson GG, Sarter M, Cacioppo JT (1998) Anxiety and cardiovascular reactivity: the basal forebrain cholinergic link. *Behav Brain Res* 94:225-248.
- Bilkey DK, Goddard GV (1985) Medial septal facilitation of hippocampal granule cell activity is mediated by inhibition of inhibitory interneurons. *Brain Res* 361:99-106.
- Birdsall NJ, Lazareno S, Matsui H (1996) Allosteric regulation of muscarinic receptors. *Prog Brain Res* 109:147-151.
- Bliss TV, Collingridge GL (1993) A synaptic model of memory: long-term potentiation in the hippocampus. *Nature* 361:31-39.
- Blitzer RD, Gil O, Landau EM (1990) Cholinergic stimulation enhances long-term potentiation in the CA1 region of rat hippocampus. *Neurosci Lett* 119:207-210.
- Bodick NC, Offen WW, Shannon HE, Satterwhite J, Lucas R, van Lier R, Paul SM (1997a) The selective muscarinic agonist xanomeline improves both the cognitive deficits and behavioral symptoms of Alzheimer disease. *Alzheimer Dis Assoc Disord* 11 Suppl 4:S16-22.

- Bodick NC, Offen WW, Levey AI, Cutler NR, Gauthier SG, Satlin A, Shannon HE, Tollefson GD, Rasmussen K, Bymaster FP, Hurley DJ, Potter WZ, Paul SM (1997b) Effects of xanomeline, a selective muscarinic receptor agonist, on cognitive function and behavioral symptoms in Alzheimer disease. *Arch Neurol* 54:465-473.
- Bonner TI, Buckley NJ, Young AC, Brann MR (1987) Identification of a family of muscarinic acetylcholine receptor genes. *Science* 237:527-532.
- Bonner TI, Young AC, Brann MR, Buckley NJ (1988) Cloning and expression of the human and rat m5 muscarinic acetylcholine receptor genes. *Neuron* 1:403-410.
- Bowen DM, Smith CB, White P, Davison AN (1976) Neurotransmitter-related enzymes and indices of hypoxia in senile dementia and other abiotrophies. *Brain* 99:459-496.
- Brady AE, Jones CK, Bridges TM, Kennedy JP, Thompson AD, Heiman JU, Breininger ML, Gentry PR, Yin H, Jadhav SB, Shirey JK, Conn PJ, Lindsley CW (2008) Centrally active allosteric potentiators of the M4 muscarinic acetylcholine receptor reverse amphetamine-induced hyperlocomotor activity in rats. *J Pharmacol Exp Ther* 327:941-953.
- Bridges TM, Marlo JE, Niswender CM, Jones CK, Jadhav SB, Gentry PR, Plumley HC, Weaver CD, Conn PJ, Lindsley CW (2009) Discovery of the first highly M5-preferring muscarinic acetylcholine receptor ligand, an M5 positive allosteric modulator derived from a series of 5-trifluoromethoxy N-benzyl isatins. *J Med Chem* 52:3445-3448.
- Brown T, Zador A (1990) Hippocampus. In: *The Synaptic Organization of the Brain* (GM S, ed), pp 346-388. New York: Oxford UP.
- Buckley NJ, Bonner TI, Brann MR (1988) Localization of a family of muscarinic receptor mRNAs in rat brain. *J Neurosci* 8:4646-4652.
- Burgard EC, Sarvey JM (1990) Muscarinic receptor activation facilitates the induction of long-term potentiation (LTP) in the rat dentate gyrus. *Neurosci Lett* 116:34-39.
- Burgard EC, Cote TE, Sarvey JM (1993) Muscarinic depression of synaptic transmission and blockade of norepinephrine-induced long-lasting potentiation in the dentate gyrus. *Neuroscience* 54:377-389.
- Bymaster FP, Felder CC (2002) Role of the cholinergic muscarinic system in bipolar disorder and related mechanism of action of antipsychotic agents. *Mol Psychiatry* 7 Suppl 1:S57-63.
- Bymaster FP, Felder C, Ahmed S, McKinzie D (2002) Muscarinic receptors as a target for drugs treating schizophrenia. *Curr Drug Targets CNS Neurol Disord* 1:163-181.
- Bymaster FP, McKinzie DL, Felder CC, Wess J (2003a) Use of M1-M5 muscarinic receptor knockout mice as novel tools to delineate the physiological roles of the muscarinic cholinergic system. *Neurochem Res* 28:437-442.
- Bymaster FP, Felder CC, Tzavara E, Nomikos GG, Calligaro DO, McKinzie DL (2003b) Muscarinic mechanisms of antipsychotic atypicality. *Prog Neuropsychopharmacol Biol Psychiatry* 27:1125-1143.
- Bymaster FP, Carter PA, Yamada M, Gomeza J, Wess J, Hamilton SE, Nathanson NM, McKinzie DL, Felder CC (2003c) Role of specific muscarinic receptor subtypes in cholinergic parasympathomimetic responses, in vivo phosphoinositide hydrolysis, and pilocarpine-induced seizure activity. *Eur J Neurosci* 17:1403-1410.
- Caccamo A, Fisher A, LaFerla FM (2009) M1 agonists as a potential disease-modifying therapy for Alzheimer's disease. *Curr Alzheimer Res* 6:112-117.
- Calabresi P, Centonze D, Gubellini P, Pisani A, Bernardi G (1998) Endogenous ACh enhances striatal NMDA-responses via M1-like muscarinic receptors and PKC activation. *Eur J Neurosci* 10:2887-2895.

- Callahan MJ, Kinsora JJ, Harbaugh RE, Reeder TM, Davis RE (1993) Continuous ICV infusion of scopolamine impairs sustained attention of rhesus monkeys. *Neurobiol Aging* 14:147-151.
- Campbell UC, Lalwani K, Hernandez L, Kinney GG, Conn PJ, Bristow LJ (2004) The mGluR5 antagonist 2-methyl-6-(phenylethynyl)-pyridine (MPEP) potentiates PCP-induced cognitive deficits in rats. *Psychopharmacology (Berl)* 175:310-318.
- Carr DB, Surmeier DJ (2007) M1 muscarinic receptor modulation of Kir2 channels enhances temporal summation of excitatory synaptic potentials in prefrontal cortex pyramidal neurons. *J Neurophysiol* 97:3432-3438.
- Caulfield MP (1993) Muscarinic receptors--characterization, coupling and function. *Pharmacol Ther* 58:319-379.
- Caulfield MP, Birdsall NJ (1998) International Union of Pharmacology. XVII. Classification of muscarinic acetylcholine receptors. *Pharmacol Rev* 50:279-290.
- Chan AS, Yeung WW, Wong YH (2005) Integration of G protein signals by extracellular signal-regulated protein kinases in SK-N-MC neuroepithelioma cells. *J Neurochem* 94:1457-1470.
- Chan WY, McKinzie DL, Bose S, Mitchell SN, Witkin JM, Thompson RC, Christopoulos A, Lazareno S, Birdsall NJ, Bymaster FP, Felder CC (2008) Allosteric modulation of the muscarinic M4 receptor as an approach to treating schizophrenia. *Proc Natl Acad Sci U S A* 105:10978-10983.
- Christopoulos A (2002) Allosteric binding sites on cell-surface receptors: novel targets for drug discovery. *Nat Rev Drug Discov* 1:198-210.
- Christopoulos A, El-Fakahany EE (1999) Qualitative and quantitative assessment of relative agonist efficacy. *Biochem Pharmacol* 58:735-748.
- Christopoulos A, Kenakin T (2002) G protein-coupled receptor allosterism and complexing. *Pharmacol Rev* 54:323-374.
- Cole AE, Nicoll RA (1984a) Characterization of a slow cholinergic post-synaptic potential recorded in vitro from rat hippocampal pyramidal cells. *J Physiol* 352:173-188.
- Cole AE, Nicoll RA (1984b) The pharmacology of cholinergic excitatory responses in hippocampal pyramidal cells. *Brain Res* 305:283-290.
- Colino A, Halliwell JV (1993) Carbachol potentiates Q current and activates a calcium-dependent non-specific conductance in rat hippocampus in vitro. *Eur J Neurosci* 5:1198-1209.
- Colom LV, Nassif-Caudarella S, Dickson CT, Smythe JW, Bland BH (1991) In vivo intrahippocampal microinfusion of carbachol and bicuculline induces theta-like oscillations in the septally deafferented hippocampus. *Hippocampus* 1:381-390.
- Conn PJ, Christopoulos A, Lindsley CW (2009a) Allosteric modulators of GPCRs: a novel approach for the treatment of CNS disorders. *Nat Rev Drug Discov* 8:41-54.
- Conn PJ, Jones CK, Lindsley CW (2009b) Subtype-selective allosteric modulators of muscarinic receptors for the treatment of CNS disorders. *Trends Pharmacol Sci* 30:148-155.
- Coward P, Chan SD, Wada HG, Humphries GM, Conklin BR (1999) Chimeric G proteins allow a high-throughput signaling assay of Gi-coupled receptors. *Anal Biochem* 270:242-248.
- Coyle JT, Price DL, DeLong MR (1983) Alzheimer's disease: a disorder of cortical cholinergic innervation. *Science* 219:1184-1190.
- Coyle JT, Tsai G, Goff DC (2002) Ionotropic glutamate receptors as therapeutic targets in schizophrenia. *Curr Drug Target CNS Neurol Disord* 1:183-189.
- Csillik B (1975) Synaptochemistry of acetylcholine metabolism in a cholinergic neuron. *Int Rev Neurobiol* 18:69-140.

- Dalley JW, Cardinal RN, Robbins TW (2004) Prefrontal executive and cognitive functions in rodents: neural and neurochemical substrates. *Neurosci Biobehav Rev* 28:771-784.
- Damasio AR, Graff-Radford NR, Eslinger PJ, Damasio H, Kassel N (1985) Amnesia following basal forebrain lesions. *Arch Neurol* 42:263-271.
- Davies P, Maloney AJ (1976) Selective loss of central cholinergic neurons in Alzheimer's disease. *Lancet* 2:1403.
- Davis KL, Thal LJ, Gamzu ER, Davis CS, Woolson RF, Gracon SI, Drachman DA, Schneider LS, Whitehouse PJ, Hoover TM, et al. (1992) A double-blind, placebo-controlled multicenter study of tacrine for Alzheimer's disease. The Tacrine Collaborative Study Group. *N Engl J Med* 327:1253-1259.
- Day J, Damsma G, Fibiger HC (1991) Cholinergic activity in the rat hippocampus, cortex and striatum correlates with locomotor activity: an in vivo microdialysis study. *Pharmacol Biochem Behav* 38:723-729.
- Day M, Carr DB, Ulrich S, Ilijic E, Tkatch T, Surmeier DJ (2005) Dendritic excitability of mouse frontal cortex pyramidal neurons is shaped by the interaction among HCN, Kir2, and K_{leak} channels. *J Neurosci* 25:8776-8787.
- Degenetais E, Thierry AM, Glowinski J, Gioanni Y (2003) Synaptic influence of hippocampus on pyramidal cells of the rat prefrontal cortex: an in vivo intracellular recording study. *Cereb Cortex* 13:782-792.
- Dekker AJ, Connor DJ, Thal LJ (1991) The role of cholinergic projections from the nucleus basalis in memory. *Neurosci Biobehav Rev* 15:299-317.
- DeSousa NJ, Beninger RJ, Jhamandas K, Boegman RJ (1994) Stimulation of GABAB receptors in the basal forebrain selectively impairs working memory of rats in the double Y-maze. *Brain Res* 641:29-38.
- Drachman DA (1977) Memory and cognitive function in man: does the cholinergic system have a specific role? *Neurology* 27:783-790.
- Drachman DA, Leavitt J (1974) Human memory and the cholinergic system. A relationship to aging? *Arch Neurol* 30:113-121.
- Dunnett SB (1985) Comparative effects of cholinergic drugs and lesions of nucleus basalis or fimbria-fornix on delayed matching in rats. *Psychopharmacology (Berl)* 87:357-363.
- Dutar P, Nicoll RA (1988) Classification of muscarinic responses in hippocampus in terms of receptor subtypes and second-messenger systems: electrophysiological studies in vitro. *J Neurosci* 8:4214-4224.
- Duttaroy A, Zimlik CL, Gautam D, Cui Y, Mears D, Wess J (2004) Muscarinic stimulation of pancreatic insulin and glucagon release is abolished in m3 muscarinic acetylcholine receptor-deficient mice. *Diabetes* 53:1714-1720.
- Eggermann E, Feldmeyer D (2009) Cholinergic filtering in the recurrent excitatory microcircuit of cortical layer 4. *Proc Natl Acad Sci U S A* 106:11753-11758.
- Eglen RM (2005) Muscarinic receptor subtype pharmacology and physiology. *Prog Med Chem* 43:105-136.
- Farber SA, Nitsch RM, Schulz JG, Wurtman RJ (1995) Regulated secretion of beta-amyloid precursor protein in rat brain. *J Neurosci* 15:7442-7451.
- Farlow M, Gracon SI, Hershey LA, Lewis KW, Sadowsky CH, Dolan-Ureno J (1992) A controlled trial of tacrine in Alzheimer's disease. The Tacrine Study Group. *JAMA* 268:2523-2529.
- Fawzi AB, Macdonald D, Benbow LL, Smith-Torhan A, Zhang H, Weig BC, Ho G, Tulshian D, Linder ME, Graziano MP (2001) SCH-202676: An allosteric modulator of both agonist and antagonist binding to G protein-coupled receptors. *Mol Pharmacol* 59:30-37.
- Felder CC, Bymaster FP, Ward J, DeLapp N (2000) Therapeutic opportunities for muscarinic receptors in the central nervous system. *J Med Chem* 43:4333-4353.

- Felder CC, Porter AC, Skillman TL, Zhang L, Bymaster FP, Nathanson NM, Hamilton SE, Gomez J, Wess J, McKinzie DL (2001) Elucidating the role of muscarinic receptors in psychosis. *Life Sci* 68:2605-2613.
- Fernandez de Sevilla D, Buno W (2003) Presynaptic inhibition of Schaffer collateral synapses by stimulation of hippocampal cholinergic afferent fibres. *Eur J Neurosci* 17:555-558.
- Fernandez de Sevilla D, Cabezas C, de Prada AN, Sanchez-Jimenez A, Buno W (2002) Selective muscarinic regulation of functional glutamatergic Schaffer collateral synapses in rat CA1 pyramidal neurons. *J Physiol* 545:51-63.
- Fernandez de Sevilla D, Nunez A, Borde M, Malinow R, Buno W (2008) Cholinergic-mediated IP3-receptor activation induces long-lasting synaptic enhancement in CA1 pyramidal neurons. *J Neurosci* 28:1469-1478.
- Fibiger HC (1991) Cholinergic mechanisms in learning, memory and dementia: a review of recent evidence. *Trends Neurosci* 14:220-223.
- Fibiger HC, Damsma G, Day JC (1991) Behavioral pharmacology and biochemistry of central cholinergic neurotransmission. *Adv Exp Med Biol* 295:399-414.
- Fink-Jensen A, Fedorova I, Wortwein G, Woldbye DP, Rasmussen T, Thomsen M, Bolwig TG, Knitowski KM, McKinzie DL, Yamada M, Wess J, Basile A (2003) Role for M5 muscarinic acetylcholine receptors in cocaine addiction. *J Neurosci Res* 74:91-96.
- Fisahn A, Yamada M, Duttaroy A, Gan JW, Deng CX, McBain CJ, Wess J (2002) Muscarinic induction of hippocampal gamma oscillations requires coupling of the M1 receptor to two mixed cation currents. *Neuron* 33:615-624.
- Fisher A (1997) Muscarinic agonists for the treatment of Alzheimer's disease: progress and perspectives. *Expert Opin Investig Drugs* 6:1395-1411.
- Fisher A (2008a) M1 muscarinic agonists target major hallmarks of Alzheimer's disease--the pivotal role of brain M1 receptors. *Neurodegener Dis* 5:237-240.
- Fisher A (2008b) Cholinergic treatments with emphasis on m1 muscarinic agonists as potential disease-modifying agents for Alzheimer's disease. *Neurotherapeutics* 5:433-442.
- Fisher A, Brandeis R, Bar-Ner RH, Kliger-Spatz M, Natan N, Sonogo H, Marcovitch I, Pittel Z (2002) AF150(S) and AF267B: M1 muscarinic agonists as innovative therapies for Alzheimer's disease. *J Mol Neurosci* 19:145-153.
- Flynn DD, Ferrari-DiLeo G, Mash DC, Levey AI (1995a) Differential regulation of molecular subtypes of muscarinic receptors in Alzheimer's disease. *J Neurochem* 64:1888-1891.
- Flynn DD, Ferrari-DiLeo G, Levey AI, Mash DC (1995b) Differential alterations in muscarinic receptor subtypes in Alzheimer's disease: implications for cholinergic-based therapies. *Life Sci* 56:869-876.
- Francis PT, Palmer AM, Snape M, Wilcock GK (1999) The cholinergic hypothesis of Alzheimer's disease: a review of progress. *J Neurol Neurosurg Psychiatry* 66:137-147.
- Frotscher M, Leranth C (1985) Cholinergic innervation of the rat hippocampus as revealed by choline acetyltransferase immunocytochemistry: a combined light and electron microscopic study. *J Comp Neurol* 239:237-246.
- Galici R, Echemendia NG, Rodriguez AL, Conn PJ (2005) A selective allosteric potentiator of metabotropic glutamate (mGlu) 2 receptors has effects similar to an orthosteric mGlu2/3 receptor agonist in mouse models predictive of antipsychotic activity. *J Pharmacol Exp Ther* 315:1181-1187.
- Gasparini F, Kuhn R, Pin JP (2002) Allosteric modulators of group I metabotropic glutamate receptors: novel subtype-selective ligands and therapeutic perspectives. *Curr Opin Pharmacol* 2:43-49.
- Gasparini F, Lingenhohl K, Stoehr N, Flor PJ, Heinrich M, Vranesic I, Biollaz M, Allgeier H, Heckendorn R, Urwyler S, Varney MA, Johnson EC, Hess SD, Rao

- SP, Sacaan AI, Santori EM, Velicelebi G, Kuhn R (1999) 2-Methyl-6-(phenylethynyl)-pyridine (MPEP), a potent, selective and systemically active mGlu5 receptor antagonist. *Neuropharmacology* 38:1493-1503.
- Gaykema RP, Luiten PG, Nyakas C, Traber J (1990) Cortical projection patterns of the medial septum-diagonal band complex. *J Comp Neurol* 293:103-124.
- Gerber DJ, Sotnikova TD, Gainetdinov RR, Huang SY, Caron MG, Tonegawa S (2001) Hyperactivity, elevated dopaminergic transmission, and response to amphetamine in M1 muscarinic acetylcholine receptor-deficient mice. *Proc Natl Acad Sci U S A* 98:15312-15317.
- Gether U (2000) Uncovering molecular mechanisms involved in activation of G protein-coupled receptors. *Endocr Rev* 21:90-113.
- Gil Z, Connors BW, Amitai Y (1997) Differential regulation of neocortical synapses by neuromodulators and activity. *Neuron* 19:679-686.
- Gill TM, Sarter M, Givens B (2000) Sustained visual attention performance-associated prefrontal neuronal activity: evidence for cholinergic modulation. *J Neurosci* 20:4745-4757.
- Gold JM (2004) Cognitive deficits as treatment targets in schizophrenia. *Schizophr Res* 72:21-28.
- Gomez J, Zhang L, Kostenis E, Felder C, Bymaster F, Brodtkin J, Shannon H, Xia B, Deng C, Wess J (1999) Enhancement of D1 dopamine receptor-mediated locomotor stimulation in M(4) muscarinic acetylcholine receptor knockout mice. *Proc Natl Acad Sci U S A* 96:10483-10488.
- Gomez J, Zhang L, Kostenis E, Felder CC, Bymaster FP, Brodtkin J, Shannon H, Xia B, Duttaroy A, Deng CX, Wess J (2001) Generation and pharmacological analysis of M2 and M4 muscarinic receptor knockout mice. *Life Sci* 68:2457-2466.
- Goto Y, O'Donnell P (2003) Altered prefrontal cortex-nucleus accumbens information processing in a developmental animal model of schizophrenia. *Ann N Y Acad Sci* 1003:398-401.
- Greenlee W et al. (2001) Muscarinic agonists and antagonists in the treatment of Alzheimer's disease. *Farmacology* 56:247-250.
- Groenewegen HJ, Uylings HB (2000) The prefrontal cortex and the integration of sensory, limbic and autonomic information. *Prog Brain Res* 126:3-28.
- Gu Z, Zhong P, Yan Z (2003) Activation of muscarinic receptors inhibits beta-amyloid peptide-induced signaling in cortical slices. *J Biol Chem* 278:17546-17556.
- Gulledge AT, Park SB, Kawaguchi Y, Stuart GJ (2007) Heterogeneity of phasic cholinergic signaling in neocortical neurons. *J Neurophysiol* 97:2215-2229.
- Gulledge AT, Bucci DJ, Zhang SS, Matsui M, Yeh HH (2009) M1 receptors mediate cholinergic modulation of excitability in neocortical pyramidal neurons. *J Neurosci* 29:9888-9902.
- Haj-Dahmane S, Andrade R (1996) Muscarinic activation of a voltage-dependent cation nonselective current in rat association cortex. *J Neurosci* 16:3848-3861.
- Haj-Dahmane S, Andrade R (1997) Calcium-activated cation nonselective current contributes to the fast afterdepolarization in rat prefrontal cortex neurons. *J Neurophysiol* 78:1983-1989.
- Haj-Dahmane S, Andrade R (1998) Ionic mechanism of the slow afterdepolarization induced by muscarinic receptor activation in rat prefrontal cortex. *J Neurophysiol* 80:1197-1210.
- Halliwel JV (1990) Physiological mechanisms of cholinergic action in the hippocampus. *Prog Brain Res* 84:255-272.
- Hamilton SE, Nathanson NM (2001) The M1 receptor is required for muscarinic activation of mitogen-activated protein (MAP) kinase in murine cerebral cortical neurons. *J Biol Chem* 276:15850-15853.

- Harvey J, Balasubramaniam R, Collingridge GL (1993) Carbachol can potentiate N-methyl-D-aspartate responses in the rat hippocampus by a staurosporine and thapsigargin-insensitive mechanism. *Neurosci Lett* 162:165-168.
- Hasselmo ME (1995) Neuromodulation and cortical function: modeling the physiological basis of behavior. *Behav Brain Res* 67:1-27.
- Hasselmo ME, Bower JM (1992) Cholinergic suppression specific to intrinsic not afferent fiber synapses in rat piriform (olfactory) cortex. *J Neurophysiol* 67:1222-1229.
- Hasselmo ME, McGaughy J (2004) High acetylcholine levels set circuit dynamics for attention and encoding and low acetylcholine levels set dynamics for consolidation. *Prog Brain Res* 145:207-231.
- Heckers S, Rauch SL, Goff D, Savage CR, Schacter DL, Fischman AJ, Alpert NM (1998) Impaired recruitment of the hippocampus during conscious recollection in schizophrenia. *Nat Neurosci* 1:318-323.
- Hersch SM, Levey AI (1995) Diverse pre- and post-synaptic expression of m1-m4 muscarinic receptor proteins in neurons and afferents in the rat neostriatum. *Life Sci* 56:931-938.
- Hersch SM, Gutekunst CA, Rees HD, Heilman CJ, Levey AI (1994) Distribution of m1-m4 muscarinic receptor proteins in the rat striatum: light and electron microscopic immunocytochemistry using subtype-specific antibodies. *J Neurosci* 14:3351-3363.
- Hirsch S, Barnes TRE (1995) Schizophrenia:pp. 440-445.
- Hounsgaard J (1978) Presynaptic inhibitory action of acetylcholine in area CA1 of the hippocampus. *Exp Neurol* 62:787-797.
- Hsiao K, Chapman P, Nilsen S, Eckman C, Harigaya Y, Younkin S, Yang F, Cole G (1996) Correlative memory deficits, A β elevation, and amyloid plaques in transgenic mice. *Science* 274:99-102.
- Huang CC, Hsu KS (2009) Activation of Muscarinic Acetylcholine Receptors Induces a Nitric Oxide-Dependent Long-Term Depression in Rat Medial Prefrontal Cortex. *Cereb Cortex*.
- Hulme (a) EC, Lu ZL, Bee MS (2003) Scanning mutagenesis studies of the M1 muscarinic acetylcholine receptor. *Receptors Channels* 9:215-228.
- Hulme EC, Birdsall NJ, Buckley NJ (1990) Muscarinic receptor subtypes. *Annu Rev Pharmacol Toxicol* 30:633-673.
- Jakubik J, El-Fakahany EE, Dolezal V (2006) Differences in kinetics of xanomeline binding and selectivity of activation of G proteins at M(1) and M(2) muscarinic acetylcholine receptors. *Mol Pharmacol* 70:656-666.
- Jakubik J, Bacakova L, El-Fakahany EE, Tucek S (1997) Positive cooperativity of acetylcholine and other agonists with allosteric ligands on muscarinic acetylcholine receptors. *Mol Pharmacol* 52:172-179.
- Jay TM, Witter MP (1991) Distribution of hippocampal CA1 and subicular efferents in the prefrontal cortex of the rat studied by means of anterograde transport of Phaseolus vulgaris-leucoagglutinin. *J Comp Neurol* 313:574-586.
- Jay TM, Thierry AM, Wiklund L, Glowinski J (1992) Excitatory Amino Acid Pathway from the Hippocampus to the Prefrontal Cortex. Contribution of AMPA Receptors in Hippocampo-prefrontal Cortex Transmission. *Eur J Neurosci* 4:1285-1295.
- Jones CK, Brady AE, Davis AA, Xiang Z, Bubser M, Tantawy MN, Kane AS, Bridges TM, Kennedy JP, Bradley SR, Peterson TE, Ansari MS, Baldwin RM, Kessler RM, Deutch AY, Lah JJ, Levey AI, Lindsley CW, Conn PJ (2008) Novel selective allosteric activator of the M1 muscarinic acetylcholine receptor regulates amyloid processing and produces antipsychotic-like activity in rats. *J Neurosci* 28:10422-10433.

- Joseph JA, Cutler R, Roth GS (1993) Changes in G protein-mediated signal transduction in aging and Alzheimer's disease. *Ann N Y Acad Sci* 695:42-45.
- Kapur S, Mizrahi R, Li M (2005) From dopamine to salience to psychosis--linking biology, pharmacology and phenomenology of psychosis. *Schizophr Res* 79:59-68.
- Katzenschlager R, Sampaio C, Costa J, Lees A (2003) Anticholinergics for symptomatic management of Parkinson's disease. *Cochrane Database Syst Rev*:CD003735.
- Kawaguchi Y (1997) Selective cholinergic modulation of cortical GABAergic cell subtypes. *J Neurophysiol* 78:1743-1747.
- Kenakin T (2003) Ligand-selective receptor conformations revisited: the promise and the problem. *Trends Pharmacol Sci* 24:346-354.
- Kenakin T (2008) Functional selectivity in GPCR modulator screening. *Comb Chem High Throughput Screen* 11:337-343.
- Khurana S, Chacon I, Xie G, Yamada M, Wess J, Raufman JP, Kennedy RH (2004) Vasodilatory effects of cholinergic agonists are greatly diminished in aorta from M3R^{-/-} mice. *Eur J Pharmacol* 493:127-132.
- Kinney GG, O'Brien JA, Lemaire W, Burno M, Bickel DJ, Clements MK, Chen TB, Wisnoski DD, Lindsley CW, Tiller PR, Smith S, Jacobson MA, Sur C, Duggan ME, Pettibone DJ, Conn PJ, Williams DL, Jr. (2005) A novel selective positive allosteric modulator of metabotropic glutamate receptor subtype 5 has in vivo activity and antipsychotic-like effects in rat behavioral models. *J Pharmacol Exp Ther* 313:199-206.
- Kirkwood A, Rozas C, Kirkwood J, Perez F, Bear MF (1999) Modulation of long-term synaptic depression in visual cortex by acetylcholine and norepinephrine. *J Neurosci* 19:1599-1609.
- Klink R, Alonso A (1997) Ionic mechanisms of muscarinic depolarization in entorhinal cortex layer II neurons. *J Neurophysiol* 77:1829-1843.
- Knapp MJ, Knopman DS, Solomon PR, Pendlebury WW, Davis CS, Gracon SI (1994) A 30-week randomized controlled trial of high-dose tacrine in patients with Alzheimer's disease. The Tacrine Study Group. *JAMA* 271:985-991.
- Kolb B (1984) Functions of the frontal cortex of the rat: a comparative review. *Brain Res* 320:65-98.
- Kolb B (1990) Animal models for human PFC-related disorders. *Prog Brain Res* 85:501-519.
- Korczyn AD (2000) Muscarinic M(1) agonists in the treatment of Alzheimer's disease. *Expert Opin Investig Drugs* 9:2259-2267.
- Krejci A, Tucek S (2002) Quantitation of mRNAs for M(1) to M(5) subtypes of muscarinic receptors in rat heart and brain cortex. *Mol Pharmacol* 61:1267-1272.
- Kremin T, Gerber D, Giocomo LM, Huang SY, Tonegawa S, Hasselmo ME (2006) Muscarinic suppression in stratum radiatum of CA1 shows dependence on presynaptic M1 receptors and is not dependent on effects at GABA(B) receptors. *Neurobiol Learn Mem* 85:153-163.
- Krnjevic K (1969) Central cholinergic pathways. *Fed Proc* 28:113-120.
- Krnjevic K (2004) Synaptic mechanisms modulated by acetylcholine in cerebral cortex. *Prog Brain Res* 145:81-93.
- Krnjevic K, Pumain R, Renaud L (1971) The mechanism of excitation by acetylcholine in the cerebral cortex. *J Physiol* 215:247-268.
- Krnjevic K, Reiffenstein RJ, Ropert N (1981) Disinhibitory action of acetylcholine in the rat's hippocampus: extracellular observations. *Neuroscience* 6:2465-2474.
- Kruglikov I, Rudy B (2008) Perisomatic GABA release and thalamocortical integration onto neocortical excitatory cells are regulated by neuromodulators. *Neuron* 58:911-924.

- Kuczewski N, Aztiria E, Leanza G, Domenici L (2005) Selective cholinergic immunolesioning affects synaptic plasticity in developing visual cortex. *Eur J Neurosci* 21:1807-1814.
- Langmead CJ, Watson J, Reavill C (2008a) Muscarinic acetylcholine receptors as CNS drug targets. *Pharmacol Ther* 117:232-243.
- Langmead CJ et al. (2008b) Characterization of a CNS penetrant, selective M1 muscarinic receptor agonist, 77-LH-28-1. *Br J Pharmacol* 154:1104-1115.
- Lanzafame A, Christopoulos A (2004) Investigation of the interaction of a putative allosteric modulator, N-(2,3-diphenyl-1,2,4-thiadiazole-5-(2H)-ylidene) methanamine hydrobromide (SCH-202676), with M1 muscarinic acetylcholine receptors. *J Pharmacol Exp Ther* 308:830-837.
- Lanzafame AA, Sexton PM, Christopoulos A (2006) Interaction studies of multiple binding sites on m4 muscarinic acetylcholine receptors. *Mol Pharmacol* 70:736-746.
- Laroche S, Jay TM, Thierry AM (1990) Long-term potentiation in the prefrontal cortex following stimulation of the hippocampal CA1/subicular region. *Neurosci Lett* 114:184-190.
- Lawrence JJ, Statland JM, Grinspan ZM, McBain CJ (2006) Cell type-specific dependence of muscarinic signalling in mouse hippocampal stratum oriens interneurons. *J Physiol* 570:595-610.
- Lazareno S (2004) Determination of allosteric interactions using radioligand-binding techniques. *Methods Mol Biol* 259:29-46.
- Lazareno S, Dolezal V, Popham A, Birdsall NJ (2004) Thiochrome enhances acetylcholine affinity at muscarinic M4 receptors: receptor subtype selectivity via cooperativity rather than affinity. *Mol Pharmacol* 65:257-266.
- Lazareno S, Gharagozloo P, Kuonen D, Popham A, Birdsall NJ (1998) Subtype-selective positive cooperative interactions between brucine analogues and acetylcholine at muscarinic receptors: radioligand binding studies. *Mol Pharmacol* 53:573-589.
- Lebois EP, Bridges TM, Lewis LM, Dawson ES, Kane AS, Xiang Z, Jadhav S, Yin H, Kennedy JP, Meiler J, Niswender CM, Jones CK, Conn PJ, Weaver CD, Lindsley CW (2009) Discovery and characterization of novel subtype-selective allosteric agonists for the investigation of M₁ receptor function in the central nervous system. *ACS Chem Neurosci*.
- Lebon G, Langmead CJ, Tehan BG, Hulme EC (2009) Mutagenic mapping suggests a novel binding mode for selective agonists of M1 muscarinic acetylcholine receptors. *Mol Pharmacol* 75:331-341.
- Lefkowitz RJ (2007) Seven transmembrane receptors: something old, something new. *Acta Physiol (Oxf)* 190:9-19.
- Lehmann J, Nagy JI, Atmadia S, Fibiger HC (1980) The nucleus basalis magnocellularis: the origin of a cholinergic projection to the neocortex of the rat. *Neuroscience* 5:1161-1174.
- Levey AI, Kitt CA, Simonds WF, Price DL, Brann MR (1991) Identification and localization of muscarinic acetylcholine receptor proteins in brain with subtype-specific antibodies. *J Neurosci* 11:3218-3226.
- Levey AI, Edmunds SM, Heilman CJ, Desmond TJ, Frey KA (1994) Localization of muscarinic m3 receptor protein and M3 receptor binding in rat brain. *Neuroscience* 63:207-221.
- Levey AI, Edmunds SM, Hersch SM, Wiley RG, Heilman CJ (1995a) Light and electron microscopic study of m2 muscarinic acetylcholine receptor in the basal forebrain of the rat. *J Comp Neurol* 351:339-356.
- Levey AI, Edmunds SM, Koliatsos V, Wiley RG, Heilman CJ (1995b) Expression of m1-m4 muscarinic acetylcholine receptor proteins in rat hippocampus and regulation by cholinergic innervation. *J Neurosci* 15:4077-4092.

- Lindsley CW, Wisnoski DD, Leister WH, O'Brien J A, Lemaire W, Williams DL, Jr., Burno M, Sur C, Kinney GG, Pettibone DJ, Tiller PR, Smith S, Duggan ME, Hartman GD, Conn PJ, Huff JR (2004) Discovery of positive allosteric modulators for the metabotropic glutamate receptor subtype 5 from a series of N-(1,3-diphenyl-1H-pyrazol-5-yl)benzamides that potentiate receptor function in vivo. *J Med Chem* 47:5825-5828.
- Liu L, Zhao R, Bai Y, Stanish LF, Evans JE, Sanderson MJ, Bonventre JV, Rittenhouse AR (2006) M1 muscarinic receptors inhibit L-type Ca²⁺ current and M-current by divergent signal transduction cascades. *J Neurosci* 26:11588-11598.
- Lu WY, Xiong ZG, Lei S, Orser BA, Dudek E, Browning MD, MacDonald JF (1999) G-protein-coupled receptors act via protein kinase C and Src to regulate NMDA receptors. *Nat Neurosci* 2:331-338.
- Ma L et al. (2009) Selective activation of the M1 muscarinic acetylcholine receptor achieved by allosteric potentiation. *Proc Natl Acad Sci U S A*.
- Ma XH, Zhong P, Gu Z, Feng J, Yan Z (2003) Muscarinic potentiation of GABA(A) receptor currents is gated by insulin signaling in the prefrontal cortex. *J Neurosci* 23:1159-1168.
- Madison DV, Nicoll RA (1986) Actions of noradrenaline recorded intracellularly in rat hippocampal CA1 pyramidal neurones, in vitro. *J Physiol* 372:221-244.
- Madison DV, Lancaster B, Nicoll RA (1987) Voltage clamp analysis of cholinergic action in the hippocampus. *J Neurosci* 7:733-741.
- Malenka RC, Bear MF (2004) LTP and LTD: an embarrassment of riches. *Neuron* 44:5-21.
- Mannaioni G, Marino MJ, Valenti O, Traynelis SF, Conn PJ (2001) Metabotropic glutamate receptors 1 and 5 differentially regulate CA1 pyramidal cell function. *J Neurosci* 21:5925-5934.
- Marino MJ, Conn PJ (2002) Direct and indirect modulation of the N-methyl D-aspartate receptor. *Curr Drug Targets CNS Neurol Disord* 1:1-16.
- Marino MJ, Rouse ST, Levey AI, Potter LT, Conn PJ (1998) Activation of the genetically defined m1 muscarinic receptor potentiates N-methyl-D-aspartate (NMDA) receptor currents in hippocampal pyramidal cells. *Proc Natl Acad Sci U S A* 95:11465-11470.
- Marino MJ, Williams DL, Jr., O'Brien JA, Valenti O, McDonald TP, Clements MK, Wang R, DiLella AG, Hess JF, Kinney GG, Conn PJ (2003) Allosteric modulation of group III metabotropic glutamate receptor 4: a potential approach to Parkinson's disease treatment. *Proc Natl Acad Sci U S A* 100:13668-13673.
- Markram H, Segal M (1990a) Electrophysiological characteristics of cholinergic and non-cholinergic neurons in the rat medial septum-diagonal band complex. *Brain Res* 513:171-174.
- Markram H, Segal M (1990b) Acetylcholine potentiates responses to N-methyl-D-aspartate in the rat hippocampus. *Neurosci Lett* 113:62-65.
- Markram H, Segal M (1992) The inositol 1,4,5-trisphosphate pathway mediates cholinergic potentiation of rat hippocampal neuronal responses to NMDA. *J Physiol* 447:513-533.
- Marlo JE, Niswender CM, Days EL, Bridges TM, Xiang Y, Rodriguez AL, Shirey JK, Brady AE, Nalywajko T, Luo Q, Austin CA, Williams MB, Kim K, Williams R, Orton D, Brown HA, Lindsley CW, Weaver CD, Conn PJ (2009) Discovery and characterization of novel allosteric potentiators of M1 muscarinic receptors reveals multiple modes of activity. *Mol Pharmacol* 75:577-588.
- Matsui M, Motomura D, Karasawa H, Fujikawa T, Jiang J, Komiya Y, Takahashi S, Taketo MM (2000) Multiple functional defects in peripheral autonomic organs in mice lacking muscarinic acetylcholine receptor gene for the M3 subtype. *Proc Natl Acad Sci U S A* 97:9579-9584.

- May LT, Leach K, Sexton PM, Christopoulos A (2007) Allosteric modulation of G protein-coupled receptors. *Annu Rev Pharmacol Toxicol* 47:1-51.
- McCoy PA, McMahon LL (2007) Muscarinic receptor dependent long-term depression in rat visual cortex is PKC independent but requires ERK1/2 activation and protein synthesis. *J Neurophysiol* 98:1862-1870.
- McCutchen E, Scheiderer CL, Dobrunz LE, McMahon LL (2006) Coexistence of muscarinic long-term depression with electrically induced long-term potentiation and depression at CA3-CA1 synapses. *J Neurophysiol* 96:3114-3121.
- McGaughy J, Dalley JW, Morrison CH, Everitt BJ, Robbins TW (2002) Selective behavioral and neurochemical effects of cholinergic lesions produced by intrabasalis infusions of 192 IgG-saporin on attentional performance in a five-choice serial reaction time task. *J Neurosci* 22:1905-1913.
- McQuiston AR, Madison DV (1999a) Muscarinic receptor activity induces an afterdepolarization in a subpopulation of hippocampal CA1 interneurons. *J Neurosci* 19:5703-5710.
- McQuiston AR, Madison DV (1999b) Muscarinic receptor activity has multiple effects on the resting membrane potentials of CA1 hippocampal interneurons. *J Neurosci* 19:5693-5702.
- Messer WS, Jr. (2002a) The utility of muscarinic agonists in the treatment of Alzheimer's disease. *J Mol Neurosci* 19:187-193.
- Messer WS, Jr. (2002b) Cholinergic agonists and the treatment of Alzheimer's disease. *Current Topics in Medicinal Chemistry* 2:353-358.
- Messer WS, Jr., Rajeswaran WG, Cao Y, Zhang HJ, el-Assadi AA, Dockery C, Liske J, O'Brien J, Williams FE, Huang XP, Wroblewski ME, Nagy PI, Peseckis SM (2000) Design and development of selective muscarinic agonists for the treatment of Alzheimer's disease: characterization of tetrahydropyrimidine derivatives and development of new approaches for improved affinity and selectivity for M1 receptors. *Pharm Acta Helv* 74:135-140.
- Miller EK, Cohen JD (2001) An integrative theory of prefrontal cortex function. *Annu Rev Neurosci* 24:167-202.
- Mirza NR, Peters D, Sparks RG (2003) Xanomeline and the antipsychotic potential of muscarinic receptor subtype selective agonists. *CNS Drug Rev* 9:159-186.
- Miyakawa T, Yamada M, Duttaroy A, Wess J (2001) Hyperactivity and intact hippocampus-dependent learning in mice lacking the M1 muscarinic acetylcholine receptor. *J Neurosci* 21:5239-5250.
- Mohler H, Fritschy JM, Rudolph U (2002) A new benzodiazepine pharmacology. *J Pharmacol Exp Ther* 300:2-8.
- Morton RA, Davies CH (1997) Regulation of muscarinic acetylcholine receptor-mediated synaptic responses by adenosine receptors in the rat hippocampus. *J Physiol* 502 (Pt 1):75-90.
- Morton RA, Manuel NA, Bulters DO, Cobb SR, Davies CH (2001) Regulation of muscarinic acetylcholine receptor-mediated synaptic responses by GABA(B) receptors in the rat hippocampus. *J Physiol* 535:757-766.
- Mrzljak L, Levey AI, Goldman-Rakic PS (1993) Association of m1 and m2 muscarinic receptor proteins with asymmetric synapses in the primate cerebral cortex: morphological evidence for cholinergic modulation of excitatory neurotransmission. *Proc Natl Acad Sci U S A* 90:5194-5198.
- Mufson EJ, Ma SY, Cochran EJ, Bennett DA, Beckett LA, Jaffar S, Saragovi HU, Kordower JH (2000) Loss of nucleus basalis neurons containing trkA immunoreactivity in individuals with mild cognitive impairment and early Alzheimer's disease. *J Comp Neurol* 427:19-30.
- Muir JL, Dunnett SB, Robbins TW, Everitt BJ (1992) Attentional functions of the forebrain cholinergic systems: effects of intraventricular hemicholinium,

- physostigmine, basal forebrain lesions and intracortical grafts on a multiple-choice serial reaction time task. *Exp Brain Res* 89:611-622.
- Munoz-Torrero D (2008) Acetylcholinesterase inhibitors as disease-modifying therapies for Alzheimer's disease. *Curr Med Chem* 15:2433-2455.
- Nilsson OG, Leanza G, Rosenblad C, Lappi DA, Wiley RG, Bjorklund A (1992) Spatial learning impairments in rats with selective immunolesion of the forebrain cholinergic system. *Neuroreport* 3:1005-1008.
- Nitsch RM, Deng M, Tennis M, Schoenfeld D, Growdon JH (2000) The selective muscarinic M1 agonist AF102B decreases levels of total Abeta in cerebrospinal fluid of patients with Alzheimer's disease. *Ann Neurol* 48:913-918.
- Noetzel MJ, Grant MK, El-Fakahany EE (2009) Mechanisms of M3 muscarinic receptor regulation by wash-resistant xanomeline binding. *Pharmacology* 83:301-317.
- O'Brien JA, Lemaire W, Chen TB, Chang RS, Jacobson MA, Ha SN, Lindsley CW, Schaffhauser HJ, Sur C, Pettibone DJ, Conn PJ, Williams DL, Jr. (2003) A family of highly selective allosteric modulators of the metabotropic glutamate receptor subtype 5. *Mol Pharmacol* 64:731-740.
- O'Brien JA, Lemaire W, Wittmann M, Jacobson MA, Ha SN, Wisnoski DD, Lindsley CW, Schaffhauser HJ, Rowe B, Sur C, Duggan ME, Pettibone DJ, Conn PJ, Williams DL, Jr. (2004) A novel selective allosteric modulator potentiates the activity of native metabotropic glutamate receptor subtype 5 in rat forebrain. *J Pharmacol Exp Ther* 309:568-577.
- O'Donnell P, Grace AA (1995) Synaptic interactions among excitatory afferents to nucleus accumbens neurons: hippocampal gating of prefrontal cortical input. *J Neurosci* 15:3622-3639.
- O'Donnell P, Lewis BL, Weinberger DR, Lipska BK (2002) Neonatal hippocampal damage alters electrophysiological properties of prefrontal cortical neurons in adult rats. *Cereb Cortex* 12:975-982.
- Ohno-Shosaku T, Matsui M, Fukudome Y, Shosaku J, Tsubokawa H, Taketo MM, Manabe T, Kano M (2003) Postsynaptic M1 and M3 receptors are responsible for the muscarinic enhancement of retrograde endocannabinoid signalling in the hippocampus. *Eur J Neurosci* 18:109-116.
- Origlia N, Kuczewski N, Aztiria E, Gautam D, Wess J, Domenici L (2006) Muscarinic acetylcholine receptor knockout mice show distinct synaptic plasticity impairments in the visual cortex. *J Physiol* 577:829-840.
- Parent MA, Wang L, Su J, Netoff T, Yuan LL (2009) Identification of the Hippocampal Input to Medial Prefrontal Cortex In Vitro. *Cereb Cortex*.
- Parikh V, Kozak R, Martinez V, Sarter M (2007) Prefrontal acetylcholine release controls cue detection on multiple timescales. *Neuron* 56:141-154.
- Passetti F, Dalley JW, O'Connell MT, Everitt BJ, Robbins TW (2000) Increased acetylcholine release in the rat medial prefrontal cortex during performance of a visual attentional task. *Eur J Neurosci* 12:3051-3058.
- Peralta EG, Ashkenazi A, Winslow JW, Smith DH, Ramachandran J, Capon DJ (1987) Distinct primary structures, ligand-binding properties and tissue-specific expression of four human muscarinic acetylcholine receptors. *EMBO J* 6:3923-3929.
- Perez-Burgos A, Perez-Rosello T, Salgado H, Flores-Barrera E, Prieto GA, Figueroa A, Galarraga E, Bargas J (2008) Muscarinic M(1) modulation of N and L types of calcium channels is mediated by protein kinase C in neostriatal neurons. *Neuroscience* 155:1079-1097.
- Perry EK, Tomlinson BE, Blessed G, Bergmann K, Gibson PH, Perry RH (1978) Correlation of cholinergic abnormalities with senile plaques and mental test scores in senile dementia. *Br Med J* 2:1457-1459.
- Phillis JW (2005) Acetylcholine release from the central nervous system: a 50-year retrospective. *Crit Rev Neurobiol* 17:161-217.

- Pitler TA, Alger BE (1990) Activation of the pharmacologically defined M3 muscarinic receptor depolarizes hippocampal pyramidal cells. *Brain Res* 534:257-262.
- Pittel Z, Heldman E, Barg J, Haring R, Fisher A (1996) Muscarinic control of amyloid precursor protein secretion in rat cerebral cortex and cerebellum. *Brain Res* 742:299-304.
- Potter LT (2001) Snake toxins that bind specifically to individual subtypes of muscarinic receptors. *Life Sci* 68:2541-2547.
- Qian J, Saggau P (1997) Presynaptic inhibition of synaptic transmission in the rat hippocampus by activation of muscarinic receptors: involvement of presynaptic calcium influx. *Br J Pharmacol* 122:511-519.
- Raedler TJ, Bymaster FP, Tandon R, Copolov D, Dean B (2007) Towards a muscarinic hypothesis of schizophrenia. *Mol Psychiatry* 12:232-246.
- Raskind MA, Cyrus PA, Ruzicka BB, Gulanski BI (1999) The effects of metrifonate on the cognitive, behavioral, and functional performance of Alzheimer's disease patients. Metrifonate Study Group. *J Clin Psychiatry* 60:318-325.
- Rees S, Morrow D, Kenakin T (2002) GPCR drug discovery through the exploitation of allosteric drug binding sites. *Receptors Channels* 8:261-268.
- Reinikainen KJ, Soininen H, Riekkinen PJ (1990) Neurotransmitter changes in Alzheimer's disease: implications to diagnostics and therapy. *J Neurosci Res* 27:576-586.
- Rogers SL, Doody RS, Mohs RC, Friedhoff LT (1998) Donepezil improves cognition and global function in Alzheimer disease: a 15-week, double-blind, placebo-controlled study. Donepezil Study Group. *Arch Intern Med* 158:1021-1031.
- Romcy-Pereira R, Pavlides C (2004) Distinct modulatory effects of sleep on the maintenance of hippocampal and medial prefrontal cortex LTP. *Eur J Neurosci* 20:3453-3462.
- Rouse ST, Levey AI (1996) Expression of m1-m4 muscarinic acetylcholine receptor immunoreactivity in septohippocampal neurons and other identified hippocampal afferents. *J Comp Neurol* 375:406-416.
- Rouse ST, Gilmor ML, Levey AI (1998) Differential presynaptic and postsynaptic expression of m1-m4 muscarinic acetylcholine receptors at the perforant pathway/granule cell synapse. *Neuroscience* 86:221-232.
- Rouse ST, Hamilton SE, Potter LT, Nathanson NM, Conn PJ (2000a) Muscarinic-induced modulation of potassium conductances is unchanged in mouse hippocampal pyramidal cells that lack functional M1 receptors. *Neurosci Lett* 278:61-64.
- Rouse ST, Edmunds SM, Yi H, Gilmor ML, Levey AI (2000b) Localization of M(2) muscarinic acetylcholine receptor protein in cholinergic and non-cholinergic terminals in rat hippocampus. *Neurosci Lett* 284:182-186.
- Salgado H, Bellay T, Nichols JA, Bose M, Martinolich L, Perrotti L, Atzori M (2007) Muscarinic M2 and M1 receptors reduce GABA release by Ca²⁺ channel modulation through activation of PI3K/Ca²⁺ -independent and PLC/Ca²⁺ -dependent PKC. *J Neurophysiol* 98:952-965.
- Sarter M, Hasselmo ME, Bruno JP, Givens B (2005) Unraveling the attentional functions of cortical cholinergic inputs: interactions between signal-driven and cognitive modulation of signal detection. *Brain Res Brain Res Rev* 48:98-111.
- Satoh K, Fibiger HC (1986) Cholinergic neurons of the laterodorsal tegmental nucleus: efferent and afferent connections. *J Comp Neurol* 253:277-302.
- Scarr E, Sundram S, Keriakous D, Dean B (2007) Altered hippocampal muscarinic M4, but not M1, receptor expression from subjects with schizophrenia. *Biol Psychiatry* 61:1161-1170.
- Scheiderer CL, Smith CC, McCutchen E, McCoy PA, Thacker EE, Kolasa K, Dobrunz LE, McMahon LL (2008) Coactivation of M(1) muscarinic and alpha1 adrenergic receptors stimulates extracellular signal-regulated protein kinase and induces

- long-term depression at CA3-CA1 synapses in rat hippocampus. *J Neurosci* 28:5350-5358.
- Scheiderer CL, McCutchen E, Thacker EE, Kolasa K, Ward MK, Parsons D, Harrell LE, Dobrunz LE, McMahon LL (2006) Sympathetic sprouting drives hippocampal cholinergic reinnervation that prevents loss of a muscarinic receptor-dependent long-term depression at CA3-CA1 synapses. *J Neurosci* 26:3745-3756.
- Seeger T, Fedorova I, Zheng F, Miyakawa T, Koustova E, Gomeza J, Basile AS, Alzheimer C, Wess J (2004) M2 muscarinic acetylcholine receptor knock-out mice show deficits in behavioral flexibility, working memory, and hippocampal plasticity. *J Neurosci* 24:10117-10127.
- Segal M (1982) Multiple action of acetylcholine at a muscarinic receptor studied in the rat hippocampal slice. *Brain Res* 246:77-87.
- Sheffler DJ, Williams R, Bridges TM, Xiang Z, Kane AS, Byun NE, Jadhav S, Mock MM, Zheng F, Lewis LM, Jones CK, Niswender CM, Weaver CD, Lindsley CW, Conn PJ (2009) A Novel Selective Muscarinic Acetylcholine Receptor Subtype 1 (M1 mAChR) Antagonist Reduces Seizures Without Impairing Hippocampal-Dependent Learning. *Mol Pharmacol*.
- Shekhar A, Potter WZ, Lightfoot J, Lienemann J, Dube S, Mallinckrodt C, Bymaster FP, McKinzie DL, Felder CC (2008) Selective muscarinic receptor agonist xanomeline as a novel treatment approach for schizophrenia. *Am J Psychiatry* 165:1033-1039.
- Sheridan RD, Sutor B (1990) Presynaptic M1 muscarinic cholinergic receptors mediate inhibition of excitatory synaptic transmission in the hippocampus in vitro. *Neurosci Lett* 108:273-278.
- Shinoe T, Matsui M, Taketo MM, Manabe T (2005) Modulation of synaptic plasticity by physiological activation of M1 muscarinic acetylcholine receptors in the mouse hippocampus. *J Neurosci* 25:11194-11200.
- Shirey JK, Xiang Z, Orton D, Brady AE, Johnson KA, Williams R, Ayala JE, Rodriguez AL, Wess J, Weaver D, Niswender CM, Conn PJ (2008) An allosteric potentiator of M4 mAChR modulates hippocampal synaptic transmission. *Nat Chem Biol* 4:42-50.
- Shirey JK, Brady AE, Jones PJ, Davis AA, Bridges TM, Kennedy JP, Jadhav SB, Menon UN, Xiang Z, Watson ML, Christian EP, Doherty JJ, Quirk MC, Snyder DH, Lah JJ, Levey AI, Nicolle MM, Lindsley CW, Conn PJ (2009) A selective allosteric potentiator of the M1 muscarinic acetylcholine receptor increases activity of medial prefrontal cortical neurons and restores impairments in reversal learning. *J Neurosci* 29:14271-14286.
- Soudijn W, van Wijngaarden I, AP IJ (2002) Allosteric modulation of G protein-coupled receptors. *Curr Opin Drug Discov Devel* 5:749-755.
- Spalding TA, Trotter C, Skjaerbaek N, Messier TL, Currier EA, Burstein ES, Li D, Hacksell U, Brann MR (2002) Discovery of an ectopic activation site on the M(1) muscarinic receptor. *Mol Pharmacol* 61:1297-1302.
- Sur C, Mallorga PJ, Wittmann M, Jacobson MA, Pascarella D, Williams JB, Brandish PE, Pettibone DJ, Scolnick EM, Conn PJ (2003) N-desmethylclozapine, an allosteric agonist at muscarinic 1 receptor, potentiates N-methyl-D-aspartate receptor activity. *Proc Natl Acad Sci U S A* 100:13674-13679.
- Tai C, Kuzmiski JB, MacVicar BA (2006) Muscarinic enhancement of R-type calcium currents in hippocampal CA1 pyramidal neurons. *J Neurosci* 26:6249-6258.
- Thinakaran G, Koo EH (2008) Amyloid precursor protein trafficking, processing, and function. *J Biol Chem* 283:29615-29619.
- Thomas RL, Mistry R, Langmead CJ, Wood MD, Challiss RA (2008) G protein coupling and signaling pathway activation by m1 muscarinic acetylcholine receptor orthosteric and allosteric agonists. *J Pharmacol Exp Ther* 327:365-374.

- Thomsen M, Woldbye DP, Wortwein G, Fink-Jensen A, Wess J, Caine SB (2005) Reduced cocaine self-administration in muscarinic M5 acetylcholine receptor-deficient mice. *J Neurosci* 25:8141-8149.
- Tsai G, Coyle JT (2002) Glutamatergic mechanisms in schizophrenia. *Annu Rev Pharmacol Toxicol* 42:165-179.
- Tzavara ET, Bymaster FP, Davis RJ, Wade MR, Perry KW, Wess J, McKinzie DL, Felder C, Nomikos GG (2004) M4 muscarinic receptors regulate the dynamics of cholinergic and dopaminergic neurotransmission: relevance to the pathophysiology and treatment of related CNS pathologies. *FASEB J* 18:1410-1412.
- Unno T, Matsuyama H, Sakamoto T, Uchiyama M, Izumi Y, Okamoto H, Yamada M, Wess J, Komori S (2005) M(2) and M(3) muscarinic receptor-mediated contractions in longitudinal smooth muscle of the ileum studied with receptor knockout mice. *Br J Pharmacol* 146:98-108.
- Valentino RJ, Dingledine R (1981) Presynaptic inhibitory effect of acetylcholine in the hippocampus. *J Neurosci* 1:784-792.
- Vertes RP (2006) Interactions among the medial prefrontal cortex, hippocampus and midline thalamus in emotional and cognitive processing in the rat. *Neuroscience* 142:1-20.
- Vinogradova OS, Brazhnik ES, Stafekhina VS, Kitchigina VF (1993) Acetylcholine, theta-rhythm and activity of hippocampal neurons in the rabbit--II. Septal input. *Neuroscience* 53:971-979.
- Vogt KE, Regehr WG (2001) Cholinergic modulation of excitatory synaptic transmission in the CA3 area of the hippocampus. *J Neurosci* 21:75-83.
- Volk LJ, Pfeiffer BE, Gibson JR, Huber KM (2007) Multiple Gq-coupled receptors converge on a common protein synthesis-dependent long-term depression that is affected in fragile X syndrome mental retardation. *J Neurosci* 27:11624-11634.
- Volpicelli LA, Levey AI (2004) Muscarinic acetylcholine receptor subtypes in cerebral cortex and hippocampus. *Prog Brain Res* 145:59-66.
- Voytko ML, Olton DS, Richardson RT, Gorman LK, Tobin JR, Price DL (1994) Basal forebrain lesions in monkeys disrupt attention but not learning and memory. *J Neurosci* 14:167-186.
- Waelbroeck M (2003) Allosteric drugs acting at muscarinic acetylcholine receptors. *Neurochem Res* 28:419-422.
- Wang L, Yuan LL (2009) Activation of M2 muscarinic receptors leads to sustained suppression of hippocampal transmission in the medial prefrontal cortex. *J Physiol* 587:5139-5147.
- Weiner DM, Levey AI, Brann MR (1990) Expression of muscarinic acetylcholine and dopamine receptor mRNAs in rat basal ganglia. *Proc Natl Acad Sci U S A* 87:7050-7054.
- Wess J (1996) Molecular biology of muscarinic acetylcholine receptors. *Crit Rev Neurobiol* 10:69-99.
- Wess J (2003) Novel insights into muscarinic acetylcholine receptor function using gene targeting technology. *Trends Pharmacol Sci* 24:414-420.
- Wess J (2005) Allosteric binding sites on muscarinic acetylcholine receptors. *Mol Pharmacol* 68:1506-1509.
- Wess J, Eglen RM, Gautam D (2007) Muscarinic acetylcholine receptors: mutant mice provide new insights for drug development. *Nat Rev Drug Discov* 6:721-733.
- Whitehouse PJ, Price DL, Struble RG, Clark AW, Coyle JT, Delon MR (1982) Alzheimer's disease and senile dementia: loss of neurons in the basal forebrain. *Science* 215:1237-1239.
- Wilkinson D, Murray J (2001) Galantamine: a randomized, double-blind, dose comparison in patients with Alzheimer's disease. *Int J Geriatr Psychiatry* 16:852-857.

- Williams S, Johnston D (1990) Muscarinic depression of synaptic transmission at the hippocampal mossy fiber synapse. *J Neurophysiol* 64:1089-1097.
- Yamada M, Lamping KG, Duttaroy A, Zhang W, Cui Y, Bymaster FP, McKinzie DL, Felder CC, Deng CX, Faraci FM, Wess J (2001a) Cholinergic dilation of cerebral blood vessels is abolished in M(5) muscarinic acetylcholine receptor knockout mice. *Proc Natl Acad Sci U S A* 98:14096-14101.
- Yamada M, Miyakawa T, Duttaroy A, Yamanaka A, Moriguchi T, Makita R, Ogawa M, Chou CJ, Xia B, Crawley JN, Felder CC, Deng CX, Wess J (2001b) Mice lacking the M3 muscarinic acetylcholine receptor are hypophagic and lean. *Nature* 410:207-212.
- Yan HD, Villalobos C, Andrade R (2009) TRPC Channels Mediate a Muscarinic Receptor-Induced Afterdepolarization in Cerebral Cortex. *J Neurosci* 29:10038-10046.
- Zhang HM, Chen SR, Matsui M, Gautam D, Wess J, Pan HL (2006) Opposing functions of spinal M2, M3, and M4 receptor subtypes in regulation of GABAergic inputs to dorsal horn neurons revealed by muscarinic receptor knockout mice. *Mol Pharmacol* 69:1048-1055.
- Zhang HM, Zhou HY, Chen SR, Gautam D, Wess J, Pan HL (2007) Control of glycinergic input to spinal dorsal horn neurons by distinct muscarinic receptor subtypes revealed using knockout mice. *J Pharmacol Exp Ther* 323:963-971.
- Zhang W, Yamada M, Gomeza J, Basile AS, Wess J (2002a) Multiple muscarinic acetylcholine receptor subtypes modulate striatal dopamine release, as studied with M1-M5 muscarinic receptor knock-out mice. *J Neurosci* 22:6347-6352.
- Zhang W, Basile AS, Gomeza J, Volpicelli LA, Levey AI, Wess J (2002b) Characterization of central inhibitory muscarinic autoreceptors by the use of muscarinic acetylcholine receptor knock-out mice. *J Neurosci* 22:1709-1717.
- Zhong P, Gu Z, Wang X, Jiang H, Feng J, Yan Z (2003) Impaired modulation of GABAergic transmission by muscarinic receptors in a mouse transgenic model of Alzheimer's disease. *J Biol Chem* 278:26888-26896.